

**Safety, pharmacokinetics and pharmacodynamics
of targeted anti-cancer drugs**

ISBN/EAN: 978-94-901-2268-3

© 2009 David Boss

Cover design: David Boss, Nieuwegein, the Netherlands
Gerie Boss, Nieuwegein, the Netherlands

Printed by: Gildeprint drukkerijen, Enschede, the Netherlands

**Safety, pharmacokinetics and pharmacodynamics
of targeted anti-cancer drugs**

Veiligheid, farmacokinetiek en farmacodynamiek van
doelgerichte anti-kanker middelen
(met een samenvatting in het Nederlands)

PROEFSCHRIFT

ter verkrijging van de graad van doctor
aan de Universiteit Utrecht
op gezag van de rector magnificus, prof. dr. J.C. Stoof,
ingevolge het besluit van het college voor promoties
in het openbaar te verdedigen
op dinsdag 27 oktober 2009 des middags te 12.45 uur

door

David Sebastiaan Boss

geboren op 8 september 1979 te Utrecht

Promotoren:

Prof. dr. J.H.M. Schellens

Prof. dr. J.H. Beijnen

The research described in this thesis was performed at the department of medical oncology of the Netherlands Cancer Institute, Amsterdam, the Netherlands, and the department of pharmacy and pharmacology of the Slotervaart hospital, Amsterdam, the Netherlands.

Publication of this thesis was financially supported by:

Eisai Ltd, Hatfield, United Kingdom

KuDOS pharmaceuticals, Cambridge, United Kingdom

AstraZeneca Nederland B.V., Zoetermeer, the Netherlands

Pfizer Nederland B.V., Capelle a/d IJssel, the Netherlands

Amgen Nederland B.V., Breda, the Netherlands

Janssen-Cilag B.V., Tilburg, the Netherlands

J.E. Jurriaanse stichting, Rotterdam, the Netherlands

The Netherlands Laboratory for Anticancer Drug Formulation, Amsterdam, the Netherlands

Boehringer Ingelheim Nederland B.V., Alkmaar, the Netherlands

Merck Sharp & Dohme B.V., Haarlem, the Netherlands

GlaxoSmithKline Nederland B.V., Zeist, the Netherlands

Roche Nederland B.V., Woerden, the Netherlands

Abbott Nederland B.V., Hoofddorp, the Netherlands

Don't you believe in flying saucers, they ask me? Don't you believe in telepathy? — in ancient astronauts? — in the Bermuda triangle? — in life after death?

No, I reply. No, no, no, no, and again no.

One person recently, goaded into desperation by the litany of unrelieved negation, burst out "Don't you believe in anything?"

"Yes", I said. "I believe in evidence. I believe in observation, measurement, and reasoning, confirmed by independent observers. I'll believe anything, no matter how wild and ridiculous, if there is evidence for it. The wilder and more ridiculous something is, however, the firmer and more solid the evidence will have to be."

Isaac Asimov

"Whenever I found out anything remarkable, I have thought it my duty to put down my discovery on paper, so that all ingenious people might be informed thereof."

Antoni van Leeuwenhoek

Voor alle patiënten
en hun families

Contents

Chapter 1: General introduction	3
Chapter 2: Novel endpoints in clinical trials: PET/CT	
2.1 Application of PET/CT in the development of novel anti-cancer drugs	9
2.2 In reply	37
Chapter 3: Aurora kinase inhibitors	
3.1 Clinical experience with Aurora kinase inhibitors: A review	43
3.2 An open-label multi-centre dose escalation phase I study of AZD1152, a selective inhibitor of Aurora B Kinase	71
Chapter 4: The CDK-inhibitor AZD5438	
4.1 Safety, tolerability, pharmacokinetics and pharmacodynamics of the oral cyclin-dependent kinase inhibitor AZD5438 when administered at continuous and intermittent dosing schedules in patients with advanced solid tumors	93
Chapter 5: Carboplatin and topotecan	
5.1 Phase I, pharmacokinetic and pharmacodynamic study of carboplatin and topotecan administered intravenously every 28 days to patients with malignant solid tumors	119
Chapter 6: The parp-inhibitor olaparib (AZD2281)	
6.1: Inhibition of poly(ADP-ribose) polymerase in tumors from BRCA mutation carriers	143
6.2: Olaparib (AZD2281) can be safely administered with therapeutic doses of paclitaxel	167

Chapter 7: The angiogenesis inhibitor E7080		
7.1	Phase I dose escalation study of E7080, an orally available multi-targeted angiogenesis inhibitor, in patients with advanced solid malignancies	183
7.2	Serum β -HCG and CA-125 as tumor-markers in a patient with osteosarcoma: A case report	203
Chapter 8: The pan-HER inhibitor PF00299804		
8.1	Phase I dose escalation study of the pan-HER inhibitor, PF00299804, in patients with advanced malignant solid tumors	217
Chapter 9: Sorafenib, gemcitabine and carboplatin		
9.1	Phase I pharmacokinetic study of sorafenib in combination with gemcitabine and carboplatin in patients with advanced solid tumors	239
Chapter 10: Conclusion and perspectives		261
Chemical structures of investigated molecules in this thesis		267
Summary		271
Samenvatting		277
Dankwoord		285
Curriculum Vitae		291
List of publications		294

1

General introduction

Chapter 1: General Introduction

With over 10 million new cases each year, cancer constitutes a major health problem worldwide (1). In the Netherlands, the incidence of new cancer cases is still increasing, with over 80.000 new cases diagnosed in 2006. Despite advances in the prevention, diagnosis, and treatment of cancer, the disease is still responsible for about 40.000 deaths per year in the Netherlands only (2). These numbers strongly advocate the search for novel, better anticancer drugs.

The last decade, cancer therapy has been hallmarked by the discovery and evaluation of numerous small molecules and monoclonal antibodies. Together, these drugs constitute the class of the so-called "targeted agents", compounds that are directed against one or more molecules that are known to be important for the malignant process. Several of these agents are now registered for the treatment of various forms of cancer. The road a candidate anticancer drug must follow in order to get its registration is time-consuming, and tremendously expensive. Following successful preclinical evaluation in *in vitro* systems and laboratory animals, the drugs must successfully pass phase I, phase II and phase III clinical trials. In brief, phase I studies aim to explore the safety of the candidate drug, while phase II studies aim to explore the activity of the compound. Finally, phase III studies are designed to test whether the candidate drug is better than the currently available drugs.

This thesis is focused on the first clinical evaluation of novel anticancer agents, as well as of combinations of anticancer agents. These studies describe the safety profiles, and aim to establish the maximum tolerable dose (MTD) and dose-limiting toxicities (DLTs), of the investigational drugs or drug combinations. Principle components in these studies are the pharmacokinetic analyses, investigating how the drug behaves in the human body. These data are essential in the course of developing a treatment schedule for any given investigational agent.

Increasingly important in phase I clinical trials is the incorporation of pharmacodynamic analyses, investigating whether the drug candidate is able to reach its target and exert its effect in a desirable way. Several of the here described phase I studies make use of pharmacodynamic endpoints, either in tumor or in surrogate tissues. Utilizing these endpoints early in the course of

clinical development is important, since they might identify failing drug candidates or ineffective treatment schedules at an early stage, thereby saving immense amounts of time and money.

Finally, response evaluations are reported in each of the here described phase I studies. Although not the primary objective, response data obtained in phase I studies can give valuable information, possibly directing the course a drug has to follow on its path to registration. Fortunately, in some of the here reported phase I studies encouraging anti-tumor activity was observed. Combined with a good safety and pharmacokinetic profile, some of the here described investigational agents passed their phase I exam successfully and moved into phase II.

References

1. GLOBOCAN 2002 database. Cancer Incidence, Mortality and Prevalence Worldwide. International Agency for Research on Cancer (<http://www-dep.iarc.fr>). 2009
2. NKR cijfers 2006. IKC 2009 (<http://www.ikcnet.nl>). 2009

Table 1: The compounds investigated in this thesis

Name	Target(s)	Mechanism of Action	Chapter
Targeted agents			
AZD1152	Aurora Kinase B	Serine/Threonine Kinase Inhibitor	3.2
AZD5438	Cyclin dependent Kinase 2	Cell cycle inhibition	4.1
olaparib (AZD2281)	Poly (ADP) ribose polymerase	Inhibition of DNA repair	6.1 6.2
E7080	VEGFR2, PDGFR-beta, FGFR1, c-kit	Angiogenesis inhibition	7.1 7.2
PF-00299804	HER1, HER2, HER4	Inhibition of HER-mediated signal transduction	8.1
sorafenib (Nexavar ®)	VEGFR-2,3, PDGFRbeta, raf-1, BRAF, C-Kit	Angiogenesis inhibition	9.1
Conventional cytotoxic agents			
carboplatin	DNA	Induction of DNA damage	5.1 9.1
topotecan (Hycamtin ®)	Topoisomerase I	Induction of DNA damage	5.1
paclitaxel (Taxol ®)	Microtubuli	Stabilizing the microtubuli	6.2
gemcitabine (Gemzar ®)	DNA	Antimetabolite	9.1

2

Novel endpoints in Clinical trials: PET/CT

CHAPTER 2.1

Application of PET/CT in the development of novel anti-cancer drugs

David S. Boss, Renato Valdes Olmos, Michiel Sinaasappel, Jos H. Beijnen, Jan H. M. Schellens

Oncologist. 2008 Jan;13(1):25-38

Abstract

Combined PET/CT is a relatively new imaging modality, combining the functional images of PET with the anatomical information of CT. Since its commercial introduction about 5 years ago, PET/CT has become an important tool in oncology. Currently, the technique is utilized for primary staging and re-staging of cancer patients, as well as for surgery and radiation therapy planning. The abilities of PET/CT to measure early treatment response as well as drug distribution within the body make this technique very useful in the development of novel anticancer drugs. In this paper recent literature about the current role of PET/CT in drug development is reviewed.

Introduction

Cancer is one of the leading causes of morbidity and mortality in developed countries, accounting for approximately 560,000 deaths in 2007 in the US only, as estimated by the American Cancer Society (1).

Imaging techniques have become indispensable to the practice of oncology for screening programs, staging, diagnosis, early response measurement and tumor surveillance during follow-up. Anatomical imaging techniques like Computed Tomography (CT) and Magnetic Resonance Imaging (MRI) have benefited from the improvements in spatial and temporal resolution over the years, and are widely used in all phases of cancer management. However, both techniques have their limitations. They rely on morphological changes, which limits discriminating pathophysiological processes such as inflammation versus metastasis in enlarged lymph nodes or fibrosis versus recurrent tumor in a residual mass. Moreover, the staging of early tumors is hampered, as morphological changes occur later in the course of the disease. MRI can also be used for functional imaging, but the technique at current stage of development is hampered by its low sensitivity. Imaging modalities like Positron Emission Tomography (PET), Single Photon Emission Computed Tomography (SPECT) and Magnetic Resonance Spectroscopy (MRS) rely on functional and metabolic changes, and have shown to be valuable for cancer imaging.

Principles of PET

PET is a popular modality in oncology. The technique is based upon the detection of photons released by annihilation of positrons emitted by radiopharmaceuticals. Positron emitting radionuclides are produced in a cyclotron by bombarding target material with accelerated protons. The positron emitting radionuclides can be used to synthesize radiopharmaceuticals that act as substrates for endogenous pathways. In the body, these radiopharmaceuticals emit positrons that undergo annihilation with nearby electrons, resulting in the release of 2 photons. These so-called annihilation photons (511 KeV) leave under a corner of 180 degrees, and are detected by coincidence imaging as they strike scintillation crystals. The resulting data can be reconstructed to reveal the distribution of radiotracer within the subject.

One of the major advantages of PET as an imaging modality is its versatility. Currently many different positron emitters with different characteristics (table

1) are available, making it possible to label a wide variety of radiopharmaceuticals (2). Availability of these novel radiopharmaceuticals enables visualization with high sensitivity of tumor metabolism, cellular proliferation, recognition of specific cell surface receptors, angiogenesis and tumor hypoxia.

Table 1: Characteristics of the most commonly used isotopes for PET imaging (2). The intrinsic spatial resolution loss is not described in literature for ^{11}C , ^{13}N and ^{15}O tracers.

Isotope	Half-life ($t_{1/2}$)	B^+ yield (%)	Mean β^+ energy (MeV)	Intrinsic spatial resolution loss (mm)
^{11}C	20.4 minutes	100	0.39	*
^{18}F	109.8 minutes	97	0.3	0.7
^{13}N	9.98 minutes	100	0.49	*
^{15}O	2.03 minutes	100	0.74	*
^{124}I	4.18 days	23	0.8	2.3
^{68}Ga	68.1 minutes	89	0.84	2.4
^{86}Y	14.7 hours	33	0.7	1.8

Abbreviations: PET, positron emission tomography;

Currently only two tracers have been approved by the FDA for applications in oncology (3). The most widely used PET tracer is ^{18}F -Fluorodeoxyglucose (^{18}F -FDG), a glucose analogue, which allows mapping of tumor glucose utilization. It is known that malignant tumors have an increased glucose metabolism (4). The value of FDG-PET for staging, re-staging and follow-up of various malignancies has been reviewed recently by Gambhir et al. (5), Rohren et al. (6), Juweid et al. (7) and others. ^{18}F -fluoride is indicated for PET imaging as a bone imaging agent to define areas of altered osteogenic activity. The value of ^{18}F -fluoride for bone imaging has been reviewed recently (8,9). All other tracers mentioned in this paper are used for research purposes.

Standardized uptake values (SUVs) provide a normalized quantitative measure of tissue FDG accumulation by normalizing the tissue radioactivity measured with PET to the injected dose and the bodyweight of the patient (10). SUVs provide highly reproducible parameters of tumor glucose utilization, allowing comparison between PET studies performed in different patients, or in the same patient at different time points (11,12). It must be noted that in order

to compare different scans, strict PET protocols have to be followed to minimize the variation between FDG-PET studies. When comparing scans it is very important that the time elapsed between injection of the FDG and the scan is constant. Dynamic scans can provide information about the tracer distribution over time. The first dynamic PET studies with FDG were performed already in the 1980s (13). Kissel et al. described a model to quantify the intracellular 5-Fluorouracil (5FU) concentration in liver metastases with dynamic PET in 1997 (14). Since then, many dynamic PET studies have been published with various tracers (15,16,17). The concept and applications of compartmental modeling and PET were reviewed recently (18).

Apart from these advantages, the technique also has its limitations. FDG is not entirely specific to malignant tissue. Some benign processes may also show enhanced glycolysis (19). This can lead to false positive FDG-PET results. Moreover, despite recent technical improvements, PET still is limited by a relatively low spatial resolution compared to anatomical imaging modalities like CT or MRI. Other disadvantages are the high costs and the need for a cyclotron in order to generate positron emitting radionuclides, as some PET radiotracers (i.e. ^{15}O , ^{13}N and ^{11}C tracers) have a short half-life, necessitating on site synthesis of the PET tracer.

Combining PET with CT

When examining the different but complementary advantages of both functional and anatomical imaging modalities, it is clear that combining these imaging modalities within one scanning gantry has great potential. In this regard, PET/CT has shown to be the most useful combination, although other combined modalities like SPECT/CT, MRS/MRI and recently PET/MRI have also shown promising results.

The PET/CT scanner is capable of acquiring accurately aligned anatomical and functional images of a patient from a single investigation (20). Temporal and spatial differences between PET and CT images are minimized as the patient remains positioned on the same bed for both imaging techniques. A combined PET/CT scan can utilize CT images for attenuation correction. Attenuation correction is generally applied to achieve count rate values independent of tissue electron density (21). Single PET machines use transmission scans for attenuation correction, which take longer (about 15 minutes) than correction

via CT scan (1 minute). The increased imaging speed is beneficial in more than one way, because it increases patient throughput (which is also beneficial for the patients because for many patients a one hour scan is too long), it leads to a more efficient use of FDG and other radiopharmaceuticals, and it reduces the imaging costs per patient (22). However, the PET examinations corrected for attenuation using CT images may be hampered by artifacts that are not seen in PET images corrected by use of transmission scans, like CT contrast agents and metal artifacts (23,24). Using segmented CT transmission maps can solve these problems. Segmentation is used to divide the CT image into regions representing different tissue types. Areas that appear denser than bone (higher CT value) are assigned to the soft tissue segment, thereby abolishing the overestimated FDG signal (25).

Since its commercial introduction about five years ago, the combined PET/CT scanner led to a dramatic change in cancer imaging, with the majority of PET systems now being sold as PET/CT machines across the world. Combined PET/CT has shown to be a powerful tool for staging of various malignancies (26,27), surgery and radiotherapy planning (28,29,30) and the assessment of response early in the course of treatment (31,32).

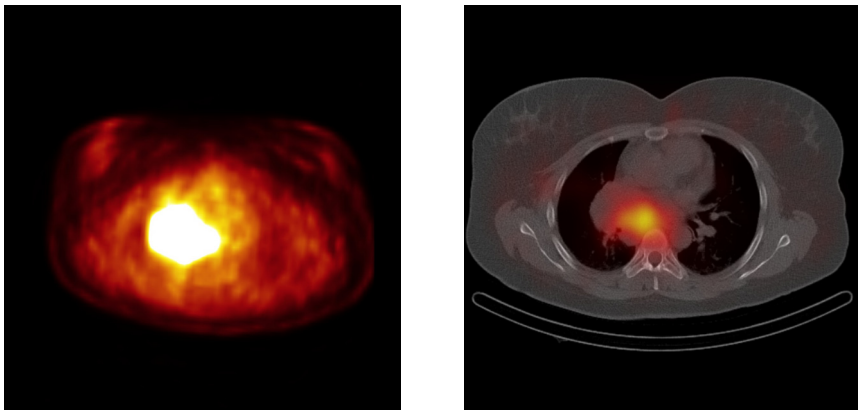


Figure 1: Combined imaging modality in a patient with a carcinoid tumor in the central area of the right lung. On the left: axial PET image showing intense tumor uptake of ^{18}F -FDG. In contrast, on the right, SPECT/CT shows uptake of ^{111}In -octreotide only in the mediastinal part of the tumor. The lack of tumor uptake of radiolabeled octreotide may be related to poor expression of membrane SSTRs whereas FDG accumulation is associated with overexpression of glucose transporters (GLUT 1 and 3) in the cell membrane. Most carcinoid tumors accumulate more octreotide than FDG due to its low growth rate and marked differentiation. However, there is variability and the individual tumor characterization may be helpful for the therapeutic choice. Abbreviations: PET, positron emission tomography; ^{18}F -FDG, ^{18}F -fluorodeoxyglucose; SPECT/CT, single photon emission computed tomography/computed tomography; SSTR, somatostatin receptor; GLUT, glucose transporter.

PET/CT in cancer drug development

The last decade, advances in tumor biology and chemistry have led to the discovery of numerous potential therapeutic cancer targets, and of lead compounds for therapeutic applications (33,34). Despite all these new targets, the number of annual new drug approvals has remained constant between 1990 and 2004, and the reason for this is likely multifactorial (35). One of the potential drawbacks in the development of new drugs are the increasing costs, which result from increasing preclinical evaluation and clinical trial expenditures (36). Earlier identification of drug failure in phase I or phase II trials could lead to a major decrease in development costs per drug (37). The combined PET/CT scanner could be a useful imaging modality in various phases of drug development. Small animal PET/CT can be used in preclinical studies, selecting drug candidates for clinical trials. PET/CT can be used to enrich the patient population of early clinical trials and for assessment of drug biodistribution by labeling the drug with a positron emitting radionuclide. Moreover, FDG-PET/CT has already shown to be a reliable predictor of treatment response. Other tracers for response evaluation are under investigation. Finally, PET/CT can be a useful tool to investigate the pharmacodynamics of novel anticancer agents.

Preclinical studies (small-animal PET/CT)

Prior to any clinical study *in vivo* preclinical studies are performed to demonstrate that the drug of interest reaches its target, has beneficial pharmacokinetics and shows a good safety profile. Drug activity in animal studies is commonly determined by measuring tumor size of tumors that have been implanted subcutaneously. External calipers are currently the standard for external repeated measurements of tumor size (38,39). However, the accuracy of these measurements have shown to be affected by subcutaneous fat layer thickness, as well as by hair and fur. In order to demonstrate metabolic responses in small animals, FDG-PET with specially designed high-resolution small-animal scanning equipment has been utilized (39,40). The spatial resolution of these PET scanners (approximately 1 mm) is superior compared to PET scanners used in the clinic (4 mm).

As with conventional PET imaging, FDG (41) and 3'-Deoxy-3'-¹⁸F-fluorothymidine (FLT) (42) are commonly used small-animal PET tracers for determining treatment response to novel anticancer agents in preclinical

mouse models. Other tracers are also used. One recent example is small-animal PET with the ^{18}F -3-hydroxymethylbutylguanine tracer, which can be used to visualize an anti-tumor immune response as a measure of immunotherapy activity (43). ^{124}I -Iodo-azomycin-galactoside is a promising tracer for imaging of hypoxia in mice with serial small-animal PET scanning (44). Another useful application of small-animal PET is the monitoring of gene expression by reporter gene systems. Target tissues expressing PET reporter genes, like herpes simplex virus type 1 thymidine kinase (45), can sequester systemically delivered PET reporter probes, enabling the monitoring of gene expression and distribution. The characteristics of the most frequently used PET reporter gene systems have been reviewed recently (46,47).

The lack of sufficient anatomical detail hampers the accuracy of single PET measurements. Combined PET/CT in animal studies was first reported using a clinical PET/CT scanner in rabbit and rat studies (48). More recently, a combined small-animal PET/CT scanner was brought into practice. The CT part of the scanner has shown to be superior in estimating tumor size when compared to the external caliper measurements (49), while FDG-PET can be used for assessing metabolic response. A disadvantage of using imaging modalities like PET/CT in preclinical studies is that it is more expensive than measurements of tumor size by external calipers.

Patient selection and response prediction

The vast majority of phase I clinical trials is performed on a broad population of patients with a wide variety of malignancies. This is due to the aim of these studies, which is not to evaluate response but rather to obtain toxicity and safety data. The introduction of many novel anticancer drug targets has for example lead to the opportunity of therapy individualization, with trastuzumab (50). Such an enrichment of patient populations in phase I studies would lead to higher response rates in these studies, and earlier identification of failing drug candidates. Functional imaging techniques like PET might aid in patient selection and prediction of response to novel anticancer agents. Examples of radiotracers used for patient selection and therapy individualization are tracers targeting various receptors involved in cell proliferation and differentiation, and tracers for imaging of multidrug resistance.

Currently, many novel PET tracers targeting cell surface receptors are being evaluated. The neuroendocrine PET tracers constitute an important class of

receptor targeted PET tracers. Neuroendocrine tumors (NETs) comprise a heterogeneous group of neoplasms originating from neural crest cells that are characterized by peptide receptors at the cell membrane and the presence of neuroamine uptake mechanisms. The role of PET and PET/CT in the imaging of NETs has been reviewed recently (51). An important PET tracer for the assessment of estrogen receptor (ER) status is 16α - ^{18}F -fluoro- 17β -estradiol (FES). Currently, the assessment ER status relies on biopsy specimens and in vitro studies. FES is a ligand for the estrogen receptor, and can be used to assess ER status in breast tumors in vivo. FES-PET has a sensitivity of 76% and specificity of 100% compared with the in vitro assay of ER status (52) and can be used to predict response to tamoxifen therapy (53). Fulvestrant is a pure ER antagonist recently approved for the treatment of hormone-sensitive breast cancer in post-menopausal women with disease progression following antiestrogen therapy. Three new 16α - ^{18}F -fluoro-fulvestrant derivatives were prepared with the aim to develop a tracer for positron emission tomography (PET) imaging capable of predicting the potential therapeutic efficacy of selective ER modulators (SERM). Unfortunately, the introduction of the 16 - ^{18}F -fluorine led to a dramatic decrease of the apparent binding affinity for ER, making these tracers unsuitable for response prediction to ER modulators (54). Other novel tracers targeting epidermal growth factor receptor (EGFR) (55), human epidermal growth factor receptor 2 (HER2) (56) and the integrin receptor $\alpha\text{v}\beta 3$ (57) are under investigation.

Overexpression of P-glycoprotein (P-gp) can result in a multidrug resistance (MDR) phenotype of cancer cells and tumors by reducing intracellular accumulation of various cytotoxic agents. The uptake of colchicine, an alkaloid that binds to tubulin, is significantly lower in resistant versus sensitive tumors (58). Colchicine has a clear intracellular target (tubulin), and is easy to label at a carbon atom, which makes it an attractive MDR tracer. ^{11}C -colchicine PET has shown to be useful for PET imaging of multidrug resistance in preclinical studies (59,60,61). PET with colchicine as a tracer can be used as a diagnostic tool to identify patients who will not respond to treatment with taxanes due to Pgp expression.

PET imaging with these kinds of tracers offers a noninvasive way of selecting patients for early clinical trials. The conventional way of patient selection for targeted therapies is by biopsy procedures, which is an invasive and logistically difficult procedure (62).

A major disadvantage of imaging with these kind of tracers is that receptor negative tumors can not be visualized. These tracers are often very specific for one receptor, and are not applicable for a wide range of malignancies.

Early response measurements in drug development

Treatment response measurements are essential in cancer therapy. It is essential to identify patients who do not respond to chemotherapy early in the course of treatment to avoid ineffective therapies and unnecessary side effects. At present, response to treatment is commonly determined by conventional imaging modalities like CT and/or MRI. Anatomical imaging modalities, including CT and MRI, assess tumor response by the size of the primary tumor and/or its metastases, which is followed over time by the clinician (63). This has its limitations, because it frequently takes several cycles of chemotherapy to demonstrate significant changes in tumor size (64,65). Furthermore, many new anticancer drugs that interfere with signal transduction pathways are cytostatic rather than cytotoxic, which activity often is associated with tumor stabilization as best treatment response. FDG-PET can measure response to treatment by assessing metabolic changes rather than changes in tumor size. Quantitative assessments of glucose uptake (SUV) before and during treatment can predict early response to treatment in a wide variety of malignancies (66,67). When compared to CT, FDG-PET was superior in predicting response to therapy early in the course of treatment in metastatic breast cancer (68), and in advanced soft tissue sarcoma (69). PET imaging employing ^{18}F -FDG is based on utilization of this substrate at sites of enhanced metabolism, i.e. tumor tissue. However, besides visualization of enhanced glucose metabolism of cancer cells, it is also possible to assess tumor response by PET by demonstrating changes in other metabolic processes of cancer cells, for instance increased amino acid metabolism. This can be determined by labeling amino acids with positron emitters, for which aim L-1- ^{11}C -tyrosine, ^{18}F -fluoro-L-proline and ^{11}C -methionine are promising tracers to determine early response. Another characteristic of cancer cells that is utilized in PET measurements is their increased proliferation potential. 3'-Deoxy-3'- ^{18}F -fluorothymidine and ^{11}C -thymidine are among the most promising PET tracers identifying cell proliferation. Application of all these relatively new tracers, reviewed recently (70,71,72), might contribute to earlier and more accurate response evaluations compared with standard CT-based response

measurements. The most striking examples of the use of PET in assessing early treatment response have been observed in studies with imatinib.

Example of assessing treatment response in drug development: imatinib

Imatinib is a receptor tyrosine-kinase inhibitor that is currently used for the treatment of chronic myelogenous leukemia (CML) and gastrointestinal stromal tumors (GIST). The development of imatinib has been reviewed extensively, since the drug is one of the first targeted anticancer drugs (73). Imatinib is a potent inhibitor of the fusion tyrosine kinase bcr-abl and of c-kit, a 145 kd transmembrane receptor tyrosine kinase that plays a role in the development of a variety of malignancies, including GIST (74). FDG-PET revealed early response to treatment with imatinib. A case report of a woman with a gastrointestinal tumor showed that the response to imatinib could be assessed by FDG-PET early after start of therapy (75). This report together with the study by van den Abbeele (76) hallmarked the use of FDG-PET for the assessment of treatment response to imatinib.

This study aimed to compare FDG-PET with anatomical CT imaging in patients with advanced GIST, who received oral daily imatinib. Twenty-three patients were imaged by CT as well as by FDG-PET at baseline, while 14 patients had subsequent FDG-PET and CT scans (1 to 3 imaging studies/patient) between 24 hours and 13 weeks after initiation of therapy. It appeared that the sites of abnormalities on FDG-PET images correlated with those seen on CT. Moreover, FDG-PET provided additional information about the extent of the disease, the metabolic activity within tumor metastases, and the response to therapy as early as 24 hours following initiation of therapy, which was far earlier compared to the measurable changes that could be observed by CT. Lack of metabolic response on FDG-PET was noted in only 1 out of 14 patients. This patient exhibited primary resistance to imatinib and tumor progression visualized by CT and conventional clinical methods (76). More recent studies confirmed the usefulness of PET in predicting early response to imatinib therapy (69,77). An example of a patient with a GIST who had an adequate metabolic response following imatinib therapy is shown in figure 2. An example of a partial metabolic response to sunitinib, a related small molecule tyrosine kinase inhibitor, is shown in figure 3.

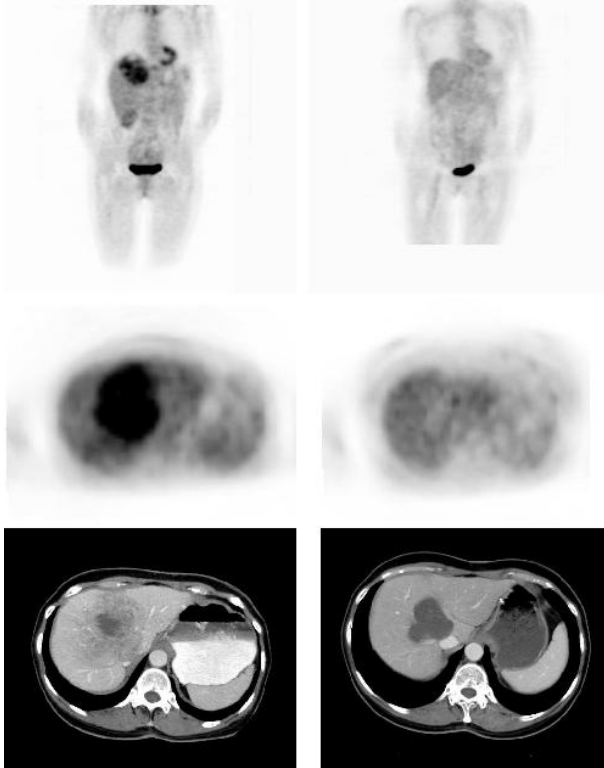


Figure 2: Left: FDG-PET scan (upper and middle figures) and CT scan (lower figure) of a patient with GIST with tumor metastases in the liver before start of imatinib therapy. This patient had a partial resection of the stomach due to a GIST. However, one year after the resection, large metastases were observed in the liver. Both the left and the right lobes of the liver show intense FDG uptake. Right: FDG-PET (upper and middle figures) and CT (lower figure) evaluation after 2 months of imatinib therapy. No pathological FDG uptake can be observed in the liver. Physiological FDG uptake can be seen in the heart, kidneys, bladder and the gut. By contrast residual tumor on CT remains considerable. Conclusion: An adequate metabolic response following imatinib treatment. Abbreviations: FDG-PET, fluorodeoxyglucose-positron emission tomography; CT, computed tomography; GIST, gastrointestinal stromal tumor.

Recently, it was shown that imatinib, via inhibition of c-kit, leads to down regulation of GLUT-1, the most prominent transporter of glucose into the cell. Moreover, imatinib inhibits the uptake of glucose into the cell by decreasing the number of a wide variety of other glucose transporters as well as their affinity for glucose (78).

These studies exemplify the importance of PET in the development of a new drug. Early response measurements are important for early screening of effective therapies. Besides for patient selection and response measurements,

PET is also used for the assessment of drug biodistribution and pharmacodynamic measurements in the course of drug development.

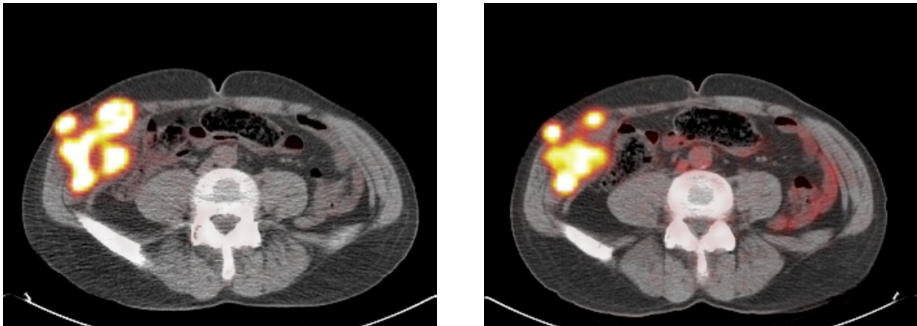


Figure 3: PET-CT fusion images of a 59 year old man with GIST recurrence in the right abdominal wall. The images show significant residual FDG tumor uptake after 2 months therapy with sunitinib. However, the SUV decreased from 13.5 (left image) to 6.4 (right image). Abbreviations: PET-CT, positron emission tomography-computed tomography; GIST, gastrointestinal stromal tumor; FDG, fluorodeoxyglucose; SUV, standardized uptake value.

Assessment of drug biodistribution

Assessment of the pharmacokinetics of novel drug candidates is one of the aims of early phase I clinical trials. Parameters including absorption, bioavailability, distribution and elimination as well as maximum plasma concentration (C_{max}) and area under the plasma-time curve (AUC) are major determinants of the toxicity profile and efficacy of any novel drug. The inter-patient variability in the pharmacokinetics of novel anticancer drugs in phase I studies is generally high. This is a limitation, because anticancer drugs often have a narrow therapeutic window and are dosed close to the maximum tolerable dose. The high inter-patient variability can be attributed to inter-individual differences in absorption, distribution metabolism and excretion of anticancer drugs (79). Recently, the influence of genetic factors on drug efficacy and toxicity was reviewed (80).

Non-steady state plasma pharmacokinetics often poorly reflect drug levels in normal or tumor tissue. Anti-cancer drug effects are mediated by interactions with targets such as receptor proteins and drug transporters. PET pharmacokinetic studies might aid in determining intratumoral drug exposure (81).

In one of the first PET studies with radiolabeled pharmaceuticals the pharmacokinetics of the opiates morphine and heroin were studied in rhesus monkeys (82). Since then it has been shown that PET analysis of radiolabeled anticancer drugs can reveal important information about the distribution of the drugs in patients. ^{18}F -fluorouracil is the most common anti-cancer drug studied with PET. This is due to the ease of ^{18}F -fluorouracil synthesis and the favorable half-life of fluorine (83). ^{18}F -fluorouracil PET studies can give important information about ^{18}F -fluorouracil biodistribution in tumor and normal tissue, as reviewed by Gupta et al. (84). A study with ^{18}F -paclitaxel (85) examined the effect of Pgp blockers on paclitaxel biodistribution, while the biodistribution, bioclearance and in vivo transformation of ^{13}N -cisplatin have also been studied with PET (86). Tumor uptake of ^{18}F -tamoxifen has been studied by PET. ^{18}F -tamoxifen uptakes in tumors with good responses were significantly higher than those with poor responses (87). Tumor uptake of ^{11}C -BCNU was compared between intra-venous and intra-arterial administration by means of PET measurements. It appeared that intra-arterial administration of ^{11}C -BCNU resulted in 50 times higher intratumoral concentrations (88).

To evaluate the distribution, pharmacokinetics and dosimetry of the somatostatin analog ^{90}Y -SMT487, a phase I study was performed with ^{86}Y -SMT487 (89). Another phase I study investigated both conventional pharmacokinetics and PET pharmacokinetics of XR5000, a topoisomerase I and II inhibitor formerly known as DACA. On the basis of conventional pharmacokinetics, a dose schedule was proposed at which potentially therapeutic plasma levels were attained. However, the PET data revealed low tumor exposure and no saturation of tumor exposure at the maximal tolerated dose (MTD) (90).

Fourteen patients scheduled for fluorouracil chemotherapy received a PET scan with ^{18}F -fluorouracil as a tracer prior to initiation of chemotherapy. Patients with a high uptake of the radiolabeled drug were more likely to achieve disease stabilization and a longer survival time, as shown in figure 4 (91). Unfortunately, we have not found a study correlating plasma pharmacokinetics with PET pharmacokinetics.

Main characteristics of the most commonly used PET radiotracers in pharmacokinetic studies are summarized in table 2.

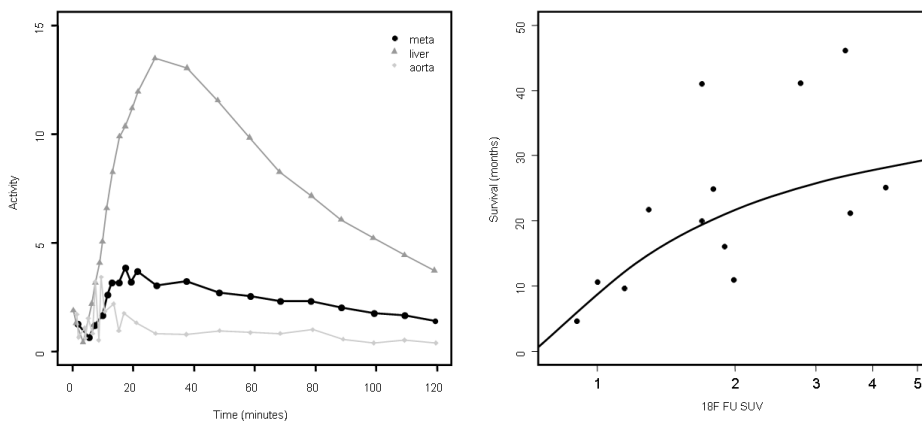


Figure 4: Left: Time-activity curve for ^{18}F -labeled fluorouracil position emission tomography in a liver metastasis, in normal liver tissue, and in normal aorta tissue. Right: Comparison of the ^{18}F -labeled fluorouracil uptake values of the liver metastasis measured with a single positron emission tomography scan 110-120 minutes post administration (SUV) and their survival time (mean overall survival) in 13 colorectal carcinoma patients with liver metastases after the onset of chemotherapy. A significant correlation coefficient of 0.65 was found between these parameters. Adapted from Moehler et al (91). Abbreviation: SUV, standardized uptake value.

Table 2: The most common radiotracers in pharmacokinetic PET studies with anticancer agents.

isotope	Labeled Drug	Information obtained
^{11}C	^{11}C -DACA, topoisomerase I/II inhibitor	Biodistribution and metabolism, potential toxicities (90,97)
	^{11}C -BCNU, alkylating agent specific for brain tissue	Biodistribution in tumor and normal tissue, comparison of administration routes (88)
^{13}N	^{13}N -Cisplatin alkylating agent	Biodistribution in tumor and normal tissue, clearance, comparison of administration routes (86)
^{18}F	^{18}F -FU, antimetabolite	Biodistribution in tumor and normal tissue, mechanism of action (84,91)
	^{18}F -Tamoxifen, estrogen receptor downregulator	Biodistribution in tumor and normal tissue, response predictions (87)
^{86}Y	^{86}Y -SMT487 somatostatin analog	Biodistribution, pharmacokinetics and dosimetry of ^{90}Y -SMT487 (89)

Abbreviation: PET, positron emission tomography

PET microdose studies

One of the major advantages of pharmacokinetic PET studies with radiolabeled drug candidates is that they can be performed at very low drug concentrations, thereby reducing or even preventing unwanted side effects. These studies, referred to as PET-microdosing studies, or phase 0 / prephase I clinical trials, can give important information about the distribution of a novel drug. However, they do not provide information about the safety and tolerability of the drug. Recently, the Committee for Human Medicinal Products (CHMP) of the European Agency for the Evaluation of Medicinal Products (EMA) proposed that a dose one-hundredth of the pharmacological dose derived of in vitro and animal models could be considered a human microdose (92). A summary of the requirements for microdose studies, as stated by the CPMP, has been given by Bergstrom et al. (93) and by the FDA in exploratory IND studies (94), and put into perspectives by Marchetti et al (95). Not many PET microdosing studies have been performed thus far, while its feasibility for studying PK in humans was demonstrated already early in the 1990s (96). An explanation for this might be the high costs of PET microdosing studies. One of the exceptions is a study with ^{11}C -DACA, an acridine carboxamide (97). This pre-phase I study, performed with a radiotracer dose equivalent to one-thousandth of the phase I starting dose, showed that valuable distribution data, including tumor concentration and early-time point PK data could be obtained using the PET technique. It should be confirmed whether the PK determined in microdosing studies is correlated with the PK determined at clinically relevant dose levels.

While PET is used as a single modality in microdosing studies, combined PET and microdialysis measurements can provide important pharmacokinetic data on intracellular drug concentrations (98). Microdialysis sampling is a minimally invasive sampling technique that can be utilized to assess unbound drug concentrations in extracellular spaces. The contribution of this technique in PK and PD studies has been reviewed recently (99). Combined PET and microdialysis measurements are not common at the moment, but might become a useful application in drug development, for which knowledge of intracellular concentrations is important (98).

Pharmacodynamics (PD)

Pharmacodynamic evaluations in drug development, are often made in phase II and III clinical studies, while phase I studies are mainly focused on dose finding, safety and tolerability of the involved new drug. Receptor binding assays for drugs that target defined receptors are a major component of these pharmacodynamic studies. Cancer is often characterized by overexpression or mutation of transmembrane molecules or specific receptors, and several new anti-cancer therapies target these specific receptors. This makes new, more specific endpoints necessary. Many studies have measured the effects of the investigational drug on surrogate tissues such as skin (100) or circulating lymphocytes (101). This approach has a number of limitations. First, this approach provides no information about the effects on the tumor tissue. Second, effects on the surrogate target correlate only partially, if at all, with response. Novel drug studies often include serial tumor biopsy sampling. This approach is not always feasible (62) and often logistically difficult. Studies in which biopsy sampling is incorporated often enroll insufficient numbers of patients to draw firm conclusions (102). In studies in which enough tumor tissue could be collected, demonstrable target inhibition did not result in tumor responses (100,103).

Imaging with PET offers a non-invasive way of assessing biological effects of novel anticancer agents. Besides tracers for imaging receptor binding, new tracers have been developed for imaging of apoptosis, antivascular activity and tissue perfusion, tumor hypoxia and choline accumulation.

FES is a tracer that can be used for the assessment of ER status and prediction of response to hormonal therapy in breast cancer patients, as mentioned in the above. However, the tracer also has value during the course of therapy. A decrease in the uptake of FES in breast cancers has been observed following treatment with tamoxifen (104). The reduction in FES uptake was found to be greater in responding patients compared with non-responding patients (105). These studies exemplify that FES-PET can be a useful tool for predicting response early in the course of hormonal treatment.

Apoptosis, or programmed cell death, is the likely mechanism behind the tumoricidal effects of both standard chemotherapeutic agents and many novel

Chapter 2.1

Isotope	Radiolabeled molecule	Rationale	Information obtained
¹¹ C	¹¹ C-Thymidine	Increased DNA proliferation of malignant cells	Early response to treatment (72)
	L-1- ¹¹ C-Tyrosine	Increased amino acid metabolism of malignant cells	Early response to treatment (70,71)
	¹¹ C-Methionine	Increased amino acid metabolism of malignant cells	Early response to treatment (70,71)
	¹¹ C-Methylcholine	Methylcholine uptake correlates with proliferation	Signal transduction (124)
	¹¹ C-Colchicine	Colchicine resistance correlates to paclitaxel resistance	Quantification of Pgp-mediated transport, multidrug resistance (59)
¹²⁴ I	¹²⁴ I-VG76e	Many tumors have overexpressed VEGF levels	Tumor VEGF levels (113)
	¹²⁴ I-Annexin V	Annexin V binds to the surface of apoptotic cells	Apoptosis (106,107)
	¹²⁴ I-Z(HER2:4)	HER2 is overexpressed in breast cancer	Predicting treatment response (56)
¹⁸ F	¹⁸ F-Fluorodeoxyglucose	Enhanced glucose uptake of malignant cells	Early response to treatment (65,66,67)
	16 α - ¹⁸ F-fluoro-17 β -oestradiol	Many breast tumors have ER overexpression	Receptor Binding, response to tamoxifen treatment (104,105)
	¹⁸ F-fluoro-L-proline	Increased amino acid metabolism of malignant cells	Early response to treatment (63,64)
	3'-Deoxy-3'- ¹⁸ F-Fluorothymidine	Increased DNA proliferation of malignant cells	Early response to treatment (70,71)
	¹⁸ F-Annexin	Annexin V binds to the surface of apoptotic cells	Apoptosis (108,109)
	¹⁸ F-fluoromisonidazole	Hypoxia predicts poor treatment response	Early response to treatment (118,119)
	¹⁸ F- fluoroazomycin arabinoside	Hypoxia predicts poor treatment response	Early response to treatment (122,123)
	¹⁸ F-fluoroerythronitroimidazole	Hypoxia predicts poor treatment response	Early response to treatment (121)
	¹⁸ F-galacto-RGD	Integrin receptor $\alpha v\beta 3$ is important for tumor growth	Predicting treatment response (57)
	¹⁸ F-ML04	EGFR is overexpressed in a wide range of malignancies	Predicting treatment response (55)
¹⁵ O	¹⁵ O-H ₂ O	Tissue perfusion is important for tumor growth and survival.	Early response to treatment (116,114,115)

Table 3 (previous page): The most common PET radiotracers for response prediction and pharmacodynamic assessments. Abbreviations: PET, positron emission tomography; DNA, deoxyribonucleic acid; EGFR, epidermal growth factor receptor; HER, human epidermal growth factor receptor 2; VEGF, vascular endothelial growth factor.

targeted anti-cancer drugs. An early event in apoptosis is the exposure of phosphatidylserines, which are normally confined internally within the cell.

Annexin V, an endogenous protein, has a high affinity for membrane bound phosphatidylserine, and is capable of detecting apoptosis in vivo.

PET studies in mice with ^{124}I labeled Annexin V showed high tracer uptake in fas-induced apoptotic tissue (106,107). ^{18}F -Annexin V uptake in non-pathological conditions appeared lower than the uptake of the SPECT tracer $^{99\text{m}}\text{Tc}$ labeled Annexin V, while the uptake of both tracers increased threefold in ischemic tissue (108). The uptake of ^{18}F -annexin V in organs of mice treated with cycloheximide correlated well with the results of terminal deoxynucleotide end-labeling (TUNEL) assays, which is an established method of measuring degrees of apoptosis (109). PET with annexin V as a tracer might be valuable for determining response to anti-cancer treatment in various malignancies, as has already been shown for SPECT/CT with $^{99\text{m}}\text{Tc}$ labeled Annexin V (110,111).

Angiogenesis is an essential process for tumors to grow beyond 2-3 cubic millimeters. The key mediator of angiogenesis is vascular endothelial growth factor (VEGF), which is therefore an appealing target for anticancer therapeutics (112).

VG76e is a monoclonal antibody that binds to human VEGF. The antibody can be labeled with ^{124}I , and used as a tracer for measuring tumor levels of VEGF, as shown in an animal PET study (113). Measuring VEGF levels by PET might be a useful method to characterize tumors and assess resistance mechanisms.

^{15}O -H₂O is another useful PET tracer that has been used extensively to measure tissue perfusion in response to antiangiogenic therapy (114,115). A recent study with ^{15}O -H₂O and labeled ^{18}F -5FU showed that treatment with nicotinamide, an amide of vitamin B₃, and carbogen, a vasoconstriction inhibitor, before administration of 5-FU, can lead to an increase in tumor perfusion. Pharmacokinetic measurements with ^{18}F -5FU PET showed a higher delivery of 5-FU to the tumor tissue. However, no differences were seen in ^{18}F -5FU tumor exposure (116).

Tumor hypoxia is associated with poor treatment outcome and survival (117). ^{18}F - labeled fluoromisonidazole (^{18}F -FMISO) is the most extensively studied PET tracer for imaging of tissue oxygenation (118). FMISO PET is a promising tool for predicting response to radiotherapy in patients with NSCLC or head and neck cancer (119). FMISO binds covalently to intracellular macromolecules upon reduction at low oxygen levels. In the presence of oxygen, the molecule is re-oxygenated to its less reactive parent compound, which is cleared from the tissue (120). However, clinical application of FMISO as a PET tracer is limited by its unfavorable biokinetics, including slow specific accumulation as well as slow clearance from normoxic tissues. Next generation PET tracers like ^{18}F -labeled fluoroazomycin arabinoside (^{18}F -FAZA) and ^{18}F -fluoroerythronitroimidazole (^{18}F -FETNIM) have been developed to achieve faster clearance by reducing lipophilicity (121,122). The feasibility of ^{18}F -FAZA for clinical PET imaging of tumor hypoxia was studied recently. ^{18}F -FAZA PET appeared feasible in head and neck cancer patients and image quality was adequate for clinical purposes (123).

Choline is a precursor of the membrane phospholipid phosphatidylcholine. The synthesis of phospholipids is tightly regulated by signal transduction cascades. The inhibition of these signal transduction pathways, can be investigated by PET with the radiolabeled choline tracer ^{11}C -methylcholine (124,125). Moreover, choline PET might be a valuable diagnostic tool to differentiate between low-grade and high-grade gliomas (126).

Conclusions and future directions

The opportunity of determining pharmacokinetic properties of novel anticancer agents, together with response evaluations early in the course of treatment clearly demonstrates the value of PET in the development of a new drug. Computed Tomography imaging procedures can not aid in measurement of pharmacokinetic characteristics of novel drugs. Furthermore, PET has superior sensitivity compared with CT to determine early response to treatment. These findings raise the question whether combined PET/CT can contribute in the development of new drugs. However, the CT part of the combined PET/CT gantry can aid in drug development. The weakness of PET imaging is its low spatial resolution, while CT is known for its superior spatial resolution. Therefore, combined PET/CT is able to generate metabolic images with improved anatomical detail. It is this combination that makes PET/CT more

accurate in determining early responses to chemotherapy when compared to either PET or CT alone. Another advantage of combining PET and CT in one modality is the faster scanning time compared to PET alone, which increases patient throughput, leads to a more efficient use of FDG and other radiopharmaceuticals, and reduces the imaging costs per patient. Despite these advantages, PET/CT is not the standard imaging modality in cancer drug development yet. At this moment PET/CT is mostly used for staging and re-staging of the disease.

Drug development is hampered by increasing costs, while the time from drug discovery to product marketing has increased over the years to more than 10 years nowadays. Less than ten percent of drugs tested in phase I studies eventually reach the market. These disappointing statistics clearly demonstrate that improvements have to be made in this field of research. Combined PET/CT might aid improving these statistics in the years to come. The combined PET/CT scanner could be useful in various preclinical and clinical phases of drug development. Earlier PD measurements in the development of novel anticancer agents might lead to earlier rejection of drug candidates, thereby increasing efficiency of drug development.

References

1. Jemal, A., Siegel, R., Ward, E. et al. Cancer statistics, 2007. *CA Cancer J.Clin.* 2007;57:43-66.
2. Pagani, M., Stone-Elander, S., and Larsson, S. A. Alternative positron emission tomography with non-conventional positron emitters: effects of their physical properties on image quality and potential clinical applications. *Eur.J.Nucl.Med.* 1997;24:1301-1327.
3. FDA guidance for industry: PET drug applications – content and format for NDAs and ANDAs. 2007;
4. Warburg, O. On the origin of cancer cells. *Science.* 1954;123:306-314.
5. Gambhir, S. S., Czernin, J., Schwimmer, J. et al. A tabulated summary of the FDG PET literature. *J.Nucl.Med.* 2001;42:1S-93S.
6. Rohren, E. M., Turkington, T. G., and Coleman, R. E. Clinical applications of PET in oncology. *Radiology.* 2004;231:305-332.
7. Juweid, M. E. and Cheson, B. D. Positron-emission tomography and assessment of cancer therapy. *N.Engl.J.Med.* 2006;354:496-507.
8. Brenner, W., Bohuslavizki, K. H., and Eary, J. F. PET imaging of osteosarcoma. *J.Nucl.Med.* 2003;44:930-942.
9. Even-Sapir, E. Imaging of malignant bone involvement by morphologic, scintigraphic, and hybrid modalities. *J.Nucl.Med.* 2005;46:1356-1367.
10. Zasadny, K. R. and Wahl, R. L. Standardized uptake values of normal tissues at PET with 2-[fluorine-18]-fluoro-2-deoxy-D-glucose: variations with body weight and a method for correction. *Radiology.* 1993;189:847-850.

11. Minn, H., Zasadny, K. R., Quint, L. E. et al. Lung cancer: reproducibility of quantitative measurements for evaluating 2-[F-18]-fluoro-2-deoxy-D-glucose uptake at PET. *Radiology*. 1995;196:167-173.
12. Weber, W. A., Ziegler, S. I., Thodtmann, R. et al. Reproducibility of metabolic measurements in malignant tumors using FDG PET. *J.Nucl.Med*. 1999;40:1771-1777.
13. Herholz, K., Ziffling, P., Staffen, W. et al. Uncoupling of hexose transport and phosphorylation in human gliomas demonstrated by PET. *Eur.J.Cancer Clin.Oncol*. 1988;24:1139-1150.
14. Kissel, J., Brix, G., Bellemann, M. E. et al. Pharmacokinetic analysis of 5-[18F]fluorouracil tissue concentrations measured with positron emission tomography in patients with liver metastases from colorectal adenocarcinoma. *Cancer Res*. 1997;57:3415-3423.
15. Zhang, X., Xiong, Z., Wu, Y. et al. Quantitative PET imaging of tumor integrin alphavbeta3 expression with 18F-FRGD2. *J.Nucl.Med*. 2006;47:113-121.
16. Schiepers, C., Chen, W., Cloughesy, T. et al. 18F-FDOPA kinetics in brain tumors. *J.Nucl.Med*. 2007;48:1651-1661.
17. Schiepers, C., Chen, W., Dahlbom, M. et al. 18F-fluorothymidine kinetics of malignant brain tumors. *Eur.J.Nucl.Med.Mol.Imaging*. 2007;34:1003-1011.
18. Watabe, H., Ikoma, Y., Kimura, Y. et al. PET kinetic analysis--compartmental model. *Ann.Nucl.Med*. 2006;20:583-588.
19. Cook, G. J., Wegner, E. A., and Fogelman, I. Pitfalls and artifacts in 18FDG PET and PET/CT oncologic imaging. *Semin.Nucl.Med*. 2004;34:122-133.
20. Beyer, T., Townsend, D. W., Brun, T. et al. A combined PET/CT scanner for clinical oncology. *J.Nucl.Med*. 2000;41:1369-1379.
21. von Schulthess, G. K. Integrated modality imaging with PET-CT and SPECT-CT: CT issues. *Eur.Radiol*. 2005;15 Suppl 4:D121-6.:D121-D126.
22. von Schulthess, G. K. Cost considerations regarding an integrated CT-PET system. *Eur.Radiol*. 2000;10 Suppl 3:S377-80.:S377-S380.
23. Dorio, P. J., Lee, F. T., Jr., Henseler, K. P. et al. Using a saline chaser to decrease contrast media in abdominal CT. *AJR Am.J.Roentgenol*. 2003;180:929-934.
24. Goerres, G. W., Ziegler, S. I., Burger, C. et al. Artifacts at PET and PET/CT caused by metallic hip prosthetic material. *Radiology*. 2003;226:577-584.
25. Mirzaei, S., Guerchraft, M., Bonnier, C. et al. Use of segmented CT transmission map to avoid metal artifacts in PET images by a PET-CT device. *BMC.Nucl.Med*. 2005;5:3-3.
26. Strunk, H., Bucerius, J., Jaeger, U. et al. PET-CT in der nachsorge des kolorektalen karzinoms: Einfluss der bildfusion auf die staginggenauigkeit. *Fortschr Röntgenstr*. 2005;177:1235-1241.
27. Antoch, G., Vogt, F. M., Freudenberg, L. S. et al. Whole-body dual-modality PET/CT and whole-body MRI for tumor staging in oncology. *JAMA*. 2003;290:3199-3206.
28. Brianzoni, E., Rossi, G., Ancidei, S. et al. Radiotherapy planning: PET/CT scanner performances in the definition of gross tumour volume and clinical target volume. *Eur.J.Nucl.Med.Mol.Imaging*. 2005;32:1392-1399.
29. Schwartz, D. L., Ford, E., Rajendran, J. et al. FDG-PET/CT imaging for preradiotherapy staging of head-and-neck squamous cell carcinoma. *Int.J.Radiat.Oncol.Biol.Phys*. 2005;61:129-136.
30. Deniaud-Alexandre, E., Touboul, E., Lerouge, D. et al. Impact of computed tomography and 18F-deoxyglucose coincidence detection emission tomography image fusion for optimization of conformal radiotherapy in non-small-cell lung cancer. *Int.J.Radiat.Oncol.Biol.Phys*. 2005;63:1432-1441.
31. Goshen, E., Davidson, T., Zwas, S. T. et al. PET/CT in the evaluation of response to treatment of liver metastases from colorectal cancer with bevacizumab and irinotecan. *Technol.Cancer Res.Treat*. 2006;5:37-43.
32. Steinert, H. C., Santos Dellea, M. M., Burger, C. et al. Therapy response evaluation in malignant pleural mesothelioma with integrated PET-CT imaging. *Lung Cancer*. 2005;49 Suppl 1:S33-5. Epub;2005 Apr 11.:S33-S35.
33. Knowles, J. and Gromo, G. A guide to drug discovery: Target selection in drug discovery. *Nat.Rev.Drug Discov*. 2003;2:63-69.
34. Lesko, L. J., Rowland, M., Peck, C. C. et al. Optimizing the science of drug development: opportunities for better candidate selection and accelerated evaluation in humans. *Pharm.Res*. 2000;17:1335-1344.
35. Glassman, R. H. and Sun, A. Y. Biotechnology: identifying advances from the hype. *Nat.Rev.Drug Discov*. 2004;3:177-183.

36. DiMasi, J. A., Hansen, R. W., and Grabowski, H. G. The price of innovation: new estimates of drug development costs. *J.Health Econ.* 2003;22:151-185.
37. DiMasi, J. A. The value of improving the productivity of the drug development process: faster times and better decisions. *Pharmacoeconomics.* 2002;20 Suppl 3:1-10.:1-10.
38. Fiennes, A. G. Growth rate of human tumour xenografts measured in nude mice by in vivo cast modelling. *Br.J.Surg.* 1988;75:23-24.
39. Myers, R. The biological application of small animal PET imaging. *Nucl.Med.Biol.* 2001;28:585-593.
40. Chatziioannou, A. F. Molecular imaging of small animals with dedicated PET tomographs. *Eur.J.Nucl.Med.Mol.Imaging.* 2002;29:98-114.
41. Zhang, Y., Saylor, M., Wen, S.et al. Longitudinally quantitative 2-deoxy-2-[18F]fluoro-D-glucose micro positron emission tomography imaging for efficacy of new anticancer drugs: a case study with bortezomib in prostate cancer murine model. *Mol.Imaging Biol.* 2006;8:300-308.
42. Oyama, N., Ponde, D. E., Dence, C.et al. Monitoring of therapy in androgen-dependent prostate tumor model by measuring tumor proliferation. *J.Nucl.Med.* 2004;45:519-525.
43. Shu, C. J., Guo, S., Kim, Y. J.et al. Visualization of a primary anti-tumor immune response by positron emission tomography. *Proc.Natl.Acad.Sci.U.S.A.* 2005;102:17412-17417.
44. Zanzonico, P., O'Donoghue, J., Chapman, J. D.et al. Iodine-124-labeled iodoazomycin-galactoside imaging of tumor hypoxia in mice with serial microPET scanning. *Eur.J.Nucl.Med.Mol.Imaging.* 2004;31:117-128.
45. Tjuvajev, J. G., Chen, S. H., Joshi, A.et al. Imaging adenoviral-mediated herpes virus thymidine kinase gene transfer and expression in vivo. *Cancer Res.* 1999;59:5186-5193.
46. Gambhir, S. S. Molecular imaging of cancer with positron emission tomography. *Nat.Rev.Cancer.* 2002;2:683-693.
47. Herschman, H. R. PET reporter genes for noninvasive imaging of gene therapy, cell tracking and transgenic analysis. *Crit Rev.Oncol.Hematol.* 2004;51:191-204.
48. Tatsumi, M., Nakamoto, Y., Traughber, B.et al. Initial experience in small animal tumor imaging with a clinical positron emission tomography/computed tomography scanner using 2-[F-18]fluoro-2-deoxy-D-glucose. *Cancer Res.* 2003;63:6252-6257.
49. Ishimori, T., Tatsumi, M., and Wahl, R. L. Tumor response assessment is more robust with sequential CT scanning than external caliper measurements. *Acad.Radiol.* 2005;12:776-781.
50. Gonzalez-Angulo, A. M., Hortobagyi, G. N., and Esteva, F. J. Adjuvant therapy with trastuzumab for HER-2/neu-positive breast cancer. *Oncologist.* 2006;11:857-867.
51. Mottaghy, F. M. and Reske, S. N. Functional imaging of neuroendocrine tumours with PET. *Pituitary.* 2006;9:237-242.
52. Mortimer, J. E., Dehdashti, F., Siegel, B. A.et al. Positron emission tomography with 2-[18F]Fluoro-2-deoxy-D-glucose and 16alpha-[18F]fluoro-17beta-estradiol in breast cancer: correlation with estrogen receptor status and response to systemic therapy. *Clin.Cancer Res.* 1996;2:933-939.
53. Linden, H. M., Stekhova, S. A., Link, J. M.et al. Quantitative fluoroestradiol positron emission tomography imaging predicts response to endocrine treatment in breast cancer. *J.Clin.Oncol.* 2006;24:2793-2799.
54. Seimbille, Y., Benard, F., Rousseau, J.et al. Impact on estrogen receptor binding and target tissue uptake of [18F]fluorine substitution at the 16alpha-position of fulvestrant (faslodex; ICI 182,780). *Nucl.Med.Biol.* 2004;31:691-698.
55. Abourbeh, G., Dissoki, S., Jacobson, O.et al. Evaluation of radiolabeled ML04, a putative irreversible inhibitor of epidermal growth factor receptor, as a bioprobe for PET imaging of EGFR-overexpressing tumors. *Nucl.Med.Biol.* 2007;34:55-70.
56. Steffen, A. C., Wikman, M., Tolmachev, V.et al. In vitro characterization of a bivalent anti-HER-2 affibody with potential for radionuclide-based diagnostics. *Cancer Biother.Radiopharm.* 2005;20:239-248.
57. Beer, A. J., Haubner, R., Wolf, I.et al. PET-based human dosimetry of 18F-galactoglycosylated radiotracer for imaging alpha v beta3 expression. *J.Nucl.Med.* 2006;47:763-769.
58. Mehta, B. M., Levchenko, A., Rosa, E.et al. Evaluation of carbon-14-colchicine biodistribution with whole-body quantitative autoradiography in colchicine-sensitive and -resistant xenografts. *J.Nucl.Med.* 1996;37:312-314.

59. Levchenko, A., Mehta, B. M., Lee, J. B. et al. Evaluation of ¹¹C-colchicine for PET imaging of multiple drug resistance. *J.Nucl.Med.* 2000;41:493-501.
60. Hendrikse, N. H. and Vaalburg, W. Imaging of P glycoprotein function in vivo with PET. *Novartis Found Symp.* 2002;243:137-145.
61. Elsinga, P. H., Hendrikse, N. H., Bart, J. et al. PET Studies on P-glycoprotein function in the blood-brain barrier: how it affects uptake and binding of drugs within the CNS. *Curr.Pharm.Des.* 2004;10:1493-1503.
62. Helft, P. R. and Daugherty, C. K. Are we taking without giving in return? The ethics of research-related biopsies and the benefits of clinical trial participation. *J.Clin.Oncol.* 2006;24:4793-4795.
63. Therasse, P., Arbuck, S. G., Eisenhauer, E. A. et al. New guidelines to evaluate the response to treatment in solid tumors. European Organization for Research and Treatment of Cancer, National Cancer Institute of the United States, National Cancer Institute of Canada. *J.Natl.Cancer Inst.* 2000;92:205-216.
64. Spaepen, K., Stroobants, S., Dupont, P. et al. Early restaging positron emission tomography with (¹⁸F)-fluorodeoxyglucose predicts outcome in patients with aggressive non-Hodgkin's lymphoma. *Ann.Oncol.* 2002;13:1356-1363.
65. Weber, W. A., Petersen, V., Schmidt, B. et al. Positron emission tomography in non-small-cell lung cancer: prediction of response to chemotherapy by quantitative assessment of glucose use. *J.Clin.Oncol.* 2003;21:2651-2657.
66. Kelloff, G. J., Hoffman, J. M., Johnson, B. et al. Progress and promise of FDG-PET imaging for cancer patient management and oncologic drug development. *Clin.Cancer Res.* 2005;11:2785-2808.
67. Weber, W. A. Use of PET for monitoring cancer therapy and for predicting outcome. *J.Nucl.Med.* 2005;46:983-995.
68. Dose, Schwarz J., Bader, M., Jenicke, L. et al. Early prediction of response to chemotherapy in metastatic breast cancer using sequential ¹⁸F-FDG PET. *J.Nucl.Med.* 2005;46:1144-1150.
69. Stroobants, S., Goeminne, J., Seegers, M. et al. ¹⁸FDG-Positron emission tomography for the early prediction of response in advanced soft tissue sarcoma treated with imatinib mesylate (Glivec). *Eur.J.Cancer.* 2003;39:2012-2020.
70. Chen, D. L. and Dehdashti, F. Advances in positron emission tomographic imaging of lung cancer. *Proc.Am.Thorac.Soc.* 2005;2:541-4, 512.
71. Wang, J. and Maurer, L. Positron Emission Tomography: applications in drug discovery and drug development. *Curr.Top.Med.Chem.* 2005;5:1053-1075.
72. Wells, P., West, C., Jones, T. et al. Measuring tumor pharmacodynamic response using PET proliferation probes: the case for 2-[(¹¹C)-thymidine. *Biochim.Biophys.Acta.* 2004;1705:91-102.
73. Capdeville, R., Buchdunger, E., Zimmermann, J. et al. Glivec (STI571, imatinib), a rationally developed, targeted anticancer drug. *Nat.Rev.Drug Discov.* 2002;1:493-502.
74. Heinrich, M. C., Griffith, D. J., Druker, B. J. et al. Inhibition of c-kit receptor tyrosine kinase activity by STI 571, a selective tyrosine kinase inhibitor. *Blood.* 2000;96:925-932.
75. Joensuu, H., Roberts, P. J., Sarlomo-Rikala, M. et al. Effect of the tyrosine kinase inhibitor STI571 in a patient with a metastatic gastrointestinal stromal tumor. *N.Engl.J.Med.* 2001;344:1052-1056.
76. Van den Abbeele, for the GIST Collaborative PET Study Group. ¹⁸F-FDG-PET Provides Early Evidence of Biological Response to STI571 in Patients with Malignant Gastrointestinal Stromal Tumors (GIST). Presented at ASCO 2001, Sarcoma abstract 1444. 2007;
77. Gayed, I., Vu, T., Iyer, R. et al. The role of ¹⁸F-FDG PET in staging and early prediction of response to therapy of recurrent gastrointestinal stromal tumors. *J.Nucl.Med.* 2004;45:17-21.
78. Cullinane, C., Dorow, D. S., Kansara, M. et al. An in vivo tumor model exploiting metabolic response as a biomarker for targeted drug development. *Cancer Res.* 2005;65:9633-9636.
79. Undevia, S. D., Gomez-Abu, G., and Ratain, M. J. Pharmacokinetic variability of anticancer agents. *Nat.Rev.Cancer.* 2005;5:447-458.
80. Bosch, T. M., Meijerman, I., Beijnen, J. H. et al. Genetic polymorphisms of drug-metabolising enzymes and drug transporters in the chemotherapeutic treatment of cancer. *Clin.Pharmacokinet.* 2006;45:253-285.

81. Brunner, M. and Langer, O. Microdialysis versus other techniques for the clinical assessment of in vivo tissue drug distribution. *AAPS.J.* 2006;8:E263-E271.
82. Hartvig, P., Bergstrom, K., Lindberg, B. et al. Kinetics of ¹¹C-labeled opiates in the brain of rhesus monkeys. *J.Pharmacol.Exp.Ther.* 1984;230:250-255.
83. Harte, R. J., Matthews, J. C., O'Reilly, S. M. et al. Sources of error in tissue and tumor measurements of 5-[¹⁸F]fluorouracil. *J.Nucl.Med.* 1998;39:1370-1376.
84. Gupta, N., Price, P. M., and Aboagye, E. O. PET for in vivo pharmacokinetic and pharmacodynamic measurements. *Eur.J.Cancer.* 2002;38:2094-2107.
85. Kurdziel, K. A., Kieseewetter, D. O., Carson, R. E. et al. Biodistribution, radiation dose estimates, and in vivo Pgp modulation studies of 18F-paclitaxel in nonhuman primates. *J.Nucl.Med.* 2003;44:1330-1339.
86. Ginos, J. Z., Cooper, A. J., Dhawan, V. et al. [¹³N]cisplatin PET to assess pharmacokinetics of intra-arterial versus intravenous chemotherapy for malignant brain tumors. *J.Nucl.Med.* 1987;28:1844-1852.
87. Inoue, T., Kim, E. E., Wallace, S. et al. Positron emission tomography using [¹⁸F]fluorotamoxifen to evaluate therapeutic responses in patients with breast cancer: preliminary study. *Cancer Biother.Radiopharm.* 1996;11:235-245.
88. Tyler, J. L., Yamamoto, Y. L., Diksic, M. et al. Pharmacokinetics of superselective intra-arterial and intravenous [¹¹C]BCNU evaluated by PET. *J.Nucl.Med.* 1986;27:775-780.
89. Jamar, F., Barone, R., Mathieu, I. et al. ⁸⁶Y-DOTA0)-D-Phe1-Tyr3-octreotide (SMT487)--a phase 1 clinical study: pharmacokinetics, biodistribution and renal protective effect of different regimens of amino acid co-infusion. *Eur.J.Nucl.Med.Mol.Imaging.* 2003;30:510-518.
90. Propper, D. J., de Bono, J., Saleem, A. et al. Use of positron emission tomography in pharmacokinetic studies to investigate therapeutic advantage in a phase I study of 120-hour intravenous infusion XR5000. *J.Clin.Oncol.* 2003;21:203-210.
91. Moehler, M., Dimitrakopoulou-Strauss, A., Gutzler, F. et al. ¹⁸F-labeled fluorouracil positron emission tomography and the prognoses of colorectal carcinoma patients with metastases to the liver treated with 5-fluorouracil. *Cancer.* 1998;83:245-253.
92. The European Agency for the Evaluation of Medicinal Products. Evaluation of Medicines for Human Use. Position paper on non-clinical safety studies to support clinical trials with a single microdose. 2003;
93. Bergstrom, M., Grahnen, A., and Langstrom, B. Positron emission tomography microdosing: a new concept with application in tracer and early clinical drug development. *Eur.J.Clin.Pharmacol.* 2003;59:357-366.
94. Guidance for Industry, Investigators, and Reviewers Exploratory IND Studies, Center for Drug Evaluation and Research (CDER); Food and Drug Administration, U.S. Department of Health and Human Services. 2007;
95. Marchetti, S. and Schellens, J. H. The impact of FDA and EMEA guidelines on drug development in relation to Phase 0 trials. *Br.J.Cancer.* 2007;97:577-581.
96. Cunningham, V. J., Pike, V. W., Bailey, D. et al. A method of studying pharmacokinetics in man at picomolar drug concentrations. *Br.J.Clin.Pharmacol.* 1991;32:167-172.
97. Saleem, A., Harte, R. J., Matthews, J. C. et al. Pharmacokinetic evaluation of N-[2-(dimethylamino)ethyl]acridine-4-carboxamide in patients by positron emission tomography. *J.Clin.Oncol.* 2001;19:1421-1429.
98. Langer, O., Karch, R., Muller, U. et al. Combined PET and microdialysis for in vivo assessment of intracellular drug pharmacokinetics in humans. *J.Nucl.Med.* 2005;46:1835-1841.
99. Zhou, Q. and Gallo, J. M. In vivo microdialysis for PK and PD studies of anticancer drugs. *AAPS.J.* 2005;7:E659-E667.
100. Baselga, J., Albanell, J., Ruiz, A. et al. Phase II and tumor pharmacodynamic study of gefitinib in patients with advanced breast cancer. *J.Clin.Oncol.* 2005;23:5323-5333.
101. Thavasu, P., Propper, D., McDonald, A. et al. The protein kinase C inhibitor CGP41251 suppresses cytokine release and extracellular signal-regulated kinase 2 expression in cancer patients. *Cancer Res.* 1999;59:3980-3984.
102. Shin, D. M., Donato, N. J., Perez-Soler, R. et al. Epidermal growth factor receptor-targeted therapy with C225 and cisplatin in patients with head and neck cancer. *Clin.Cancer Res.* 2001;7:1204-1213.

103. Rojo, F., Tabernero, J., Albanell, J. et al. Pharmacodynamic studies of gefitinib in tumor biopsy specimens from patients with advanced gastric carcinoma. *J.Clin.Oncol.* 2006;24:4309-4316.
104. McGuire, A. H., Dehdashti, F., Siegel, B. A. et al. Positron tomographic assessment of 16 alpha-[18F] fluoro-17 beta-estradiol uptake in metastatic breast carcinoma. *J.Nucl.Med.* 1991;32:1526-1531.
105. Dehdashti, F., Flanagan, F. L., Mortimer, J. E. et al. Positron emission tomographic assessment of "metabolic flare" to predict response of metastatic breast cancer to antiestrogen therapy. *Eur.J.Nucl.Med.* 1999;26:51-56.
106. Keen, H. G., Dekker, B. A., Disley, L. et al. Imaging apoptosis in vivo using 124I-annexin V and PET. *Nucl.Med.Biol.* 2005;32:395-402.
107. Dekker, B., Keen, H., Lyons, S. et al. MBP-annexin V radiolabeled directly with iodine-124 can be used to image apoptosis in vivo using PET. *Nucl.Med.Biol.* 2005;32:241-252.
108. Murakami, Y., Takamatsu, H., Taki, J. et al. 18F-labelled annexin V: a PET tracer for apoptosis imaging. *Eur.J.Nucl.Med.Mol.Imaging.* 2004;31:469-474.
109. Yagle, K. J., Eary, J. F., Tait, J. F. et al. Evaluation of 18F-annexin V as a PET imaging agent in an animal model of apoptosis. *J.Nucl.Med.* 2005;46:658-666.
110. Kartachova, M., Haas, R. L., Olmos, R. A. et al. In vivo imaging of apoptosis by 99mTc-Annexin V scintigraphy: visual analysis in relation to treatment response. *Radiother.Oncol.* 2004;72:333-339.
111. Kartachova, M. S., Valdes Olmos, R. A., Haas, R. L. et al. Mapping of treatment-induced apoptosis in normal structures: 99mTc-Hynic-rh-annexin V SPECT and CT image fusion. *Eur.J.Nucl.Med.Mol.Imaging.* 2006;33:893-899.
112. Ferrara, N. VEGF as a therapeutic target in cancer. *Oncology.* 2005;69 Suppl 3:11-6. Epub;2005 Nov 21.:11-16.
113. Collingridge, D. R., Carroll, V. A., Glaser, M. et al. The development of [(124)I]iodinated-VG76e: a novel tracer for imaging vascular endothelial growth factor in vivo using positron emission tomography. *Cancer Res.* 2002;62:5912-5919.
114. Herbst, R. S., Mullani, N. A., Davis, D. W. et al. Development of biologic markers of response and assessment of antiangiogenic activity in a clinical trial of human recombinant endostatin. *J.Clin.Oncol.* 2002;20:3804-3814.
115. Anderson, H. L., Yap, J. T., Miller, M. P. et al. Assessment of pharmacodynamic vascular response in a phase I trial of combretastatin A4 phosphate. *J.Clin.Oncol.* 2003;21:2823-2830.
116. Gupta, N., Saleem, A., Kotz, B. et al. Carbogen and nicotinamide increase blood flow and 5-fluorouracil delivery but not 5-fluorouracil retention in colorectal cancer metastases in patients. *Clin.Cancer Res.* 2006;12:3115-3123.
117. Nordsmark, M. and Overgaard, J. A confirmatory prognostic study on oxygenation status and loco-regional control in advanced head and neck squamous cell carcinoma treated by radiation therapy. *Radiother.Oncol.* 2000;57:39-43.
118. Padhani, A. R. Where are we with imaging oxygenation in human tumours? *Cancer Imaging.* 2005;5:128-30.:128-130.
119. Eschmann, S. M., Paulsen, F., Reimold, M. et al. Prognostic impact of hypoxia imaging with 18F-misonidazole PET in non-small cell lung cancer and head and neck cancer before radiotherapy. *J.Nucl.Med.* 2005;46:253-260.
120. Thorwarth, D., Eschmann, S. M., Paulsen, F. et al. A kinetic model for dynamic [18F]-Fmiso PET data to analyse tumour hypoxia. *Phys.Med.Biol.* 2005;50:2209-2224.
121. Lehtio, K., Oikonen, V., Gronroos, T. et al. Imaging of blood flow and hypoxia in head and neck cancer: initial evaluation with [(15)O]H(2)O and [(18)F]fluoroerythronitroimidazole PET. *J.Nucl.Med.* 2001;42:1643-1652.
122. Sorger, D., Patt, M., Kumar, P. et al. [18F]Fluoroazomycinarabinofuranoside (18FAZA) and [18F]Fluoromisonidazole (18FMISO): a comparative study of their selective uptake in hypoxic cells and PET imaging in experimental rat tumors. *Nucl.Med.Biol.* 2003;30:317-326.
123. Souvatzoglou, M., Grosu, A. L., Roper, B. et al. Tumour hypoxia imaging with [(18)F]FAZA PET in head and neck cancer patients: a pilot study. *Eur.J.Nucl.Med.Mol.Imaging.* 2007;20:.
124. Roivainen, A., Forsback, S., Gronroos, T. et al. Blood metabolism of [methyl-11C]choline; implications for in vivo imaging with positron emission tomography. *Eur.J.Nucl.Med.* 2000;27:25-32.

125. Liu, D., Hutchinson, O. C., Osman, S. et al. Use of radiolabelled choline as a pharmacodynamic marker for the signal transduction inhibitor geldanamycin. *Br.J.Cancer.* 2002;87:783-789.
126. Ohtani, T., Kurihara, H., Ishiuchi, S. et al. Brain tumour imaging with carbon-11 choline: comparison with FDG PET and gadolinium-enhanced MR imaging. *Eur.J.Nucl.Med.* 2001;28:1664-1670.

CHAPTER 2.2

In Reply

David S. Boss, Renato Valdes Olmos, Michiel Sinaasappel, Jos H.
Beijnen, Jan H. M. Schellens

Oncologist. 2008 Jun;13(6):736-37

In response to:
Oncologist. 2008 Jun;13(6):734-35

We read with interest the letter entitled ^{18}F -Fluorodeoxyglucose Positron Emission Tomography for Monitoring Response to Sorafenib Treatment in Patients with Hepatocellular Carcinoma by Siemerink et al.

Because of a lack of tumor uptake, there is as yet no defined role for ^{18}F -FDG-PET in the staging of HCC, but ^{18}F -FDG-PET might be valuable for the assessment of therapy response in patients with demonstrated tumor uptake at baseline. This is stated in the review by Hain and Fogelman (1). However, we have found no prospective study in which ^{18}F -FDG-PET scans were made at baseline and early in the course of therapy in patients with HCC. The studies that Hain and Fogelman (1) refer to in their review include one retrospective study (2) and one study in which baseline ^{18}F -FDG uptake levels were correlated with clinical outcome (3). In other words, at this moment there is no evidence that ^{18}F -FDG-PET is valuable for early response measurements in patients with HCC. Perhaps this makes the findings of Siemerink et al. even more interesting.

Sorafenib is, in our opinion, an attractive drug for evaluation of its antitumor activity by ^{18}F -FDG-PET. It is a multikinase inhibitor, with platelet-derived growth factor receptor, vascular endothelial growth factor receptor, Raf kinase, and c-Kit as predominant targets. The latter is of importance when considering ^{18}F -FDG-PET response measurements. It has been shown that c-Kit inhibition leads to a downregulation of Glut-1, the most important transporter of glucose into the cell (4). Consequently, treatment with sorafenib, as with imatinib, might lead to reduced ^{18}F -FDG uptake.

In the letter by Siemerink et al., ^{18}F -FDG-PET scans were made at baseline and after 3 weeks of treatment. After treatment with imatinib, ^{18}F -FDG-PET responses can already be observed after 1 week of therapy, or even earlier (5). Perhaps responses to sorafenib can also be seen after 1 week of therapy. In our opinion, it would be valuable to study ^{18}F -FDG-PET uptake even earlier in the course of treatment, for example, after 1 week of drug treatment.

In conclusion, the use of ^{18}F -FDG-PET for assessment of response to sorafenib therapy might be valuable, as stated by Siemerink et al. We share their opinion that these results should be confirmed in a larger population. We

suggest measuring the response to sorafenib treatment even earlier in the course of therapy.

References

1. Hain SF, Fogelman I. Recent Advances in Imaging Hepatocellular Carcinoma: Diagnosis, Staging and Response Assessment: Functional Imaging. *Cancer Journal* 2004;10:121-27
2. Wudel LJ Jr, Delbeke D, Morris D et al. The role of [18F]fluorodeoxyglucose positron emission tomography imaging in the evaluation of hepatocellular carcinoma. *Am Surg* 2003;69:117-24
3. Shiomi S, Nishiguchi S, Ishizu H et al. Usefulness of positron emission tomography with fluorine-18-fluorodeoxyglucose for predicting outcome in patients with hepatocellular carcinoma. *Am J Gastroenterol* 2001;96:1877-80
4. Culinane C, Dorow DS, Kansara M et al. An in vivo tumor model exploiting metabolic response as a biomarker for targeted drug development. *Cancer Res.* 2005 ;65:9633-6.
5. Van den Abbeele, for the GIST Collaborative PET study group. F18-FDG PET provides early evidence of biological response to STI571 in patients with malignant gastrointestinal stromal tumors (GIST). Presented at the 2001 American Society of Clinical Oncology Annual Meeting, San Francisco, May 12-15, 2001.

3

Aurora kinase inhibitors

CHAPTER 3.1

**Clinical experience with aurora kinase
inhibitors: A review**

David S. Boss, Jos H. Beijnen, Jan H. M. Schellens

Oncologist. 2009;14(8):780-93

Abstract

The aurora kinase family of serine/threonine kinases comprises three members, designated aurora A, B and C. Aurora A and B are essential components of the mitotic pathway, ensuring proper chromosome assembly, formation of the mitotic spindle and cytokinesis. The role of Aurora C is less well clear. Overexpression of aurora A and B has been observed in several tumor types, and has been linked with a poor prognosis of cancer patients. Several small molecules targeting aurora kinase A, B or both have been evaluated preclinically and in early phase I trials. In this review we aim to summarize the most recent advances in the development of aurora kinase inhibitors, with a focus on the clinical data.

Introduction

Mitosis, the process by which an eukaryotic cell separates a complete copy of its duplicated genome into two identical sets in two daughter cells, is an extremely complex and tightly regulated process (1). Central players in the mitotic process are the microtubules forming the mitotic spindle as well as the centrosome, an organelle that has an important role in regulating tubulin dynamics (2). Defects in mitotic signaling pathways, including those involving tubulin dynamics, might lead to unrestrained growth, one of the hallmarks of cancer cells. The effectiveness of the taxanes and vinca-alkaloids in the treatment of many tumor types indicates the significance of the mitotic/tubulin machinery as a validated drug target (3,4). Recently, other mitosis regulating molecules have been proposed as targets for anticancer drug development, including cyclin-dependent kinases (5), survivin (6), polo-like kinases (7), and the aurora kinases that will be discussed in this review. Members of the aurora kinase family have emerged as key regulators of the mitotic process. Furthermore, they are frequently overexpressed in various human malignancies, and overexpression in cancer patients correlates with a poor prognosis, exemplifying their significance for tumor formation and progression. These factors clearly demonstrate the feasibility of the aurora kinases as promising drug targets, which is underlined by the possibility to inhibit the auroras with small molecules. Several small molecules targeting one or more of the aurora family members have emerged, and are currently being tested in clinical studies.

The aurora family

The aurora family of serine/threonine kinases contains three members in mammalian cells, designated aurora A, B and C, which share the highest degree of sequence homology in their catalytic domains (8).

However, their expression pattern and cellular localization differ markedly. Aurora A and B are expressed in many different cell types, while the expression of aurora C seems to be restricted to testicular tissue (9). Activation of the aurora kinases is dependent on co-factors, and many

different co-factors are involved in the activation of aurora A, B and C, respectively, although the precise mechanisms of aurora activation remain to be elucidated. The roles of aurora kinases A, B and, to a much lesser extent, aurora kinase C, in mitosis have been extensively studied (figure 1) as described in an excellent review by Vader and Lens (10). Aurora A is required for centrosome maturation and division. Subsequently, the divided centrosomes migrate to opposite sites of the dividing cell to define the poles of the bipolar mitotic spindle (10). This process, as well as the formation of the mitotic spindle, also requires aurora A function (11). Entry into mitosis is also regulated by aurora A due to an effect on CDK1/cyclinB complexes, making aurora A also a cell cycle regulating protein (12). Aurora B is the catalytic component of the chromosomal passenger complex, which consists of three additional proteins: Survivin, borealin and INCENP (13,14). This complex regulates chromosome condensation, probably via direct phosphorylation of histone H3 by aurora B (15). Subsequently, aurora B directs the proper orientation of the chromosomes (16), the assembly of the mitotic spindle (17), and the correct attachment of the mitotic spindle to the chromosomes by destabilizing defective microtubule-chromosome attachments, leading to abrogation of the mitotic process (18). These processes are controlled by the spindle checkpoint, a quality control circuit that blocks the onset of mitosis until all chromosomes have achieved a bipolar attachment to the mitotic spindle (19). The spindle checkpoint also requires aurora B function (14). Finally, aurora B has a critical role in cytokinesis, the process whereby the cytoplasm of a single cell is divided to form two daughter cells. Abrogation of aurora B function results in polyploidy (a state when there are more than two homologous sets of chromosomes) as a result of cytokinesis failure (20). The role of aurora C in mitosis is less well studied, although the protein has been implicated as a chromosomal passenger protein as well (21). It is believed that aurora C function overlaps and complements the function of aurora B in mitose (22). The protein is known to play an important role during spermatogenesis (23,24).

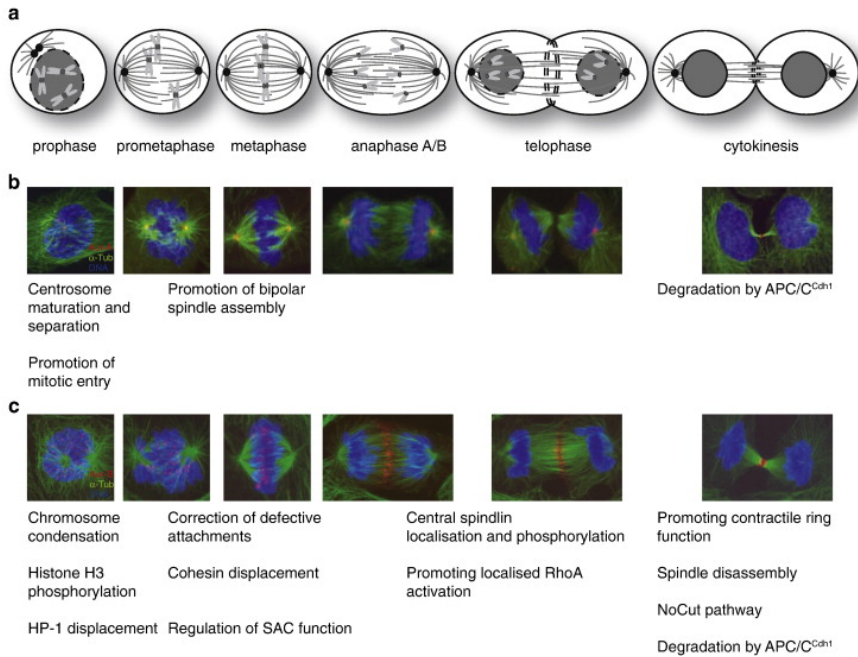


Figure 1: Localisation and functions of aurora kinases A and B during mitosis. (a) Schematic representation of the different mitotic phases and (b, c) the localisation pattern and functions of aurora-A (b) and aurora-B (c). DNA is in blue, aurora-A/B in red and α -tubulin in green (10). Figure and legend reprinted from *Biochimica et Biophysica Acta*, 1786, The aurora kinase family in cell division and cancer, pages 60-72, Copyright 2008, with permission from Elsevier.

Role of the auroras in cancer

The important roles of the aurora kinases A and B in mitotic processes raised the inevitable question whether these proteins might be involved in tumorigenesis. Both aurora A and B are overexpressed in various tumor types, as summarized recently by Gautschi et al. (25). The human aurora A gene resides at chromosome 20q13.2, a region frequently amplified in breast cancer (26). Overexpression of aurora A or amplification of the aurora A gene has been identified in several malignancies including breast (27,28), lung (29), head and neck (30), and colon cancer (31). In these studies, aurora A overexpression was associated with poor differentiated tumors (29), a poor prognosis (27,30), and genomic instability (31). Also, several polymorphisms in the gene encoding for aurora A have been identified, of which the

polymorphic substitution of isoleucine for phenylalanine at residue 31 (F31I) has been correlated with an increased risk to develop colon and breast cancer (32,33). The human gene encoding for aurora B is located on chromosome 17p13.1, a region that is not commonly amplified in human tumors. Overexpression of the aurora B gene has been observed in NSCLC (34), glioblastoma (35) and oral squamous cell carcinoma (36), and overexpression was correlated with poor differentiation (34), lymph node involvement (34), metastatic potential (36), and a shortened survival (35). One study found a polymorphism in the aurora kinase B gene that predisposes for breast cancer (37). Finally, a mutation in the gene encoding for aurora kinase C was described in a patient with NSCLC (38).

Despite their overexpression in various tumors, no clear role for the aurora kinases in tumorigenesis has been established. Aurora A overexpression leads to centrosome amplification, chromosome instability and oncogenic transformation in mammalian cells, probably via inactivation of the p53 pathway (39,40). Vice versa, aurora A activity also depends on p53, since p53 can inhibit aurora A function either by directly binding to its catalytic domain (41), or via induction of Gadd45, a protein that inhibits aurora A function (42). The tight relation between aurora A and p53 is confirmed by the correlation between aurora A expression and p53 status in mouse models and human tumors (43). Aurora A alone is not a potent inducer of cellular transformation in primary cells and it is thought that additional oncogenic events, such as Ras activation, are needed for this to occur (44). Moreover, it is not known whether the observed effects following aurora A overexpression can be attributed to aurora A kinase activity, since overexpression of kinase-dead aurora A caused a similar phenotype (45). Altogether, aurora A is thought to be an important oncoprotein, despite the lack of direct evidence linking this protein with the process of tumor formation. Aurora B is believed to be of less importance for tumorigenesis, although one study concluded that aurora B expression increased invasiveness in xenograft experiments (46), and another study reported enhanced cellular transformation in cells expressing oncogenic Ras when aurora B was overexpressed (47). Finally, no role in tumorigenesis has been suggested for aurora C.

Targeting the auroras

The clearly established role for the aurora kinases A and B in mitosis, accompanied by the evidence suggesting that deregulated aurora A and B expression is linked to tumorigenesis, raised the hypothesis that inhibiting these kinases might be a powerful antitumor strategy. Preclinical experiments revealed that knocking out either aurora A or aurora B leads to distinct phenotypes, in accordance with the different functions of both kinases (figure 2).

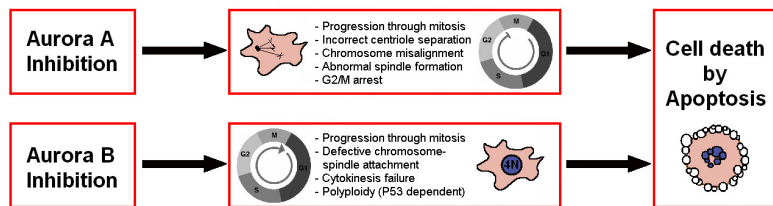


Figure 2: Expected phenotypes from inhibition of aurora A and aurora B. The given phenotypes were observed in RNA interference experiments, and in experiments with selective small molecules directed against the aurora kinases.

RNA interference (RNAi) experiments showed that loss of aurora A leads to incorrect centrosome duplication and misalignment of chromosomes during metaphase (48). Also, aurora A inhibition delayed the entry in mitosis, and finally caused cells to arrest at the G2/M checkpoint (49). In contrast with aurora A deficient cells, cells without aurora B function can progress through mitosis without delay. However, several defects arise without proper aurora B function, including abnormal chromosome-spindle attachments and cytokinesis failure (50). The progression through subsequent rounds of mitosis without cell division depends on p53 function. p53 wild-type cells will arrest following endoreduplication, while p53 mutated cells are able to pass through another cell cycle, leading to polyploidy (51). Eventually, these cells will die by apoptosis. These results led to the development of several small molecule inhibitors of these kinases. Hesperadin (Boehringer Ingelheim) and ZM447439 (AstraZeneca) were the first proven small molecule inhibitors of aurora kinases. Hesperadin is a specific inhibitor of aurora kinase B (Hespera was the opponent of Aurora in Greek mythology). The compound induced polyploidy in

HeLa cells (52), and stopped cell growth of prostate and breast cancer cells (53). In vitro, ZM447439 inhibits both aurora kinase A and B, leading to failure of chromosome alignment, segregation, and cytokinesis, followed by cell death (54,55). Both compounds never entered clinical trials, probably due to the emergence of more potent and specific inhibitors of the aurora kinases. We will discuss the most relevant aurora kinase inhibitors that are in clinical development, starting with the pan-aurora kinase inhibitors, inhibitors that target multiple aurora family members. Subsequently, we will discuss inhibitors targeting aurora kinase A and finally, we will discuss AZD1152, the only selective aurora kinase B inhibitor that has entered clinical trials. An overview of all compounds is given in table 1, the chemical structures are presented in figure 3.

Clinical experience with inhibitors targeting multiple aurora family members (pan-aurora inhibitors):

Tozasertib

Tozasertib, originally developed as VX-680 by Vertex and later renamed MK-0457 by Merck pharmaceuticals, was the first aurora kinase inhibitor to be tested in clinical trials. The drug, a pyrimidine derivative, has affinity for all aurora family members at nanomolar concentrations with inhibitory constant values ($K_{i(\text{app})}$) of 0.6, 18 and 4.6 nM for aurora A, aurora B and aurora C, respectively (56). Preclinical studies confirmed that tozasertib inhibited both aurora A and aurora B kinase activity (57), and activity has been reported against prostate (58), thyroid (59), ovarian (60) and oral squamous cancer cell lines (61). Upon treatment with tozasertib, cells accumulate with a 4N DNA content due to a failure of cytokinesis. This ultimately leads to apoptosis, preferentially in cells with a compromised p53 function (62). The first phase I study in patients with advanced solid tumors reported a good tolerability of tozasertib up to doses of 8 mg/m²/h, when administered by continuous 5-day intravenous infusion every 28 days. The dose limiting toxicity (DLT) was asymptomatic neutropenia at 12 mg/m²/h, and escalation up to 10 mg/m²/h was underway at the time of the report at ASCO 2006. Three of the 16 treated patients achieved stable disease, and two of them completed 6 cycles (63). Of

interest is the observed activity of tozasertib in patients with T315I Abl-mutated chronic myeloid leukemia (CML) or Philadelphia chromosome-positive acute lymphocytic leukemia (ALL) (64). This phenomenon is caused by the binding of the drug to the active conformation of the Abl kinase domain, thereby preventing phosphorylation of the protein kinase domain. This, together with the avoidance of the innermost cavity of the Abl kinase domain by tozasertib, explains the significant effectiveness of this compound against imatinib- and dasatinib resistant forms of Abl (65). Further structural studies explained the high affinity of tozasertib for both the aurora kinases, and imatinib-resistant forms of Abl by showing that the compound exploits a hydrophobic pocket in the active site that is only present in an inactive kinase conformation (66). Tozasertib appeared to be particularly effective in bone marrow mononuclear cells obtained from acute myeloid leukemia (AML) patients with high aurora A expression. Therefore, aurora A expression may serve as a prognostic marker for leukemia patients treated with tozasertib (67). A phase I study in patients with leukemia was initiated in 2005. The study has been completed, but no reports have entered the public domain. Other clinical studies that were initiated include a phase I study in patients with CML and Philadelphia positive-ALL, a study in patients with colorectal cancer, a phase II study in patients with lung cancer, and a phase II study in patients with T315I mutant CML and Philadelphia chromosome-positive ALL (data obtained from clinicaltrials.gov). In November 2007, Merck suspended enrolment in clinical trials with tozasertib, pending a full analysis of all efficacy and safety data for this drug. The decision was based on preliminary safety data, in which a QTc prolongation was observed in one patient. However, recently at ASCO 2009, data of a phase I study of concomitant and consecutive treatment with dasatinib and tozasertib in CML and ALL patients were presented. Three patients (two patients with Ph+ ALL, and one with CML in blast crisis), all previously unsuccessfully treated with imatinib, were enrolled. The two ALL patients, both in hematological response after three months of treatment with dasatinib, subsequently received a 6-hour biweekly infusion of tozasertib at 64 mg/m²/hr. Both patients maintained the hematological response. The CML patient progressed on dasatinib, and was subsequently treated with a 5-day continuous infusion of tozasertib at 10 mg/m²/hr, every 4 weeks. This patient obtained a complete hematological

response after one cycle of treatment, and the authors concluded that the sequential and concomitant administration of dasatinib and tozasertib is a promising strategy for refractory Ph+ CML and ALL (68).

PHA-739358

PHA-739358 (Nerviano medical sciences) is a small molecule 3-aminopyrazole derivative with strong activity against aurora kinases A, B and C (IC₅₀ values of 13, 79 and 61 nM, respectively) (69). Interestingly, this compound also inhibits several cancer-related tyrosine kinases at the nanomolar range, including fibroblast growth factor receptor-1 (FGFR-1), Ret, Trk-a and Abl (69). The crystal structure of PHA-739358 in complex with the T315I Abl mutant has been unraveled, providing an explanation for the activity of PHA-739358 on the T315I mutation (70). In accordance with these findings, PHA-739358 is very effective against BCR-ABL-positive leukemia cell lines, including the imatinib resistant cell lines harboring the T315I mutation (71). Other sensitive tumor cell lines included several carcinomas, including those of the colon, breast, ovaries and prostate (69). Data of the first clinical phase I studies were presented at ASCO 2008. In the first study, PHA-739358, administered as 24h infusions once every 2 weeks, was well tolerated up to doses of 500 mg/m², which was considered the MTD. The DLT was febrile neutropenia. The most frequently observed hematological toxicities included grade 3 and 4 neutropenia and lymphocytopenia, non-hematological toxicities were mostly mild (grade I/II). The pharmacokinetic parameters were independent of dose and time, and characterized by a low inter-patient variability. Clinically relevant disease stabilizations were observed in several patients. The second part of the study, where patients received colony stimulating factor as bone marrow support, was still recruiting patients at the time of the report (72). The second study investigated the safety, tolerability, and pharmacokinetics of PHA-739358 when administered as a 6h or 3h infusion on days 1,8 and 15 every 4 weeks. During the first part of the study, patients received the drug as a 6h infusion.

Table 1: Aurora kinase inhibitors in clinical development

	Aurora Inhibition	Status	DLT	Response	References
Pan-aurora inhibitors					
680	Tozasertib (MK-0457, VX-680)	Phase II	Neutropenia	SD, response in CML and ALL patients	(63,68)
	Aurora A (K _i 0.6 nM)				
	Aurora B (K _i 18 nM) Aurora C (K _i 4.6 nM)				
PHA-739358	Aurora A (IC ₅₀ 13 nM)	Phase II	Neutropenia	SD response in CML patients	(72,73,74)
	Aurora B (IC ₅₀ 79 nM)				
	Aurora C (IC ₅₀ 61 nM)				
AS703569 (R763)	Not published	Phase I	Diarrhea Mucositis Neutropenic infection	PR	(76,77)
AT9283	Aurora A (IC ₅₀ ≈ 3 nM) Aurora B (IC ₅₀ ≈ 3 nM)	Phase I	Neutropenia	PR	(80,81)
SNS-314	Aurora A (IC ₅₀ 9 nM) Aurora B (IC ₅₀ 31 nM)	Phase I	Not reached	SD	(83)
PF-03814735	Not published	Phase I	Neutropenia	SD	(84)
Aurora A inhibitors					
MLN8054	Aurora A (IC ₅₀ 4 nM)	Phase I	Somnolence	SD	(88,87,89)
	Aurora B (IC ₅₀ 172 nM)				
MLN8237	Not published	Phase I	Neutropenia Mucositis Somnolence	PR	(92,93)
Aurora B inhibitor					
AZD1152	Aurora A (K _i 1369 nM) Aurora B (K _i 0.36 nM) Aurora C (K _i 17nM)	Phase I/II	Neutropenia	SD	(100)

Abbreviations: K_i, inhibitory constant; IC₅₀, half maximal inhibitory concentration; DLT, dose limiting toxicity; SD, stable disease; PR, partial response; CML, chronic myeloid leukemia; ALL, acute lymphoblastic leukemia; AML, acute myeloid leukemia

DLTs in this part of the study were observed in 6 patients, and neutropenia was the DLT for this schedule. The recommended phase II dose was identified at 330 mg/m². The most frequently observed adverse events included grade I/II anorexia, nausea, fatigue and diarrhea. Pharmacokinetics were dose/time independent, and clinically relevant disease stabilizations were observed in several patients. Pharmacodynamic analyses of skins biopsy samples revealed inhibition of histone H3 phosphorylation, a biomarker of aurora B inhibition, at doses of 190 mg/m² and higher. The second part of the study was ongoing at the time of the report, but the 330 mg/m² dose given as a 3hr infusion appeared to be less well tolerated, with 2 DLTs (grade 4 neutropenia and grade 3 fatigue) out of 7 treated patients (73). Phase II studies with PHA-739358 are ongoing in patients with CML and refractory prostate cancer, and results of the study in patients with CML were reported recently. Twelve patients were included, and received doses from 250 to 400 mg/m²/day by a once-weekly 6-hour infusion, for 3 consecutive weeks every 4 weeks. Two patients, both with T315I mutated BCR-ABL, achieved a complete hematological response at 330 mg/m². The drug was, in accordance with the phase I results, well tolerated, with neutropenia as principle toxicity. Pharmacodynamic data were also in agreement with phase I data, and pharmacodynamic analyses revealed treatment-associated decreases of CRKL (V-crk sarcoma virus CT10 oncogene homolog (avian)-like) phosphorylation, a biomarker of BCR-ABL activity, in 10 out of 11 evaluable patients (74).

AS703569

AS703569 (R763), developed by Merck-Serono and Rigel pharmaceuticals, is an orally available ATP-competitive inhibitor of aurora A, B and C. The compound also inhibits other cancer-related kinases, including FLT3, making this compound a good candidate for evaluation in patients with hematological malignancies. The drug demonstrated potent inhibition of several tumor cell lines in vitro, and in xenograft studies (75). Three Phase I studies are ongoing, two of which were recently presented at international meetings. The first trial, presented at ASCO 2007, is a two-arm phase I study that is conducted in patients with advanced solid tumors. Patients included in this study received AS703569 orally on day 1 and 8 (arm 1), or on day 1, 2 and 3 (arm 2) in 21-

day cycles. At the time of the report, a total of 15 patients was included at two dose levels (6 and 12 mg/m²). The drug was well tolerated, and no study related DLTs or serious adverse events (SAEs) were observed. No pharmacokinetic and pharmacodynamic data were available at the time of the report (76). Recently, data of a second phase I trial with AS703569 were presented. In this phase I study in patients with advanced hematological malignancies, 2 dosing regimens were tested: days 1-3 and 8-10 of a 21-day cycle (regimen 1) and days 1-6 of a 21 day cycle (regimen 2). In regimen 1, 24 patients were treated up to dose levels of 47 mg/m². At this dose level, 2 DLTs were reported (both grade 3 diarrhea). In regimen 2, 21 patients were treated up to dose levels of 47 mg/m², and 3 DLTs were seen at this dose level (neutropenic infection and two cases of grade 4 mucositis). Consequently, in both regimens the doses were de-escalated to 37 mg/m², and enrolment was ongoing at the time of the report. The most frequently observed grade ≥ 3 toxicities included infections, neutropenia, thrombocytopenia, anemia, and gastrointestinal disorders. One patient with CML (T315I) had a hematological and cytogenetic response, three patients with AML achieved reduction in BM and/or peripheral blasts and one patient with CML achieved a partial response. Several other patients had disease stabilizations (77). The third phase I study is evaluating R763/AS703569 in combination with standard of care therapy in patients with advanced malignancies. This study was recently initiated, and is currently recruiting patients

AT9283

AT9283 (Astex pharmaceuticals) is a multi-targeted kinase inhibitor, with potent activity against aurora kinase A and B (IC₅₀ of approximately 3 nM) (78). A variety of other cancer-related protein kinases is also inhibited by AT9283, including Abl kinase, JAK2, JAK3, Ret and GSK3 beta. The inhibitory potential of AT9283 against the T315I Abl mutant makes this compound an attractive option for the treatment of imatinib-resistant patients with CML (79). Clinical studies with this compound are ongoing, and preliminary results of a phase I study in patients with refractory leukemia were presented at ASCO 2008. Twenty-nine patients were included at the time of the report.

AT9283 was administered by 72h continuous IV infusions once every 3 weeks. The MTD was identified at a dose level of 108 mg/m²/day, as DLTs were observed at the next higher dose level of 162 mg/m²/day. The DLTs included grade IV elevation of serum aminotransferases in 2 patients. Another patient died from myocardial infarction shortly after completion of the AT9283 infusion. AT9283 administration was associated with predictable myelosuppression, particularly neutropenia. Several patients experienced clinical benefit following AT9283 treatment, including reductions in BM blasts in approximately 1/3 of the treated patients with AML. Also, two patients with refractory CML exhibited a hematological response. Pharmacodynamic and clinical observations in this trial suggest that expanding the duration of the infusion will increase the biological effect of AT9283, a hypothesis that will be explored in the near future (80). A second phase I study, conducted in patients with advanced solid malignancies, was presented at ASCO 2009. Thirty-three patients had been treated up to doses of 12 mg/m²/day. This dose level was found to be intolerable, because 3 out of 6 treated patients experienced a DLT (neutropenia in all cases). The MTD was set at 9mg/m²/day. Pharmacokinetic analyses suggested an exposure that increased linearly with dose. Seven patients included in the study received an oral dose of AT9283 one week prior to starting IV treatment. Pharmacokinetic analysis revealed a median oral bioavailability of 27 percent. Biological evidence of aurora B inhibition, manifest as a reduction in histone H3 phosphorylation in skin biopsies during the infusion, was observed at all dose levels. Best response in this study was a partial response in a patient with NSCLC, who was ongoing at the time of the report. Prolonged disease stabilizations were observed in 4 patients with various tumor types (81). Currently, another phase I study is ongoing in patients with solid tumors or refractory non-Hodgkin lymphoma, investigating 24h infusions on days 1 and 8 every three weeks.

SNS-314

SNS-314 (Sunesis pharmaceuticals) is a novel aminothiazole-derived urea that selectively inhibits aurora A, B and C in the low nanomolar range, exhibits potent activity against various tumor cell lines, and also displays activity in xenograft models (82). Recently, preliminary data of the first phase I study in

patients with advanced solid tumors were presented at ASCO 2009. Thirty-two patients were included at the time of the report, at doses ranging from 30 to 1800 mg/m². The drug was administered as a 3h IV infusion on days 1, 8 and 15 in 28 day cycles. A DLT of grade 3 neutropenia preventing administration of all three doses was observed at 1440 mg/m², but the MTD was not established at the time of the report. SNS-314 was generally well tolerated at the studied dose-levels, with grade 1-2 gastrointestinal complaints and fatigue as the most frequently observed toxicities. The plasma pharmacokinetics were dose-proportional, and there were no signs of drug accumulation following weekly administration of SNS-314. Pharmacodynamic analyses of pre- and post-dose skin biopsies suggested aurora B inhibition at doses of 240 mg/m² and higher. Six patients had stable disease as their best response, and the study was ongoing at the time of the report (83).

PF-03814735

PF-03814735 (Pfizer) is an orally available aurora kinase inhibitor that is currently in phase I clinical trials. The compound inhibits aurora kinase A and B, and has a broad spectrum of clinical activity. Preclinical data have not been published; data of the first phase I study were presented at ASCO 2008. Twenty patients were recruited, and received doses up to 100 mg/day for 5 consecutive days in 3-week cycles. At this dose level, 2 out of 7 patients experienced a DLT (neutropenia), and the next lower dose level was considered the MTD (80 mg/day). Pharmacokinetics were linear up to the highest dose level, and two patients had prolonged disease stabilization. The second part of the study will investigate a 10 consecutive days in 3-week cycles treatment schedule. This schedule was recruiting patients at the time of the report (84).

Clinical experience with selective inhibitors of aurora kinase A:

MLN8054

MLN8054 (Millenium pharmaceuticals) is an orally available selective inhibitor of aurora kinase A (IC₅₀ = 4nM), with a high selectivity over aurora kinase B

(IC_{50} = 172 nM), and a panel of other selected kinases (85). Inhibition of aurora A by MLN8054 leads to the formation of abnormal mitotic spindles, and alignment defects during metaphase, ultimately resulting in aneuploidy and cell death (86). The compound inhibited the growth of colorectal, prostate, NSCLC, breast and ovarian cancer cell lines, and prostate and colorectal xenografted tumors in preclinical experiments (85). Data of the first phase I study were presented at ASCO 2007. Initially, the drug was given once daily for 7 consecutive days, repeated every 21 days. At the time of the report, 22 patients had been treated, at doses up to 40 mg/day. Reversible grade 3 somnolence was observed in 2 out of 4 patients treated at 40 mg/day, after which it was decided to change drug administration to divided doses on a QID schedule. Sixteen additional patients were treated at this schedule up to doses of 55 mg/day. Two out of 4 patients treated at 55 mg/day experienced reversible grade 3 somnolence, resulting in a MTD of 45 mg/day at a QID schedule. In contrast with the other aurora kinase inhibitors, no myelosuppression was observed at any dose with either schedule. The occurrence of somnolence can be explained by the structural similarity of MLN8054 to benzodiazepines. MLN8054 binds to the gamma-aminobutyric acid alpha 1 benzodiazepine (GABAA α 1 BZD) receptor. Therefore, it was decided to continue dose escalation with the co-administration of methylphenidate. Unfortunately, no accumulation of cells in mitosis was observed in skin biopsies of patients treated with MLN8054, suggesting insufficient target inhibition (87). Recently, the final results of another phase I study with MLN8054 were presented. In this study, patients with advanced solid tumors received the drug once daily on days 1-5 and 8-12 or on days 1-14 in four divided doses, in 28-day cycles. Forty-three patients received doses up to 80mg/day, dose escalation was stopped at this dose-level because of DLTs (grade 3 somnolence, liver function elevations, neutropenia and mucositis, respectively). No responses were reported, although pharmacodynamic markers suggested aurora A inhibition at the higher dose levels (88,89). Following these results, MLN8054 was replaced by MLN8237, a second generation aurora kinase A inhibitor.

MLN8237

MLN8237 (Millenium pharmaceuticals) is the follow-up compound for MLN8054, with an increased potency of inhibition and a decreased benzodiazepine-like effect on the central nervous system (90). MLN8237 demonstrated promising anti-tumor activity in preclinical models, particularly against neuroblastoma and ALL xenograft panels (91). Results of the first phase I study were presented at an EORTC symposium last year. The compound was administered orally once daily to patients with advanced solid tumors for 7 days in 21-day cycles. Twenty-three patients had been treated at doses up to 150 mg/day, DLTs were observed in 3 out of 6 patients treated at the highest dose level (neutropenia, grade 3 mucositis and grade 3 somnolence). Upon administration, MLN8237 was rapidly absorbed, exposure increased with dose, and efficacious exposure was observed at the highest dose levels. One patient with metastatic ovarian cancer had preliminary evidence of anti-tumor activity; four patients had prolonged disease stabilization following treatment with MLN8237. Interestingly, no clinically significant benzodiazepine-like side effects were observed. The investigators planned to evaluate alternate dose groups including 110 mg once daily, 70-100 mg twice daily and lower doses over 14-21 days (92). Recently, results of another phase I study with MLN8237 were reported at ASCO 2009. In this study, MLN8237 was administered to patients with advanced solid tumors once or twice daily for 7 days, followed by a 14 day recovery period. Twenty-seven patients had been treated, and DLTs were observed at the higher dose levels, when the drug was administered bi-daily (BID). The DLTs included stomatitis and neutropenia in 2 patients and stomatitis and pancytopenia in another patient treated at 100 mg BID, stomatitis and neutropenia, and neutropenia in two patients treated at 75 mg BID, and neutropenia and somnolence in two patients treated at the 60 mg BID dose level. The 50 mg BID dose-level was considered safe, with no DLTs in three patients. Preliminary PK analysis showed dose-dependent increases in exposure and maximum plasma concentrations, and PD analyses revealed Aurora A inhibition following MLN8237 dosing. Antitumor activity was observed in a patient with liposarcoma, treated at 100 mg MLN8237 BID. The authors concluded that these results would support the future phase II development of MLN8237 (93).

Clinical experience with a selective inhibitor of aurora kinase B:

AZD1152

AZD1152 (AstraZeneca) is a dihydrogen phosphate prodrug of a pyrazoloquinazoline aurora kinase inhibitor (AZD1152-hydroxyquinazoline pyrazol anilide, AZD1152-HQPA), and is converted rapidly to the active moiety in plasma (94). AZD1152-HQPA is a potent and selective inhibitor of aurora kinase B ($K_{i(\text{app})} = 0.36 \text{ nM}$), compared with aurora kinase A ($K_{i(\text{app})} = 1369 \text{ nM}$), and has a high specificity over a panel of 50 other kinases (95). AZD1152 potently inhibited the growth of human colon, NSCLC and promyelocytic leukemia tumor xenografts in preclinical studies (96). Moreover, the compound induced growth arrest and apoptosis in various leukemia cell lines, suggesting that AZD1152 is a promising new agent for treatment of individuals with leukemia (97,98). Another study showed encouraging antitumor activity of AZD1152 against a panel of myeloma cells, expressing high levels of aurora B, and suggested AZD1152 alone or in combination with dexamethasone as a potential treatment for patients with myeloma (99). The first clinical study is completed, although no definite report has been published. In this phase I trial, presented at ASCO 2006, AZD1152 was administered as a 2h infusion once every week to patients with advanced solid malignancies, and was tolerated well up to doses of 300mg. DLT was grade 4 neutropenia in 3 patients treated at 450 mg, and bone marrow recovery was generally noted by 2 weeks post dose. Pharmacokinetic analyses revealed a rapid conversion to the active drug in plasma, and linear pharmacokinetics of both the prodrug and the active moiety. Significant disease stabilizations were observed in five out of 13 treated patients (100). Several other studies with AZD1152 are ongoing, including a phase I and a phase I/II study in patients with AML.

Other aurora kinase inhibitors

Other aurora kinase inhibitors that are currently being evaluated in phase I clinical trials include CYC116 (Cyclacel pharmaceuticals), and MK5108 (VX-689), developed by Merck and Vertex. However, data of these studies have not entered the public domain as far as we know. Recently, the development

of another aurora kinase inhibitor MK6592 (VX-667) was terminated by Merck and Vertex, after the compound did not meet pharmacokinetic objectives in a phase I study. Aurora kinase inhibitors that demonstrated anti-tumor activity in preclinical studies, but have not entered clinical trials (yet), include the aforementioned hesperadin (52,53) and ZM447439 (54,55), PHA-680632 (101), PHA-680626 (102), AKI-001 (103), Jadomycin B (104), and Reversine (105).

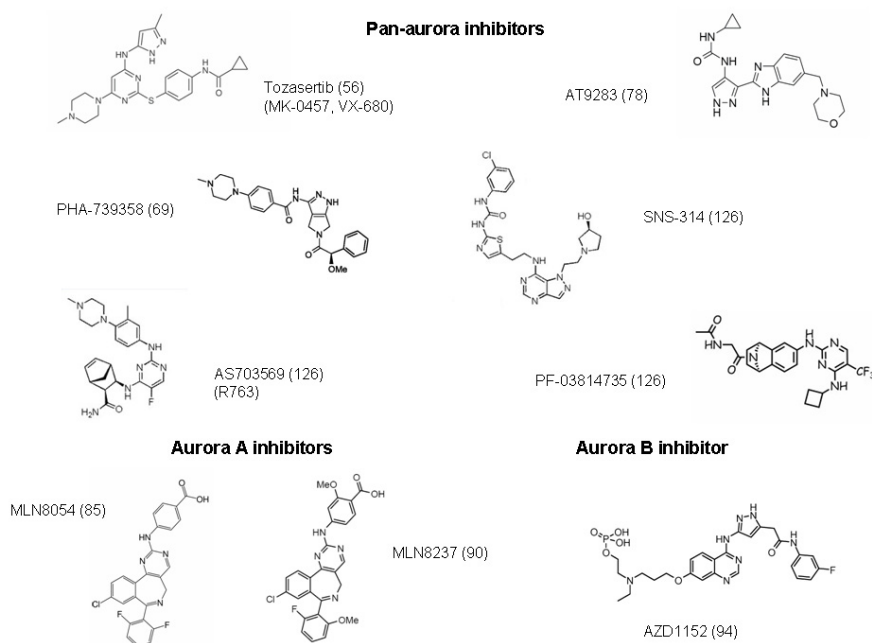


Figure 3: Chemical structures of aurora kinase inhibitors that are currently in clinical trials. References indicate the source of the chemical structures.

Discussion

The mitotic/tubulin machinery is a validated drug target, exemplified by the success of the taxanes and vinca-alkaloids. Aurora kinase inhibitors potentially have a benefit over these agents, because they only target those cells that enter mitosis, possibly improving specificity for dividing cells. The aurora

kinases have shown to be promising drug targets in preclinical models, and several agents have entered the clinic.

In most phase I studies described in this review, the aurora kinase inhibitors were well tolerated, showing reversible neutropenia as the DLT in the great majority of the tested compounds. This might constitute a problem in future combination studies with chemotherapeutic agents, since neutropenia is a dose-limiting side-effect of several anti-cancer drugs. A strategy to reduce the severity of myelosuppression might be to co-administer granulocyte colony stimulating factor, which has already been done in one of the here described phase I studies (72). Interestingly, no thrombocytopenia was observed following treatment with the aurora kinase inhibitors described in this overview. This might be due to downregulation of aurora A and aurora B during maturation of megakaryocytes, the thrombocyte producing bone marrow cells (106). This down regulation leads to polyploidization, a step that is thought to be essential for megakaryocyte maturation and subsequent thrombocyte production (107).

Overall, the responses seen in the phase I studies reported in this overview in patients with solid tumors are rather disappointing. The majority of reports had disease stabilizations as best response, with the exception of two partial responses in patients treated with AT9283 (NSCLC) and MLN8237 (ovarian). The promising activity seen in patients with hematological malignancies is probably due to cross reactivity of the aurora kinase inhibitors with BCR-ABL, the fusion protein that is aberrantly expressed in these patients. The lack of objective responses in patients with solid tumors could be due to many different factors, including incomplete target inhibition or the occurrence of mutations in the targeted proteins. The latter issue was recently addressed (108). Combining the existing aurora inhibitors with novel agents targeting mutated aurora kinases might overcome these problems in the future.

A matter of debate in the field of the aurora kinases is which of the auroras is the best drug target. This issue was addressed by several groups, and contradictory results have been reported. Results of experiments in pancreatic cell lines, using antisense oligonucleotides, showed that targeting aurora A has

advantages over targeting aurora B, while no advantage was observed when both proteins were targeted simultaneously (109). On the other hand, experiments in colon cells showed an advantage of aurora B inhibition over aurora A inhibition (110), suggesting that the role of the different aurora kinases might be cell line dependent. Intriguing are the preclinical results with the dual aurora kinase inhibitors tozasertib (VX-680) and ZM447439. Following administration of these small molecules, phenotypes identical to inactivation of aurora B alone were observed, indicating that dual inhibitors act primarily via inhibition of aurora B (110,56). Also contributing to the ongoing debate are several recent publications regarding the role of aurora kinase A. One study found no role for aurora kinase A in RAS-MAPK mediated cellular transformation (111), while another study concluded that aurora A is essential for maintaining genomic stability, and that aurora A is a tumor suppressor protein (112). Altogether, these results question whether aurora A is the favorable drug target (113). It is also uncertain whether in tumor cells aurora overexpression is the cause or consequence of tumorigenesis. It is plausible that the upregulation of cell cycle regulating proteins is due to the increased turn-over rate of cancer cells, and that inhibition of these proteins will not destroy the source of the malignant process. This hypothesis does not apply to leukemias expressing BCR-ABL. This aberrant protein is known to be the cause of the malignant transformation, thereby explaining the impressive activity of aurora kinase inhibitors with cross reactivity towards this protein.

In order to increase the anti-tumor activity of the aurora kinase inhibitors in the clinic, combination therapy with cytotoxic anti-cancer agents, radiotherapy or other targeted agents might be employed in the future. Several preclinical studies have addressed this issue. Transcriptional silencing of aurora kinase A potentiates the effect of tubulin targeting agents, including vincristine (114) and taxanes (115). This synergy is also observed after treatment with tozasertib in combination with docetaxel (60). Treatment with AZD1152, an aurora B inhibitor, was found to be synergistic with a variety of chemotherapeutic agents, including irinotecan, docetaxel, vinorelbine, gemcitabine, oxaliplatin and 5-fluorouracil (116), and with vincristine and topoisomerase inhibitors in leukemia cell lines (98). Moreover, this compound also potentiates the radiation response in p53-deficient cancer cells,

suggesting synergy with radiotherapy (117). Recently, synergy between tozasertib and vorinostat, a histone deacetylase inhibitor, was demonstrated in several leukemia cell lines (118,119). Finally, at ASCO 2009 it was reported that MLN8237 and rituximab, an anti CD20 monoclonal antibody, reduced tumor burden in a synergistic mechanism in multiple diffuse large B-cell lymphoma tumor models (120).

Future studies should employ validated biomarkers to assess the degree of target inhibition in patients who are treated with aurora kinase inhibitors. In some of the phase I trials described in this review, phosphorylation of Histone H3 was used as a biomarker (73,84,121,122). This event is associated with aurora B activity, since aurora B directly phosphorylates histone H3 on serine 10, making it a useful tool for evaluating the degree of aurora B inhibition (123,124). Histone H3 phosphorylation is critical for the transformation of cancer cells, and might therefore be an anticancer target on its own (125). The mitotic index constitutes a biomarker for aurora A activity, because inhibition of aurora A in cancer cells resulted in accumulation in mitosis (92,87). Another biomarker for aurora A activity is the degree of autophosphorylation on threonine at residue 288 (T288). This event, together with an increase in mitotic cells (measured by phosphorylation of histone H3) was found to be a promising biomarker for aurora A inhibition by MLN8054 (85).

Patient selection based on aurora A and/or aurora B overexpression may be a useful strategy to test whether these subpopulations will benefit from therapy with aurora kinase inhibitors. Some histologically aggressive lymphomas, for instance, are known to overexpress the aurora kinase A gene (50). Finally, more work needs to be done to determine the optimal treatment regimen for this class of molecules. One of the here described phase I studies suggested that prolonged inhibition of the aurora kinases is beneficial (80). If this holds true, there is a need for orally available aurora kinase inhibitors. Fortunately, several of these agents have entered clinical trials.

In conclusion, the aurora kinases were considered promising drug targets when their inhibitors first entered the clinic. However, the clinical activity of the aurora kinase inhibitors in patients with solid tumors has been rather

disappointing. Future studies with aurora kinase inhibitors should focus on the possibility of combining these agents with radiotherapy, chemotherapy, or other targeted anticancer agents. As single agents, the aurora kinase inhibitors only seem to have a future in patients with leukemias expressing BCR-ABL, or in patients with fast growing tumors with aurora kinase overexpression. Biomarkers of response are necessary for better evaluation of this class of anti cancer drugs.

References

1. Pines, J. and Rieder, C. L. Re-staging mitosis: a contemporary view of mitotic progression. *Nat.Cell Biol.* 2001;3:E3-E6.
2. Schatten, H. The mammalian centrosome and its functional significance. *Histochem.Cell Biol.* 2008;129:667-686.
3. Morris, P. G. and Fornier, M. N. Microtubule active agents: beyond the taxane frontier. *Clin.Cancer Res.* 2008;14:7167-7172.
4. Zhou, J. and Giannakakou, P. Targeting microtubules for cancer chemotherapy. *Curr.Med.Chem.Anticancer Agents.* 2005;5:65-71.
5. Sharma, P. S., Sharma, R., and Tyagi, R. Inhibitors of cyclin dependent kinases: useful targets for cancer treatment. *Curr.Cancer Drug Targets.* 2008;8:53-75.
6. Mita, A. C., Mita, M. M., Nawrocki, S. T.et al. Survivin: key regulator of mitosis and apoptosis and novel target for cancer therapeutics. *Clin.Cancer Res.* 2008;14:5000-5005.
7. Warner, S. L., Stephens, B. J., and Von Hoff, D. D. Tubulin-associated proteins: Aurora and Polo-like kinases as therapeutic targets in cancer. *Curr.Oncol.Rep.* 2008;10:122-129.
8. Keen, N. and Taylor, S. Aurora-kinase inhibitors as anticancer agents. *Nat.Rev.Cancer.* 2004;4:927-936.
9. Kimura, M., Matsuda, Y., Yoshioka, T.et al. Cell cycle-dependent expression and centrosome localization of a third human aurora/Ipl1-related protein kinase, AIK3. *J.Biol.Chem.* 1999;274:7334-7340.
10. Vader, G. and Lens, S. M. The Aurora kinase family in cell division and cancer. *Biochim.Biophys.Acta.* 2008;1786:60-72.
11. Liu, Q. and Ruderman, J. V. Aurora A, mitotic entry, and spindle bipolarity. *Proc.Natl.Acad.Sci.U.S.A.* 2006;103:5811-5816.
12. Satinover, D. L., Brautigam, D. L., and Stukenberg, P. T. Aurora-A kinase and inhibitor-2 regulate the cyclin threshold for mitotic entry in *Xenopus* early embryonic cell cycles. *Cell Cycle.* 2006;5:2268-2274.
13. Ruchaud, S., Carmena, M., and Earnshaw, W. C. Chromosomal passengers: conducting cell division. *Nat.Rev.Mol.Cell Biol.* 2007;8:798-812.
14. Vader, G., Maia, A. F., and Lens, S. M. The chromosomal passenger complex and the spindle assembly checkpoint: kinetochore-microtubule error correction and beyond. *Cell Div.* 2008;3:10.:10-
15. Goto, H., Yasui, Y., Nigg, E. A.et al. Aurora-B phosphorylates Histone H3 at serine28 with regard to the mitotic chromosome condensation. *Genes Cells.* 2002;7:11-17.
16. Tanaka, T. U., Rachidi, N., Janke, C.et al. Evidence that the Ipl1-Sli15 (Aurora kinase-INCENP) complex promotes chromosome bi-orientation by altering kinetochore-spindle pole connections. *Cell.* 2002;108:317-329.
17. Sampath, S. C., Ohi, R., Leismann, O.et al. The chromosomal passenger complex is required for chromatin-induced microtubule stabilization and spindle assembly. *Cell.* 2004;118:187-202.
18. Lampson, M. A., Renduchitala, K., Khodjakov, A.et al. Correcting improper chromosome-spindle attachments during cell division. *Nat.Cell Biol.* 2004;6:232-237.
19. Musacchio, A. and Salmon, E. D. The spindle-assembly checkpoint in space and time. *Nat.Rev.Mol.Cell Biol.* 2007;8:379-393.

20. Terada, Y., Tatsuka, M., Suzuki, F. et al. AIM-1: a mammalian midbody-associated protein required for cytokinesis. *EMBO J.* 1998;17:667-676.
21. Yan, X., Cao, L., Li, Q. et al. Aurora C is directly associated with Survivin and required for cytokinesis. *Genes Cells.* 2005;10:617-626.
22. Sasai, K., Katayama, H., Stenoien, D. L. et al. Aurora-C kinase is a novel chromosomal passenger protein that can complement Aurora-B kinase function in mitotic cells. *Cell Motil.Cytoskeleton.* 2004;59:249-263.
23. Kimmins, S., Crosio, C., Kotaja, N. et al. Differential functions of the Aurora-B and Aurora-C kinases in mammalian spermatogenesis. *Mol.Endocrinol.* 2007;21:726-739.
24. Tang, C. J., Lin, C. Y., and Tang, T. K. Dynamic localization and functional implications of Aurora-C kinase during male mouse meiosis. *Dev.Biol.* 2006;290:398-410.
25. Gautschi, O., Heighway, J., Mack, P. C. et al. Aurora kinases as anticancer drug targets. *Clin.Cancer Res.* 2008;14:1639-1648.
26. Sen, S., Zhou, H., and White, R. A. A putative serine/threonine kinase encoding gene BTAK on chromosome 20q13 is amplified and overexpressed in human breast cancer cell lines. *Oncogene.* 1997;14:2195-2200.
27. Nadler, Y., Camp, R. L., Schwartz, C. et al. Expression of Aurora A (but not Aurora B) is predictive of survival in breast cancer. *Clin.Cancer Res.* 2008;14:4455-4462.
28. Tanaka, T., Kimura, M., Matsunaga, K. et al. Centrosomal kinase AIK1 is overexpressed in invasive ductal carcinoma of the breast. *Cancer Res.* 1999;59:2041-2044.
29. Xu, H. T., Ma, L., Qi, F. J. et al. Expression of serine threonine kinase 15 is associated with poor differentiation in lung squamous cell carcinoma and adenocarcinoma. *Pathol.Int.* 2006;56:375-380.
30. Reiter, R., Gais, P., Jutting, U. et al. Aurora kinase A messenger RNA overexpression is correlated with tumor progression and shortened survival in head and neck squamous cell carcinoma. *Clin.Cancer Res.* 2006;12:5136-5141.
31. Nishida, N., Nagasaka, T., Kashiwagi, K. et al. High copy amplification of the Aurora-A gene is associated with chromosomal instability phenotype in human colorectal cancers. *Cancer Biol.Ther.* 2007;6:525-533.
32. Chen, J., Sen, S., Amos, C. I. et al. Association between Aurora-A kinase polymorphisms and age of onset of hereditary nonpolyposis colorectal cancer in a Caucasian population. *Mol.Carcinog.* 2007;46:249-256.
33. Lo, Y. L., Yu, J. C., Chen, S. T. et al. Breast cancer risk associated with genotypic polymorphism of the mitosis-regulating gene Aurora-A/STK15/BTAK. *Int.J.Cancer.* 2005;115:276-283.
34. Vischioni, B., Oudejans, J. J., Vos, W. et al. Frequent overexpression of aurora B kinase, a novel drug target, in non-small cell lung carcinoma patients. *Mol.Cancer Ther.* 2006;5:2905-2913.
35. Zeng, W. F., Navaratne, K., Prayson, R. A. et al. Aurora B expression correlates with aggressive behaviour in glioblastoma multiforme. *J.Clin.Pathol.* 2007;60:218-221.
36. Qi, G., Ogawa, I., Kudo, Y. et al. Aurora-B expression and its correlation with cell proliferation and metastasis in oral cancer. *Virchows Arch.* 2007;450:297-302.
37. Tchatchou, S., Wirttenberger, M., Hemminki, K. et al. Aurora kinases A and B and familial breast cancer risk. *Cancer Lett.* 2007;247:266-272.
38. Davies, H., Hunter, C., Smith, R. et al. Somatic mutations of the protein kinase gene family in human lung cancer. *Cancer Res.* 2005;65:7591-7595.
39. Katayama, H., Sasai, K., Kawai, H. et al. Phosphorylation by aurora kinase A induces Mdm2-mediated destabilization and inhibition of p53. *Nat.Genet.* 2004;36:55-62.
40. Liu, Q., Kaneko, S., Yang, L. et al. Aurora-A abrogation of p53 DNA binding and transactivation activity by phosphorylation of serine 215. *J.Biol.Chem.* 2004;279:52175-52182.
41. Chen, S. S., Chang, P. C., Cheng, Y. W. et al. Suppression of the STK15 oncogenic activity requires a transactivation-independent p53 function. *EMBO J.* 2002;21:4491-4499.
42. Shao, S., Wang, Y., Jin, S. et al. Gadd45a interacts with aurora-A and inhibits its kinase activity. *J.Biol.Chem.* 2006;281:28943-28950.
43. Mao, J. H., Wu, D., Perez-Losada, J. et al. Crosstalk between Aurora-A and p53: frequent deletion or downregulation of Aurora-A in tumors from p53 null mice. *Cancer Cell.* 2007;11:161-173.

44. Tatsuka, M., Sato, S., Kitajima, S. et al. Overexpression of Aurora-A potentiates HRAS-mediated oncogenic transformation and is implicated in oral carcinogenesis. *Oncogene*. 2005;24:1122-1127.
45. Meraldi, P., Honda, R., and Nigg, E. A. Aurora-A overexpression reveals tetraploidization as a major route to centrosome amplification in p53^{-/-} cells. *EMBO J*. 2002;21:483-492.
46. Ota, T., Suto, S., Katayama, H. et al. Increased mitotic phosphorylation of histone H3 attributable to AIM-1/Aurora-B overexpression contributes to chromosome number instability. *Cancer Res*. 2002;62:5168-5177.
47. Kanda, A., Kawai, H., Suto, S. et al. Aurora-B/AIM-1 kinase activity is involved in Ras-mediated cell transformation. *Oncogene*. 2005;24:7266-7272.
48. Marumoto, T., Honda, S., Hara, T. et al. Aurora-A kinase maintains the fidelity of early and late mitotic events in HeLa cells. *J.Biol.Chem*. 2003;278:51786-51795.
49. Rojanala, S., Han, H., Munoz, R. M. et al. The mitotic serine threonine kinase, Aurora-2, is a potential target for drug development in human pancreatic cancer. *Mol.Cancer Ther*. 2004;3:451-457.
50. Adams, R. R., Maiato, H., Earnshaw, W. C. et al. Essential roles of Drosophila inner centromere protein (INCENP) and aurora B in histone H3 phosphorylation, metaphase chromosome alignment, kinetochore disjunction, and chromosome segregation. *J.Cell Biol*. 2001;153:865-880.
51. Tsuno, T., Natsume, A., Katsumata, S. et al. Inhibition of Aurora-B function increases formation of multinucleated cells in p53 gene deficient cells and enhances anti-tumor effect of temozolomide in human glioma cells. *J.Neurooncol*. 2007;83:249-258.
52. Hauf, S., Cole, R. W., LaTerra, S. et al. The small molecule Hesperadin reveals a role for Aurora B in correcting kinetochore-microtubule attachment and in maintaining the spindle assembly checkpoint. *J.Cell Biol*. 2003;161:281-294.
53. Ladygina, N. G., Latsis, R. V., and Yen, T. [Effect of the pharmacological agent hesperadin on breast and prostate tumor cultured cells]. *Biomed.Khim*. 2005;51:170-176.
54. Ditchfield, C., Johnson, V. L., Tighe, A. et al. Aurora B couples chromosome alignment with anaphase by targeting BubR1, Mad2, and Cenp-E to kinetochores. *J.Cell Biol*. 2003;161:267-280.
55. Gadea, B. B. and Ruderman, J. V. Aurora kinase inhibitor ZM447439 blocks chromosome-induced spindle assembly, the completion of chromosome condensation, and the establishment of the spindle integrity checkpoint in *Xenopus* egg extracts. *Mol.Biol.Cell*. 2005;16:1305-1318.
56. Harrington, E. A., Bebbington, D., Moore, J. et al. VX-680, a potent and selective small-molecule inhibitor of the Aurora kinases, suppresses tumor growth in vivo. *Nat.Med*. 2004;10:262-267.
57. Tyler, R. K., Shpiro, N., Marquez, R. et al. VX-680 inhibits Aurora A and Aurora B kinase activity in human cells. *Cell Cycle*. 2007;6:2846-2854.
58. Lee, E. C., Frolov, A., Li, R. et al. Targeting Aurora kinases for the treatment of prostate cancer. *Cancer Res*. 2006;66:4996-5002.
59. Arlot-Bonnemains, Y., Baldini, E., Martin, B. et al. Effects of the Aurora kinase inhibitor VX-680 on anaplastic thyroid cancer-derived cell lines. *Endocr.Relat Cancer*. 2008;15:559-568.
60. Lin, Y. G., Immaneni, A., Merritt, W. M. et al. Targeting aurora kinase with MK-0457 inhibits ovarian cancer growth. *Clin.Cancer Res*. 2008;14:5437-5446.
61. Pan, C., Yan, M., Yao, J. et al. Aurora kinase small molecule inhibitor destroys mitotic spindle, suppresses cell growth, and induces apoptosis in oral squamous cancer cells. *Oral Oncol*. 2008;44:639-645.
62. Gizatullin, F., Yao, Y., Kung, V. et al. The Aurora kinase inhibitor VX-680 induces endoreduplication and apoptosis preferentially in cells with compromised p53-dependent postmitotic checkpoint function. *Cancer Res*. 2006;66:7668-7677.
63. Rubin, E. H., Shapiro, G. I., Stein, M. N. et al. A phase I clinical and pharmacokinetic (PK) trial of the aurora kinase (AK) inhibitor MK-0457 in cancer patients. *J.Clin.Oncol*. 2006;24:Abstract 3009-
64. Giles, F. J., Cortes, J., Jones, D. et al. MK-0457, a novel kinase inhibitor, is active in patients with chronic myeloid leukemia or acute lymphocytic leukemia with the T315I BCR-ABL mutation. *Blood*. 2007;109:500-502.
65. Young, M. A., Shah, N. P., Chao, L. H. et al. Structure of the kinase domain of an imatinib-resistant Abl mutant in complex with the Aurora kinase inhibitor VX-680. *Cancer Res*. 2006;66:1007-1014.

66. Cheetham, G. M., Charlton, P. A., Golec, J. M. et al. Structural basis for potent inhibition of the Aurora kinases and a T315I multi-drug resistant mutant form of Abl kinase by VX-680. *Cancer Lett.* 2007;251:323-329.
67. Huang, X. F., Luo, S. K., Xu, J. et al. Aurora kinase inhibitory VX-680 increases Bax/Bcl-2 ratio and induces apoptosis in Aurora-A-high acute myeloid leukemia. *Blood.* 2008;111:2854-2865.
68. Papayannidis, C., Iacobucci, I., Soverini, S. et al. Innovative phase I study of concomitant and consecutive treatment with dasatinib and MK-0457 in refractory Ph+ CML and ALL patients. *J.Clin.Oncol.* 2009;27:Abstract 7080-
69. Carpinelli, P., Ceruti, R., Giorgini, M. L. et al. PHA-739358, a potent inhibitor of Aurora kinases with a selective target inhibition profile relevant to cancer. *Mol.Cancer Ther.* 2007;6:3158-3168.
70. Modugno, M., Casale, E., Soncini, C. et al. Crystal structure of the T315I Abl mutant in complex with the aurora kinases inhibitor PHA-739358. *Cancer Res.* 2007;67:7987-7990.
71. Gontarewicz, A., Balabanov, S., Keller, G. et al. Simultaneous targeting of Aurora kinases and Bcr-Abl kinase by the small molecule inhibitor PHA-739358 is effective against imatinib-resistant BCR-ABL mutations including T315I. *Blood.* 2008;111:4355-4364.
72. Cohen, R. B., Jones, S. F., von Mehren, M. et al. Phase I study of the pan aurora kinases (AKs) inhibitor PHA-739358 administered as a 24 h infusion without/with G-CSF in a 14-day cycle in patients with advanced solid tumors. *J.Clin.Oncol.* 2008;26:Abstract 2520-
73. De Jonge, M., Steeghs, N., Verweij, J. et al. Phase I study of the aurora kinases (AKs) inhibitor PHA-739358 administered as a 6 and 3-h IV infusion on Days 1, 8, 15 every 4 wks in patients with advanced solid tumors. *J.Clin.Oncol.* 2008;26:Abstract 3507-
74. Paquette, R., Shah, N., Sawyers, C. et al. PHA-739358: a pan-aurora kinase inhibitor. *Hematology Meeting Reports.* 2008;2:92-93.
75. Gianella-Borradori, A. Aurora kinase inhibitor: AS703569. *Hematology Meeting Reports.* 2008;2:90-91.
76. Renshaw, J. S., Patnaik, A., Gordon, M. et al. A phase I two arm trial of AS703569 (R763), an orally available aurora kinase inhibitor, in subjects with solid tumors: preliminary results. *J.Clin.Oncol.* 2007;25:Abstract 14130-
77. Sonet, A., Graux, C., Maertens, J. et al. Phase I, Dose-Escalation Study of 2 Dosing Regimens of AS703569, An Inhibitor of Aurora and Other Kinases, Administered Orally in Patients with Advanced Hematological Malignancies. 2008;
78. Howard, S., Berdini, V., Boulstridge, J. A. et al. Fragment-based discovery of the pyrazol-4-yl urea (AT9283), a multitargeted kinase inhibitor with potent aurora kinase activity. *J.Med.Chem.* 2009;52:379-388.
79. Tanaka, R., Squires, M. S., Kimura, S. et al. Activity of the multi-targeted kinase inhibitor, AT9283 on Imatinib-resistant CML models. 2008;
80. Foran, J. M., Ravandi, F., O'Brien, S. M. et al. Phase I and pharmacodynamic trial of AT9283, an aurora kinase inhibitor, in patients with refractory leukemia. *J.Clin.Oncol.* 2008;26:Abstract 2518-
81. Kristeleit, R., Calvert, H., Arkenau, H. et al. A phase I study of AT9283, an aurora kinase inhibitor, in patients with refractory solid tumors. *J.Clin.Oncol.* 2009;27:Abstract 2566-
82. Oslob, J. D., Romanowski, M. J., Allen, D. A. et al. Discovery of a potent and selective aurora kinase inhibitor. *Bioorg.Med.Chem.Lett.* 2008;18:4880-4884.
83. Robert, F., Verschraegen, C., Hurwitz, H. et al. A phase I trial of sns-314, a novel and selective pan-aurora kinase inhibitor, in advanced solid tumor patients. *J.Clin.Oncol.* 2009;27:Abstract 2536-
84. Jones, S. F., Burris, H. A., Dumez, H. et al. Phase I accelerated dose-escalation, pharmacokinetic (PK) and pharmacodynamic study of PF-03814735, an oral aurora kinase inhibitor, in patients with advanced solid tumors: Preliminary data. *J.Clin.Oncol.* 2008;26:Abstract 2517-
85. Manfredi, M. G., Ecsedy, J. A., Meetze, K. A. et al. Antitumor activity of MLN8054, an orally active small-molecule inhibitor of Aurora A kinase. *Proc.Natl.Acad.Sci.U.S.A.* 2007;104:4106-4111.
86. Hoar, K., Chakravarty, A., Rabino, C. et al. MLN8054, a small-molecule inhibitor of Aurora A, causes spindle pole and chromosome congression defects leading to aneuploidy. *Mol.Cell Biol.* 2007;27:4513-4525.

87. Jones, S. F., Cohen, R. B., Dees, E. C. et al. Phase I clinical trial of MLN8054, a selective inhibitor of Aurora A kinase. *J.Clin.Oncol.* 2007;25:Abstract 3577-
88. Cervantes, A., Macarulla, T., Rosello, S. et al. MLN8054, a selective inhibitor of Aurora A kinase: final results of a phase I clinical trial. 2008;
89. Macarulla, T., Rodriguez-Braun, E., Taberero, J. et al. Phase I pharmacokinetic (PK) and pharmacodynamic (PD) study of the selective aurora A kinase (AAK) inhibitor MLN8054 in patients with advanced solid tumors. *J.Clin.Oncol.* 2009;27:Abstract 2578-
90. Sells, T, Ecsedy, J. A., Stroud, Set al. MLN8237: An orally active small molecule inhibitor of aurora A kinase in phase I clinical trials. *Proc Am Assoc Cancer Res (AACR).* 2008;49:Abstract 2997-
91. Smith, M. A., Houghton, P. J., Morton, C. et al. Pediatric preclinical testing program (PPTP) stage 2 testing of the aurora A kinase inhibitor MLN8237. 2008;
92. Infante.J., Dees, E. C., Cohen, R. B. et al. Phase I study of the safety, pharmacokinetics (PK), and pharmacodynamics (PD) of MLN8237, a selective aurora A kinase inhibitor, in the United States. 2008;
93. Cervantes-Ruiperez, A., Elez, M. E., Rosello, S. et al. Phase I pharmacokinetic (PK) and pharmacodynamic (PD) study of MLN8237, a novel selective aurora A kinase (AAK) inhibitor, in patients (pts) with advanced solid tumors. *J.Clin.Oncol.* 2009;27:Abstract 2565-
94. Mortlock, A. A., Foote, K. M., Heron, N. M. et al. Discovery, synthesis, and in vivo activity of a new class of pyrazoloquinazolines as selective inhibitors of aurora B kinase. *J.Med.Chem.* 2007;50:2213-2224.
95. Keen, N., Brown, E., Crafter, C. et al. Biological characterisation of AZD1152, a highly potent and selective inhibitor of aurora kinase activity. *Clin.Cancer Res.* 2005;11:B220-
96. Wilkinson, R. W., Odedra, R., Heaton, S. P. et al. AZD1152, a selective inhibitor of Aurora B kinase, inhibits human tumor xenograft growth by inducing apoptosis. *Clin.Cancer Res.* 2007;13:3682-3688.
97. Walsby, E., Walsh, V., Pepper, C. et al. Effects of the aurora kinase inhibitors AZD1152-HQPA and ZM447439 on growth arrest and polyploidy in acute myeloid leukemia cell lines and primary blasts. *Haematologica.* 2008;93:662-669.
98. Yang, J., Ikezoe, T., Nishioka, C. et al. AZD1152, a novel and selective aurora B kinase inhibitor, induces growth arrest, apoptosis, and sensitization for tubulin depolymerizing agent or topoisomerase II inhibitor in human acute leukemia cells in vitro and in vivo. *Blood.* 2007;110:2034-2040.
99. Evans, R. P., Naber, C., Steffler, T. et al. The selective Aurora B kinase inhibitor AZD1152 is a potential new treatment for multiple myeloma. *Br.J.Haematol.* 2008;140:295-302.
100. Schellens, J. H., Boss, D., Witteveen, P. O. et al. Phase I and pharmacological study of the novel aurora kinase inhibitor AZD1152. *J.Clin.Oncol.* 2006;24:3008-
101. Soncini, C., Carpinelli, P., Gianellini, L. et al. PHA-680632, a novel Aurora kinase inhibitor with potent antitumoral activity. *Clin.Cancer Res.* 2006;12:4080-4089.
102. Gontarewicz, A., Balabanov, S., Keller, G. et al. PHA-680626 exhibits anti-proliferative and pro-apoptotic activity on Imatinib-resistant chronic myeloid leukemia cell lines and primary CD34+ cells by inhibition of both Bcr-Abl tyrosine kinase and Aurora kinases. *Leuk.Res.* 2008;32:1857-1865.
103. Rawson, T. E., Ruth, M., Blackwood, E. et al. A pentacyclic aurora kinase inhibitor (AKI-001) with high in vivo potency and oral bioavailability. *J.Med.Chem.* 2008;51:4465-4475.
104. Fu, D. H., Jiang, W., Zheng, J. T. et al. Jadomycin B, an Aurora-B kinase inhibitor discovered through virtual screening. *Mol.Cancer Ther.* 2008;7:2386-2393.
105. D'Alise, A. M., Amabile, G., Iovino, M. et al. Reversine, a novel Aurora kinases inhibitor, inhibits colony formation of human acute myeloid leukemia cells. *Mol.Cancer Ther.* 2008;7:1140-1149.
106. Kawasaki, A., Matsumura, I., Miyagawa, J. et al. Downregulation of an AIM-1 kinase couples with megakaryocytic polyploidization of human hematopoietic cells. *J.Cell Biol.* 2001;152:275-287.
107. Pang, L., Weiss, M. J., and Poncz, M. Megakaryocyte biology and related disorders. *J.Clin.Invest.* 2005;115:3332-3338.
108. Girdler, F., Sessa, F., Patercoli, S. et al. Molecular basis of drug resistance in aurora kinases. *Chem.Biol.* 2008;15:552-562.

Chapter 3.1

109. Warner, S. L., Munoz, R. M., Stafford, P. et al. Comparing Aurora A and Aurora B as molecular targets for growth inhibition of pancreatic cancer cells. *Mol.Cancer Ther.* 2006;5:2450-2458.
110. Girdler, F., Gascoigne, K. E., Eyers, P. A. et al. Validating Aurora B as an anti-cancer drug target. *J.Cell Sci.* 2006;119:3664-3675.
111. Kosik, A., Bekier, M. E., Katusin, J. D. et al. Investigating the role of Aurora kinases in RAS signaling. *J.Cell Biochem.* 2008;
112. Lu, L. Y., Wood, J. L., Ye, L. et al. Aurora A is essential for early embryonic development and tumor suppression. *J.Biol.Chem.* 2008;283:31785-31790.
113. Cochran, A. G. Aurora A: target invalidated? *Chem.Biol.* 2008;15:525-526.
114. Lentini, L., Amato, A., Schillaci, T. et al. Aurora-A transcriptional silencing and vincristine treatment show a synergistic effect in human tumor cells. *Oncol.Res.* 2008;17:115-125.
115. Hata, T., Furukawa, T., Sunamura, M. et al. RNA interference targeting aurora kinase a suppresses tumor growth and enhances the taxane chemosensitivity in human pancreatic cancer cells. *Cancer Res.* 2005;65:2899-2905.
116. Nair, J. S., Tse, A., Keen, N. et al. A novel Aurora B kinase inhibitor with potent anticancer activity either as a single agent or in combination with chemotherapy. *J.Clin.Oncol.* 2004;22:Abstract 9568-
117. Tao, Y., Zhang, P., Girdler, F. et al. Enhancement of radiation response in p53-deficient cancer cells by the Aurora-B kinase inhibitor AZD1152. *Oncogene.* 2008;27:3244-3255.
118. Dai, Y., Chen, S., Venditti, C. A. et al. Vorinostat synergistically potentiates MK-0457 lethality in chronic myelogenous leukemia cells sensitive and resistant to imatinib mesylate. *Blood.* 2008;112:793-804.
119. Fiskus, W., Wang, Y., Joshi, R. et al. Cotreatment with vorinostat enhances activity of MK-0457 (VX-680) against acute and chronic myelogenous leukemia cells. *Clin.Cancer Res.* 2008;14:6106-6115.
120. Zhang, M., Huck, J., Hyer, M. et al. Effect of Aurora A kinase inhibitor MLN8237 combined with rituximab on antitumor activity in preclinical B-cell non-Hodgkin's lymphoma models. *J.Clin.Oncol.* 2009;27:Abstract 8553-
121. Plummer, E. R., Calvert, H., Arkenau, H. et al. A dose-escalation and pharmacodynamic study of AT9283 in patients with refractory solid tumours. *J.Clin.Oncol.* 2008;26:Abstract 2519-
122. Robert, F., Hurwitz, H., Uronis, H. et al. Phase I trial of SNS-314, a novel selective inhibitor of aurora kinases A,B and C, in advanced solid tumor patients. 2008;
123. Carpinelli, P. and Moll, J. Aurora kinase inhibitors: identification and preclinical validation of their biomarkers. *Expert.Opin.Ther.Targets.* 2008;12:69-80.
124. Hsu, J. Y., Sun, Z. W., Li, X. et al. Mitotic phosphorylation of histone H3 is governed by Ipl1/aurora kinase and Glc7/PP1 phosphatase in budding yeast and nematodes. *Cell.* 2000;102:279-291.
125. Dong, Z. and Bode, A. M. The role of histone H3 phosphorylation (Ser10 and Ser28) in cell growth and cell transformation. *Mol.Carcinog.* 2006;45:416-421.
126. KinasePro website. <http://kinasepro.wordpress.com>

CHAPTER 3.2

Clinical evaluation of AZD1152, an intravenous inhibitor of aurora B kinase, in patients with solid malignant tumors

David S. Boss, Petronella O. Witteveen, Jana van der Sar, Martijn Lolkema, Emile E. Voest, Paul K. Stockman, Jan H. M. Schellens

Abstract

Purpose: To determine, for each of two dosing schedules, the dose-limiting toxicity (DLT) and maximum-tolerated dose (MTD) of AZD1152, an aurora B kinase inhibitor, and to evaluate its safety, biological activity and pharmacokinetics (PK).

Patients and Methods: Patients with advanced solid malignancies were treated with escalating doses (100 to 650mg) of AZD1152, administered as a 2-hr infusion every 7 days (schedule A) or every 14 days (schedule B). Safety was assessed throughout and PK evaluated for each schedule.

Results: Fifty-nine patients were treated; 19 in schedule A and 40 in schedule B. The MTDs were determined as 200 mg and 450 mg, respectively. Neutropenia (with or without fever) was the DLT and the most frequent toxicity in each schedule. Common Terminology Criteria of Adverse Events (CTCAE) grade ≥ 3 neutropenia occurred in 57.9% and 42.5% of patients in schedules A and B, respectively, and grade ≥ 3 leukopenia in 10.5% and 20%, respectively. Other AE, mainly hematological or GI toxicities, were generally of mild or moderate intensity. No deaths occurred as a result of an AE. No objective tumor responses were observed at any dose or schedule although stable disease was achieved in 15 patients (25%) overall. Systemic exposure to AZD115-hQPA was observed by 1 hour into the infusion, and exhibited linear PK.

Conclusions: AZD1152 was generally well tolerated on either regimen. Neutropenia was the most frequent and dose-limiting toxicity. Future investigations should explore AZD1152 as a monotherapy in hematological malignancies or as part of a combination regimen in solid tumors.

Introduction

The aurora kinase family is comprised of three highly conserved serine/threonine kinases (aurora A, Aurora B and Aurora C) that have key regulatory roles at critical points of the cell cycle (0,2). aurora A is commonly amplified in solid tumors and has been established as an oncogene, while aurora B overexpression leads to defects in mitosis and increased tumor invasiveness. The aurora kinases have been suggested as promising targets for cancer therapy due to their frequent overexpression in a variety of tumors (1). While aurora A has historically been most associated with tumorigenesis, several studies have highlighted a role for aurora B in oncogenic transformation (3,4).

Compared with more established inhibitors of cell division, such as the anti-tubulins (5), aurora-selective small molecule inhibitors have the potential to provide similar efficacy with fewer side effects, because they only target cells entering mitosis. Several small-molecule inhibitors of aurora kinases have been developed as anticancer agents, a number of which are being evaluated clinically (6). One of these, AZD1152, is an acetanilide substituted pyrazole-aminoquinazoline phosphate pro-drug that is converted to the active moiety hydroxy-quinazoline pyrazole anilide of AZD1152 (AZD1152-hQPA) in plasma (7). AZD1152-hQPA is a highly potent and selective inhibitor of aurora B compared with aurora A (8). Consistent with inhibition of aurora B kinase, addition of AZD1152-hQPA to tumor cells in vitro inhibits cytokinesis, but allows endoreduplication, such that large multinucleated giant cells are formed with greater than 4N DNA content. This phenomenon consequently reduces cell viability and ultimately induces apoptosis (8). In an in vivo panel, AZD1152 significantly inhibited the growth of human tumor xenografts (9). Together these data suggest that AZD1152 may exhibit activity against multiple tumor types, and a phase I study was undertaken to determine the MTD, DLT, PK profile, and recommended dosing schedule for further evaluation.

Patients and methods

Patient selection

Eligibility criteria included patients aged ≥ 18 years with histologically- or cytologically-confirmed solid malignancies refractory to standard therapy or for whom no standard therapy existed; World Health Organization (WHO) performance status of 0 to 2; at least one measurable or non-measurable site of disease as defined by modified Response Evaluation Criteria in Solid Tumors (RECIST) (10) (lesions ≥ 2 cm diameter were required for PET scan assessments); previous chemotherapy > 4 weeks before first dose; and adequate bone marrow, hepatic and renal function.

Trial design and procedures

This phase I, open-label, multi-centre, dose escalation study assessed the safety, tolerability, anti-tumor activity and PK of AZD1152 administered as 2 separate dosing schedules: schedule A, a 2-hour iv infusion given every 7 days and schedule B, a 2-hour iv infusion given every 14 days.

At screening, informed consent was obtained and a complete medical history, including concomitant medication, electrocardiograms, and WHO performance score was recorded. A physical examination, and routine clinical chemistry, hematology and urinalysis assessments were also performed, and these were repeated within 24 hours of each dose in cycle 1, before every first dose in subsequent cycles, and at withdrawal/study completion. AEs were monitored throughout the trial using CTCAE version 3.0. Patients could continue treatment with AZD1152 at the same dose for as long as they were considered by the investigator to be receiving benefit. Administration of G-CSF was not allowed during treatment with AZD1152. All patients were monitored until progression of disease, loss to follow-up, or commencement of another anticancer treatment.

Dosing schedules and dose escalation

The sequence of dosing schedules is presented in Figure 1. schedule A was conducted to determine the DLT and MTD of AZD1152, and used a modified accelerated titration design (11) with a starting dose (determined from animal toxicology studies) of 100 mg. Drug was administered on days 1, 8 and 15 of

a 21-day cycle with initial cohorts of 1 patient (until evidence of a \geq grade 2 drug-related toxicity) and subsequent cohorts of between 3 and 6 patients. When 2 or more patients from the same cohort experienced a DLT, this dose was defined as the non-tolerated dose and there were no further dose escalations. The dose level below the non-tolerated dose was defined as the MTD. The MTD established in schedule A was used as the starting dose for schedule B, and initial cohorts of 3 patients were given AZD1152 as a 2-hour IV infusion every 14 days of a 28-day cycle. Doses were escalated until evidence of a DLT at which point the dose level was expanded to 6. If no additional DLTs were observed, dose escalation continued. If 2 or more of the 6 patients experienced DLT, the next lower dose (the MTD) was expanded to 6 patients. Once determined, the MTD dose level was expanded further, and additional patients were treated to further evaluate the safety and tolerability of the MTD. It was originally intended that expansion at the MTD level would apply to both dose regimens (A and B); however, due to tolerability issues and dose delays, it was decided that only the MTD for schedule B would be expanded.

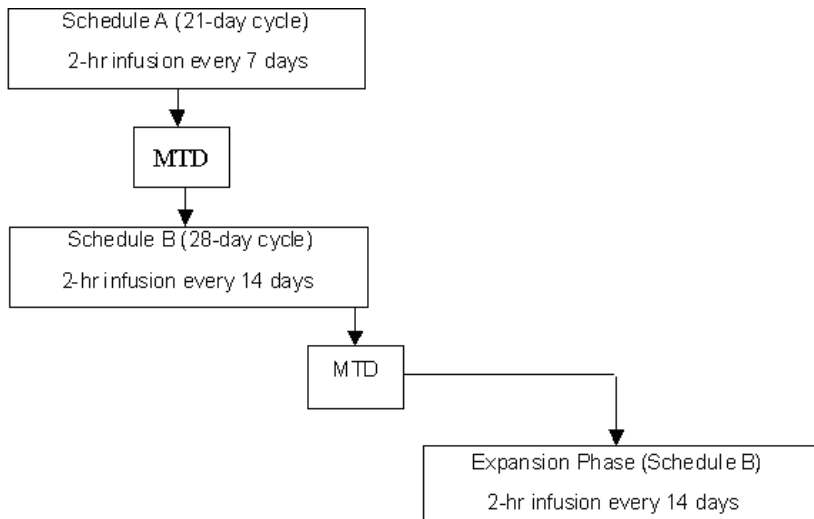


Figure 1: Sequence of dosing schedules
Abbreviation: MTD, maximum tolerated dose

Toxicity criteria

The incidence and severity of AEs were evaluated and coded according to the National Cancer Institute CTCAE, version 3.0. AZD1152-related DLT was defined as follows: any grade 4 toxicity (grade 4 neutropenia for > 3 days), grade \geq 3 neutropenia with fever, grade 3 or 4 thrombocytopenia associated with bleeding (excluding patients receiving systemic anticoagulation), or any grade 3 or 4 non-hematological toxicity. Any grade 3 liver function test (or \geq 2x baseline values for patients entered with abnormal liver enzymes) was also considered dose limiting, as was any drug-related toxicity resulting in a dose interruption in cycle 1 of more than 7 days.

Pharmacokinetic analysis

For each dosing schedule, plasma concentrations of AZD1152 and AZD1152-hQPA were determined following the first dose of AZD1152. Venous blood samples (4mL) were taken at the following times: pre-dose, 1hr after the start of the infusion, 5 minutes before the end of infusion (EOI) and at 0.25, 0.5, 0.75, 1, 1.5, 2, 3, 4, 6, 8, 10, 12, 20 and 22 hours following EOI. During the next 3 infusions (if given), blood samples were taken pre-dose, 5 minutes before EOI and 1, 3 and 6 hours after EOI.

Plasma PK parameters of AZD1152 and AZD1152-hQPA were determined by non-compartmental methods, using WinNonlin Enterprise Version 4.1 (Pharsight Corporation, Mountain View, CA, USA).

Tumor measurement and response evaluation

Tumor measurements were obtained at baseline by radiological techniques or, if appropriate, by physical examination. Tumor response was evaluated by RECIST criteria every 6-8 weeks. Each lesion measured at baseline was measured by the same method throughout the study so that the comparison was consistent. If a response was observed, a confirmation scan after 4-8 weeks was required. Data from patients with correlative serological biomarkers of their tumor (eg, PSA, CEA) were also collected; however, very few patients had sufficient measurements (baseline plus at least one follow-up visit) to allow accurate evaluation of these biomarkers as surrogates for tumor response. Attenuation-corrected FDG-PET scans (axial extent base of skull to mid femur) were performed after a fasting period of 6 hours. FDG-PET

assessments were performed only on patients entering the defined MTD cohort of schedule B within 7 days of receiving their first dose (baseline) and after completion of at least 1 cycle of treatment (post-treatment; Day 30 ± 3). Biological activity of AZD1152 was to be measured by comparison to the baseline scan.

Results

Patient characteristics

Baseline patient characteristics are listed in table 1 for each dosing schedule. In total, 59 patients received treatment, 19 in schedule A and 40 in schedule B (16 of these in the MTD expansion phase). In schedule A, 18/19 patients (94.7%) received at least 1 cycle of treatment across 4 dose levels (100, 200, 300 and 450 mg). Twelve patients (63.2%) received at least 2 cycles of treatment, and the maximum number of cycles received was 27, by 1 patient on 300 mg. Five of 19 patients (26.3%) had a dose reduction, and 13 (64.8%) had a dose delay. In schedule B, all 40 patients completed at least 1 cycle of treatment across 5 dose levels (200, 300, 450, 550 and 650 mg). Thirty-two of 40 patients (80%) received at least 2 cycles of treatment, and the maximum number of cycles received was 10, by 1 patient on 450 mg. Five of 40 patients (12.5%) had a dose reduction, and 6 (15%) had a dose delay. In each schedule, the maximum duration of dose delay was 2 weeks, and the majority of dose reductions or delays were due to neutropenia.

MTDs and DLTs

The MTD of AZD1152 was defined as 200 mg in schedule A, and 450 mg in schedule B. In each schedule the DLT was neutropenia (with or without fever, or causing a dose delay of > 7 days). Dose escalation sequences were as follows: Schedule A, 100 mg (1 patient, no DLT), 200 mg (6 patients, no DLTs), 300 mg (3 patients; no DLTs), 450 mg (6 patients, 3 DLTs), 300 mg, (3 patients, 2 DLTs); schedule B, 200 mg (4 patients, no DLTs), 300 mg (3 patients, no DLTs), 450 mg (7 patients, no DLTs), 650 mg (5 patients, 2 DLTs), 550 mg (5 patients, 2 DLTs). The 650 mg and 550 mg doses were confirmed as non-tolerated doses and the 450 mg dose expanded as the MTD. A subsequent 16 patients were treated at this dose.

Table 1: Patient characteristics

Characteristic	Dosing schedule A (N=19)		Dosing schedule B (N=40)	
	Patients		Patients	
	No.	%	No.	%
Sex				
Male	14	74	30	75
Female	5	26	10	25
Age, years				
median	59		59	
range	40-71		25-73	
Race				
Caucasian	19	100	38	95
Black	0	0	0	0
Oriental	0	0	2	5
Prior therapy*				
Chemotherapy+	19	100	32	80
Hormonal	4	21	2	5
Radiotherapy	10	53	19	48
WHO Performance Status				
0	1	5	9	23
1	16	84	28	70
2	2	11	3	8
Cancer Types				
Colorectal	8	42	9	23
Skin/soft tissue	3	16	10	25
Head & Neck	2	11	5	13
Prostate	2	11	0	0
Pancreas	1	5	3	8
Esophagus	1	5	2	5
Lung	0	0	3	8
Stomach	0	0	2	5
Other#	2	11	6	15

Abbreviations: WHO, World Health Organization.

*Patients may have had more than one prior therapy.

+ Patients may have had more than one kind of chemotherapy.

Schedule A: one patient each, pleura and renal; Schedule B: one patient each, bladder, pleura, renal, ureter, ovary, and adenocarcinoma of unknown primary

Adverse events and laboratory data

An overview of the adverse events that occurred during the study is shown in table 2. There were no deaths as the result of an adverse event in either schedule. In schedule A, all 19 patients had at least 1 adverse event.

Table 2: Number (%) of patients by dose and dosing schedule with at least 1 adverse event in any category

AE Category	DOSING SCHEDULE A Number (%) of patients* Dose (mg)				Total (N=19)	DOSING SCHEDULE B Number (%) of patients* Dose (mg)					Total (N=40)
	100 (N=1)	200 (N=6)	300 (N=6)	450 (N=6)		200 (N=4)	300 (N=3)	450 (N=23)	550 (N=5)	650 (N=5)	
Any AE	1	6 (100)	6 (100)	6 (100)	19 (100)	4 (100)	3 (100)	22 (96)	5 (100)	5 (100)	39 (98)
Any AE with CTC Grade 3 or 4	0	4 (67)	5 (83)	6 (100)	15 (79)	1 (25)	2 (67)	11 (48)	5 (100)	5 (100)	24 (60)
AE leading to death	0	0	0	0	0	0	0	0	0	0	0
Serious AE	0	1 (17)	0	2 (33)	3 (16)	0	2 (67)	7 (30)	1 (20)	1 (20)	11 (28)
Drug related	0	0	0	1 (17)	1 (5)	0	0	2 (9)	1 (20)	1 (20)	4 (10)
Any AE leading to drug withdrawal	0	1 (17)	0	2 (33)	3 (16)	0	1 (33)	2 (9)	1 (20)	0	4 (10)
Drug related	0	0	0	0	0	0	0	0	0	0	0

*Patients with multiple events in the same category are counted once in that category. Patient with events in more than one category are counted once in each of those categories

Table 3: Most frequent adverse events by dose and schedule occurring in ≥ 10% of patients

Preferred term	DOSING SCHEDULE A Number (%) of patients* Dose (mg)				Total (N=19)	Preferred term	DOSING SCHEDULE B Number (%) of patients* Dose (mg)				Total (N=40)	
	100 (N=1)	200 (N=6)	300 (N=6)	450 (N=6)			200 (N=4)	300 (N=3)	450 (N=23)	550 (N=5)		650 (N=5)
Neutropenia	0	4 (67)	5 (83)	4 (67)	13 (68)	Neutropenia	0	3 (100)	12 (52)	5 (100)	25 (63)	
Constipation	1 (100)	2 (33)	2 (33)	2 (33)	7 (37)	Nausea	3 (75)	1 (33)	11 (48)	3 (60)	4 (80)	22 (55)
Fatigue	0	3 (50)	1 (17)	2 (33)	6 (32)	Leukopenia	0	1 (33)	10 (44)	4 (80)	3 (60)	18 (45)
Diarrhea	0	2 (33)	3 (50)	0	5 (26)	Fatigue	0	1 (33)	11 (48)	1 (20)	2 (40)	15 (38)
Leukopenia	0	3 (50)	1 (17)	1 (17)	5 (26)	Pyrexia	3 (75)	1 (33)	9 (39)	1 (20)	1 (20)	15 (38)
Nausea	0	3 (50)	1 (17)	1 (17)	5 (26)	Vomiting	1 (25)	2 (67)	6 (26)	3 (60)	1 (20)	13 (33)
Vomiting	1 (100)	2 (33)	1 (17)	1 (17)	5 (26)	Alopecia	0	0	7 (30)	1 (20)	2 (40)	10 (25)
Pyrexia	0	1 (17)	1 (17)	2 (33)	4 (21)	Constipation	1 (25)	0	5 (22)	2 (40)	1 (20)	9 (23)
Alopecia	0	1 (17)	1 (17)	1 (17)	3 (16)	Proteinuria	2 (50)	0	4 (17)	2 (40)	1 (20)	9 (23)
Anemia	0	1 (17)	1 (17)	1 (17)	3 (16)	Nasopharyngitis	0	0	7 (30)	0	2 (40)	9 (23)
Cough	0	1 (17)	1 (17)	1 (17)	3 (16)	Anorexia	2 (50)	2 (67)	2 (9)	0	2 (40)	8 (20)
Dyspepsia	0	2 (33)	0	1 (17)	3 (16)	Cough	1 (25)	0	7 (30)	0	0	8 (20)
Hemoglobin decrease	0	1 (17)	1 (17)	1 (17)	3 (16)	Diarrhea	0	0	5 (22)	2 (40)	1 (20)	8 (20)
Abdominal pain	0	1 (17)	1 (17)	0	2 (11)	Abdominal pain	1	0	4 (17)	1 (20)	0	6 (15)
Abdominal pain upper	0	1 (17)	1 (17)	0	2 (11)	Anemia	0	0	4 (17)	1 (20)	1 (20)	6 (15)
Dry mouth	0	0	1 (17)	1 (17)	2 (11)	Hematuria	1 (25)	0	3 (13)	1 (20)	0	5 (13)
Eczema	0	0	2 (33)	0	2 (11)	Dyspnea	0	0	2 (9)	1 (20)	1 (20)	4 (10)
Headache	1 (100)	0	0	1 (17)	2 (11)	Flank pain	1 (25)	1 (33)	1 (20)	0	1 (20)	4 (10)
Hyperhidrosis	0	2 (33)	0	0	2 (11)							
Lymphadenopathy	0	2 (33)	0	0	2 (11)							
Paresthesia	0	1 (17)	1 (17)	0	2 (11)							
Stomatitis	0	2 (33)	0	0	2 (11)							

*Patients with multiple events in the same category are counted only once in that category; patients with events in more than one category are counted once in each of those categories

Three patients (16%) experienced serious adverse events (leukopenia, neutropenia, pyrexia and vomiting); one of these was considered to be drug related. Three patients (16%) had adverse events that led to drug withdrawal (lymphadenopathy, pulmonary embolism, pyrexia); none was considered to be related to AZD1152. In schedule B, 39 of 40 patients (98%) had at least 1 adverse event. Eleven patients (28%) had at least 1 serious adverse event. Of these, febrile neutropenia, leukopenia and sepsis were considered to be drug related. Four patients (10%) discontinued treatment as the result of adverse events (femur fracture and pyrexia, lumbar vertebral fracture, malaise and osteomyelitis); none was considered to be related to AZD1152. The most frequently reported adverse events ($\geq 10\%$ of patients) are listed in Table 3 by dose and schedule. These events, mainly of hematological or GI origin, were generally of mild or moderate intensity and included neutropenia, nausea, leukopenia, fatigue, pyrexia, constipation, vomiting and diarrhea; the profile of events was similar for each schedule. Fifteen of 19 patients (79%) in schedule A and 24 of 40 (60%) patients in schedule B experienced adverse events of CTCAE grade ≥ 3 (Table 4). The most common CTCAE Grade 3 or 4 events were neutropenia (58% and 43% of patients in schedules A and B, respectively) and leukopenia (11% and 20%, respectively). With the exception of neutropenia, there were no clinically relevant changes from baseline in any of the laboratory data.

Antitumor activity

No objective tumor response, as defined by RECIST criteria, was observed at any dose in either dosing schedule during this trial. The best response observed was stable disease, which occurred in 7 of 19 patients (37%) in schedule A (1 patient in the 100 mg group, and 2 in each of the 200, 300 and 450 mg groups), and 8 of 40 patients (20%) in schedule B (6 patients in the 450 mg group and 2 in the 650 mg group). Some of these patients remained stable over a long period of time, including a patient with adenoid cystic carcinoma treated at 200 mg in schedule A and a patient in schedule B with SCLC who had remained stable for 10 months by the time of the database lock. Progressive disease was observed in 7 patients (37%) in schedule A and 21 patients (53%) in schedule B. Five patients (26%) in schedule A and 11 patients (28%) in schedule B were unevaluable.

Table 4: Number (%) of patients by dose and dosing schedule with at least 1 adverse event of CTC ≥ Grade 3

Preferred term	DOSING SCHEDULE A Number (%) of patients* Dose (mg)				Total (N=19)	Preferred term	DOSING SCHEDULE B Number (%) of patients* Dose (mg)				Total (N=40)	
	100 (N=1)	200 (N=6)	300 (N=6)	450 (N=6)			200 (N=4)	300 (N=3)	450 (N=23)	550 (N=5)		650 (N=5)
At least 1 AE CTC ≥ Grade 3	0	4 (67)	5 (83)	6 (100)	15 (79)	At least 1 AE CTC ≥ Grade 3	1 (25)	2 (67)	11 (48)	5 (100)	5 (100)	24 (60)
Neutropenia	0	3 (50)	4 (67)	4 (67)	11 (58)	Neutropenia	0	2 (67)	5 (22)	5 (100)	5 (100)	17 (43)
Leukopenia	0	1 (17)	0	1 (17)	2 (11)	Leukopenia	0	0	1 (4)	4 (80)	3 (60)	8 (20)
ALT increased	0	1 (17)	0	0	1 (5)	Febrile neutropenia	0	0	1 (4)	1 (20)	1 (20)	3 (8)
AST increased	0	1 (17)	0	0	1 (5)	Fatigue	0	0	1 (4)	0	0	2 (5)
Back pain	0	1 (17)	0	0	1 (5)	Abdominal pain	0	0	1 (4)	0	0	1 (3)
Blood ALP increased	0	1 (17)	0	0	1 (5)	Anorexia	0	1 (33)	0	0	0	1 (3)
GGT increased	0	1 (17)	0	0	1 (5)	ASP increased	0	0	1 (4)	0	0	1 (3)
Granulocytopenia	0	0	1 (17)	0	1 (5)	Bacteremia	0	0	1 (4)	0	0	1 (3)
Musculoskeletal pain	0	0	1 (17)	0	1 (5)	Constipation	0	0	0	0	0	1 (3)
Neutrophil count increased	0	0	0	1 (17)	1 (5)	Cough	1 (25)	0	0	0	0	1 (3)
Pain in extremity	0	1 (17)	0	0	1 (5)	Drug toxicity	0	1 (33)	0	0	0	1 (3)
Pulmonary embolism	0	0	0	1 (17)	1 (5)	Dyspnea	0	0	1 (4)	0	0	1 (3)
Spinal cord compression	0	0	1 (17)	0	1 (5)	Int. vena caval occlusion	0	0	0	0	1 (20)	1 (3)
Vomiting	0	1 (17)	0	0	1 (5)	Intl norm. ratio increased	0	1 (33)	0	0	0	1 (3)
						Malaise	0	0	0	1 (20)	0	1 (3)
						Pain in extremity	0	0	1 (4)	0	0	1 (3)
						Pneumonia	0	0	1 (4)	0	0	1 (3)
						Post-op wound infection	0	0	1 (4)	0	0	1 (3)
						Pyrexia	0	0	1 (4)	0	0	1 (3)
						Sepsis	0	0	1 (4)	0	0	1 (3)
						Vomiting	0	0	1 (4)	0	0	1 (3)

* Patients with multiple events in the same category are counted only once in that category; patients with events in more than one category are counted once in each of those categories

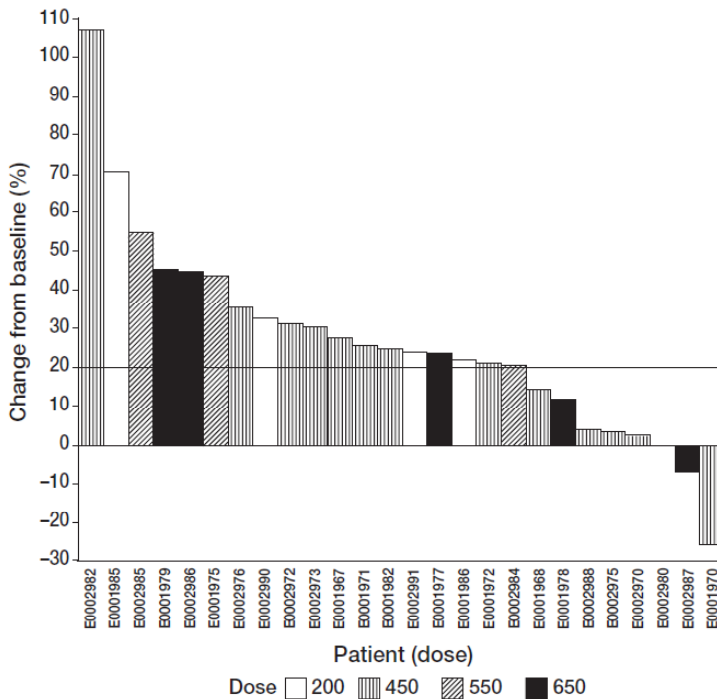


Figure 2: Percentage change in total lesion length from baseline to week 6 assessment (N=26/40). Schedule B: 2-hr infusion, once every 2 weeks

Figure 2 shows the percentage change in total lesion length from baseline to week 6 (± 7 days) for evaluable patients in schedule B.

Pharmacokinetics

Plasma PK parameters of AZD1152 and AZD1152-hQPA for schedule B are shown in table 5; these being similar for the equivalent doses for schedule A. After the end of infusion (EOI), plasma concentrations of AZD1152 declined rapidly with gmean terminal elimination half-lives of 3 to 9 hours; by 24 hours post dose concentrations were at, or approaching, the limit of quantification (LoQ) of the assay (0.25 ng/mL), irrespective of dose level.

Systemic exposure to AZD1152-hQPA was observed by the time of the first sample taken at 1 hour into the infusion with the maximum plasma concentration at the EOI. Plasma concentrations then declined in a biphasic manner with gmean terminal elimination half-lives of 6.5 to 7.4 hours; by 24 hours post dose they were still markedly higher than the LoQ with evidence of a 3rd phase with very low but quantifiable plasma concentrations in the pre-dose sample taken before the start of Cycle 2. The terminal half-life of this

phase was estimated to be about 50 hours. However, the majority of the exposure was determined up to 24 hours post dose and no accumulation of AZD1152-hQPA was observed for either regimen; for the MTD (schedule B) the gmean AUCs for Cycles 1 and 3 were similar, at 21780 and 19590 ng.h/mL, respectively. The exposure to AZD1152-hQPA was higher than that to AZD1152 by 2- to 6-fold, and this exposure increased with increasing dose in a dose-proportional manner. Both inter- and intra-patient variability in exposure was low; that for inter-patient ranging from 1.1- to 2.3-fold, and that for intra-patient up to a maximum of only 1.3-fold. The gmean plasma clearance of AZD1152-hQPA ranged from 15 to 27 L/h and the gmean volume of distribution at steady state ranged from 50 to 88 L.

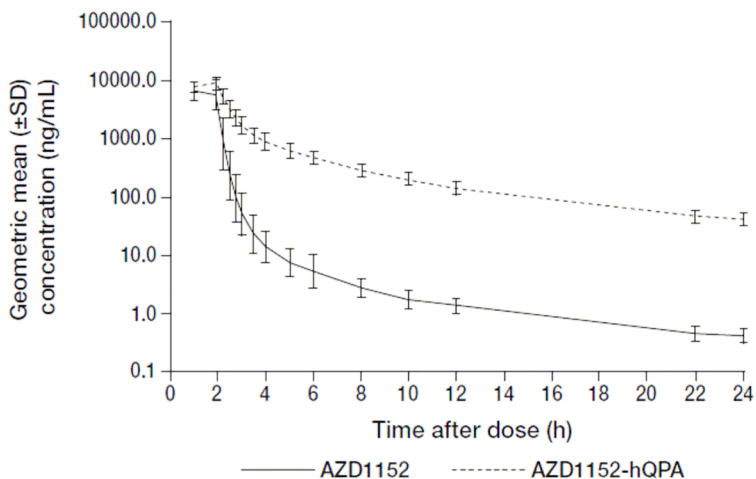


Figure 3: Geometric mean (\pm SD) plasma concentrations (ng/ml) versus time of AZD1152 and AZD1152-hQPA after a 2-hr infusion of 450 mg (MTD: Schedule B)

Other biologic activity

Thirteen of 23 patients receiving the MTD in schedule B (450 mg) had assessable baseline and follow-up FDG-PET scans. Changes in FDG-PET standard uptake value (SUVmax) averaged over lesions from baseline to post-dose for each of these patients showed no significant reduction in averaged SUVmax. However, one patient with SCLC had a 20% reduction in PET signal, most probably indicating anti-tumor activity of the study drug.

Table 5: Plasma pharmacokinetic parameters of AZD1152 and hQPA*, following a single 2-hr infusion every 2 weeks (Dosing Schedule B)

Parameter (unit)	200 mg (N=4)		300 mg (N=3)		450 mg (N=23)		550 mg (N=5)		650 mg (N=5)	
	AZD1152	hQPA	AZD1152	hQPA	AZD1152	hQPA	AZD1152	hQPA	AZD1152	hQPA
C_{max} (ng/mL)	Gmean (1168) (CV[%]) (19.4)	2879 (6.4)	2470 (50.0)	7696 (15.3)	7037 (34.9)	9215 (22.7)	6613 (42.8)	11230 (8.5)	11830 (24.8)	13010 (24.5)
AUC (ng.h/mL)	Gmean (1807) (CV[%]) (15.0)	7470 (4.5)	3572 (52.2)	19990 (11.7)	10460 (7.1)	21780 (22.6)	10620 (47.8)	30010 (1.9)	19280 (26.7)	33640 (23.4)
$t_{1/2}$ (h)	Gmean (4.785) (CV[%]) (65.0)	7.001 (4.2)	9.292 (5.0)	6.727 (11.4)	6.629 (16.1)	6.548 (18.7)	7.373 (19.9)	6.738 (23.5)	7.080 (8.7)	6.915 (12.1)
CL (L/h)	Gmean (110.7) (CV[%]) (16.3)	26.77 (4.4)	83.98 (43.0)	15.01 (11.6)	43.01 (46.6)	20.66 (20.5)	51.77 (71.6)	18.33 (1.9)	33.72 (34.2)	19.32 (23.7)
V_{ss} (L)	Gmean (53.31) (CV[%]) (33.6)	88.42 (7.5)	35.95 (27.0)	50.12 (16.2)	19.62 (63.2)	54.94 (22.6)	19.85 (81.1)	53.26 (21.8)	15.61 (55.4)	57.61 (28.4)

CV Coefficient of variation; NC Not calculable

Discussion

The most frequently reported CTCAE grade ≥ 3 adverse events in this study were neutropenia and leukopenia, toxicities that had been anticipated from preclinical experience with AZD1152, and that have also been observed clinically with other aurora kinase inhibitors (12,13,14). With the exception of neutropenia, there were no other clinically relevant changes in laboratory data. The number of patients who permanently discontinued study treatment due to a treatment-related adverse event was very low, although some patients required a dose reduction or dose delay due to an adverse event. The majority of patients received at least 2 cycles of treatment. It would be of interest to explore safety and antitumor activity of AZD1152 at higher exposure levels for which G-CSF could be used.

The best observed responses in this trial were prolonged disease stabilizations in several patients. Other researchers have also reported stable disease as the best response to aurora kinases in solid tumors but, as yet, no partial or complete responses have been observed (12,13,14). Preliminary results have recently been presented for a number of other inhibitors of aurora A or aurora B, including MLN8237 (15), AT9283 (16), AS703569 (R763) (17) SNS-314 (18) and PF-03814735 (19). The debate continues as to which of the aurora kinases, A or B, represents the best drug target: A recent publication addressing this issue came down in favor of aurora B (20).

The lack of clinical responses following treatment with aurora kinase inhibitors raises the question as to whether these drugs reach their target and, to answer this, future studies should employ biomarkers of response. Indeed, recent phase I trials using aurora kinase B inhibitors have used phosphorylation of histone H3 as a biomarker (14,16,19,21). This event is associated with aurora B activity, since aurora B directly phosphorylates histone H3 on serine 10, making it a useful tool for evaluating the degree of aurora B inhibition (22,23).

The lack of tumor responses in this study, as opposed to the impressive preclinical results, might be the result of differences between the growth rate of tumor cell lines *in vitro*, and tumor cells *in vivo*. It is anticipated from the working mechanism of AZD1152, that tumor cells need to proliferate a few times before they kill themselves. In preclinical models, tumors have an extremely high proliferation rate which makes them more susceptible to the

actions of AZD1152. In humans, however, the growth rate is slower and perhaps we need to be more patient and even accept initial growth before growth reduction is seen. This may explain the lack of responses in solid tumors whereas hematological malignancies may be more prone to respond.

With regards to the optimal treatment schedule for this class of agents, the present study investigated a 2-hour infusion. However, preclinical studies with AZD1152 have revealed prolonged drug administration to be more effective (AstraZeneca: Data on file) and a phase I study using the aurora kinase inhibitor AT9283 has also reported this (24). Phase I studies with prolonged infusions of AZD1152 are currently underway.

Whether efficacy exists if AZD1152 is used in combination with other drug classes remains to be seen. Treatment with AZD1152, was found to be synergistic with a variety of chemotherapeutic agents in preclinical studies, including irinotecan, docetaxel, vinorelbine, gemcitabine, oxaliplatin and 5-fluorouracil (25), and with vincristine and topoisomerase inhibitors in leukemia cell lines (26). Combining AZD1152 with radiotherapy might also provide a promising strategy, since the compound potentiates the radiation response in p53 deficient cancer cells (27). Further examination of tumor types that may be more susceptible to aurora kinase inhibitors is also warranted and would include hematological malignancies such as AML. Indeed, a recent report has shown evidence of aurora kinase activity in patients with imatinib-refractory CML and AML (24).

In summary, neutropenia and leukopenia were the main toxicities of AZD1152 in this patient population. Overall, the drug displayed a manageable tolerability profile on either dosing regimen, and there were no associated safety concerns that would preclude its further development. The data provide a good safety basis for future combination studies with AZD1152 in patients with solid tumors, or for future studies with AZD1152 monotherapy in patients with hematological malignancies.

References

1. Andrews PD. Aurora kinases: shining lights on the therapeutic horizon? *Oncogene* 2005;24:5005-15.
2. Carmena M, Earnshaw WC. The cellular geography of aurora kinases. *Nat Rev Mol Cell Biol* 2003;4:842-54.
3. Kanda A, Kawai H, Suto S, et al. Aurora-B/AIM-1 kinase activity is involved in Ras-mediated cell transformation. *Oncogene* 2005;24: 7266-7272.
4. Ota T, Suto S, Katayama H, et al. Increased Mitotic Phosphorylation of Histone H3 A ttributable to AIM-1/Aurora-B Overexpression Contributes to Chromosome Number Instability. *Cancer Res* 2002;62:5168-5177.
5. Wood KW, Cornwell WD, Jackson JR. Past and future of the mitotic spindle as an oncology target. *Curr Opin Pharmacol* 2001;1:370-7.
6. Gautschi O, Heighway J, Mack PC, et al. Aurora kinases as anticancer drug targets. *Clin Cancer Res* 2008;14:1639-1648.
7. Mortlock AA, Foote KM, Heron NM, et al. Discovery, synthesis and in vivo activity of a new class of pyrazoloquinazolines as selective inhibitors of aurora B kinase. *J Med Chem* 2007;50:2213-24.
8. Keen N, Brown E, Crafter C, et al. Biological characterization of AZD1152, a highly potent and selective inhibitor of aurora kinase activity. *Clin Cancer Res* 2005;11:B220.
9. Wilkinson RW, Odedra R, Heaton SP et al. AZD1152, a selective inhibitor of Aurora B Kinase, inhibits human tumor xenograft growth by inducing apoptosis. *Clin Cancer Res.*, 2007; 13 (12); 3682-3688.
10. Therasse P, Arbuck SG, Eisenhauer EA, et al. New guidelines to evaluate the response to treatment in solid tumors: European Organization for Research and Treatment of Cancer, National Cancer Institute of the United States, National Cancer Institute of Canada. *J Natl Cancer Inst* 2000;92:205-216.
11. Simon R, Freidlin B, Rubinstein L, et al. Accelerated titration designs for phase I clinical trials in oncology. *J Natl Cancer Inst* 1997;89:1138-1147.
12. Rubin EH, Shapiro GI, Stein MN, et al. A phase I clinical and pharmacokinetic (PK) trial of the aurora kinase (AK) inhibitor MK-0457 in cancer patients. *J Clin Oncol* 2006;24 (June 20 Supplement; abstr 3009).
13. De Jonge M, Steeghs N, Verweij J et al. Phase I study of the aurora kinases (AKs) inhibitor PHA-739358 administered as a 6 and 3-h IV infusion on Days 1, 8, 15 every 4 wks in patients with advanced solid tumors. *J Clin Oncol* 2008;26:(May 20 Suppl; abstr 3507).
14. Cohen RB, Jones SF, von Mehren M et al. Phase I study of the pan aurora kinases (AKs) inhibitor PHA-739358 administered as a 24 h infusion without/with G-CSF in a 14-day cycle in patients with advanced solid tumors. *J Clin Oncol* 2008;26:(May 20 Suppl; abstr 2520).
15. Infante J, Dees EC Cohen RB, et al. Phase I study of the safety, pharmacokinetics (PK), and pharmacodynamics (PD) of MLN8237, a selective Aurora A kinase inhibitor, in the United States. *Eur J Cancer suppl* 2008;6(12):Abstract 280.
16. Plummer ER, Calvert H, Arkenau H, et al. A dose-escalation and pharmacodynamic study of AT9283 in patients with refractory solid tumours. *J Clin Oncol* 2006;26:(May 20 suppl; abstr 2519).
17. Renshaw JS, Patnaik A, Gordon M et al. A phase I two arm trial of AS703569 (R763), an orally available aurora kinase inhibitor, in subjects with solid tumors: preliminary results. *J Clin Oncol* 2007;25:(June 20 Suppl; abstr 14130).
18. Robert F, Hurwitz H, Verschraegen CF et al. Phase I trial of SNS-314, a novel selective inhibitor of aurora kinases A, B and C in advanced solid tumor patients. *J Clin Oncol* 2008;26:(May 20 suppl; abstr 14642).
19. Jones SF, Burris III HA, Dumez H et al. Phase I accelerated dose-escalation, pharmacokinetic (PK) and pharmacodynamic study of PF-03814735, an oral aurora kinase inhibitor, in patients with advanced solid tumors; preliminary results. *J Clin Oncol* 2008;26:(May 20 suppl; abstr 2517).
20. Girdler F, Sessa F, Patercoli S, et al. Molecular Basis of Drug Resistance in Aurora Kinases. *Chem.Biol* 2008;15:552-562.
21. Robert F, Hurwitz H, Uronis H. Phase 1 trial of SNS-314, a novel selective inhibitor of Aurora kinases A, B, and C, in advanced solid tumor patients. *Eur J Cancer suppl* 2008;6(12) Abstract 283.

22. Hsu J-Y, Sun Z-W, Li X, et al. Mitotic phosphorylation of Histone H3 is governed by Ipl1/aurora Kinase and Glc7/PP1phosphatase in budding yeast and nematodes. *Cell* 2000;102:279-291.
23. Carpinelli P, Moll J. Aurora kinase inhibitors: identification and preclinical validation of their biomarkers. *Expert.Opin.Ther.Targets* 2008;12:69-80.
24. Foran JM, Ravandi F, O'Brien SM et al. Phase I and pharmacodynamic trial of AT9283, an aurora kinase inhibitor, in patients with refractory leukemia. *J Clin Oncol* 2008;26:(May 20 suppl; abstr 2518).
25. Nair JS, Tse A, Keen N, et al. A novel aurora B kinase inhibitor with potent anticancer activity either as a single agent or in combination with chemotherapy. *J Clin Oncol* 2004;45:851s, (suppl; abstr 9568).
26. Yang J, Ikezoe T, Kishioka C, et al. AZD1152, a novel and selective aurora B kinase inhibitor, induces growth arrest, apoptosis, and sensitization for tubulin depolymerizing agent or topoisomerase II inhibitor in human acute leukemia cells in vitro and in vivo. *Blood* 2007;110:2034-2040.
27. Tao Y, Zhang P, Girdler F, et al. Enhancement of radiation response in p53-deficient cancer cells by the Aurora-B kinase inhibitor AZD1152. *Oncogene* 2008;27:3244-3255.

4

The CDK inhibitor

AZD5438

CHAPTER 4.1

Safety, tolerability, pharmacokinetics and pharmacodynamics of the oral cyclin-dependent kinase inhibitor AZD5438 when administered at continuous and intermittent dosing schedules in patients with advanced solid tumors

David S. Boss, Gary K. Schwartz, Mark R. Middleton, Dereck D. Amakye, Helen Swaisland, Rachel S. Midgley, Malcolm Ranson, Susan Danson, Hilary Calvert, Ruth Plummer, Clive Morris, Richard D. Carvajal, Lucean R. Chirieac, Jan H.M. Schellens, Geoffrey I. Shapiro

Annals of Oncology. In press

Abstract

Background: AZD5438 is an orally bioavailable inhibitor of cyclin E-cdk2, cyclin A-cdk2 and cyclin B-cdk1 complexes. Three phase I studies assessed the clinical safety, tolerability, pharmacokinetics and pharmacodynamics of AZD5438 when administered in different dosing schedules.

Patients and methods: AZD5438 was administered four times daily, once every seven days (study 1), for 14 consecutive days followed by 7 days of rest (study 2), or continuously (study 3), to patients with advanced solid tumors. Dose escalation proceeded until the emergence of dose-limiting toxicities.

Results: Sixty-four patients were included across the three studies (19, 17, and 28, respectively). Nausea and vomiting were the most common adverse events. When dosed continuously, 40 mg four times daily was considered intolerable, and due to safety issues, all studies were terminated prematurely. Consequently, no intolerable dose was identified during the weekly schedule. Pharmacokinetics demonstrated dose proportional exposure, high inter-patient variability, and accumulation after multiple doses. Skin biopsies suggested reduced retinoblastoma protein phosphorylation at cdk2 phospho-sites, other pharmacodynamic assessments did not reveal consistent trends.

Conclusions: AZD5438 was generally well tolerated in a weekly dosing schedule, but not in continuous schedules. The clinical development program for AZD5438 was discontinued owing to tolerability and exposure data from these studies.

Introduction

Cyclins and cyclin-dependent kinases (CDKs) are core components of the cell cycle machinery, and drive the transition between cell cycle phases. During the progression from G1 to S, cyclin D- and cyclin E-dependent kinases 4, 6 and 2 sequentially phosphorylate the Rb protein (Rb) (1), disrupting pRb-mediated E2F-1 repression, and allowing transcription of genes required for S phase transit (2, 3). CDK2 also plays a role in S-phase and G2-phase progression, while CDK1 controls the G2/M transition (4). Dysregulation of cell cycle CDK activity occurs universally in human cancer (5) so that CDKs have generated considerable interest as novel anti-neoplastic targets (6, 7).

AZD5438, is an orally bio-available inhibitor of cyclin E-CDK2, cyclin A-CDK2 and cyclin B-CDK1 complexes (IC_{50} 0.006 μ M, 0.045 μ M and 0.016 μ M, respectively), with 75-fold selectivity over cyclin D1-CDK4 (IC_{50} 0.45 μ M) (8). AZD5438 inhibits phosphorylation of the CDK2 substrates pRb and p27^{Kip1}, and phosphorylation of the CDK1 substrates nucleolin and protein phosphatase 1 α , in a dose-dependent manner. In a panel of 23 cell lines (including lung, colorectal, breast, prostate and hematological tumor cells) IC_{50} 's varied from 0.17 μ M (MCF-7 human breast cancer) to 1.7 μ M (ARH-77 plasma cell leukemia). In exponentially growing tumor cells, acute exposure to AZD5438 induces S- and G2-phase arrest. G1 arrest is evident in synchronized tumor cell populations. These observations are consistent with a CDK1/2 inhibitory phenotype (9-11).

Preclinical and healthy volunteer studies (12) demonstrated a promising safety and efficacy profile, prompting clinical dose-escalation and scheduling studies. In this report, we describe three clinical studies investigating the safety and tolerability of AZD5438 in patients with advanced solid tumors. The studies assessed weekly dosing and continuous daily dosing schemes with and without varying periods off therapy.

In all three studies, AZD5438 was administered four-times daily. Preclinical data demonstrated that the daily dose could be split to either twice-daily or four-times daily dosing, while maintaining tumor growth inhibition and avoiding peak plasma drug concentration (C_{max}) effects. The most efficacious models were associated with evidence of a sustained reduction in the levels of phosphorylated Rb by approximately 50% for up to 16 hours post-dose.

Furthermore, in healthy volunteer studies, pharmacokinetics demonstrated a relatively short plasma half-life, with C_{max} achieved 0.5-3 hrs post-dose. Dose-limiting toxicity at 160 mg was nausea and vomiting, with only one episode of grade 1 nausea among subjects receiving either 60 or 80 mg. The 160 mg dose level was also associated with a trend toward an increased QTc interval (12). Pharmacodynamic data demonstrated up to 30% reduction in phosphorylated Rb levels in buccal mucosa biopsies at 1.5 hours after a 40 or 60 mg dose; this effect was not maintained at 6 hours post-dose (13). Taken together, the preclinical and clinical data suggested that four-times daily dosing could mitigate C_{max} -related toxicities, while sustaining target coverage despite the rapid elimination of AZD5438, and was therefore chosen for investigation.

Patients and methods

Patients

All three studies included patients aged ≥ 18 years of age with histologically or cytologically confirmed solid malignant tumors that were refractory to standard therapies, or for whom no standard treatment exists. Patients were required to have an Eastern Cooperative Oncology Group (ECOG) performance status of 0–2, adequate hematological, renal and hepatic function, and should have received no more than three prior cytotoxic chemotherapy regimens. Patients were excluded if they had active intracerebral metastases, treatment with potent cytochrome P-450 inhibitors or inducers or if they had received radiation or chemotherapy within 3 weeks of the start of study treatment. All patients provided written informed consent. The study was conducted in accordance with the Declaration of Helsinki, local institutional review board ethical approval, Good Clinical Practice and applicable regulatory requirements.

Study design

Three open-label, dose-escalation multi-centre phase I studies were performed. AZD5438 was administered orally in all studies. In study 1, cohorts of three or four patients received four doses of AZD5438 orally on day 1 and subsequently every 7 days. The starting dose was 40 mg/day in four divided doses (10 mg q.i.d., 50% of the maximum tolerated dose (MTD) observed in a previously conducted single ascending dose study in healthy volunteers). If a

dose limiting toxicity (DLT) was observed in one patient in a cohort within 21 days of commencing treatment, additional patients were to be recruited (to increase the cohort up to six) and treated at the same dose level. If a DLT was observed in two or more patients at a dose level, that dose was declared the non-tolerated dose (NTD) and no further dose escalation occurred. The maximum-tolerated dose (MTD) was defined as one dose level below the NTD. The cohort of patients at the MTD was expanded to six patients for confirmation. Using Common Terminology Criteria for Adverse Events (CTCAE), dose-limiting toxicities (DLTs) were defined as any of the following treatment-related events occurring during the first treatment cycle: Any grade 4 hematological event (excluding leucocytopenia and neutropenia if duration \leq 8 days); grade 3 or 4 neutropenia with fever; Thrombocytopenia associated with bleeding; grade \geq 2 vomiting (2–5 episodes in 24 hours) despite optimal anti-emetic therapy; any other grade 3 or 4 non-hematological event (including biochemical findings) despite adequate supportive care; unscheduled interruption of dosing of $>$ 7 days; QTc $>$ 500 ms or increase $>$ 60 ms. The dose escalation plans of studies 2 and 3, as well as the definitions for NTD, MTD and DLT were similar. In study 2, eligible patients received a single dose of AZD5438 on day 1 followed by four-times daily dosing for 14 consecutive days, followed by a 7-day rest period. The starting dose was 20 mg/day (5 mg q.i.d.), which was 25% of the maximum well-tolerated dose observed in the previously mentioned single-ascending dose study in healthy volunteers. In study 3, patients received a single dose of AZD5438 on the first day of the first cycle, followed by q.i.d. dosing thereafter in 28-day cycles, starting at 10mg/day (2.5 mg q.i.d.). With this lower dose, a dose-intensity comparable with study 2 was obtained.

Measurement of study variables

At enrollment, demographics were recorded, along with ECOG performance status, concomitant medications and radiological assessments from within the previous 28 days documented according to Response Evaluation Criteria in Solid Tumors (RECIST) (14). Each patient underwent a physical examination, measurement of vital signs; a pregnancy test if applicable and assessment of adequate contraception; resting ECG, standard biochemistry, urinalysis and hematology tests. Assessments were performed serially during study therapy. Electronic ECGs were collected and centrally analyzed prior to each dose-escalation decision. Adverse events (AEs) were reported according to the

National Cancer Institute CTCAE version 3.0. Tumor response was evaluated by RECIST every 8 weeks. No formal statistical analyses were performed.

Pharmacokinetics

Single-dose pharmacokinetic parameters were measured using venous blood samples taken prior to and at various time points following the first dose of AZD5438. In study 1, blood samples were taken on day 1 pre-dose and at 0.5, 1, 1.5, 2, 3, 4 and 5 hours post-dose. In studies 2 and 3 there was a single dose administered on day 1, enabling blood sampling up to 24 hours post dose. In these studies, blood samples were drawn on day 1 pre-dose and at 0.5, 1, 1.5, 2, 3, 4, 5, 8 and 24 hours post dose. In study 2, additional PK samples were taken on day 7 (pre-dose and 1.5 hours post-dose) and on day 14 (pre-dose and up to 5 hours post dose). In study 3, additional PK samples were taken at days 8, 15 and 22 (pre-dose and 1.5 hours post-dose), and on day 28 (pre-dose and up to 5 hours post-dose).

A validated high-performance liquid chromatography assay with tandem mass spectrometry detection was used to determine the total drug concentration in plasma. The following pharmacokinetic parameters were determined by non-compartmental analysis using WinNonLin version 3.1 (Pharsight corporation): maximum plasma concentration (C_{max}), time to reach the C_{max} (t_{max}), area under the plasma concentration–time curve from time zero to 5 hours ($AUC_{(0-5)}$), area under the plasma concentration–time curve from time zero to the time of the last measurable concentration ($AUC_{(0-t)}$), area under the plasma concentration–time curve from time zero to infinity (AUC), terminal half-life ($t_{1/2}$), total plasma clearance following oral dosing (CL/F) and volume of distribution at steady state following oral dosing (V_{dss}/F).

Exploratory pharmacodynamic endpoints

To investigate the effects of AZD5438 on various biomarkers in surrogate proliferating tissues, studies were performed in stimulated peripheral blood mononuclear cells (PBMCs) (in the presence of pre- and post-treatment plasma), as well as in hair follicles and keratinocytes. Peripheral blood samples were taken pre-dose on day 1, and 1.5 hours post first dose on days 1 and 8 (studies 1 and 3), or pre-dose on day 1, and 1.5 hours post first dose on days 1 and 7 (study 2). PBMCs were extracted and frozen together with autologous

plasma. Alternatively, stimulated healthy volunteer PBMCs were mixed with pre- and post-treatment plasma. Proliferation of PBMCs stimulated by OKT3 *ex vivo* in the presence of pre- and post-treatment plasma was assessed after a 48-hour incubation at 37°C by measuring the incorporation of ³H-thymidine into cellular DNA, administered with a 42-hour incubation pulse. Cells were harvested using a Tomtek 96 harvester and counted with a Wallac 1205 BetaPlate liquid scintillation counter. Additionally, levels of phosphorylated p27^{Kip1}, phosphorylated pRb and Ki67 were measured from scalp hair taken on days 1 and 8 of the first treatment cycle (study 1), on days 1 and 7 of the first treatment cycle (study 2), or on days 1 and 8 of every treatment cycle (study 3). Up to 40 hair follicles were plucked. Follicles in the first phase of the hair cycle were analyzed using methodology previously described (13). In a subset of participants treated at the Dana-Farber Cancer Institute (part of study 3), skin biopsies were performed pre-treatment and within 2 hours of the first dose on either day 15 or 22 of treatment and analyzed immunohistochemically for expression of phospho-Rb, total Rb, p27^{Kip1}, cyclin D1, p53 and Ki67, as previously described (15, 16).

Results

Early study termination

A review of emerging safety data from studies 2 and 3, as well as the available clinical pharmacokinetic and pharmacodynamic data, led to a decision by AstraZeneca to discontinue the development of AZD5438 as a potential anticancer agent. Therefore, all three studies described in this report were terminated prematurely.

Study population

A total of 64 patients with advanced solid malignancies, whose characteristics are summarized in table 1, were entered into the studies. Fifteen of the 19 patients who entered study 1 completed the first cycle (21 days). Four patients were removed during the first cycle due to non-drug related AEs ($n = 2$, 60 mg q.i.d. cohort) or disease progression ($n = 1$, 40 mg q.i.d. cohort; $n = 1$, 60 mg q.i.d. cohort), and were deemed not fully evaluable for toxicity and replaced. The 15 patients who completed the first cycle were later withdrawn from the study due to disease progression ($n = 13$), AEs ($n = 1$) or withdrawal

Table 1: Patient characteristics

Patient characteristics	Study 1 (N=19)	Study 2 (N=17)	Study 3 (N=28)
Median age, years (range)	57.5 (41–71)	61.3 (44–79)	58.3(33–84)
Male/female, <i>n</i>	12/7	12/5	18/10
Race/ethnicity,			
Caucasian	19	16	26
Asian (non-Japanese)		1	1
Black			1
Primary tumor location, <i>n</i>			
Lung	5		3
Pancreas	5		
Colorectal	4	4	7
Renal		4	
Skin/soft tissue			3
Adrenal			2
Head & Neck			2
Esophagus			2
Other	5	9	9

of consent ($n = 1$). Five patients died during the study: four due to disease progression (40 mg q.i.d., $n = 1$; 60 mg q.i.d., $n = 3$), and one due to pneumonia CTC grade 4 (60 mg q.i.d.).

Seventeen patients were enrolled in study 2, of whom three (all from the 40 mg q.i.d. cohort) did not complete the first cycle due to intestinal obstruction ($n = 1$), disease progression ($n = 1$), and fatal acute renal failure ($n = 1$). The 14 patients who completed the first cycle were later discontinued for disease progression ($n = 11$), intercurrent illness ($n = 1$), nausea and vomiting ($n = 1$) and premature study termination ($n = 1$).

Twenty-eight patients were enrolled in study 3. Thirteen patients did not complete the first treatment cycle: two in the 10 mg q.i.d. cohort due to disease progression; seven in the 20 mg q.i.d. cohort due to withdrawal of consent ($n = 3$), disease progression ($n = 2$), and AEs ($n = 2$); and four in the 40 mg q.i.d. cohort due to withdrawal of consent ($n = 2$) and AEs ($n = 2$). The 15 patients who completed the first cycle were later discontinued for disease progression ($n = 13$), withdrawal of consent ($n = 1$) and discontinuation at the investigator's discretion ($n = 1$). Three patients died during study 3; one due

to disease progression and two due to AEs detailed below. Dose-levels and numbers of enrolled are shown in table 2.

Table 2: Dose escalation schemes

Dose-escalation schemes			
Study 1: weekly dosing			
Dose level, mg q.i.d.	Patients, <i>n</i>	Number of days on treatment*, range	Number of patients with DLT in cycle 1
10	3	36–106	0
20	3	51–106	0
40	4	8–58	0
60	6	1–141	0
90	3	50–106	0
Study 2: fourteen days continuous dosing, one week rest			
Dose level, mg q.i.d.	Patients, <i>n</i>	Number of days on treatment*, range	Number of patients with DLT in cycle 1
5	3	55–77	0
10	3	55–98	0
20	3	55–119	0
40	8	5–161	2 (G2 nausea and vomiting; G5 acute renal failure)
Study 3: continuous dosing			
Dose level, mg q.i.d.	Patients, <i>n</i>	Number of days on treatment*, range	Number of patients with DLT in cycle 1
2.5	3	35–56	0
5	3	29–56	0
10	5	19–87	0
20	11	1–226	0
40	6	3–56	2 (fatal pericarditis; G3 fatigue)

DLT, dose-limiting toxicity.

*Period from first to last dose of AZD5438 treatment.

Safety and tolerability

In all three studies, the most frequently reported treatment-emergent AEs were gastrointestinal in origin (table 3), and most were CTC grade 1–2. The number of patients reporting gastrointestinal AEs increased in a dose-

dependent manner. When administered four times daily once every week (study 1), AZD5438 was well tolerated up to doses of 90 mg q.i.d. At this dose, CTC grade 3 fatigue was reported, although none of the other observed safety findings over the dose range of 10-90 mg q.i.d. satisfied DLT criteria. Also, no treatment-related SAEs were reported. Due to early study termination, neither the NTD nor MTD was established for this schedule.

Administration of AZD5438 four times daily in continuous schedules (studies 2 and 3) led to substantially increased toxicities. All 17 patients who received AZD5438 in study 2 experienced at least one AE. Most AEs were mild to moderate (CTC grade 1 or 2, see Table 3). Eleven patients experienced AEs considered to be related to study drug, including nausea ($n = 7$), vomiting ($n = 4$), fatigue ($n = 2$) and lethargy ($n = 2$). DLTs were encountered at 40 mg q.i.d. in two patients (CTC grade 2 nausea and vomiting and CTC grade 5 acute renal failure). The first patient, a 48-year-old female diagnosed with advanced breast cancer with liver and bone metastasis, reported nausea, anorexia, fatigue and diarrhea 4 days after initiating AZD5438 treatment. Despite anti-emetic treatment, her symptoms deteriorated, resulting in admission to hospital on day 5. Lactate dehydrogenase and C-reactive protein were elevated (337 UI/l and 95 mg/l, respectively), alkaline phosphatase, aspartate aminotransferase and alanine aminotransferase levels increased transiently, and serum sodium levels decreased to 126 mmol/l. There were ECG features of pericarditis without evidence of myocardial infarction (normal creatinine kinase, troponin-T and echocardiogram). These symptoms resolved after study treatment was stopped.

The second patient, a 67-year-old woman with metastatic colorectal carcinoma and a history of pulmonary embolism, reported lethargy and nausea from the first day of therapy, with vomiting from day 3 despite anti-emetic treatment. On day 5 she complained of increased weakness, reduced fluid intake, diaphoresis and generalized abdominal pain. On admission to hospital she was dehydrated, hypotensive (blood pressure 84/60 mmHg) and tachycardic (heart rate 125 bpm). Chest x-ray was normal, ECG showed sinus tachycardia, and chemistries showed serum creatinine of 252 mmol/l (baseline 102 mmol/l), normal serum electrolytes (K^+ and Na^+), and slightly elevated blood urea (12.5 mmol/l). Despite fluid therapy (central venous pressure +10 and recovery of blood pressure) the patient remained anuric. There was no response to high-dose furosemide, and serum creatinine elevated further to

Table 3: Treatment-emergent adverse events occurring in ≥3 patients irrespective of causality

Number of patients experiencing AE	Study 1 AZD5438 dose (mg, q.i.d.)						Study 2 AZD5438 dose (mg, q.i.d.)						Study 3 AZD5438 dose (mg, q.i.d.)					
	10 (3)	20 (3)	40 (4)	60 (6)	90 (3)	Total n (%) (19)	5 (3)	10 (3)	20 (3)	40 (8)	Total n (%) (17)	2.5 (3)	5 (3)	10 (5)	20 (11)	40 (6)	Total n (%) (28)	
Nausea	1	3	3*	4	2	13 (68)	1	2	3	7*	13 (76)	1	1	3	5	4	14 (50)	
Vomiting	0	1	3*	4	3	11 (58)	1	0	2	4	7 (41)	1	0	4	4*	3	12 (43)	
Diarrhoea	1	1	0	4*	1	7 (37)	0	0	1	3	4 (24)	1	0	0	1	2	4 (14)	
Constipation	2	1	2*	1	0	6 (32)	0	1	1	3	5 (29)	1	0	2	3	0	6 (21)	
Abdominal pain	0	0	0	2	1	3 (16)	0	0	0	3	3 (18)							
Fatigue	1	1	1	1	2*	6 (32)	1	1	1	5	8 (47)	1	2	2	5	5*	15 (54)	
Pyrexia	0	2	0	3	0	5 (26)	0	0	0	3	3 (18)	0	0	1	1	2	4 (14)	
Nasopharyngitis	1	1	1	0	1	4 (21)												
Anorexia	0	0	1	1	1	3 (16)	0	2	2	3	7 (41)	0	0	1	3*	1	5 (18)	
Back pain	0	0	0	3*	0	3 (16)	1	0	1	1	3 (18)							
Headache	1	0	2	0	2	5 (26)	1	0	1	1	3 (18)	0	0	1	2	1	4 (14)	
Urinary retention	0	0	1	2	0	3 (16)												
Dyspnoea	1	0	0	1*	1 [†]	3 (16)						0	0	1*	2	2	5 (18)	
Lethargy							1	1	2	1	5 (29)							
Cough							1	0	0	3	4 (24)	1	0	1	1	0	3 (11)	
Dyspepsia							1	0	1	1	3 (18)							
Dehydration							0	0	0	2	1	0	0	0	2	1	3 (11)	
Dizziness							0	1	0	2	0	0	1	0	2	0	3 (11)	
Oedema							0	1	0	1*	1	0	1	0	1*	1	3 (11)	

AE, adverse event. All AEs were CTC grade 1 or 2 except for CTC grade 3 AEs (n=1) in categories marked*, and a single CTC grade 4 AE in the category marked[†].

404 mmol/l within 12 hours of admission. Further aggressive management and dialysis were declined. The patient deteriorated and died on day 6. Blood culture was negative and C-reactive protein was elevated markedly (220 mg/l, baseline unknown). The cause of death was dehydration and acute renal failure, which was deemed to be study treatment related. Post-mortem exam was not performed.

Of the six other patients treated with 40 mg q.i.d., two experienced elevations in C-reactive protein, white cell count and serum creatinine, which resolved after cessation of treatment. Treatment was resumed at 20 mg q.i.d. in one patient without recurrence of the elevations; the other patient was not re-treated with AZD5438. As DLTs were experienced by two out of six evaluable patients at 40 mg q.i.d., this dose was considered to be the NTD for the 14-days-on, 7-days-off schedule. The MTD could not be established due to study termination.

A total of 166 AEs were reported by 27 patients during study 3. Consistent with the other studies, the majority of AEs were gastrointestinal in origin, with the number of reports increasing in a dose-dependent manner. Of these, the AEs considered to be causally related to AZD5438 by the investigator were nausea ($n = 8$ patients), vomiting ($n = 7$ patients), diarrhea ($n = 3$ patients) and abdominal pain ($n = 1$ patient). Six patients experienced a total of nine non-fatal SAEs, of which myocardial ischemia, CTC grade 2 (20 mg q.i.d.), in a patient with hypertension, was considered to be possibly related to the study drug.

Two patients died due to AEs. The first patient was a 53-year-old female in the 20 mg q.i.d. cohort with a primary tumor of the ampulla of Vater, who had a history of hypertension and rheumatic heart disease. On study day 4, she reported worsening bouts of vomiting that had started on day 1, following initiation of study treatment. AZD5438 was discontinued and she received i.v. fluids. Hours later, she became lethargic and confused, with respiratory distress, hypoxia, hypotension, hyponatremia, marked leukocytosis, increased serum creatinine and markedly elevated aspartate aminotransferase, D-dimer and brain natriuretic peptide levels. ECG initially showed no acute changes, but there was evidence of previous myocardial infarction. Despite intubation, intravenous fluids and antibiotics, she decompensated and died on day 5. ECG showed changes consistent with acute myocardial infarction. No post-mortem

examination was performed. In the opinion of the investigator, a pulmonary embolism may have caused hypoxia and right heart failure (high BNP) with passive liver congestion (elevated aspartate aminotransferase). Additionally, with a history of rheumatic heart disease and strong family history for coronary artery disease, this patient may have suffered a myocardial infarction, leading to fatality. The event was not considered to be related to AZD5438.

The second patient, a 58-year-old female in the 40 mg cohort, died on study day 4. This patient, with previously untreated liposarcoma with liver metastases, had a medical history of hysterectomy, tubal ligation, and three radical resections of retroperitoneal sarcoma (including right nephrectomy and adrenalectomy). Following initiation of AZD5438, she experienced a prodrome of fatigue, nausea and vomiting, which progressively worsened. On admission on day 3, study treatment was stopped. At presentation, she was hypotensive with white blood cell count 20,000 and elevated serum creatinine. ECG showed no acute changes, but low voltage, with unremarkable echocardiogram. Chest x-ray showed bilateral hilar infiltrates suggestive of aspiration pneumonia. Despite treatment for septic shock with antibiotics, pressors and a TNF α inhibitor, she became acidotic and anuric and died on day 4. Blood cultures were negative. A post-mortem examination concluded that the cause of death was pericarditis. The investigator considered this fatal event to be treatment-related, and therefore a DLT.

A second DLT was also observed in the 40 mg q.i.d. cohort presented as severe fatigue, CTC grade 3. This episode of fatigue, in a 60-year-old male with esophageal carcinoma and liver metastases, emerged on treatment day 3, after nausea and vomiting the previous day. The condition improved significantly following discontinuation of study therapy. As a result of these DLTs, AZD5438 40 mg q.i.d. was delineated as the NTD for the continuous dosing schedule. Due to the premature termination of this study, the MTD was not established.

Pharmacokinetics

Pharmacokinetic data obtained following administration of single oral doses (all three studies) and multiple oral doses (studies 2 and 3) of AZD5438 are summarized in Table 4. Absorption of AZD5438 after single oral doses was

Table 4: Derived pharmacokinetic parameters following administration of a single dose and multiple doses of ADZ5438.

Single dose (studies 1, 2 and 3)	ADZ5438 dose							
	2.5 mg Study 3	5 mg Studies 2+3	10 mg All studies	20 mg All studies	40 mg All studies	60 mg Study 1 only	90 mg Study 1 only	
C_{max} (ng/ml)	14.2 median (range) n	21.3 (12.5-37.5) 6 1	88 (10.7-182) 11 1	134 (30.9-301) 17 1.5	261 (25.1-754) 18 1.0	708 (239-1690) 6 1.0	438 (51.3-602) 3 1.0	
T_{max} (h)	1.0 median (range) n	1.25 (1.0-2.0) 3 6	1.0 (0.5-2.0) 11 1	1.5 (0.5-3.25) 17 1.5	1.0 (0.5-4.0) 18 1.0	1.0 (0.5-1.5) 6 1.0	1.0 (0.5-2.0) 3 1.0	
AUC (ng·h/ml)	62.9 median (range) n	89.3 (53.0-342) 5 1	256 (44.4-715) 9 1	411 (107-3246) 16 1	1028 (59.8-4550) 15 1	1655 (346-2964) 2 1	751 (109-1393) 2 1	
$AUC_{(0-5)}$ (ng·h/ml)	38.8 median (range) n	44.9 (34.7-121) 6 1	169 (34.1-382) 10 1	303 (88.9-942) 17 1	724 (50.7-1607) 18 1	2220 (343-4510) 6 1	1179 (100-1272) 2 1	
Half-life (h)	2.32 median (range) n	2.54 (1.68-7.24) 3 1	2.09 (1.27-5.28) 9 1	2.0 (1.31-8.09) 17 1	2.60 (1.31-7.61) 15 1	1.27 (0.72-0.82) 2 1	1.18 (1.01-1.34) 2 1	
CL/F (l/h)	172 median (range) n	56 (14.6-94.4) 5 1	39.1 (14.0-225) 9 1	49 (6.2-188) 16 1	38.9 (8.8-669) 15 1	96.6 (20.2-173) 2 1	444 (64.6-824) 2 1	
V_{dss}/F (l)	511 median (range) n	321 (144-662) 5 1	113 (64.7-839) 9 1	168 (73.2-690) 16 1	136 (70.4-1851) 15 1	126 (61.8-190) 2 1	1203 (143-2262) 2 1	
AZD5438 dose								
Multiple doses (Studies 2 and 3)	2.5 mg Study 3	5 mg Study 2	5 mg Study 3	10 mg Study 2	10 mg Study 3	20 mg Study 2	40 mg Study 2	40 mg Study 3
C_{mass} (ng/ml)	24.2 median (range) n	33.5 (33-41.2) 3 1	27.7 (22.1-36.8) 3 1	135 (22.3-284) 3 1	150 (97.3-202) 2 1	177 (86.9-197) 3 1	178.5 (173-184) 2 1	155 (72.4-171) 3 1
T_{mass} (h)	0.5 median (range) n	1.0 (0.5-1.5) 3 1	1.0 (0.5-1.0) 3 1	2.0 (0.5-2.0) 3 1	1.25 (1.0-1.5) 2 1	1.0 (1.0-3.0) 3 1	0.75 (0.5-1.0) 2 1	1.0 (1.0-2.0) 3 1
$AUC_{(0-5)}$ (ng·h/ml)	58.7 median (range) n	94.9 (93.0-95.5) 3 1	62.2 (36.7-110) 3 1	422 (53.3-809) 3 1	411 (309-531) 1 1	420 (309-531) 2 1	367 (115-426) 1 1	392 (115-426) 3 1
$C_{min,ss}$ (ng/ml)	5.39 median (range) n	7.84 (0.5-21.1) 3 1	4.53 (2.19-15.1) 3 1	78.9 (7.09-92.9) 3 1	33.9 (54.2-318) 1 1	71.3 (3.9-47.5) 3 1	16.3 (1.08-2.28) 1 1	32.8 (0.78-1.08) 3 1
Predictability	0.59 median (range) n	1.06 (0.25-0.94) 2 1	0.51 (0.32-0.69) 2 1	0.70 (0.59-1.46) 3 1	0.90 (1.08-2.28) 2 1	1.68 (1.08-2.28) 2 1	0.82 (0.78-1.08) 1 1	0.89 (0.78-1.08) 3 1
Accumulation ratio	1.51 median (range) n	2.65 (1.07-2.16) 3 1	0.91 (0.89-1.3) 3 1	1.1 (0.76-2.64) 3 1	1.11 (1.61-3.48) 1 1	2.55 (1.61-3.48) 2 1	0.92 (1.08-1.40) 1 1	1.21 (1.08-1.40) 3 1

AUC, area under the plasma concentration-time curve; $AUC_{(0-5)}$, area under the plasma concentration-time curve from time zero to 5 hours; CL/F, total apparent drug clearance; C_{max} , maximum plasma drug concentration; C_{mass} , maximum plasma drug concentration at steady state; $C_{min,ss}$, minimum plasma drug concentration at steady state; t_{max} , time to reach maximum plasma drug concentration; t_{mass} , time to reach maximum plasma drug concentration at steady state; V_{dss}/F , apparent volume of distribution at steady state. *Concentration present at 5 hours after dosing; †Assessment of how well predicted the multiple-dose exposure is from the single-dose data (ratio of day 14 $AUC_{(0-5)}$: day 1 AUC for study 2 and ratio of day 28 $AUC_{(0-5)}$: day 1 AUC for study 3).

rapid, with time to maximum plasma drug concentration generally ranging between 0.5 and 4 hours post-dose across the doses studied. Beyond the peak, plasma concentrations declined rapidly over the time period studied (up to 24 hours after dose administration). The half-life ranged from 0.72 to 8.09 hours. The variability in exposure between patients within a dose cohort was high (figure 1), but exposure (area under the plasma concentration–time curve [AUC] and maximum plasma drug concentration [C_{max}]) generally increased with increasing dose.

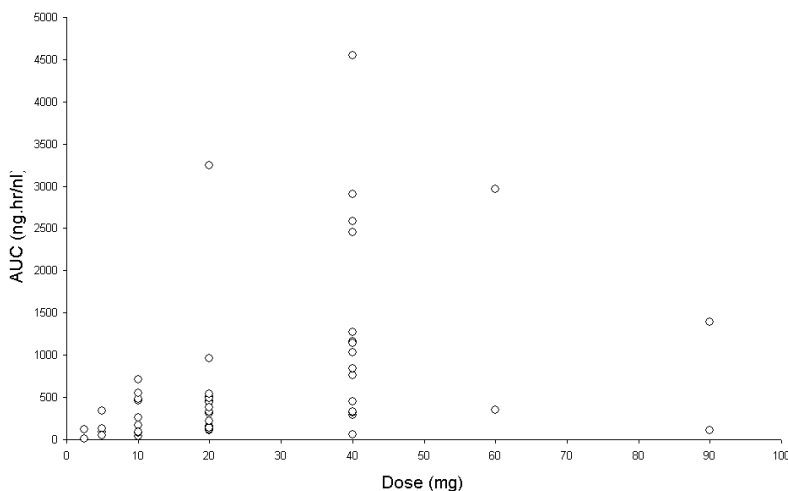


Figure 1: The area under the curve (AUC) as a function of AZD5438 dose. The AUCs were calculated after a single dose of AZD5438, on day 1 of treatment. There is a dose-proportional increase in exposure, but a high inter-patient variability in exposure to AZD5438.

Following multiple oral dosing of AZD5438, C_{max} was again achieved rapidly after dosing with concentrations declining rapidly thereafter. Consistent with the single-dose data, exposure following multiple dosing of AZD5438 increased with increasing dose. Comparison of the plasma drug concentrations achieved on days 7 and 14 (study 2) and on days 8, 15 and 22 compared with drug levels obtained on day 29 (study 3) indicated that steady state was achieved within the first 7 days of dosing with AZD5438.

An assessment of the predictability of multiple-dose exposure from the single-dose data (ratio of day 14 AUC (study 2) or day 28 AUC (study 3) from time zero to 5 hours to day-1 AUC for the same patient) showed that multiple-dose pharmacokinetics were not well predicted from single-dose pharmacokinetics.

Accumulation occurred in some patients following multiple oral dosing of AZD5438 q.i.d. for 14 consecutive days (study 2) or continuously for 28 days (study 3). Among nine patients evaluated in study 2, the accumulation ratio ranged from 0.76 to 3.48; in eleven patients evaluated in study 3, the accumulation ratio ranged from 0.86 to 2.16.

Tumor response

In all three studies, no objective responses were observed. Overall, 26 patients could not be evaluated for tumor response as they withdrew early. Of the 38 evaluable patients, 24 had progressive disease and 14 had stable disease as best response (supplementary table 1).

Exploratory pharmacodynamic findings

Evaluation of stimulated patient PBMCs combined with autologous plasma was not possible across the three studies because the majority of PBMC samples had few or no viable cells. An alternative method involved using stimulated PBMCs from a healthy volunteer donor in combination with the patients' pre- and post-treatment plasma to assess the drug effect. By this approach, plasma samples from 12 patients in study 1 generated informative data (stimulated proliferation counts >5000 cpm) at three time points. However, no consistent trends were observed across dose levels. In study 2, using the alternative approach, 24 out of 37 pre-treatment plasma samples generated stimulated proliferation counts >5000 cpm. No meaningful effect on proliferation count was observed with post-treatment plasma obtained from patients receiving 5 or 10 mg ($n = 3$). Two out of three samples in the 20 mg q.i.d. cohort and seven out of eight samples in the 40 mg q.i.d. cohort had reduced proliferation counts, when plasma obtained 1.5 hours post-dose was compared to pre-treatment plasma on day 1. In study 3, with volunteer cells plus pre-treatment patient plasma, 11 samples demonstrated ≥ 2 values above 5000 cpm. No consistent trends were observed in reduction of ^3H incorporation using post-treatment plasma in the 10 mg q.i.d. cohort. At 20 mg q.i.d. and 40 mg q.i.d, there were reductions in proliferation counts at 1.5 hours post-dose compared with pre-dose on day 1 in five out of six patients and in all patients, respectively. However, among small sample sets available, these trends were not confirmed with plasma obtained 1.5 hours post-dose on day 7 (study 2) or day 8 (study 3).

For hair follicle analysis, there were insufficient data to evaluate a treatment effect on biomarkers, since only 17% of follicles collected in study 1, 38% collected in study 2, and 21% collected in study 3, had staining present.

Seven paired skin biopsies were analyzed over the course of study 3. Among samples obtained from patients receiving doses of 5 mg q.i.d. or higher ($n = 5$), the percent positive nuclei (scored as 1+ or 2+) staining for phospho-Rb at the S249/T252 and S780 epitopes declined post-treatment, while total Rb staining was similar in pre- and post-treatment samples. Representative skin biopsies for one patient, treated at the 40 mg q.i.d. dose level, are shown in Figure 2, along with quantification of Rb staining. No significant change was seen in staining at S807/811 or T356 phospho-sites post treatment, with variable changes observed at the S795 epitope. Additionally, the reduction in Rb phosphorylation at the S249/T252 and S780 sites was incomplete and was not associated with a reduction in Ki67 staining post-treatment. Among the 7 paired samples, most demonstrated stable or increased p27^{Kip1} staining post treatment, although decreased staining was observed in 2 samples. No significant changes in cyclin D1 or p53 staining were observed post treatment.

Post-hoc analysis: exposure versus tolerability

In light of the high variability in exposure, a *post-hoc* analysis was performed to investigate the relationship between drug exposure and tolerability. This analysis included the 45 patients treated with AZD5438 continuous dosing schedules in studies 2 and 3. Patients were divided into three categories: death and/or DLT; withdrawal within 1 week of starting treatment; and completed >1 week of treatment. There was a trend associating increased exposure with decreased tolerability (Figure 3).

Discussion

AZD5438 is one of a number of CDK inhibitors that have recently undergone clinical evaluation. The therapeutic benefit of these agents, including flavopiridol, seliciclib and BMS-387032 (SNS-032), has proved difficult to demonstrate in single-agent solid tumor studies (6), although recently it was shown that treatment with seliciclib can induce responses in patients with nasopharyngeal cancer (17). AZD5438 had an advantage over some existing

agents in being orally bio-available, allowing sustained daily dosing, likely necessary for tumor growth inhibition in the absence of induction of apoptosis. This report covers three phase I studies designed to investigate different dosing schedules for AZD5438.

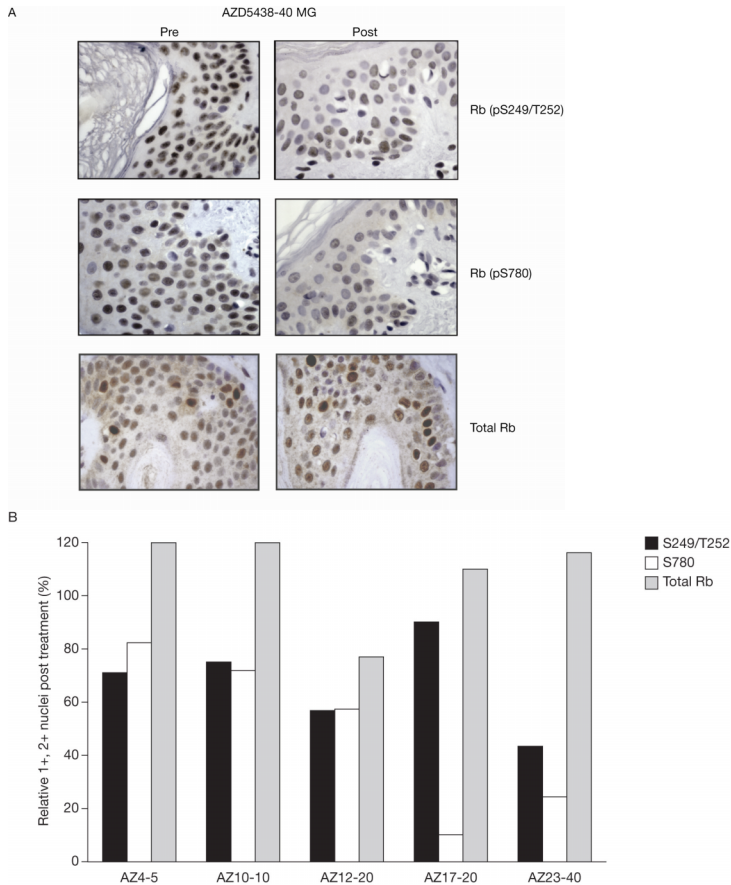
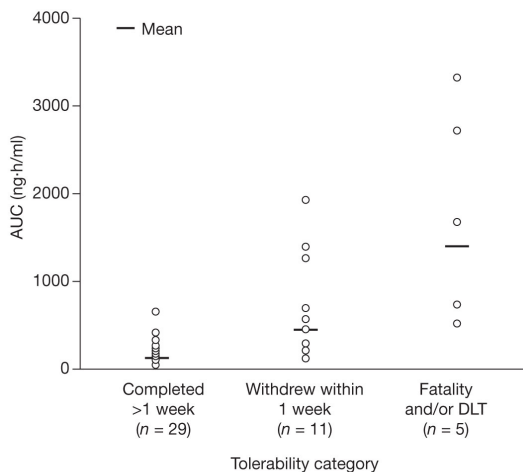


Figure 2: Total and phospho-Rb staining in skin biopsies. (A) Skin biopsies were obtained pre-treatment (pre) and 2 hours after the first dose on day 22 of continuous ADZ5438 dosing. Five-micrometer sections from formalin-fixed, paraffin-embedded samples were subjected to immunohistochemistry with the indicated antibodies. Results from patient #23 are shown (treated at the 40 mg dose level), demonstrating reduced Rb staining at the S249/T252 and S780 phosho-sites in the keratinocyte layers, suggestive of reduced CDK activity post treatment. Total Rb staining is maintained in the post-treatment sample. (B) Immunohistochemical data were quantified by scoring the nuclei of 100–200 keratinocytes as 0, 1+ or 2+. The percentage of positive nuclei was considered as 100 for each pre-treatment sample. Bars indicate the percent positive staining (1+, 2+) in each post-treatment sample, relative to the pre-treatment sample. The x-axis designations indicate the patient number and the dose of AZD5438 administered. In these samples, reductions in phospho-Rb staining were noted, while total Rb staining was maintained post treatment.



AUC, area under the concentration–time curve; DLT, dose-limiting toxicity.

Figure 3. Post-hoc analysis: exposure to AZD5438 and tolerability outcome in continuous dosing studies. Owing to the lack of multiple-dose data for many of the patients, the total daily AUC was calculated from day 1 pharmacokinetic measurements. Tolerability categories were: (1) patients who completed at least the initial safety assessment period (21 or 28 days) or withdrew after 1 week due to disease progression; (2) patients who withdrew within 1 week of starting treatment due to poor tolerability or for disease-related reasons; (3) patients who discontinued due to fatality and/or DLT.

The majority of toxicities observed in all three studies were gastrointestinal in origin, and increased in a dose-dependent manner, consistent with the toxicity profiles in preclinical and healthy volunteer studies with AZD5438 (12), and also in line with clinical experiences with other CDK inhibitors (6). The weekly schedule was well tolerated up to 90 mg q.i.d., and no NTD was established due to the adverse safety findings from the continuous studies. Both studies with continuous AZD5438 administration progressed sufficiently to identify a NTD of 40 mg q.i.d., with both non-fatal gastrointestinal and constitutional DLTs, as well as fatal DLTs.

Continuous dosing of AZD5438 was associated with profound anorexia and fatigue in some patients, accompanied by nausea and vomiting. This symptom complex occurred within the first few days of starting AZD5438 therapy and was associated with tachycardia, hypotension, hyponatremia and increases in white blood cell counts, C-reactive peptide and serum creatinine. Given the complex nature of the events, and the presence of significant medical comorbidities in this patient population, a clear etiology for these events has not yet been established. Nonetheless, these cases share certain similarities, such

as the complex of anorexia, lethargy/fatigue, nausea and vomiting leading to sudden decompensation that was seen in all three patients who experienced fatal events on the continuous dosing schedules. In light of the full profile of SAEs that subsequently emerged, the fatal myocardial infarction (suspected) in this study might retrospectively be considered to be possibly treatment related. It is notable that cardiovascular events, including myocardial infarction has been reported in studies of flavopiridol (18, 19). However, the severity of AEs observed in these studies were not expected, and are not comparable with those observed in studies with other CDK inhibitors.

Single-dose pharmacokinetic evaluation in all three studies showed that AZD5438 was rapidly absorbed and eliminated. After q.i.d. dosing, multiple-dose pharmacokinetics were not well predicted from the single-dose data, with evidence of drug accumulation (studies 2 and 3). Exposure to AZD5438 showed high inter-patient variability. The factors accounting for this variability have not been identified. Notwithstanding this variability, exposure generally increased with increasing dose.

In the here describes studies, the analyses of pharmacodynamic markers in PBMCs and hair follicles led to disappointing results, with no observed treatment-related trends at all. The biological activity of flavopiridol, another CDK inhibitor, had been successfully investigated in PBMCs before (18,20), and PBMC and hair follicle analyses were employed successfully in a study of AZD5438 in healthy volunteers (13). The results of the here described studies highlight the difficulties inherent in transferring surrogate tissue biomarker measurements from well-tolerated healthy volunteer studies to a setting of metastatic cancer in which patients have numerous confounding factors including previous and concurrent therapies, as well as their underlying disease.

The analyses of paired skin biopsies in study 3 revealed inhibition of CDK2, indicated by stable P27^{Kip1} expression (21) and reduced phosphorylation of Rb at the S249/T252 phospho-site (9,10). In buccal mucosae from healthy volunteers, no changes were induced by AZD5438 at this phospho-site (13), potentially reflecting differences in the tissues examined and the analysis after only a single dose, compared with a minimum of 15 days of dosing prior to post-treatment sampling here. Interestingly, reduced phosphorylation of Rb at S780 was also observed, a site reported to be phosphorylated by CDK4 (22).

AZD5438 is significantly less potent against CDK4, although phosphorylation at this site could be affected by cell-cycle position, induced by combined CDK2/CDK1 inhibition (11). Similarly, in the buccal mucosae of healthy volunteers, reduced phosphorylation at S807/811 was noted, which is another CDK4-specific site (23, 24). In both data sets, changes in Rb phosphorylation did not translate to reduced Ki67 staining, suggesting the necessity for more complete inhibition of CDK targets in order to achieve antiproliferative effects.

A *post-hoc* analysis of observed exposure and tolerability outcome in the 45 patients treated with AZD5438 continuous dosing showed a clear trend to poorer outcome with increasing exposure. However, the high degree of variability in inter-individual exposure and the inability to identify factors underlying this variability make it difficult to predict tolerable doses in individual patients. Together with the unpredictable nature of the serious toxicities, this variability in exposure constituted a major clinical development challenge for the compound. The exposure-related toxicity might have resulted from accumulation of the drug in these patients, although the onset of severe toxicities was frequently observed early in the course of treatment. In contrast to the exposure-related intolerability, dose-related efficacy was not observed. Clinical exposures did not reach the exposures associated with preclinical efficacy, even at NTDs. There appeared to be only minimal clinical efficacy, manifested by disease stabilization for more than 4 months in three out of a total of 64 patients dosed across all three studies. Thus, the probability of obtaining a viable dose and schedule for further clinical evaluation of AZD5438 as a potential anticancer agent was considered to be minimal or non-existent.

In conclusion, the phase I AZD5438 clinical study program has failed to establish an appropriate risk–benefit profile for this novel agent, and therefore its clinical development has been discontinued. The utility of CDK inhibitors as anticancer agents, as monotherapy or in combination regimens, remains to be established.

Acknowledgements

This study was supported financially by AstraZeneca. The Dana-Farber sub-study (part of study 3) was funded by AstraZeneca as well as the Dana-Farber/Harvard Cancer Center (DF/HCC) Specialized Program of Research

Excellence (SPORE) in Lung Cancer, NIH grant P20 CA90578, and NIH grant R01 CA90687.

We thank Cheryl Forder and Hazel Weir for technical assistance with PBMC assay development, Fiona Smith, Cheryl Forder and Syngenta for analyzing PBMC and hair follicles, Kate Byth, Gareth D. Hughes, Robert Wilkinson and Alexandra McGregor for the conduct of supporting preclinical translational studies, Jim Growcott, Shampa Das, David Wilson, Andrew Hughes, and Louise Garside for contribution to the clinical program and analysis of clinical data, and Matthew Lewis of Mudskipper Bioscience for editorial assistance. Susan Rigby, Anita Lindsay, John Freeman and Chris Bowen provided study logistics management. We thank Anat Stemmer-Rachamimov, Anna Kreshock, Donna Skinner, Janice Williams and Anna Levitz of the DF/HCC Pathology Core for assistance with skin biopsy processing and immunohistochemistry. We thank Drs. Leonard J. Appleman and Andrew X. Zhu for assisting with recruitment at Dana-Farber/Harvard Cancer Center.

References

1. Reed SI. Control of the G1/S transition. *Cancer Surv* 1997; 29: 7-23.
2. Lundberg AS, R.A. W. Functional inactivation of the retinoblastoma protein requires sequential modification by at least two distinct cyclin-cdk complexes. *Mol. Cell. Biol.* 1998; 18: 753-761.
3. Harbour JW, Luo RX, Dei Santi A et al. Cdk phosphorylation triggers sequential intramolecular interactions that progressively block Rb functions as cells move through G1. *Cell* 1999; 98: 859-869.
4. Pines J. The cell cycle kinases. *Semin Cancer Biol* 1994; 5: 305-313.
5. Sherr CJ. Cancer cell cycles. *Science* 1996; 274: 1672-1677.
6. Shapiro GI. Cyclin-dependent kinase pathways as targets for cancer treatment. *J Clin Oncol* 2006; 24: 1770-1783.
7. Schwartz GK, Shah MA. Targeting the cell cycle: a new approach to cancer therapy. *J Clin Oncol* 2005; 23: 9408-9421.
8. Wheeler C, Stephens T, Byth K. Novel approaches in oncology at AstraZeneca. *Eur J Cancer Suppl* 2003; 1: 3-8.
9. Cai D, Byth KF, Shapiro GI. AZ703, an imidazo[1,2-a]pyridine inhibitor of cyclin-dependent kinases 1 and 2, induces E2F-1-dependent apoptosis enhanced by depletion of cyclin-dependent kinase 9. *Cancer Res* 2006; 66: 435-444.
10. Byth KF, Geh C, Forder CL et al. The cellular phenotype of AZ703, a novel selective imidazo[1,2-a]pyridine cyclin-dependent kinase inhibitor. *Mol Cancer Ther* 2006; 5: 655-664.
11. Cai D, Latham VM, Jr., Zhang X, Shapiro GI. Combined depletion of cell cycle and transcriptional cyclin-dependent kinase activities induces apoptosis in cancer cells. *Cancer Res* 2006; 66: 9270-9280.
12. Camidge DR, Smethurst D, Growcott J et al. A first-in-man phase I tolerability and pharmacokinetic study of the cyclin-dependent kinase-inhibitor AZD5438 in healthy male volunteers. *Cancer Chemother Pharmacol* 2007; 60: 391-398.
13. Camidge DR, Pemberton M, Growcott J et al. A phase I pharmacodynamic study of the effects of the cyclin-dependent kinase-inhibitor AZD5438 on cell cycle markers within the buccal mucosa, plucked scalp hairs and peripheral blood mononucleocytes of healthy male volunteers. *Cancer Chemother Pharmacol* 2007; 60: 479-488.

14. Therasse P, Arbuck SG, Eisenhauer EA et al. New guidelines to evaluate the response to treatment in solid tumors. *Journal of the National Cancer Institute* 2000; 92: 205-216.
15. Haddad RI, Weinstein LJ, Wiczonek TJ et al. A phase II clinical and pharmacodynamic study of E7070 in patients with metastatic, recurrent, or refractory squamous cell carcinoma of the head and neck: modulation of retinoblastoma protein phosphorylation by a novel chloroindolyl sulfonamide cell cycle inhibitor. *Clin Cancer Res* 2004; 10: 4680-4687.
16. Loda M, Cukor B, Tam SW et al. Increased proteasome-dependent degradation of the cyclin-dependent kinase inhibitor p27 in aggressive colorectal carcinomas. *Nature Med.* 1997; 3: 231-234.
17. Hsieh WS, Soo R, Peh BK et al. Pharmacodynamic effects of seliciclib, an orally administered cell cycle modulator, in undifferentiated nasopharyngeal cancer. *Clin Cancer Res.* 2009; 15: 1435-42.
18. Stadler WM, Vogelzang NJ, Amato R et al. Flavopiridol, a novel cyclin-dependent kinase inhibitor, in metastatic renal cancer: a University of Chicago phase II consortium study. *Journal of Clinical Oncology* 2000; 18: 371-375.
19. George S, Kasimis BS, Cogswell J et al. Phase I study of flavopiridol in combination with Paclitaxel and Carboplatin in patients with non-small-cell lung cancer. *Clin Lung Cancer* 2008; 9: 160-165.
20. Bible KC, Lensing JL, Nelson SA et al. Phase 1 trial of flavopiridol combined with cisplatin or carboplatin in patients with advanced malignancies with the assessment of pharmacokinetic and pharmacodynamic end points. *Clin Cancer Res* 2005; 11: 5935-5941.
21. Zhang GJ, Safran M, Wei W et al. Bioluminescent imaging of Cdk2 inhibition in vivo. *Nat Med* 2004; 10: 643-648.
22. Kitagawa M, Higashi H, Jung HK et al. The consensus motif for phosphorylation by cyclin D1-cdk4 is different from that for phosphorylation by cyclin A/E-cdk2. *EMBO J* 1996; 15: 7060-7069.
23. Zarkowska T, Mitnacht S. Differential phosphorylation of the retinoblastoma protein by G1/S cyclin-dependent kinases. *J. Biol. Chem.* 1997; 272: 12738-12746.
24. Brantley MA, Harbour JW. Inactivation of retinoblastoma protein in uveal melanoma by phosphorylation of sites in the COOH-terminal region. *Cancer Res* 2000; 60: 4320-4323.

Supplementary table 1: Primary tumor response assessments

Primary tumor response assessments				
Study 1: weekly dosing	Best overall objective response (n)			
Dose level, mg q.i.d.	Progression	Stable disease	Not evaluated	All
10	3	0	0	3
20	3	0	0	3
40	0	1	3	4
60	1	1	4	6
90	1	2	0	3
Total	8	4	7	19
Study 2: fourteen days continuous dosing, one week rest				
Dose level, mg q.i.d.	Progression	Stable disease	Not evaluated	All
5	1	1	1	3
10	1	2	0	3
20	3	0	0	3
40	2	2	4	8
Total	7	5	5	17
Study 3: continuous dosing				
Dose level, mg q.i.d.	Progression	Stable disease	Not evaluated	All
2.5	2	1	0	3
5	1	1	1	3
10	1	2	2	5
20	3	1	7	11
40	2	0	4	6
Total	9	5	14	28

5

Carboplatin and topotecan

CHAPTER 5.1

Phase I, pharmacokinetic and pharmacodynamic study of carboplatin and topotecan administered intravenously every 28 days to patients with malignant solid tumors

David S. Boss, Wandena S. Siegel-Lakhai, Nadja E. van Egmond-Schoemaker, Dick Pluim, Hilde Rosing, Wim W. ten Bokkel Huinink, Jos H. Beijnen, Jan H. M. Schellens

Clin Cancer Res. 2009;15(13):4475-83

Abstract

Purpose: Preclinical studies have shown that the combination of topotecan and carboplatin is synergistic. To evaluate the schedule dependency of this interaction, the following phase I trial was designed to determine the safety and maximum tolerated dose (MTD), pharmacokinetics and pharmacodynamics of carboplatin and topotecan in patients with malignant solid tumors.

Experimental design: In part 1, patients received carboplatin on day 1 and topotecan on days 1, 2 and 3 (C→T schedule). In part 2, topotecan was administered on days 1, 2, and 3, followed by carboplatin on day 3 (T→C schedule). Pharmacokinetics were determined in plasma and TopI catalytic activity and Pt-DNA adducts in white blood cells (WBC) and tumor tissue.

Results: Forty-one patients were included. Dose-limiting toxicities (DLTs) during the C→T schedule were grade 4 thrombocytopenia and febrile neutropenia (MTD: carboplatin target AUC 4 min.mg/mL; topotecan 0.5 mg/m²/day). DLTs during the T→C schedule included grade 4 neutropenia, thrombocytopenia, neutropenic fever and grade 4 nausea and vomiting (MTD: carboplatin target AUC 6 min.mg/mL; topotecan 0.9 mg/m²/day). One complete and five partial responses were observed. The clearance of and exposure to carboplatin and topotecan did not depend on the sequence of drug administration. No schedule dependent effects were seen in Pt-DNA levels and TopI catalytic activity in WBC and tumor tissue. However, myelotoxicity was clearly more evident in the C→T schedule.

Conclusion: The T→C schedule was better tolerated as both hematological and non-hematological toxicities were milder. Other than the investigated PD factors must explain the schedule dependent differences in toxicities.

Introduction

Topotecan and carboplatin are both active anticancer drugs with an established use in the clinic. Topotecan, a water-soluble semisynthetic analogue of camptothecin, is licensed for the treatment of Small-Cell Lung Cancer (SCLC), cervical cancer, and metastatic ovarian carcinoma (1, 2, 3, 4). Carboplatin is an analogue of cisplatin, but with a milder non-hematological toxicity profile and a broad spectrum of antitumor activity (5, 6). Topotecan undergoes pH dependent reversible hydrolysis from the active lactone form into the carboxylate form and vice versa (7, 8). Topotecan inhibits DNA topoisomerase I (TopI) by binding to the cleavable complex (consisting of TopI covalently bound to DNA). The stabilized cleavable complex results in irreversible DNA double-strand breaks leading to cell death (9, 10, 11). The antineoplastic effect of carboplatin involves the formation of a covalent interaction with DNA after which several Pt-DNA adducts are formed, ultimately leading to cell death. Approximately 90 % of an administered dose of carboplatin is eliminated by glomerular filtration (12). This makes it possible to individualize the dose of carboplatin based on renal function as estimated by creatinine clearance (13, 14). The rationale for combining carboplatin and topotecan is the synergistic cytotoxicity observed between platinum agents and topoisomerase I inhibitors in preclinical models (15, 16, 17, 18). To explain this synergism a mechanistic model has been established, in which the TopI enzyme directly binds to the Pt-DNA adduct. Subsequently, topotecan binds to this complex, which yields large stabilized lesions to the DNA that are difficult to repair (17, 18). Preclinical studies have shown that the sequence of cisplatin or carboplatin followed by topotecan was the most active sequence (17, 18). This is in agreement with results from clinical studies: Increased hematological toxicity was observed when cisplatin or carboplatin was given before topotecan compared to the reversed schedule (19, 20, 21, 22, 23, 24). To evaluate the schedule dependency of this interaction, the following phase I trial was designed to determine the safety and maximum tolerated dose (MTD), pharmacokinetics and pharmacodynamics of carboplatin and topotecan in patients with advanced solid malignancies.

Patients and methods

Eligibility

Patients were eligible if they had a histologically or cytologically confirmed solid tumor and a metastatic tumor accessible for biopsy. Other eligibility criteria included age ≥ 18 years, WHO performance status ≤ 2 and an estimated life expectancy ≥ 3 months. Previous chemotherapy had to be discontinued for at least 4 weeks before entry into the study or 6 weeks in the case of mitomycin C or nitrosourea. Patients had to have acceptable hematological blood values (WBC $\geq 3.5 \times 10^9/L$, absolute neutrophil count (ANC) $\geq 1.5 \times 10^9/L$, platelets $\geq 100 \times 10^9/L$, hemoglobin level (Hb) ≥ 9.0 g/dL), as well as acceptable renal and hepatic function (creatinine clearance ≥ 60 mL/min, serum bilirubin ≤ 1.5 times the normal upper limit and ASAT and ALAT ≤ 2 times the normal upper limit (or ≤ 5 times the normal upper limit in the presence of hepatic metastases)). The study protocol was approved by the Medical Ethics Committee of the hospital and all patients had to give written informed consent.

Treatment plan and study design

In the first part of the study, patients received carboplatin as a 60 min i.v. infusion on day 1 and topotecan as a 30 min i.v. infusion on days 1 (after carboplatin administration), 2 and 3 (C→T schedule). Carboplatin dosage was calculated using the target area under the free carboplatin plasma concentration versus time curve (AUC in min.mg/mL). For carboplatin, it has been shown in several studies that the CL is linearly related to the glomerular filtration rate (GFR) and therefore the AUC is also related to the GFR (25). We calculated the carboplatin dose using the Calvert formula (13), with GFR estimated using the formula of Cockcroft and Gault (26). The starting dose (topotecan 0.5 mg/m²/day, carboplatin target AUC 4 min.mg/mL) was based on the experience in other clinical trials (22,23). At least three patients were entered at each dose level. The MTD was defined as the highest dose level not producing DLTs during the first treatment cycle in more than 2/6 patients. The sequence of drug administration was reversed in the second part of the study (T→C schedule): Topotecan administered at days 1, 2, and 3, followed by carboplatin at day 3 (carboplatin administered after administration of topotecan on day 3). Dose escalation during the T→C schedule was started at

the established MTD of the C→T schedule. Subsequently, the dose was escalated further according to the original plan. Treatment cycles in both parts of the study were repeated every 28 days.

Drug product

Topotecan (Hycamtin) was provided by GlaxoSmithKline Beecham Pharmaceuticals (Harlow, United Kingdom). Each vial contained topotecan as lyophilised cake that was equivalent to 4 mg of the free base. To prepare the drug for i.v. infusion, the lyophilised formulation was reconstituted with 4 mL of sterile water for injection prior to dilution in 0.9% NaCl. Carboplatin was supplied by Pharmachemie B.V. (Haarlem, the Netherlands), and prepared according to the local procedure.

Patient evaluation and follow-up

Pre-treatment evaluation included a complete medical history and physical examination. Before and during every cycle, the following was assessed at defined time points: vital signs (days 1,2 and 3), physical examination including ECG (day 1), urinalysis (day 1) and laboratory assessments (chemistry on days 1 and 15, and complete blood cell counts on days 1, 8, 15 and 21). Tumor measurements were performed at baseline and every other cycle and were evaluated according to the WHO criteria (27). All toxicities were graded according to the National Cancer Institute Common Toxicity Criteria (NCI-CTC) version 2.0 (28). Dose-limiting toxicities (DLTs) were defined as any of the following events occurring during the first treatment cycle and related to study treatment: 1) grade 4 neutropenia lasting ≥ 7 days or associated with fever/infection, 2) grade 4 thrombocytopenia or requiring platelet transfusion, 3) mucositis grade ≥ 3 lasting ≥ 7 days, 4) grade 3 or 4 non-hematological toxicity excluding alopecia, untreated nausea and vomiting (grade 3) or severe musculoskeletal pain (grade 3).

Pharmacokinetic studies

To determine the pharmacokinetics of topotecan, blood sampling was performed during the C→T schedule on day 1 and during the T→C schedule on day 3 (day of carboplatin infusion). Samples were taken pre-dose and at 30 min, 1, 1.5, 2, 3, 4, 8 and 12 hours after start of the infusion. Limited blood

sampling for the determination of topotecan pharmacokinetics, according to a method that was previously established (29), was performed during the C→T schedule on day 2 and 3 during cycle 1 and at day 1 during cycle 2. During the T→C schedule blood samples were taken during cycle 1 at day 1 and 2 and during cycle 2 at day 3. Samples were taken prior to infusion and at exactly 2.5 hours after the start of the 30 min infusion. The levels of total topotecan (lactone + hydroxy acid) and topotecan lactone were determined using a validated high performance liquid chromatography assay (29). To describe carboplatin pharmacokinetics, sampling was performed during the C→T schedule on day 1 of the first and second cycle. During the T→C schedule, sampling was performed on day 3 of the first and second cycle. Blood samples were taken pre-dose and at 30 min, 1, 1.5, 2, 4, 7 and 24 hours after start of the infusion during the first cycle of both schedules. During the second cycle, blood samples were taken pre-dose and at 1, 2, 4, 7 and 24 hours after start of the infusion. For the determination of free platinum, plasma ultrafiltrate was prepared by adding 1 mL of plasma to the MPS-1 system equipped with 3 kDa YMT membranes (Amicon Division, Danvers, MA, USA). Analysis was performed using a validated Zeeman atomic absorption spectrometry method (30).

Pharmacodynamic studies

A tumor biopsy was obtained from each patient during cycle 1, 24 hours after the infusion of carboplatin. In the C→T schedule the biopsy was taken on day 2, and in the T→C schedule a tumor biopsy was taken on day 4. After collecting tumor tissue, samples were washed with 0.9% NaCl and subsequently divided in two aliquots and snap frozen in liquid nitrogen. One aliquot was used for the determination of intrastrand platinum-DNA adducts (Pt-GG and Pt-AG) and TopI protein levels and one aliquot was used to determine TopI catalytic activity. Pt-DNA adducts were quantified using a sensitive ³²P-postlabelling assay, that was validated in vitro and in vivo (31). The TopI catalytic activity was assayed by relaxation of supercoiled pBR322 DNA as described previously (16). The TopI catalytic activity was expressed as the lowest nuclear extract concentration (μg protein/mL) at which the supercoiled DNA was completely relaxed. The TopI protein levels were determined by Western blotting using the human IGROV1 ovarian cell line as reference (32). TopI levels were expressed relative to the TopI level present in 10 μg IGROV1 cell lysate. For the determination of Pt-DNA adducts in WBC,

samples were taken during cycle 1 and 2, on day 1 during the C→T schedule and on day 3 during the T→C schedule. Samples were taken prior to infusion and at 4 and 21 hours after the start of the carboplatin infusion, and WBC fractions were isolated and purified as previously described (31). For the determination of TopI catalytic activity in WBC, blood samples were collected in three CPT_{tm} vacutainers (Becton Dickinson, USA). Samples were taken during the C→T schedule on day 1 and during the T→C schedule on day 3 of the first and second cycle. Samples were taken before infusion, at the end of carboplatin infusion and at the end of topotecan infusion. An additional sample was taken during both schedules directly after the tumor biopsy sample.

Pharmacokinetic and pharmacodynamic analyses

The pharmacokinetic parameters of topotecan and carboplatin during the first cycle on day 1 (C→T schedule) or day 3 (T→C schedule) were determined by non-compartmental analysis with WinNonLin software (version 4.1, Pharsight Corporation, Mountain View, CA). The area under the concentration-time curve (AUC) and total plasma clearance (CL) of total topotecan, topotecan lactone and free carboplatin were calculated. On the other days of topotecan administration, a limited sampling method was used to estimate topotecan CL, which employed one sample 2 hours after the end of the 30 min infusion as previously described (33). The area under the adduct curve (AUA, in fmol*h/μg DNA) of platinum-DNA adducts were calculated in WBC by the linear-logarithmic trapezoidal method up to the last measured data point without extrapolation (34). Statistical analyses were performed using the SPSS software package for Windows (Version 11.0, SPSS Inc, Chicago, Illinois, USA). Details about the statistical analyses can be found in the supplementary information.

Results

Patient characteristics

Patient characteristics are shown in table 1a, the number of patients included at the different dose levels are summarized in table 1b. Initially, 3 patients were included at dose level 1. No study related DLT was observed. At dose level 2, three out of six patients experienced a DLT. Subsequently, dose level 1 was expanded with another three patients and no DLTs were observed. Dose

Table 1a: Patient characteristics

Patient characteristics	n
gender	
male	23
female	18
age	
median	55
range	(34-76)
tumor types	
ovarium	9
NSCLC	9
SCLC	6
melanoma	5
esophagus	3
stomach	4
ACUP	2
undifferentiated large cell	1
bileduct	1
mesothelioma	1
WHO performance status	
0	14
1	19
2	8
previous therapy	
chemotherapy	17
chemotherapy + surgery	9
chemotherapy + radiotherapy	8
chemotherapy + surgery + radiotherapy	6
no previous treatment	1

Table 1b: Number of patients treated at each dose level

Schedule	Dose level	Carboplatin (AUC)	Topotecan (mg/m ² /day)	n
C→T	1	4	0.5	6
C→T	2	5	0.5	6
T→C	1	4	0.5	3
T→C	2	5	0.5	4
T→C	3	5	0.6	3
T→C	4	6	0.7	3
T→C	5	6	0.8	3
T→C	6	6	0.9	6
T→C	7	6	1.1	7

level 1 (carboplatin target AUC 4 min.mg/mL; topotecan 0.5 mg/m²/day) was the MTD at the C→T schedule. During the T→C schedule, at dose level 2, one patient had to be replaced because the tumor biopsy failed. No DLTs were observed up to dose level 7. At this dose level, one patient experienced DLT and subsequently this cohort was expanded with another four patients. One extra patient was treated at dose level 7 due to ethical considerations, since the patient was already informed about this study, and very eager to participate when it appeared that all slots had been filled. Subsequently, one

of these additional patients also experienced DLT. Although the number of patients with DLT at dose level 7 was two out of seven, it was decided to reduce the dose to level 6. This decision was taken because five out of seven patients experienced grade 3-4 thrombocytopenia during cycle one (two patients) or subsequent cycles. Thus, further dose-escalation was expected to result in unmanageable thrombocytopenia. One DLT was observed at level 6 (out of 6 patients) and therefore it was decided that dose level 6 (carboplatin target AUC 6 min.mg/mL; topotecan 0.9 mg/m²/day) was safe at the T→C schedule. In total, 170 cycles were administered to the 41 patients (median 4; range 1-12, supplementary table 1).

Adverse events

All patients were evaluable for toxicity. The treatment related hematological and non-hematological toxicities are presented in table 2a and 2b. Hematological toxicity, primarily thrombocytopenia, was dose limiting for the combination of topotecan and carboplatin using the C→T schedule. At dose level 2 (C→T schedule), three of the six patients included developed DLT. Two patients had thrombocytopenia grade 4 and one patient thrombocytopenia grade 4 combined with febrile neutropenia grade 4. Three patients in the C→T schedule had a dose reduction of both drugs due to severe hematological toxicities after receiving 1, 1 and 3 cycles. In the T→C schedule, at level 7, two patients experienced DLT. The first patient had grade 4 neutropenia, thrombocytopenia and neutropenic fever and also grade 3 nausea and grade 4 vomiting, despite prophylactic anti-emetics. The second patient experienced grade 3 thrombocytopenia and was hospitalized because of epistaxis. At dose-level 6, one out of three extra patients experienced a DLT (grade 4 thrombocytopenia and neutropenic fever). Five patients in the T→C schedule had a dose reduction of both drugs and one patient of topotecan due to severe hematological toxicities after receiving 3, 4, 4, 1, 1 and 1 cycle, respectively. From table 2a it can be concluded that the incidence of grade 3-4 hematological toxicities and the number of cycles causing these toxicities were higher during the C→T schedule. Grade 3-4 thrombocytopenia was the main hematological toxicity observed during both schedules, but the incidence during the C→T schedule (58% of all patients, 20% of all cycles) was higher compared to the T→C schedule (41% of all patients, 13% of all cycles). Non-hematological toxicity was frequently observed but generally mild. Main toxicities were grade 1-2 fatigue, nausea and vomiting. In general, the

Table 2a: Incidence of treatment emergent hematological toxicities for all cycles in patients treated with the combination of carboplatin and topotecan

Dose level	Schedule	Patients (n)	Nr. of cycles (n)	Anemia		Febrile neutropenia		Neutropenia		Leucocytopenia		Thrombocytopenia	
				Gr 1-2	Gr 3-4	Gr 1-2	Gr 3-4	Gr 1-2	Gr 3-4	Gr 1-2	Gr 3-4	Gr 1-2	Gr 3-4
1	C→T	6	24	2/4 ^a	1/4	0/0	1/1	1/1	2/2	1/1	3/3	0/0	1/1
2	C→T	6	30	4/4	3/5	1/1	1/1	1/1	3/3	1/3	3/3	0/5	6/10
Total		12	54	50%/15% ^b	33%/17%	8%/2%	17%/4%	17%/4%	42%/9%	17%/7%	50%/11%	0%/9%	58%/20%
1	T→C	3	18	2/2	0/0	0/0	0/0	0/0	2/2	3/4	0/0	0/0	0/0
2	T→C	4	18	2/2	0/0	0/0	0/0	1/1	0/0	0/0	0/0	0/3	2/2
3	T→C	3	8	1/1	0/0	0/0	0/0	0/0	0/0	1/1	0/0	0/0	0/0
4	T→C	3	5	0/0	0/0	0/0	0/0	0/0	1/1	0/0	1/1	0/0	1/2
5	T→C	3	25	2/4	0/0	0/0	0/0	0/1	1/1	0/0	0/0	1/4	1/1
6	T→C	6	21	2/4	2/3	0/0	1/1	0/0	2/2	1/1	1/1	0/0	3/4
7	T→C	7	21	3/4	1/1	0/0	1/1	1/1	3/3	1/1	0/0	1/1	5/6
Total		29	116	41%/15% ^b	10%/3%	0%/0%	7%/2%	7%/3%	31%/8%	24%/6%	7%/2%	7%/7%	41%/13%

^a Number of patients experienced toxicity / number of cycles causing toxicity

^b Relative number of patients experienced toxicity / relative number of cycles causing toxicity

Table 2b: Incidence of treatment emergent non-hematological toxicities for all cycles in patients treated with the combination of carboplatin and topotecan

Dose level	Schedule	Patients (n)	Nr. of cycles (n)	Fatigue		Nausea		Vomiting		Diarrhea ^c		Alopecia		Neuropathy ^c		Constipation ^c	
				Gr 1-2	Gr 3-4	Gr 1-2	Gr 3-4	Gr 1-2	Gr 3-4	Gr 1-2	Gr 3-4	Gr 1-2	Gr 3-4	Gr 1-2	Gr 3-4	Gr 1-2	Gr 3-4
1	C→T	6	24	2/2 ^a	0/0	4/6	0/0	3/3	0/0 ^a	0/0	0/0	0/0	0/0	0/0	2/2	4/4	
2	C→T	6	30	4/4	1/1	6/7	0/0	4/5	3/7	1/1	1/1	0/0	0/0	1/1	4/4		
Total		12	54	50%/11% ^b	8%/2%	83%/24%	0%/0%	58%/15%	25%/13% ^b	8%/2%	0%/0%	0%/0%	8%/2%	50%/11%			
1	T→C	3	18	1/1	0/0	2/3	0/0	1/1	1/1	0/0	0/0	0/0	0/0	0/0			
2	T→C	4	18	1/2	1/1	2/2	0/0	0/0	1/1	0/0	0/0	0/0	0/0	0/0			
3	T→C	3	8	2/2	0/0	0/0	1/1	0/0	1/1	1/1	1/1	1/1	0/0	0/0			
4	T→C	3	5	2/2	0/0	2/2	0/0	2/2	1/1	0/0	0/0	0/0	1/1	1/1			
5	T→C	3	25	2/3	0/0	2/2	0/0	1/1	2/2	3/3	0/0	0/0	0/0	0/0			
6	T→C	6	21	3/5	1/1	2/7	0/0	2/6	1/1	1/1	0/0	0/0	0/0	1/1			
7	T→C	7	21	3/3	0/0	2/2	1/1	0/0	2/2	3/3	1/1	1/1	0/0	0/0			
Total		29	116	48%/16% ^b	7%/2%	41%/16%	7%/2%	21%/9%	24%/6% ^b	28%/7%	7%/2%	3%/1%	7%/2%				

^a Number of patients experienced toxicity / number of cycles causing toxicity

^b Relative number of patients experienced toxicity / relative number of cycles causing toxicity

^c No Grade 3-4 toxicity was observed

incidence of non-hematological toxicities was lower during the T→C schedule compared to the C→T schedule, excluding grade 1-2 obstipation. Two patients treated at the T→C schedule experienced grade 3 nausea and grade 4 vomiting and went off-study after receiving 1 and 2 cycles, respectively.

Pharmacokinetics

Plasma samples for determining carboplatin, topotecan lactone and topotecan total pharmacokinetics were obtained from 36, 32 and 37 patients, respectively. During the C→T and T→C schedule, the mean AUC of carboplatin was about 1-2 min.mg/mL lower than the target AUC, as calculated by the method of Calvert with GFR estimated from the Cockcroft and Gault formula (supplementary figure 1) [13]. The AUC levels of unbound platinum, topotecan lactone and total topotecan are shown in table 3a. There were no significant differences in CL of unbound platinum ($p = 0.14$, table 3b), topotecan lactone ($p = 0.96$, table 3c) and total topotecan ($p = 0.08$, table 3c) between the two schedules. When comparing topotecan CL during the C→T and T→C schedule between days 1, 2 and 3 of cycle 1 and days 1 or 3 of cycle 2, it was shown that the effect of day of treatment on total topotecan CL was not significant ($p = 0.67$). There was also no significant effect of schedule on total topotecan CL measured on different days ($p = 0.54$). Finally, there was no significant interaction between day of treatment and schedule on total topotecan CL ($p = 0.15$).

Table 3a Mean (SD) AUC levels of unbound platinum and topotecan during C→T and T→C schedule

Dose levels	n	Topot. dose (mg/m ² /d)	Carbo target AUC	Carboplatin measured AUC (min.mg/mL)	Topotecan _{lac} AUC (h.ng/mL)	Topotecan _{tot} AUC (h.ng/mL)
1 C→T	6	0.5	4	3.1 (0.5)	12.6 (4.9)	39.7 (12.8)
2 C→T	6	0.5	5	3.6 (0.3) ¹	13.4 (4.7) ³	47.8 (13.9) ³
1 T→C	3	0.5	4	2.5 (0.4)	11.8 (2.4)	35.2 (8.9)
2 T→C	4	0.5	5	2.7 (0.5)	11.3 (1.8)	32.7 (2.2)
3 T→C	3	0.6	5	3.1 (0.4)	12.5 (10.1-15.0) ²	51.9 (25.3)
4 T→C	3	0.7	6	4.0 (3.4-4.6) ²	17.8 (14.1-21.5) ²	59.6 (44.2-74.9) ²
5 T→C	3	0.8	6	4.0 (0.4)	18.4 (4.4)	37.8 (10.6)
6 T→C	6	0.9	6	4.3 (0.5)	22.2 ⁵	76.5 (18.6)
7 T→C	7	1.1	6	3.9 (0.7) ⁴	31.7(12.6) ⁴	60.5 (28.4) ³

¹ n = 3, ² n = 2, ³ n = 5, ⁴ n = 6, ⁵ n = 1

Table 3b: Mean (SD) clearance of unbound platinum during C→T and T→C schedules

variable	units	C→T (n = 9)	T→C (n = 27)	p - value ¹
Unbound platinum				
CL	(mL/min)	0.6 (0.1)	0.7 (0.1)	0.14

¹2-sided p-value for testing a difference between the two schedules (student t test)

Table 3c Mean (SD) clearance of topotecan during C→T and T→C schedules

variable	units	C→T (n = 11)	T→C (n = 26)	p - value ¹
CL	(L/h)	Topotecan_{lactone} 84.5 (32.5)	83.7 (18.3) ²	0.96
CL	(L/h)	Topotecan_{total} 24.1 (6.4)	29.6 (8.9)	0.08

¹2-sided p-value for testing a difference between the two schedules (student t test)

²n = 21

Pharmacodynamics

The incidence of thrombocytopenia was related to carboplatin AUC, and was more evident during the C→T schedule compared to the T→C schedule (figure 1a, b and c). When comparing the same dose level, measured AUC of carboplatin or topotecan between the two schedules, the mean platelet decrease after all cycles was significantly higher during the C→T schedule (83.7% at the C→T and 59.3% at the T→C schedule, $p = 0.0005$). The decreases in ANC (78.3% at the C→T and 70.2% at the T→C schedule) and leucocytes (70.3% at the C→T and 57.0% at the T→C schedule) after all cycles were also more evident in the C→T schedule, although not statistically significant ($p = 0.36$ and 0.13 , respectively). The results of the TopI catalytic activity in WBC during the C→T schedule and T→C schedule are summarized in supplementary table 2a and b. Topotecan and carboplatin administration had a significant effect on the TopI catalytic activity ($p = 0.006$). However, this effect was not schedule dependent ($p = 0.32$). Moreover, there was no significant interaction between topotecan/carboplatin infusion and schedule on the TopI catalytic activity ($p = 0.15$). We also found no significant correlation between the TopI catalytic activity and TopI protein levels in tumor cells and there was no schedule dependency ($R^2 = 0.04$, $p > 0.05$, supplementary figure 2).

Pt-DNA adduct levels could be determined in 10 patients during cycle 1 of the C→T schedule and in 20 patients of the T→C schedule in WBC. During the C→T

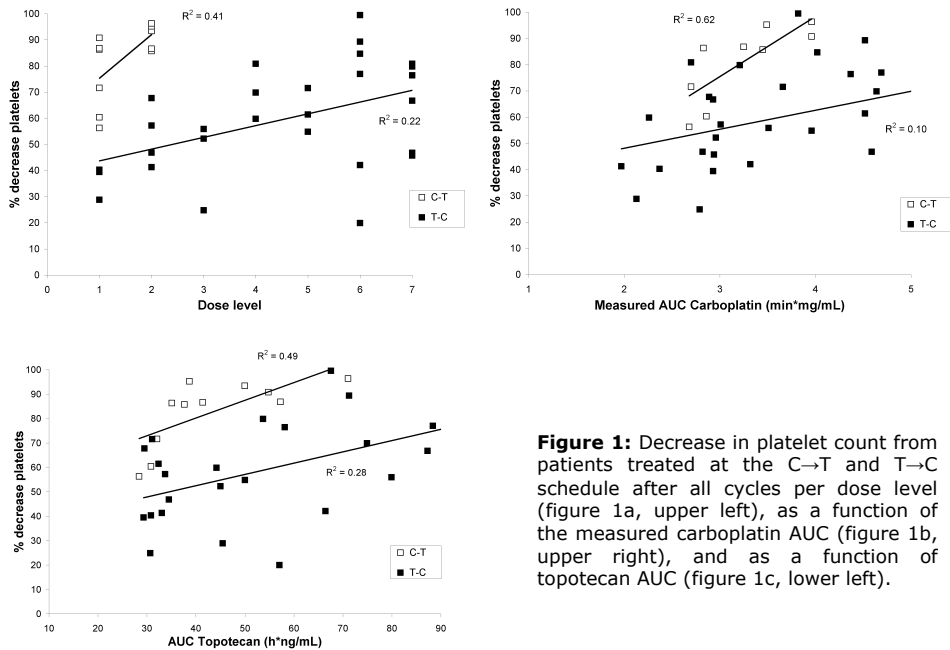


Figure 1: Decrease in platelet count from patients treated at the C→T and T→C schedule after all cycles per dose level (figure 1a, upper left), as a function of the measured carboplatin AUC (figure 1b, upper right), and as a function of topotecan AUC (figure 1c, lower left).

schedule, the AUA Pt-GG and Pt-AG values were in the range of 0.44-4.13 fmol*h/ μ g DNA and 0.02-1.95 fmol*h/ μ g DNA, respectively. During the T→C schedule the AUA values were in the range of 0.22-6.07 fmol*h/ μ g DNA for Pt-GG and 0.00-2.14 fmol*h/ μ g DNA for Pt-AG. Figure 2a and b present a scatter plot of the AUA of Pt-GG as a function of the measured AUC of carboplatin. During both schedules, it was shown that there was a significant increase in AUA of Pt-GG in WBC when the measured AUC of carboplatin increased. When comparing the AUA Pt-GG values between the C→T and T→C schedule, no significant difference was found ($p = 0.09$). The AUA Pt-GG values were corrected for the measured AUC of carboplatin.

During the C→T schedule, Pt-GG and Pt-AG adduct levels in tumor tissue could be determined in 11 and 10 patients, respectively. The Pt-GG and Pt-AG levels were in the range of 0.20-0.96 fmol/ μ g DNA and 0.01-0.21 fmol/ μ g DNA, respectively. During the T→C schedule, Pt-GG and Pt-AG adduct levels in tumor tissue could be determined in 16 patients. The Pt-GG and Pt-AG levels were in the range of 0.62-1.81 fmol/ μ g DNA and 0.11-0.33 fmol/ μ g DNA, respectively. The Pt-GG levels in tumor tissue were compared with the Pt-GG levels in WBC that were taken at the time-point of tumor biopsy. The results are depicted in figure 2c. No significant correlation was found between the Pt-

Chapter 5.1

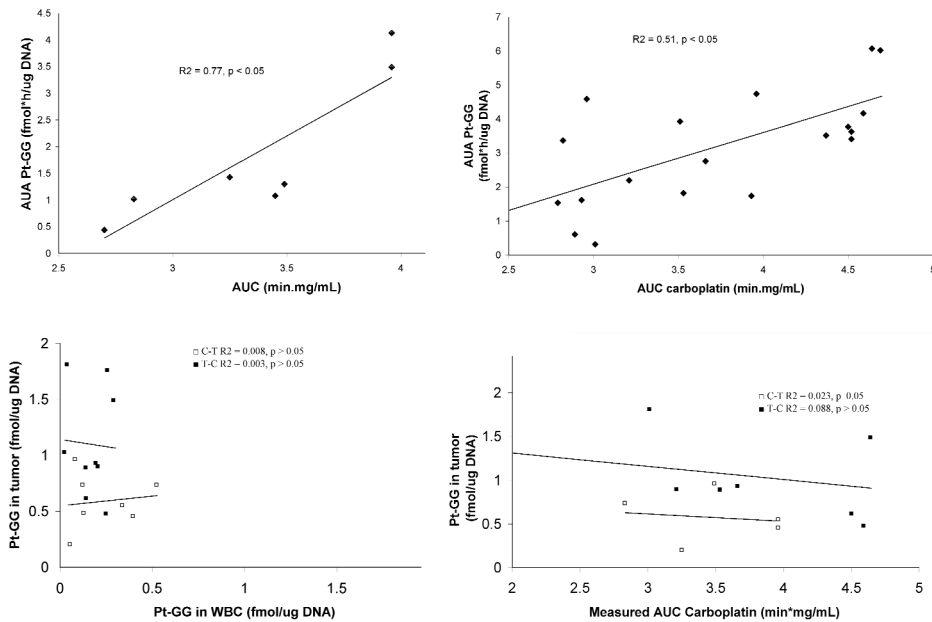


Figure 2: Relationship between the AUA of Pt-GG and the measured AUC of carboplatin during the C→T schedule, cycle 1. N = 7 (figure 2a, upper left); Relationship between the AUA of Pt-GG and the measured AUC of carboplatin during the T→C schedule, cycle 1. N = 19 (figure 2b, upper right); Pt-GG adduct levels in WBC versus tumor tissue. C→T schedule N = 7 and T→C schedule N = 9 (figure 2c, lower left); Pt-GG adduct levels in tumor tissue versus measured AUC of carboplatin. C→T schedule N = 5 and T→C schedule N = 8 (figure 2d, lower right).

GG adduct levels in WBC and tumor tissue during both schedules. The levels found in tumor tissue were significantly higher than in WBC in the C→T schedule ($p = 0.02$) as well as in the T→C schedule ($p = 0.0005$). Figure 2d shows the relationship between tumor Pt-GG adduct levels and the measured AUC of carboplatin. No significant correlation was found. To investigate schedule dependency, the tumor Pt-GG adduct levels were corrected for the measured AUC. No significant difference was found between the C→T and T→C schedule ($p = 0.14$).

Response

Of the 41 patients, 39 patients had at least one post baseline response evaluation (supplementary table 3). One patient (2%) with relapsed SCLC, had a confirmed complete response. Partial responses were documented in five patients (12%), two of which were treated at the C→T schedule (both ovarian cancer patients). The partial responses in the T→C schedule were observed in

patients with ovarian cancer, SCLC and gastric cancer, respectively. In addition to these objective responses, twenty-one patients (51%) had stable disease varying between 1 and 8 months. Twelve patients (29%) had disease progression.

Discussion

In this trial, we examined the combination of carboplatin and topotecan in two different treatment schedules. The MTD for the C→T schedule was established at topotecan 0.5 mg/m²/day and carboplatin target AUC 4 min.mg/mL, while dose escalation could be continued up to level 6 (topotecan 0.9 mg/m²/day and carboplatin AUC 6 min.mg/mL) in the reversed schedule. These results are in agreement with other studies (24). We individualized the dose of carboplatin using the Calvert formula, and found a considerable variability between the target AUC and the measured AUC. This could be due to the Cockcroft and Gault formula that was used to calculate the creatinine clearance. Previously, it has been shown that using this method results in underexposure to carboplatin (35,36,37). Calculation of the creatinine clearance by a ⁵¹CrEDTA-measurement might have resulted in lower variability between the target and measured AUC. However, the observed difference between target and measured AUC of carboplatin has in our view not affected the main outcome of the study.

The observed myelotoxicity was clearly different between the two schedules. This effect could not be attributed to a pharmacokinetic interaction, since we found no significant difference in the CL of carboplatin and topotecan between the C→T and T→C schedule. The observed schedule dependent toxicity could also not be attributed to the here addressed pharmacodynamic factors. During both schedules we found an increase in the concentration of nuclear extract needed for complete relaxation of supercoiled DNA, and the concentration of the nuclear extract needed for relaxation of DNA was highest when both agents were present. However, there was no schedule dependency. Also, no correlation was found between TopI catalytic activity and TopI protein levels in tumor cells. It was expected that higher concentrations of TopI protein frequently found in tumor cells (38) were correlated with higher TopI catalytic activity, but this was not confirmed in our trial. The lack of correlation between TopI protein levels and TopI catalytic activity was also shown in other studies (39, 40). During both schedules, we found a significant increase in AUA of Pt-

GG in WBC when the measured AUC of carboplatin increased. However, when comparing the AUA Pt-GG values between the C→T and T→C schedule, no significant difference was found. This result is in accordance with the findings *in vitro* of the combination of topotecan and cisplatin where no schedule dependent effect could be found in the Pt-DNA adduct levels in WBC (17). To our knowledge, this is the first report addressing the relationship between Pt-GG adduct levels in WBC and tumor tissue following treatment with carboplatin. Unfortunately, no correlations were found between the measured AUC of carboplatin and the Pt-GG adduct levels in tumor tissue, and between the Pt-GG adduct levels in WBC and tumor tissue. The levels found in tumor tissue were significantly higher during both schedules compared to WBC. These results have also been reported for cisplatin recently (41). The difference in Pt-GG adduct levels in tumor tissue compared to WBC could be due to: differences in DNA repair mechanisms in tumor cells compared to WBC; differences in pH of tumor cells that can effect delivery (42); differences in scavenging thiol levels; or overexpression of multidrug resistance proteins MRP2 or the copper transporting P-type ATPase ATP7B (43, 44).

We hypothesize that other than the here described pharmacodynamic factors must explain the schedule dependent differences in toxicities. In clinical studies, the most important pharmacodynamic parameter (the fixation of the cleavable complex by topotecan) can't be measured. This is due to the rapid reversibility of the reaction and the lack of a sufficiently sensitive assay. It is plausible that the same pharmacodynamic interaction between carboplatin and topotecan takes place in myeloid precursor cells as identified in tumor cells *in vitro*. This synergy would explain the schedule dependent myelotoxicity. Future studies are needed to determine any differential effect of carboplatin-topotecan in tumor versus myeloid cells. Although higher doses of topotecan and carboplatin could be administered in the T→C schedule, the results of the preclinical and our clinical studies indicate that the C→T schedule at a dose of topotecan 0.5 mg/m²/day and carboplatin target AUC 4 min.mg/mL is preferred for further investigation. This schedule showed synergy with regard to toxicity (myelosuppression) and there may similarly be a positive antitumor synergy with the lower doses of carboplatin and topotecan. Future studies randomizing the two schedules of carboplatin and topotecan are needed to unravel any difference in antitumor activity.

Acknowledgement

The study was supported by an unrestricted grant from GlaxoSmithKline, Research Triangle Park, NC, USA.

References

1. Kollmannsberger C, Mross K, Jakob A, Kanz L, Bokemeyer C. Topotecan – A novel topoisomerase I inhibitor: pharmacology and clinical experience. *Oncol* 56: 1-12, 1999.
2. Von Pawel J, Schiller JH, Shepherd FA et al. Topotecan versus cyclophosphamide, doxorubicin, and vincristine for the treatment of recurrent small-cell lung cancer. *J Clin Oncol* 17: 658-667, 1999.
3. Long HJ 3rd, Bundy BN, Grendys EC Jr et al. Randomized phase III trial of cisplatin with or without topotecan in carcinoma of the uterine cervix: a Gynecologic Oncology Group Study. *J Clin Oncol*. 20;23(21):4626-33, 2005.
4. Gordon A, Carmichael J, Malfetano J et al. Final analysis of a phase III, randomised study of topotecan versus paclitaxel in advanced epithelial ovarian carcinoma: international topotecan study group. *Proc Am Soc Clin Oncol* 17: 356a, 1998.
5. Lokich J, Anderson N. Carboplatin versus cisplatin in solid tumors: An analysis of the literature. *Ann Oncol* 9: 13-21, 1998.
6. Go RS, Adjei A. Review of the comparative pharmacology and clinical activity of cisplatin and carboplatin. *J Clin Oncol* 17: 409-422, 1999.
7. Hertzberg RP, Caranfa MJ, Holden KG et al. Modification of the hydroxy lactone ring of camptothecin: inhibition of mammalian topoisomerase I and biological activity. *J Med Chem* 32: 715-720, 1989.
8. Beijnen JH, Smith BR, Keijer WJ et al. High-performance liquid chromatographic analysis of the new antitumour drug SK&F 104864-A (NSC 609699) in plasma. *J Pharm Biomed Anal* 8: 789-794.
9. Hsiang Y-H, Liu LF. Identification of mammalian DNA topoisomerase I as an intracellular target of the anticancer drug camptothecin. *Cancer Res* 48: 1722-1729, 1988.
10. Hsiang Y-H, Lihou MG, Liu LF. Arrest of replication forks by drug-stabilized topoisomerase I-DNA cleavable complexes as a mechanism of cell killing by camptothecin. *Cancer Res* 49: 5077-5082, 1989.
11. Eng W-K, Faucette L, Johnson RK, Sternglanz R. Evidence that DNA topoisomerase I is necessary for the cytotoxic effects of camptothecin. *Mol Pharmacol* 34: 755-760, 1988.
12. Reed E, Kohn K. Platinum analogues, in Chabner BA, Collins JM (eds): *Cancer Chemotherapy: Principles and Practice*. Philadelphia, PA, Lippincott: 465-490, 1990
13. Calvert AH, Newell DR, Gumbrell LA et al. Carboplatin dosage: Prospective evaluation of a simple formula based on renal function. *J Clin Oncol* 7: 1748-1756, 1989.
14. Jodrell DI, Egorin MJ, Canetta RM et al. Relationships between carboplatin exposure and tumor response and toxicity in patients with ovarian cancer. *J Clin Oncol* 4: 520-528, 1992.
15. Romanelli S, Perego P, Pratesi G, Carenini N, Tortoreto M, Zunino F. In vitro and in vivo interaction between cisplatin and topotecan in ovarian carcinoma systems. *Cancer Chemother Pharmacol* 41: 385-390, 1998.
16. Ma J, Maliepaard M, Nooter K et al. Synergistic cytotoxicity of cisplatin and topotecan or SN-38 in a panel of eight solid-tumor cell lines in vitro. *Cancer Chemother & Pharmacol* 41: 307-16, 1998.
17. Van Waardenburg RCAM, De Jong LA, van Eijndhoven MA et al. Platinated DNA adducts enhance poisoning of DNA topoisomerase I by camptothecin. *J Biol Chem* 279: 54502-54509, 2004.
18. Van Waardenburg RCAM, De Jong LA, van Delft F et al. Homologous recombination is a highly conserved determinant of the synergistic cytotoxicity between cisplatin and DNA topoisomerase I poisons. *Mol Cancer Ther* 3: 393-402, 2004.

Chapter 5.1

19. Rowinsky EK, Kaufmann SH, Baker SD et al. Sequences of topotecan and cisplatin: Phase I, pharmacologic, and in vitro studies to examine sequence dependence. *J Clin Oncol* 14: 3074-3084, 1996.
20. De Jonge MJ, Loos WJ, Gelderblom H et al. Phase I pharmacologic study of oral topotecan and intravenous cisplatin: Sequence dependent hematologic side effects. *J Clin Oncol* 18: 2104-2115, 2000.
21. Pujol JL, von Pawel J, Tumolo S et al. Preliminary results of combined therapy with topotecan and carboplatin in advanced non-small cell lung cancer. *Oncol* 61: 47-54, 2001.
22. Simpson A, Twelves C, Boddy A et al. Schedule dependency of carboplatin and topotecan: Phase I and pharmacokinetic studies. *Proc Am Soc Clin Oncol* 18: 785 (abstr), 1998.
23. Bowman A, Rye T, Ross G, Wheatley A, Smyth JF. Effective dosing of topotecan and carboplatin in relapsed ovarian cancer: a phase I/II study. *J Clin Oncol*. 19: 3255-3259, 2001.
24. Estape RE, Angioli R, Mendez L et al. 3-Day topotecan and carboplatin in first line treatment of ovarian cancer: a phase II trial. *Proc Am Soc Clin Oncol* 20: 874 (abstr), 2001.
25. Wagstaff AJ, Ward A, Benfield P, Heel RC. Carboplatin, a preliminary review of its pharmacodynamic and pharmacokinetic properties and therapeutic efficacy in the treatment of cancer. *Drugs* 37: 162-190, 1989.
26. Cockcroft DW, Gault MH. Prediction of creatinine clearance from serum creatinine. *Nephron* 16: 31-41, 1976.
27. World Health Organisation (WHO): WHO handbook for reporting results of cancer treatment. Geneva, Switzerland, World Health Organisation, 1979.
28. National Cancer Institute (NCI): Guidelines for reporting adverse drug reactions. Bethesda, MD, USA, Division of Cancer Treatment, National Cancer Institute, 1988.
29. Rosing H, Doyle E, Davies BE, Beijnen JH. High-performance liquid chromatographic determination of the novel anti-tumor drug topotecan and topotecan as the total of the lactone and carboxylate forms, in human plasma. *J Chrom B* 668: 107-111, 1995.
30. Van Warmerdam LJC, van Tellingen O, Maes RAA, Beijnen JH. Validated method for the determination of carboplatin in biological fluids by Zeeman atomic spectrometry. *Fresenius J Anal Chem* 351: 1820-1824, 1995.
31. Pluim D, Maliepaard M, van Waardenburg RC, Beijnen JH, Schellens JH. 32P-postlabeling assay for the quantification of the major platinum-DNA adducts. *Analyt Biochem* 275: 30-38, 1999.
32. Schoemaker NE, Herben VM, de Jong LA et al. Topoisomerase I levels in white blood cells of patients with ovarian cancer treated with paclitaxel-cisplatin-topotecan in a phase I study. *Anticancer Drugs* 13: 87-91, 2002.
33. Van Warmerdam LJC, Verweij J, Rosing H, Schellens JH, Maes RA, Beijnen JH. Limited sampling models for topotecan pharmacokinetics. *Ann Oncol* 5: 259-264, 1994.
34. Schellens JH, Ma J, Planting AS et al. Relationship between the exposure to cisplatin, DNA adduct formation in leucocytes and tumor response in patients with solid tumors. *Br J Cancer* 73: 1569-1575, 1996.
35. Nannan Panday VR, van Warmerdam LJ, Huizing MT et al. Carboplatin dosage formulae can generate inaccurate predictions of Carboplatin exposure in carboplatin/paclitaxel combination regimens. *Clin Drug Investig.* 15(4):327-35, 1998
36. Millward MJ, Webster LK, Toner GC et al. Carboplatin dosing based on measurement of renal function--experience at the Peter MacCallum Cancer Institute. *Aust N Z J Med.* 26(3):372-9, 1996.
37. Van Warmerdam LJC, Rodenhuis S, Ten Bokkel Huinink WW, Maes RA, Beijnen JH. Evaluation of formulas using serum creatinine level to calculate the optimal dosage of carboplatin. *Cancer Chemother Pharmacol.* 37: 266-270, 1996.
38. Bronstein IB, Vorobyev S, Timofeev A, Jolles CJ, Alder SL, Holden JA. Elevations of DNA topoisomerase I catalytic activity and immunoprotein in human malignancies. *Oncol Res.* 8: 17-25, 1996.
39. Minagawa Y, Kigawa J, Itamochi H, Tirakawa M. The role of topoisomerase I inhibitor in cisplatin-resistant ovarian cancer. *Hum Cell.*14: 237-243, 2001.
40. Chen BM, Chen JY, Kao M, Lin JB, Yu MH, Roffler SR. Elevated topoisomerase I activity in cervical cancer as a target for chemoradiation therapy. *Gynecol Oncol.* 79: 272-280, 2000.

41. Hoebbers F, Pluim D, Hart AA et al. Cisplatin-DNA adduct formation in patients treated with cisplatin-based chemoradiation: lack of correlation between normal tissues and primary tumor. *Cancer Chemother Pharmacol.* 61:1075-81, 2008
42. Huang Z, Huang Y. The change of intracellular pH is involved in the cisplatin-resistance of human lung adenocarcinoma A549/DDP cells. *Cancer Invest* 23: 26-32, 2005.
43. Kawabe T, Chen ZS, Wada M et al. Enhanced transport of anticancer agents and leukotriene C4 by the human canalicular multispecific organic anion transporter (cMOAT/MRP2). *FEBS Lett.* 456(2):327-31, 2008.
44. Komatsu M, Sumizawa T, Mutoh M et al. Copper-transporting P-type adenosine triphosphatase (ATP7B) is associated with cisplatin resistance. *Cancer Res.* 60(5):1312-6, 2000.

Supplementary information

Statistical analysis

The measured AUC of carboplatin was compared with the target AUC calculated by the method of Calvert using linear regression analysis. The differences in CL of carboplatin and topotecan between the two schedules were tested using a two-sided student t-test. The difference in CL of topotecan when administered alone or in combination with carboplatin was tested using a two-way ANOVA. The two-sided student t-test was used to compare the myelosuppression during both schedules. Myelosuppression was defined as the percentage decrease in leucocytes, platelet count and absolute neutrophil count (ANC), as calculated with the following equation: $[100\% \times (\text{pre-treatment value} - \text{nadir value})] / \text{pre-treatment value}$. The concentration of nuclear extract needed in the TopI catalytic activity assay in WBC for the relaxation of supercoiled DNA was compared between each sampling time point and schedule using a two-way ANOVA. To study the effect of topotecan and carboplatin administration on TopI catalytic activity in tumor cells, one-way ANOVA and post-hoc Scheffé tests were performed. The TopI catalytic activity in tumor cells was compared with the TopI protein levels in tumor cells by linear regression analysis. The same analysis was performed to compare the Pt-adduct concentrations between WBC and tumor cells, and to describe the relationship between the AUA of Pt-adducts with the AUC of carboplatin during both schedules. To investigate a possible schedule dependency, the AUA of Pt-adducts corrected for the measured AUC of carboplatin were compared between the two schedules, using a two-sided student t-test. The tumor adduct levels were also corrected for the measured AUC of carboplatin, to make a comparison between the two schedules possible, presuming there is a linear relation between carboplatin exposure and tumor adduct levels. All

statistical tests were two-tailed and the level of significance was set at 0.05. The statistical analyses were performed using the SPSS software package for Windows (Version 11.0, SPSS Inc, Chicago, Illinois, USA).

Supplementary tables and figures

Supplementary table 1: Number of cycles per patient

Nr. of cycles	N
1-2	17
3-4	8
5-6	12
> 7	4

Supplementary table 2a: TopI catalytic activity in white blood cells during the C→T schedule (day 1 of cycle 1 and 2). Values are expressed as mean (SD) nuclear extract (μg protein/mL) needed for complete relaxation of supercoiled DNA. Sample at time-point of tumor biopsy was only taken during cycle 1

C→T	Before infusion	End carboplatin infusion	End topotecan infusion	At time-point of tumor biopsy
	t0	t1	t1.5	t21.5
Cycle 1	35 (42) ¹	36 (25) ²	40 (23) ²	56 (50) ³
Cycle 2	40 (30) ²	36 (28) ⁴	126 (214) ²	

¹ n = 10, ² n = 9, ³ n = 5, ⁴ n = 8

Supplementary table 2b: TopI catalytic activity in white blood cells during the T→C schedule (day 3 of cycle 1 and 2). Values are expressed as mean (SD) nuclear extract (μg protein/mL) needed for complete relaxation of supercoiled DNA. Sample at time-point of tumor biopsy was only taken during cycle 1

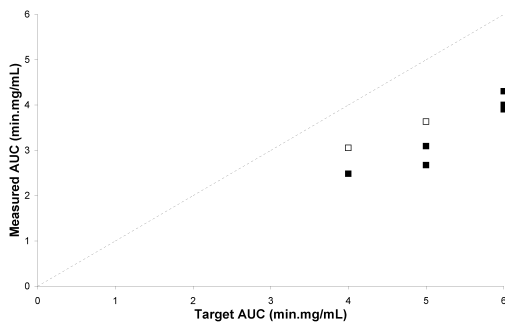
T→C	Before infusion	End topotecan infusion	End carboplatin infusion	At time-point of tumor biopsy
	t0	t0.5	t1.5	t21.5
Cycle 1	25 (29) ¹	34 (22) ²	63 (51) ¹	98 (53) ³
Cycle 2	29 (30) ⁴	65 (72) ³	105 (142) ³	

¹ n = 23, ² n = 22, ³ n = 19, ⁴ n = 20

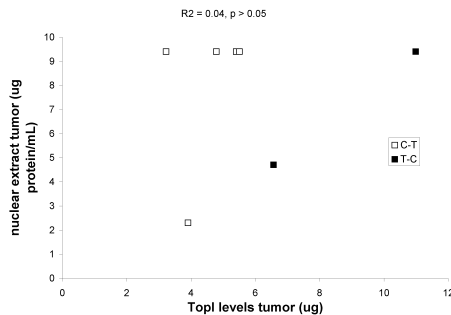
Supplementary table 3: Best response during treatment according to WHO criteria.

Dose level	Schedule	n	Complete response (CR)	Partial response (PR)	Stable disease (SD)	Progressive disease (PD)	Not evaluable (NE)
1	C→T	6		1	3	2	
2	C→T	6		1	4	1	
1	T→C	3		2	1		
2	T→C	4			3	1	
3	T→C	3			2		1
4	T→C	3			1	2	
5	T→C	3	1		2		
6	T→C	6		1	2	3	
7	T→C	7			3	3	1
No of patients (%)		41	1 (2%)	5 (12%)	21 (51%)	12 (29%)	2 (5%)

Supplementary Figure 1: Linear regression analysis for target AUC and mean measured AUC of carboplatin. □ C→T schedule; ■ T→C schedule. The dotted line is the line of identity (x = y)



Supplementary Figure 2: TopI catalytic activity versus TopI protein levels in tumor tissue
 C→T schedule: 5 patients treated at 0.5 mg/m2/day topotecan
 T→C schedule: 2 patients treated at 0.6 mg/m2/day topotecan;
 data adjusted to 0.5 mg/m2/day topotecan



6

**The parp inhibitor
olaparib (AZD2281)**

CHAPTER 6.1

Inhibition of poly(ADP-ribose) polymerase in tumors from BRCA mutation carriers

Peter C. Fong, David S. Boss, Timothy A. Yap, Andrew Tutt, Peijun Wu, Marja Mergui-Roelvink, Peter Mortimer, Helen Swaisland, Alan Lau, Mark J. O'Connor, Alan Ashworth, James Carmichael, Stan B. Kaye, Jan H. M. Schellens, Johann S. de Bono

N Engl J Med. 2009;361(2):123-34

Abstract

Background: Inhibiting poly(ADP)-ribose polymerase (PARP) is a potential synthetic lethal strategy for the treatment of cancers with specific DNA repair defects, including those arising in BRCA1 and BRCA2 (BRCA1/2) mutation carriers. Olaparib (AZD2281) is a novel, potent, orally active PARP inhibitor.

Methods: A first-in-man Phase I trial was conducted with detailed pharmacokinetic-pharmacodynamic (PK-PD) studies. The patient population was planned to be enriched with BRCA1/2 mutation carriers.

Results: 60 patients were treated; 22 were BRCA1/2 mutation carriers with a further patient with a strong BRCA family history declining testing. Dose level and schedule increased from 10 mg daily for 2 out of 3 weeks, to 600 mg bid continuously. Olaparib was well tolerated. Reversible dose-limiting toxicities were seen in 1/6 patients at 400 mg bid (grade 3 mood alteration and fatigue) and 2/6 patients at 600 mg bid (grade 4 thrombocytopenia; grade 3 somnolence). This led to an expansion cohort at 200 mg bid in BRCA1/2 mutation carriers only. Other toxicities included mild gastrointestinal symptoms. There was no increased toxicity observed in BRCA1/2 mutation carriers. PK data indicated rapid absorption and elimination; PD studies confirmed PARP inhibition in surrogate and tumor tissue. Substantial and durable antitumor activity was reported only in BRCA1/2 mutation carriers, in patients with heavily pre-treated ovarian, breast and prostate cancers.

Conclusions: This is the first clinical trial to validate the concept of synthetic lethality with a PARP inhibitor. Olaparib is well tolerated, inhibits PARP and has substantial antitumor activity in BRCA1/2 mutation associated cancers.

Introduction

Cellular DNA is continually subject to damage and coordinated pathways act to repair this, maintaining genomic integrity and cell survival (1-3). The poly(ADP)-ribose polymerases (PARPs) comprise a large family of multi-functional enzymes, the most abundant of which is PARP-1 which plays a key role in the repair of DNA single-strand breaks (SSBs) via the base excision repair (BER) pathway (4-5). PARP inhibition leads to the accumulation of DNA SSBs, which can result in DNA double-strand breaks (DSBs) at replication forks. Normally these are effectively repaired by the error-free homologous recombination (HR) double-strand DNA repair pathway (6), key components of which are the tumor suppressor proteins BRCA1 and BRCA2 (7).

Germline heterozygous mutations in one BRCA1 or BRCA2 allele are associated with a high risk of development of a number of malignancies, including breast, ovarian and prostate (8-10). Cells carrying heterozygous loss-of-function BRCA mutations can lose the remaining wild-type allele, resulting in deficient HR DNA repair, causing genetic aberrations driving carcinogenesis in BRCA carriers; this somatic loss of the wild-type allele in the tumor is thought to be an obligate step in this process. This leads to the emergence of a tumor that carries a DNA repair defect that is not shared by the rest of the normal tissues of the carrier. This tumor-specific defect can be exploited using PARP inhibitors to induce selective tumor cytotoxicity, sparing normal cells. PARP inhibition in these HR repair-deficient tumor cells generates unrepaired DNA SSBs which are likely to cause the accumulation of DSBs and collapsed replication forks (11-13). Conversely, the normal tissue compartment is composed of cells heterozygous for BRCA mutations that retain HR function and have PARP inhibitor sensitivity similar to wild-type cells, suggesting a large therapeutic index for PARP inhibition in BRCA carriers (14, 15). This effect has been described as "synthetic lethality", which occurs when there is a potent and lethal synergy between two otherwise non-lethal events: a highly specific PARP inhibitor induced DNA lesion and a tumor-restricted genetic loss of function for the DNA repair pathway required to repair it (HR) (13) (Supplementary Figure 1). We have shown that inhibiting a DNA repair enzyme in the absence of an exogenous DNA-damaging agent to selectively kill tumor cells represents a novel approach to cancer therapy (11). In vitro, BRCA1 and BRCA2-deficient cells were up to 1000-fold more sensitive to PARP inhibition than wild-type cells and tumor growth inhibition was also demonstrated in BRCA2-deficient

xenografts (11, 12, 16). Here, we describe the first clinical evaluation of a novel, potent, orally active PARP inhibitor olaparib (previously AZD2281 and KU-0059436; Supplementary Figure 2) (17), with a focus on BRCA mutation carriers.

Methods

Patients

This study was performed at the Royal Marsden Hospital (RMH, United Kingdom) and the Netherlands Cancer Institute (NKI, Netherlands). Eligibility criteria were: ≥ 18 years of age; disease refractory to standard therapies or with no suitable effective standard treatments; ECOG performance status ≤ 2 ; adequate bone marrow, hepatic and renal function and a washout period after previous anticancer therapy of ≥ 4 weeks. BRCA1 or BRCA2 mutation carrier status was not initially required for eligibility, although provisions were made in the protocol to permit BRCA1 or BRCA2 mutation carrier enrichment. In the expansion phase, only BRCA1 or BRCA2 mutation carrier patients were enrolled. The study was approved by institutional review boards and ethics committees and commenced in June 2005.

Study design

Dose escalation utilized a modified accelerated titration design (18). Briefly, this involved treating 3 patients per dose level with 100% dose escalation between dose levels in the absence of grade 2 or greater toxicity. Six patients were treated if one dose-limiting toxicity (DLT) was observed at a dose level; the maximum administered dose was defined if 2 DLTs were observed at a dose level, when dose escalation was stopped. Drug-related grade 3 or 4 toxicity occurring in the first cycle was considered a DLT. Olaparib was initially given once daily in 3-weekly cycles at 10 mg for 2 out of 3 weeks, but this was subsequently modified to a continuous twice-daily schedule in 4-weekly cycles from 100 mg (Supplementary Table 1). Since this was a 'first-in-man' trial, the objectives were to determine safety, tolerability, DLT, maximum-tolerated dose (MTD), PARP inhibitory dose and pharmacokinetic (PK) and pharmacodynamic (PD) profiles in both surrogate and tumor tissue. Once these had been established, a key aim was to test the hypothesis that patients with BRCA1 and BRCA2 mutation associated cancers would demonstrate

objective responses to single-agent treatment with this approach, since this had never previously been observed in clinical practice.

Assessment of toxicity, PK/PD, and response

Safety evaluations were conducted at baseline and weekly. All subjects had a history taken and physical examination performed; investigations including complete blood count, clotting, electrolytes, liver and renal function tests and electrocardiograph tracing. Adverse events were graded by the Common Terminology Criteria for Adverse Events (CTCAE) version 3.0 (19). PK and PD studies were performed at baseline and during cycles 1 and 2. Plasma was analyzed by solid-phase extraction followed by high-performance liquid chromatography with mass spectrometric detection to determine olaparib plasma concentrations. The plasma concentration-time data were analyzed using non-compartmental analysis [WinNonLin version 4.1; Pharsight Corporation, CA94041, USA] to derive PK parameters following the first dose (single-dose parameters) and dosing on day 14 (multiple-dose parameters). PARP inhibition was evaluated in PD studies utilizing a functional assay (Mesoscale Discovery®, Maryland 20877, USA) by analyzing poly(ADP)-ribose (PAR) formation from peripheral blood mononuclear cells (PBMCs) and tumor tissue cell lysates, all normalized to the amount of PARP-1 protein present (20). The formation of γ H2AX foci, a marker of DNA DSBs, was evaluated at dose levels ≥ 100 mg bid of olaparib. This was performed before, and at multiple time points following treatment utilizing plucked eyebrow hair follicles (Supplementary Figure 3) (20). Tumor radiological assessments by CT or MRI scans were carried out every 2 cycles and graded according to RECIST criteria (21). Additional disease evaluation with serum tumor markers, including cancer antigen 125 (CA125) and prostate-specific antigen (PSA) assessed by the Gynecologic Cancer Intergroup (GCIg) (22) and PSA Working Group (PSAWG) (23) criteria respectively, were carried out where appropriate. Tumor marker response in ovarian and prostate cancer was taken as decline $>50\%$ sustained at least 4 weeks later. Patient response was defined as the number of patients with CR and PR, while the clinical benefit rate was defined as the number of patients with radiological or tumor marker response, or stable disease for ≥ 4 months.

Table 1: Patient demographics (n=60)

Characteristics		Number (%)
Sex	Male	20 (33.3)
	Female	40 (66.7)
Age, years	Mean	54.8
	Range	19–82
Tumor type	Ovarian¶ [15 BRCA1;1 BRCA2]	21 (33.3)
	Breast [3 BRCA2]	9 (15)
	Colorectal	8 (13.3)
	Melanoma	4 (6.7)
	Sarcoma	4 (6.7)
	Prostate [1 BRCA2]	3 (5)
	Other*	11 (18.3)
ECOG performance status	0	18 (30)
	1	37 (61.7)
	2	5 (8.3)
No. of prior treatments	1	6 (10)
	2	11 (18.3)
	3	11 (18.3)
	≥4	32 (53.3)

All patients (n=60)							
	<100 mg bid n=18	100 mg bid 2 of 3 wks n=4	100 mg bid n=5	200 mg bid n=20	400 mg bid n=8	600 mg bid n=5	Overall n=60
BRCA1	1	1	1	7	6	1	17
BRCA2	0	0	0	5	0	0	5
BRCA wild-type or unknown	17	3#	4	8	2	4	38#

Ovarian cancer subgroup (n=21)							
	<100 mg bid n=4	100 mg bid 2 of 3 wks n=2	100 mg bid n=1	200 mg bid n=7	400 mg bid n=6	600 mg bid n=1	Overall n=21
BRCA1	1	1	1	5	6	1	15
BRCA2	0	0	0	1	0	0	1
BRCA wild-type or unknown	3	1#	0	1	0	0	5#

¶ Ovarian cancer includes 1 primary peritoneal cancer and 1 fallopian tube cancer. *Uterine and vaginal (n=3), lung (n=3), pancreas (n=2), mesothelioma (n=2), kidney (n=1) cancers; # Includes 1 patient with a strong family history of BRCA-mutated cancers, but who declined BRCA mutation testing.

Study responsibilities

The study (KU36-92; D0810C00002; NCT00516373) was designed by academic investigators at the Royal Marsden Hospital, Institute of Cancer Research and representatives of KuDOS Pharmaceuticals Ltd, the sponsor of this trial. Drs Yap, Fong and de Bono wrote the first draft of the manuscript, which was then finalized by the co-authors. Data were collected and analyzed under the supervision of the academic investigators. Data management and descriptive statistics were performed by Theradex with additional analyses performed by The Institute of Cancer Research.

Results

Patients

Sixty patients with histologically or cytologically confirmed advanced solid tumors were enrolled; their demographics are presented in Table 1. Evaluated olaparib dose levels utilizing 10 separate cohorts are described in Supplementary Table 1. Minimal toxicity, with impressive antitumor activity in BRCA1 and BRCA2 mutation associated cancers was reported, confirming that this agent's safety profile is very different to that of cytotoxic chemotherapy.

Dose-limiting toxicity and maximum administered dose

Three DLTs in course 1 were observed at the 400 mg and 600 mg bid dose cohorts. At 400 mg bid, a 47-year-old patient with advanced ovarian carcinoma experienced grade 3 mood alteration and fatigue on the first day of treatment. These symptoms completely resolved within 24 hours of drug discontinuation, recurring on re-challenge at 200 mg bid, resulting in treatment discontinuation. A 59-year-old patient with mesothelioma, who had just completed mitomycin, vinblastine and carboplatin chemotherapy that had resulted in prolonged myelosuppression, experienced grade 4 thrombocytopenia at 600 mg bid during the first month of treatment. This thrombocytopenia resolved within two weeks of drug discontinuation. The third DLT was observed in a 47-year-old metastatic breast carcinoma patient at 600 mg bid who experienced grade 3 somnolence on day 8 of treatment that resolved completely within 24 hours of drug discontinuation; grade 1

Chapter 6.1

	<100 mg bid n (%)	100 mg bid 2 of 3 wks n (%)	100 mg bid contin. n (%)	200 mg bid contin. n (%)	400 mg bid contin. n (%)	600 mg bid contin. n (%)	Total n (%)
Anemia							
Grade 1-2	1 (5.6%)	0	0	0	0	1 (20.0%)	2 (3.3%)
Grade 3-4	0	0	0	1 (5.0%)	0	0	1 (1.7%)
Lymphopenia							
Grade 1-2	0	0	0	0	0	0	0
Grade 3-4	0	0	0	2 (10.0%)	1 (12.5%)	0	3 (5.0%)
Diarrhea							
Grade 1-2	0	0	0	2 (10.0%)	1 (12.5%)	0	3 (5.0%)
Grade 3-4	0	0	0	0	0	0	0
Dyspepsia							
Grade 1-2	0	0	0	1 (5.0%)	1 (12.5%)	2 (40.0%)	4 (6.7%)
Grade 3-4	0	0	0	0	0	0	0
Nausea							
Grade 1-2	6 (33.3%)	1 (25%)	0	7 (35.0%)	0	3 (60.0%)	17 (28.3%)
Grade 3-4	0	0	0	0	1 (12.5%)	1 (20.0%)	2 (3.3%)
Stomatitis							
Grade 1-2	0	0	0	3 (15.0%)	0	0	3 (5.0%)
Grade 3-4	0	0	0	0	0	0	0
Vomiting							
Grade 1-2	2 (11.1%)	1 (25%)	0	5 (25.0%)	0	3 (60.0%)	11 (18.3%)
Grade 3-4	0	0	0	0	1 (12.5%)	0	1 (1.7%)
Anorexia							
Grade 1-2	3 (16.7%)	0	0	2 (10%)	0	2 (40%)	7 (11.7%)
Grade 3-4	0	0	0	0	0	0	0
Dysgeusia							
Grade 1-2	0	2 (50%)	0	2 (10.0%)	1 (12.5%)	3 (60.0%)	8 (13.3%)
Grade 3-4	0	0	0	0	0	0	0
Fatigue							
Grade 1-2	3 (16.7%)	0	1 (20.0%)	4 (20.0%)	5 (62.5%)	4 (80.0%)	17 (28.3%)
Grade 3-4	0	0	0	1 (5.0%)	0	0	1 (1.7%)
Dizziness							
Grade 1-2	0	0	0	1 (5.0%)	0	1 (20.0%)	2 (3.3%)
Grade 3-4	0	0	0	0	1 (12.5%)	0	1 (1.7%)

*Adverse events at least possibly, probably and definitely related to olaparib in the safety population Note: no grade 5-related adverse events were reported at that time of this analysis

Table 2 (left page): Olaparib-related adverse events* with a frequency of $\geq 5\%$ in the safety population

somnolence recurred on re-challenge at 400 mg bid. These DLTs led to a defined maximum administered dose of 600 mg bid and a MTD of 400 mg bid.

Safety

Toxicities in this study were largely mild (grade 1–2) and included nausea (19 patients; 31.7%), fatigue (18; 30%), vomiting (12; 20%), taste alteration (8; 13.3%) and anorexia (7; 11.7%). A low incidence of myelosuppression was reported; 3 patients (5%) experienced anemia and 2 patients (3%) experienced grade 4 thrombocytopenia (Table 2).

One patient with advanced non-small-cell lung carcinoma and a history of recurrent lower respiratory tract infections experienced fatal respiratory failure and died after 4 months on olaparib. Another patient with ovarian cancer died from Gram-negative septicemia after 1 month on olaparib in the absence of neutropenia; she had pelvic nodal disease with cutaneous involvement that was colonized with similar organisms. Both cases were deemed unlikely to be olaparib related.

No obvious increase in frequency or grade of toxicities was observed when comparing known BRCA1 or BRCA2 mutation carriers and non-carriers.

Pharmacokinetic studies

PK studies indicate that olaparib absorption is rapid with peak plasma concentration (C_{max}) observed 1–3 hours post-dosing (Supplementary Figure 4). Following this, plasma concentrations declined bi-phasically with a terminal elimination half-life of approximately 5–7 hours (Supplementary Table 2). The exposure achieved increased with increasing dose up to 100 mg, but increased less proportionally as the dose was increased further (Figures 1A and 1B). The mean volume of distribution was 40.3 L and mean plasma clearance was 4.55 L/hr. Following daily administration of 10, 20, 40 and 80 mg of olaparib for 14 days, exposure did not increase markedly over that achieved with a single dose (AUC₀₋₂₄ increased by $\sim 26\%$). Following twice-daily dosing with 60, 100, 200, 400 and 600 mg of olaparib, exposure increased by an average of 49%; there was no marked time dependency in the PK of olaparib.

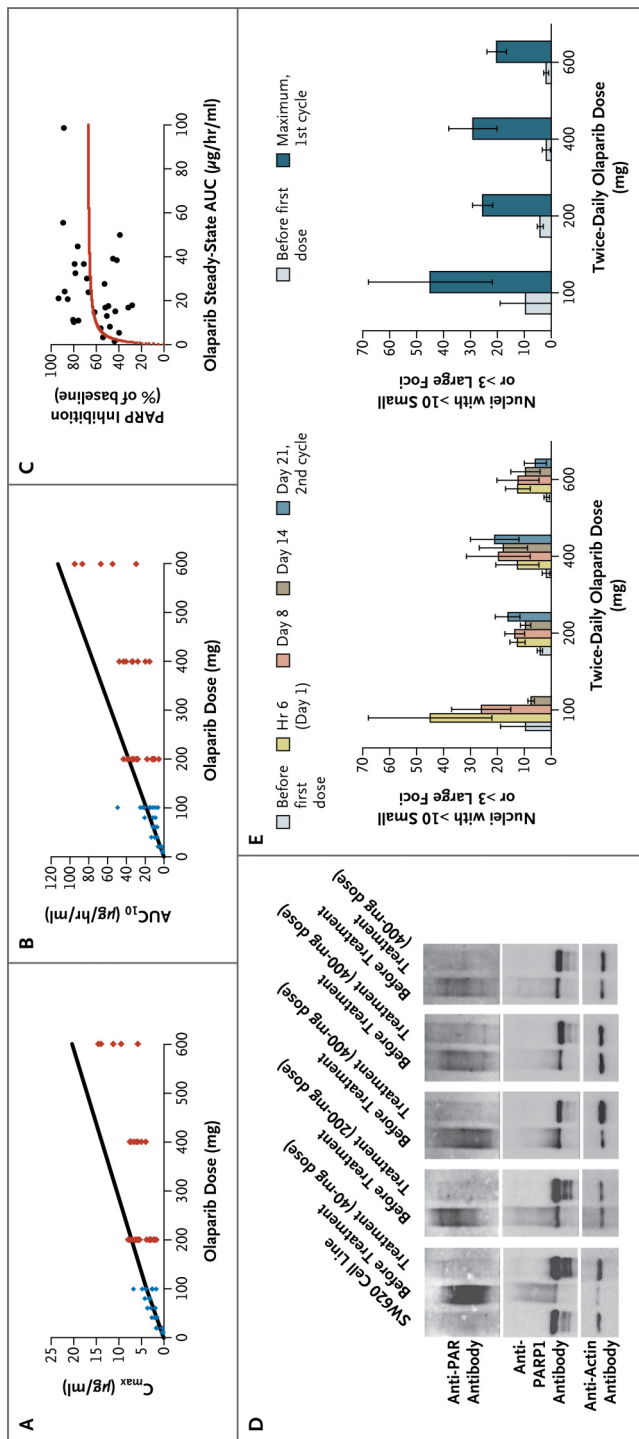


Figure 1 (left page): Results of pharmacokinetic and pharmacodynamic studies of olaparib. The results of pharmacokinetic studies of olaparib are shown after receipt of a single dose. The peak plasma concentration (C_{max}) of olaparib (Panel A) and the area under the plasma concentration–time curve over a 10-hour period after dosing (AUC_{10}) (Panel B) are shown according to the olaparib dose administered. Blue data points represent doses for which exposure increased proportionally with dose, and red data points represent doses for which the increase in exposure was less than proportional to dose. The black line depicts the dose-proportional relationship between exposure and dose that was achieved at doses up to 100 mg and the predicted average exposure that would be expected at doses greater than 100 mg if dose proportionality were maintained across the range of doses. Panel C shows the results of pharmacokinetic–pharmacodynamic analyses. Samples of peripheral-blood mononuclear cells (PBMCs) were collected before and after administration of olaparib for each patient. Poly(adenosine diphosphate [ADP]–ribose) polymerase (PARP) activity was determined through an ex vivo PARP-activation assay. The data points represent PARP inhibition after receipt of olaparib, expressed as a percentage of PARP activity before receipt of olaparib and averaged over time for each patient in each dosing group. These values are plotted against the drug exposure achieved in the patient after multiple doses of olaparib (the steady-state AUC). The red line represents the line of best fit of a simple E_{max} (maximum-effect) model to the data. The results of pharmacodynamic assays, reflecting the inhibition of PARP activity in tumors from patients treated with olaparib, are shown in Panel D. Immunoblots of tumor whole-cell extracts from patients were prepared before the start of continuous olaparib administration and 8 days afterward. Blots were probed with antibodies against poly(ADP-ribose) (PAR), PARP1, and actin (the loading control). Unstimulated SW620 cells (those in which PARP1 was not activated) show no PAR signal and were used as a negative control. Active PARP1 modifies itself with PAR polymers; therefore, the loss of PAR signal after treatment (top row) indicates inhibition of PARP activity. Reprobing of the same blots with anti-PARP1 antibody (middle row) reveals upward smearing of PARP1 proteins before but not after olaparib treatment, confirming inhibition of PARP activity. In pharmacodynamic assays with the use of eyebrow-hair follicles (Panel E), the percentage of cell nuclei with at least 10 small or 3 large foci of γ H2AX, the phosphorylated form of histone H2A histone family, member X (H2AX) at serine 139 is shown before and after olaparib administration (left), and the peak γ H2AX induction during the first cycle is shown for the cohort of patients receiving each dose of olaparib. A minimum of 100 nuclei were scored for each data point, by an observer who was unaware of the olaparib dose. There was significant induction of γ H2AX for each dose shown. The numbers of patients with samples tested were as follows: 2 in the 100-mg cohort, 18 in the 200-mg cohort, 5 in the 400-mg cohort, and 4 in the 600-mg cohort. I bars indicate the standard error.

Evidence for PARP inhibition

Figure 1C depicts the average percentage PARP inhibition in PBMC from patients in each cohort with increasing doses of olaparib, plotted against steady state exposure to olaparib. Substantial PARP inhibition of >90% was observed in patients treated at doses ≥ 60 mg bid. Immunoblots of cell extracts prepared from tumor biopsies collected pre-dose and after 8 days of treatment with olaparib are shown in Figure 1D. PARP inhibition is evidenced by the loss of PAR signal (a biomarker for PARP activity) in treated samples. PD analysis was also carried out on plucked eyebrow hair follicles to measure γ H2AX foci formation following treatment (24). γ H2AX foci induction 6 hours post-olaparib (Figure 1E) indicated that PARP inhibition was rapidly associated with downstream induction of arrested DNA replication forks and DNA DSBs as predicted by preclinical models.¹¹ This induction of γ H2AX was sustained at all

Table 3: Tumor responses divided into subgroups for all evaluable *BRCA1/2* ovarian, breast and prostate cancer patients

Subgroup	Number of patients by subgroup and dose level	Radiological response by RECIST criteria		Tumor marker decline >50% (response)	Radiological and/or tumor marker response	Clinical Benefit (radiological or tumor marker response or SD ≥4 months)
		PR/CR	SD ≥4 months (actual duration)			
Evaluable <i>BRCA1/2</i> ovarian, breast and prostate cancer patients§	19	9 (8 Ov, 1 Br)	2 (1 Ov, 1 Br)	7 (6 Ov, 1 Pr)	10 (8 Ov, 1 Br, 1 Pr)	12 (9 Ov, 2 Br, 1 Pr)
<100 mg bid	1	0	0	0	0	0
100 mg bid for 2 of 3 weeks	2#	1#	0	1#	1#	1#
100 mg bid	1	0	0	0	0	0
200 mg bid	10	4	2 (6, 7 months)	3	5	7
400 mg bid	4	4~	0	3	4	4
600 mg bid	1	0	0	0	0	0
Evaluable <i>BRCA1/2</i> ovarian cancer patients§	15	8	1	6	8	9
<100 mg bid	1	0	0	0	0	0
100 mg bid for 2 of 3 weeks	2#	1#	0	1#	1#	1#
100 mg bid	1	0	0	0	0	0
200 mg bid	6	3	1 (6 months)	2	3	4
400 mg bid	4	4~	0	3~	4~	4~
600 mg bid	1	0	0	0	0	0
All patients	60	9	7*	7	10	17

Ov: Ovarian cancer. Br: Breast cancer. Pr: Prostate cancer. #Includes 1 patient with a strong family history of *BRCA*-mutated cancers, but who declined *BRCA* mutation testing. §2 patients were non-evaluable for tumor response; 1 stopped due to DLT (received only 2 doses), 1 died of unrelated sepsis after receiving 1 cycle of olaparib (with a CA125 decline). ~One *BRCA1* ovary patient was treated off trial due to an incidental brain metastasis found on cycle 1 day 14 and subsequently responded systemically to olaparib. *1 *BRCA2* breast cancer, 1 *BRCA2* ovarian cancer, 2 non-*BRCA* breast cancer, 1 sarcoma, 1 renal cell carcinoma, 1 non-small cell lung cancer

later time points. There was no significant increase in foci induction above 100 mg bid at which these analyses commenced.

Figure 2: Radiologic evidence of tumor response to olaparib

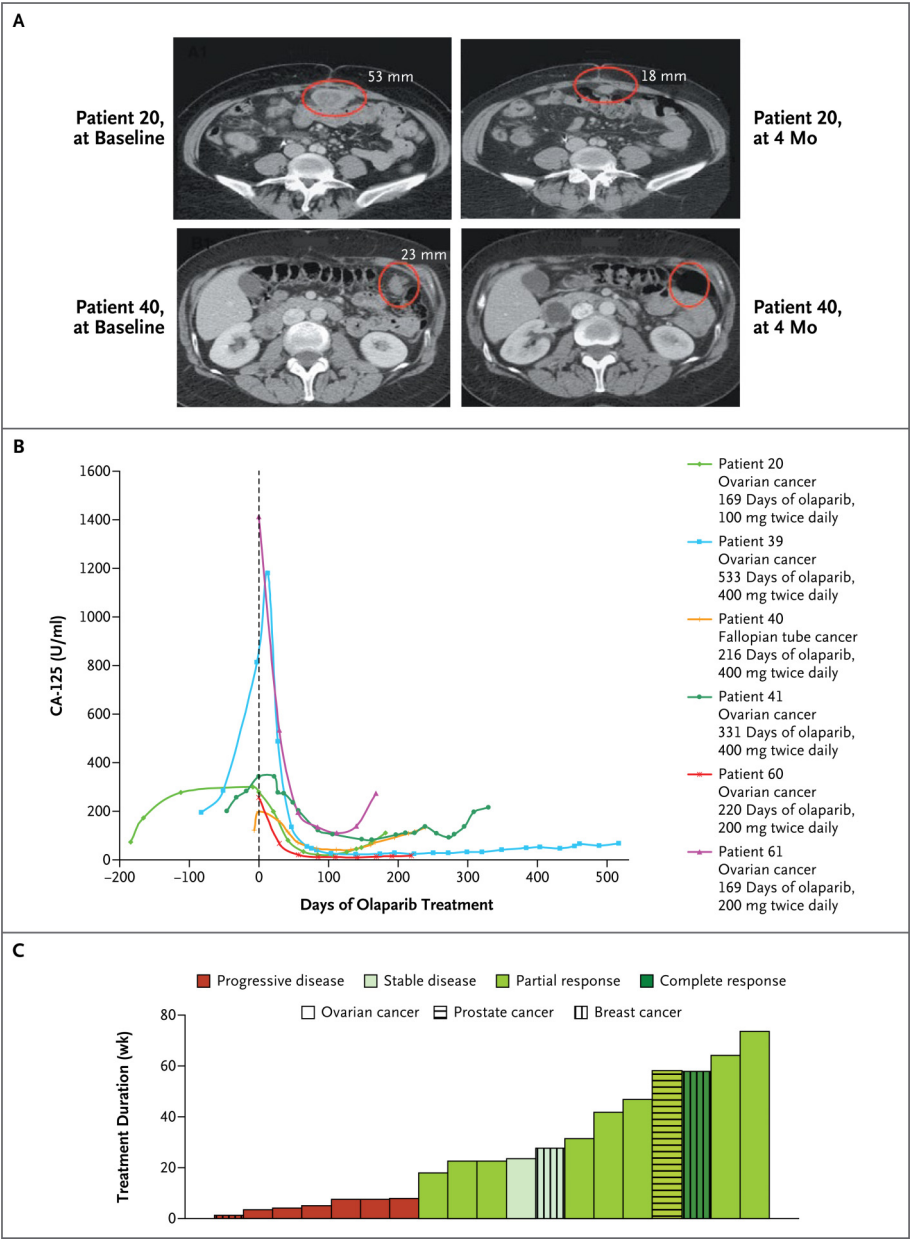


Figure 2 (previous page): Radiologic evidence of tumor response to olaparib. Computed tomographic (CT) scans of the abdomen in a patient with advanced ovarian cancer (Patient 20), who had a very strong family history suggestive of BRCA deficiency but who declined to undergo BRCA testing, show a reduction in the size of a peritoneal tumor nodule (encircled in red) by 66% over a 4-month treatment period (top right), as compared with baseline (top left). She received olaparib at a dose of 100 mg, twice daily, for 2 of every 3 weeks. CT scans of the abdomen in another patient with advanced ovarian cancer (Patient 41), who had a BRCA1 mutation (4693delAA), show complete regression of a peritoneal tumor nodule over a 4-month treatment period (bottom right), as compared with baseline (bottom left). Patient 41 received olaparib (200 mg, twice daily) for a year. Panel B shows biochemical evidence of antitumor activity, measured as cancer antigen 125 (CA-125) levels over time for six patients with advanced ovarian or fallopian-tube cancer who had a response to olaparib therapy according to Gynecologic Cancer Intergroup criteria. The maximum decline in the CA-125 level was 98%, in Patient 39 (from 1180 U per millimeter at baseline to a normal value of 22 U per milliliter). All patients also had a partial response, according to Response Evaluation Criteria in Solid Tumors (RECIST), as evaluated on CT. Panel C shows the duration of treatment and the best response seen in the 19 BRCA mutation carriers with ovarian, breast, or prostate cancer who could be evaluated for tumor response. Objective antitumor response was defined as the number of patients with a complete or partial response on radiologic assessment, according to RECIST, whereas the rate of clinical benefit was defined as the number of patients with a radiologic or tumor-marker response or stable disease, for 4 or more months. Tumor-marker response was defined as a decline of more than 50% in tumor-marker levels, sustained for at least 4 weeks.

Antitumor activity: Evidence for synthetic lethality

Durable antitumor activity was only observed in confirmed BRCA1 or BRCA2 mutation carriers apart from one patient with a very strong BRCA family history who declined BRCA mutation testing but was deemed to be a BRCA carrier (Table 3; Figure 2). Overall, 23 BRCA carrier patients were treated. Two patients were not evaluable for antitumor response; one only received 2 doses of drug due to DLT; the other had ovarian cancer-associated fatal septicemia after 4 weeks of olaparib with a falling CA125. Of the remaining 21 patients, 2 had tumors not typically associated with BRCA carrier status; a small cell lung carcinoma and a vaginal adenocarcinoma patient. Both patients were on 200 mg bid olaparib and progressed rapidly within 2 and 7 weeks of treatment respectively. The remaining 19 BRCA carrier patients had ovarian, breast and prostate cancers; 12/19 (63%) of these evaluable BRCA mutation carriers derived clinical benefit from olaparib with radiological or accepted tumor marker criteria responses or meaningful disease stabilization (≥ 4 months). Nine BRCA carrier patients responded by RECIST, with one patient remaining in response for >76 weeks (Figure 2C; Table 3). Further details on the specific BRCA1 and BRCA2 mutations and responses are provided in Supplementary Table 3. No objective antitumor responses were observed in the unselected patient population.

Overall, 8 advanced ovarian cancer patients achieved radiological PR by RECIST criteria (Table 3; Figure 2A). Using GCIG criteria for assessing CA125 response in ovarian cancer, 6 patients achieved a GCIG CA125 response of >50% (Table 3; Figure 2B). Of the 3 BRCA2 breast cancer patients, 1 achieved a CR by RECIST and another had disease stabilization for 7 months; both had a corresponding decline in serum tumor markers (Figure 2C). The BRCA2 breast cancer patient who achieved a CR lasting >60 weeks was estrogen, progesterone and HER2-receptor negative. She had pulmonary and lymph node metastases and had previously progressed through anthracycline-based chemotherapy. A breast cancer patient who did not undergo BRCA testing had regression of multiple sub-centimeter brain metastasis (previously unirradiated and not on corticosteroids) and a >50% fall in serum tumor markers of carcinoembryonic antigen (CEA) and cancer antigen 15-3 (CA15-3).

A BRCA2 castration-resistant prostate cancer patient had >50% PSA decline with resolution of his bone metastases, was on study >58 weeks at data cut off (he remains on study at 2 years; Figure 2C; Supplementary Figure 5).

Discussion

This is the first report of treatment of human cancer with a PARP inhibitor as a single agent. Since it is a 'first-in-man' trial of olaparib, we describe our findings relating to safety, tolerability, PK and PD. This oral drug is very well-tolerated with satisfactory PK-PD characteristics and without the toxicity of cytotoxic cancer chemotherapy. Importantly, patients who were carriers of BRCA1 or BRCA2 mutations did not have an increased risk of toxicity, as suggested by our preclinical studies (11) Of special interest is the remarkable degree of antitumor activity in patients with BRCA mutation associated cancers, and the lack of antitumor responses in unselected patients.

These data indicate that targeting a specific DNA repair pathway with PARP inhibition has the necessary selectivity profile and wide therapeutic window for BRCA-deficient cells and support the clinical relevance of the hypothesis that these cancers are indeed susceptible to "synthetic lethality" (25) Predictive biomarkers identifying tumor cell HR DNA repair deficiency are now urgently required to evaluate the broader utility of this promising therapeutic strategy. 6 HR repair defects can also be caused by loss of function of proteins other than BRCA1 and BRCA2, including RAD51, ATM, ATR, CHK1, CHK2 and

components of the Fanconi anemia repair pathway (26). Loss of these proteins also sensitizes to PARP inhibition.⁶ Importantly, such HR repair defects may be relatively common in some sporadic cancers including breast (27) and ovarian (28), making this therapeutic strategy potentially more widely useful as an anticancer treatment.

Not all BRCA1 or BRCA2 carrier patients responded to olaparib. Different BRCA1 or BRCA2 mutations may have resulted in differing HR defects and sensitivities to PARP inhibition. This could also have resulted from pre-existing genetic resistance; we and others have shown previously that secondary BRCA2 mutations may restore BRCA function and therefore HR, causing resistance to PARP inhibitors and platinum compounds (29, 30). Assays of HR proficiency will be vital to the study of primary or acquired resistance to PARP inhibitors, as well as for identifying HR-defective sporadic tumors. Molecular studies of ovarian cancer have, for example, suggested that up to half of high-grade serous cancers may lose BRCA1 or BRCA2 function through genetic or epigenetic events (28). Such sporadic tumors appear to phenocopy BRCA1 or BRCA2-deficient ones without actually bearing germline mutations in either BRCA1 or BRCA2 genes, a phenomenon which has been described as 'BRCAness' (31).

Finally, this study raises the possibility that for some anticancer drugs, the traditional clinical development and registration process needs to be altered. Due consideration must now be given to developing selected rationally designed, molecularly targeted therapeutics for patients whose tumors have the same molecular defect but arise from different origins such as ovarian, breast and prostate. Such a radical change in the drug evaluation and registration process may be key to accelerating anticancer drug development.

Acknowledgments

The Royal Marsden Hospital and The Institute of Cancer Research Drug Development Unit is supported by Cancer Research UK through a Program Grant to the Section of Medicine, The Institute of Cancer Research and through an Experimental Cancer Medical Centre (ECMC) grant (Ref.: C51/A7401). It is also supported by the Department of Health through the ECMC grant and as part of the NIHR Biomedical Research Centre at the Royal Marsden Hospital. Dr Fong, Dr Yap, Dr Tutt, Prof Ashworth, Prof Kaye and Dr de Bono are

employees of The Institute of Cancer Research. Olaparib (AZD2281), previously known as KU-0059436, was incorporated into the AstraZeneca pipeline following acquisition of KuDOS Pharmaceuticals Ltd. KuDOS Pharmaceuticals Ltd is a wholly owned subsidiary of AstraZeneca PLC. Editorial assistance was provided by Ms Sarah Jane Mason from Mudskipper Bioscience, funded by AstraZeneca.

References

1. Lindahl T. Instability and decay of the primary structure of DNA. *Nature* 1993;362(6422):709-15.
2. Jackson SP. Detecting, signalling and repairing DNA double-strand breaks. *Biochem Soc Trans* 2001;29(Pt 6):655-61.
3. Hoeijmakers JH. Genome maintenance mechanisms for preventing cancer. *Nature* 2001;411(6835):366-74.
4. Ame JC, Spenlehauer C, de Murcia G. The PARP superfamily. *Bioessays* 2004;26(8):882-93.
5. Dantzer F, de La Rubia G, Menissier-De Murcia J, Hostomsky Z, de Murcia G, Schreiber V. Base excision repair is impaired in mammalian cells lacking Poly(ADP-ribose) polymerase-1. *Biochemistry* 2000;39(25):7559-69.
6. McCabe N, Turner NC, Lord CJ, et al. Deficiency in the repair of DNA damage by homologous recombination and sensitivity to poly(ADP-ribose) polymerase inhibition. *Cancer Res* 2006;66(16):8109-15.
7. Gudmundsdottir K, Ashworth A. The roles of BRCA1 and BRCA2 and associated proteins in the maintenance of genomic stability. *Oncogene* 2006;25(43):5864-74.
8. Wooster R, Weber BL. Breast and ovarian cancer. *N Engl J Med* 2003;348(23):2339-47.
9. Stratton JF, Gayther SA, Russell P, et al. Contribution of BRCA1 mutations to ovarian cancer. *N Engl J Med* 1997;336(16):1125-30.
10. Edwards SM, Kote-Jarai Z, Meitz J, et al. Two percent of men with early-onset prostate cancer harbor germline mutations in the BRCA2 gene. *Am J Hum Genet* 2003;72(1):1-12.
11. Farmer H, McCabe N, Lord CJ, et al. Targeting the DNA repair defect in BRCA mutant cells as a therapeutic strategy. *Nature* 2005;434(7035):917-21.
12. Bryant HE, Schultz N, Thomas HD, et al. Specific killing of BRCA2-deficient tumours with inhibitors of poly(ADP-ribose) polymerase. *Nature* 2005;434(7035):913-7.
13. Ashworth A. A Synthetic Lethal Therapeutic Approach: Poly(ADP) Ribose Polymerase Inhibitors for the Treatment of Cancers Deficient in DNA Double-Strand Break Repair. *J Clin Oncol* 2008.
14. Tutt AN, Lord CJ, McCabe N, et al. Exploiting the DNA repair defect in BRCA mutant cells in the design of new therapeutic strategies for cancer. *Cold Spring Harb Symp Quant Biol* 2005;70:139-48.
15. Brody LC. Treating cancer by targeting a weakness. *N Engl J Med* 2005;353(9):949-50.
16. Evers B, Drost R, Schut E, et al. Selective inhibition of BRCA2-deficient mammary tumor cell growth by AZD2281 and cisplatin. *Clin Cancer Res* 2008;14(12):3916-25.
17. AstraZeneca. Investigator's Brochure: AZD2281 Poly ADP-ribose polymerase-1 inhibitor (PARPi), KU-0059436: Astra Zeneca; 2008 14 Jan 2008. Report No.: 4.
18. Simon R, Freidlin B, Rubinstein L, Arbuuck SG, Collins J, Christian MC. Accelerated titration designs for phase I clinical trials in oncology. *J Natl Cancer Inst* 1997;89(15):1138-47.
19. Common Terminology Criteria for Adverse Events v3.0 (CTCAE). DCTD, NCI, NIH, DHHS, 2006. (Accessed at <http://ctep.cancer.gov/forms/CTCAEv3.pdf>.)
20. Camidge DR, Randall KR, Foster JR, et al. Plucked human hair as a tissue in which to assess pharmacodynamic end points during drug development studies. *Br J Cancer* 2005;92(10):1837-41.

21. Therasse P, Arbuuck SG, Eisenhauer EA, et al. New guidelines to evaluate the response to treatment in solid tumors. European Organization for Research and Treatment of Cancer, National Cancer Institute of the United States, National Cancer Institute of Canada. *J Natl Cancer Inst* 2000;92(3):205-16.
22. Rustin GJ, Quinn M, Thigpen T, et al. Re: New guidelines to evaluate the response to treatment in solid tumors (ovarian cancer). *J Natl Cancer Inst* 2004;96(6):487-8.
23. Bubley GJ, Carducci M, Dahut W, et al. Eligibility and response guidelines for phase II clinical trials in androgen-independent prostate cancer: recommendations from the Prostate-Specific Antigen Working Group. *J Clin Oncol* 1999;17(11):3461-7.
24. Fernandez-Capetillo O, Celeste A, Nussenzweig A. Focusing on foci: H2AX and the recruitment of DNA-damage response factors. *Cell Cycle* 2003;2(5):426-7.
25. Kaelin WG, Jr. The concept of synthetic lethality in the context of anticancer therapy. *Nat Rev Cancer* 2005;5(9):689-98.
26. Venkitaraman AR. A growing network of cancer-susceptibility genes. *N Engl J Med* 2003;348(19):1917-9.
27. Turner NC, Reis-Filho JS, Russell AM, et al. BRCA1 dysfunction in sporadic basal-like breast cancer. *Oncogene* 2007;26(14):2126-32.
28. Press JZ, De Luca A, Boyd N, et al. Ovarian carcinomas with genetic and epigenetic BRCA1 loss have distinct molecular abnormalities. *BMC Cancer* 2008;8:17.
29. Edwards SL, Brough R, Lord CJ, et al. Resistance to therapy caused by intragenic deletion in BRCA2. *Nature* 2008;451(7182):1111-5.
30. Sakai W, Swisher EM, Karlan BY, et al. Secondary mutations as a mechanism of cisplatin resistance in BRCA2-mutated cancers. *Nature* 2008;451(7182):1116-20.
31. Turner N, Tutt A, Ashworth A. Hallmarks of 'BRCAness' in sporadic cancers. *Nat Rev Cancer* 2004;4(10):814-9.

Supplementary tables and figures

Supplementary table 1: Dose-escalation scheme; dosing schedule was adapted based on the acquired pharmacokinetic-pharmacodynamic data.

Dose level and schedule	Number of patients	Total number of cycles	Median number of cycles	Number of dose-limiting toxicities in cycle 1 (%)
10 mg daily, 2 out of 3 weeks	3	12	2	0 (0)
20 mg daily, 2 out of 3 weeks	3	5	2	0 (0)
40 mg daily, 2 out of 3 weeks	5	15	2	0 (0)
80 mg daily, 2 out of 3 weeks	3	9	4	0 (0)
60 mg bid, 2 out of 3 weeks	4	10	2	0 (0)
100 mg bid, 2 out of 3 weeks	4	15	3	0 (0)
100 mg bid, continuously	5	8	2	0 (0)
100 mg bid, continuously	20	94	4	0 (0)
100 mg bid, continuously	8	41	25	1 (12.5)
100 mg bid, continuously	5	13	2	2 (40.0)

Supplementary table 2A: Derived pharmacokinetic parameters following administration of a single dose of olaparib at a range of dose levels

Parameter	Statistic	Dose (mg)								
		10 mg (n = 3)	20 mg (n = 3)	40 mg (n = 5)	60 mg (n = 4)	80 mg (n = 3)	100 mg (n = 8)	200 mg (n = 20)	400 mg (n = 8)	600 mg (n = 5)
Cmax (µg/ml)	Gmean (CV)	0.38 (36)	1.04 (81)	1.94 (22)	2.55 (33)	3.49 (20)	3.32 (46)	4.22 (50)	6.08 (22)	10.5 (38)
	Range	0.25-0.48	0.46-1.66	1.50-2.68	1.95-3.77	3.02-4.35	1.68-6.77	1.69-7.88	4.04-7.47	5.90-14.5
tmax (h)	Median	2.0	1.5	1.5	2.25	1.5	1.0	1.5	1.75	3.0
	Range	0.5-2.0	1.0-1.5	1.0-4.0	0.5-3.0	1.5-1.5	1.0-3.0	1.0-4.0	1.5-8.0	2.0-4.0
AUC0-12 (µg.h/ml)	Gmean (CV)	1.26* (37)	3.74* (52)	9.80* (23)	9.82 (22)	13.2* (43)	19.7 (60)	20.9** (60)	33.5 (47)	68.7 (53)
	Range	0.92-1.86	2.29-6.07	7.12-13.3	7.47-12.2	9.25-20.8	8.95-54.9	9.71-45.8	15.8-59.5	31.4-108.9
AUC0-24 (µg.h/ml)	Gmean (CV)	1.45 (40)	4.80 (46)	13.1 (30)	NC	16.5 (56)	NC	NC	NC	NC
	Range	1.05-2.21	3.35-7.79	9.44-20.6		10.6-29.4				
AUC (µg.h/ml)	Gmean (CV)	1.50 (40)	5.04 (44)	13.9 (32)	NC	17.1 (59)	NC	NC	NC	NC
	Range	1.10-2.31	3.62-8.11	9.97-22.9		10.8-31.2				
t½ (h)	Amean (SD)	6.67 (0.29)	6.10 (0.48)	6.14 (0.90)	NC	5.48 (0.31)	NC	NC	NC	NC
	Range	6.41-6.99	5.67-6.62	5.16-7.19		5.12-5.66				
CL/F (L/h)	Amean (SD)	6.97 (2.43)	4.20 (1.57)	2.98 (0.85)	NC	5.11 (2.44)	NC	NC	NC	NC
	Range	4.33-9.11	2.46-5.52	1.75-4.01		2.56-7.43				
V/F (L)	Amean (SD)	67.6 (26.0)	37.6 (16.4)	25.8 (6.67)	NC	39.8 (17.3)	NC	NC	NC	NC
	Range	40.0-91.8	20.2-52.7	18.2-36.0		20.9-54.8				

Amean = arithmetic mean; CV = coefficient of variation; Gmean = geometric mean; NC = not calculated (sampling stopped at 12 hours after dosing); SD = standard deviation.

* Value reported is actually AUC₀₋₁₀ because no 12-hour sample was collected.

** n = 17

Supplementary table 2B: Derived pharmacokinetic parameters on Day 14 of multiple oral dosing of olaparib at a range of dose levels

Parameter	Statistic	Dose (mg)									
		10 mg (n = 3)	20 mg (n = 2)	40 mg (n = 4)	60 mg (n = 3)	80 mg (n = 3)	100 mg (n = 8)	200 mg (n = 17)	400 mg (n = 6)	600 mg (n = 5)	
C_{max} (µg/ml)	Gmean (CV)	0.49 (43)	NC	1.78 (7)	2.08 (12)	4.82 (14)	3.67 (31)	5.62 (50)	7.65 (27)	11.5 (42)	
	Range	0.38-0.79	1.42-1.94	1.66-1.93	1.90-2.37	4.13-5.46	2.81-5.86	2.83-17.1	5.28-10.5	6.49-17.6	
t_{max} (h)	Median	1.0	NC	1.75	3.0	1.5	1.5	1.5	2.0	1.5	
	Range	0.5-2.0	1.0-1.0	1.0-4.0	1.0-6.0	1.0-2.0	1.0-4.0	1.0-6.0	1.5-3.0	1.0-3.0	
C_{min} (µg/ml)	Gmean (CV)	0.008 (76)	NC	0.12 (37)	0.26 (238)	0.14 (152)	0.45 (90)	0.96**	1.29 (76)	2.18 (177)	
	Range	0.005-0.018	0.029-0.054	0.086-0.190	0.064-1.00	0.060-0.47	0.12-0.98	(133) 0.21-2.95	0.66-3.89	0.39-5.95	
AUC₀₋₁₂ (µg.h/ml)	Gmean (CV)	1.67* (36)	NC	9.20* (19)	11.5 (54)	19.0* (30)	20.5 (52)	33.3** (75)	44.9 (39)	86.8† (42)	
	Range	1.31-2.50	4.48-6.51	7.04-10.5	7.46-20.0	13.9-25.1	10.7-48.9	11.2-162.4	27.7-78.7	55.4-119.4	
AUC₀₋₂₄ (µg.h/ml)	Gmean (CV)	1.94 (40)	NC	13.0 (21)	NC*	24.5 (40)	NC*	NC*	NC*	NC*	
	Range	1.48-3.03	5.38-8.06	9.54-15.0		16.8-36.5					
CL_{ss}/F (L/h)	Amean (SD)	5.39 (1.84)	NC	3.13 (0.72)	5.67 (2.54)	3.43 (1.29)	5.38 (2.39)	7.63**	9.44 (3.35)	7.31†	
	Range	3.30-6.76	2.48-3.72	2.66-4.19	2.99-8.04	2.19-4.76	2.05-9.30	(4.40) 1.23-17.9	5.08-14.4	(1.38) 5.03-10.8	
t_{1/2} (h)	Amean (SD)	NC	NC	9.52 (1.64)	NC	8.05 (0.70)	NC	NC	NC	NC	
	Range	8.26-12.2	9.34-12.0	7.95-11.0		7.27-8.62					

Amean = arithmetic mean; CV = coefficient of variation; Gmean = geometric mean; NC = not calculated (n = 2); NC* = NC (sampling stopped at 12 hours after dosing); SD = standard deviation.

* Value reported is actually AUC₀₋₁₀ because no 12 hour sample was collected.

** n = 14; † n=3.

Supplementary table 3: Pharmacogenomics of PARP inhibitors; radiological and biochemical responses for ovarian, breast and prostate cancer patients according to BRCA1 or BRCA2 mutation sequence found (where available)

Pat, no.	Tumor type	Gene	Mutation	Response to olaparib [§]	Dose
11	Ovary	<i>BRCA1</i>	5382insC	No	40 mg qd (14 out of 21 days)
20	Ovary	–	Not tested*	Yes	100 mg bid (14 out of 21 days)
21	Peritoneum	<i>BRCA1</i>	3875delGTCT	No	100 mg bid (14 out of 21 days)
26	Ovary	<i>BRCA1</i>	4184del4	No	100 mg bid
36	Ovary	<i>BRCA1</i>	185delAG	No	400 mg bid
37	Ovary	<i>BRCA1</i>	185delAG	Yes	400 mg bid
39	Ovary	<i>BRCA1</i>	185delAG	Yes	400 mg bid
40 [#]	Fallopian tube	<i>BRCA1</i>	4184delTCAA	Yes	400 mg bid
41	Ovary	<i>BRCA1</i>	185delAG	Yes	400 mg bid
42	Ovary	<i>BRCA1</i>	C.4357+1delG	No	400 mg bid
44	Ovary	<i>BRCA1</i>	Unavailable	No	600 mg bid
47	Ovary	<i>BRCA1</i>	4693delAA	Yes	200 mg bid
48	Ovary	<i>BRCA2</i>	8206T>G	No	200 mg bid
49	Breast	<i>BRCA2</i>	3715delG	Yes	200 mg bid
50	Prostate	<i>BRCA2</i>	6174del T	Yes	200 mg bid
53	Breast	<i>BRCA2</i>	902delC	Yes	200 mg bid
54	Breast	<i>BRCA2</i>	4684del4	No	200 mg bid
55	Ovary	<i>BRCA1</i>	Deletion exon 15–17	No	200 mg bid
59	Ovary	<i>BRCA1</i>	6kb ins exon 13	No	200 mg bid
60	Ovary	<i>BRCA1</i>	5396+1 G>A	Yes	200 mg bid
61	Ovary	<i>BRCA1</i>	1185C>T (Q356X)	Yes	200 mg bid

*Patient with a strong family history of *BRCA*-mutated cancers, but who declined *BRCA* mutation testing

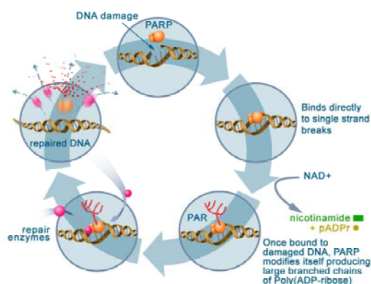
§ Clinical benefit was defined as response by RECIST or accepted tumor marker criteria or disease stabilization ≥ 4 months.

Patient was treated off-trial due to incidental brain metastases and subsequently responded systemically to olaparib.

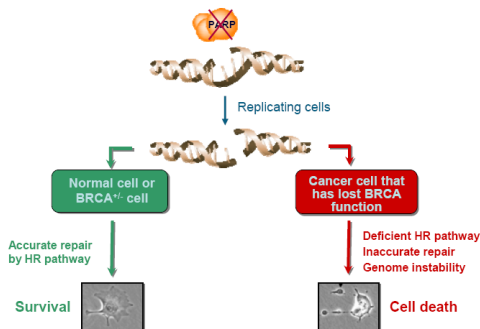
Mutations in bold denote the 3 most common Ashkenazi founder mutations.

Supplementary figure 1: Synthetic lethality induced by PARP inhibition in a BRCA-deficient genetic background. (A) PARP plays a key role in the repair of DNA single-strand breaks that occur all the time as a consequence of normal cell function. (B) When PARP is inhibited, unrepaired single-strand breaks are converted into DNA double-strand breaks during DNA replication. In normal or BRCA heterozygous cells (BRCA+/-) the double-strand breaks are effectively repaired by homologous recombination DNA repair. PARP inhibition is therefore not toxic to cells with wild-type BRCA1 or BRCA2. Tumor-specific defects in BRCA1 and BRCA2 lead to a defect in DNA repair by homologous recombination and are, due to this synthetic lethal interaction, exquisitely sensitive to PARP inhibition (13).

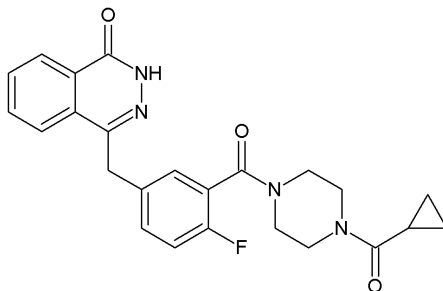
(A) Repair of DNA single strand breaks by PARP



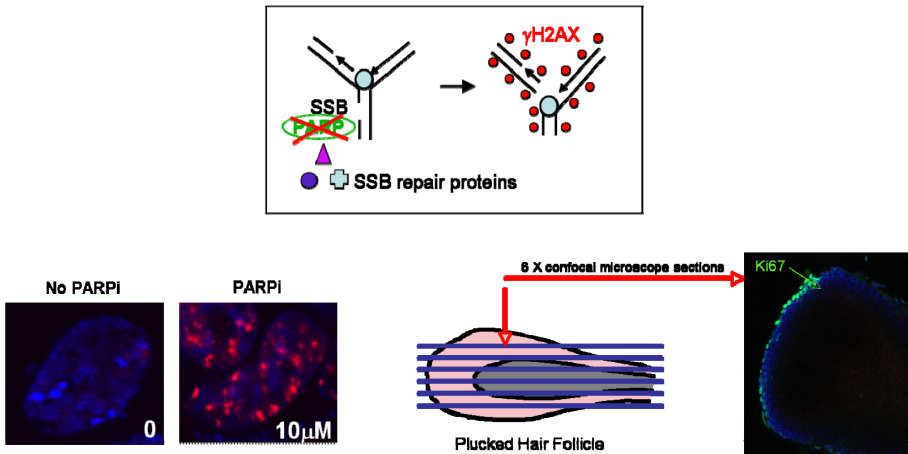
(B) Tumour specific killing by olaparib



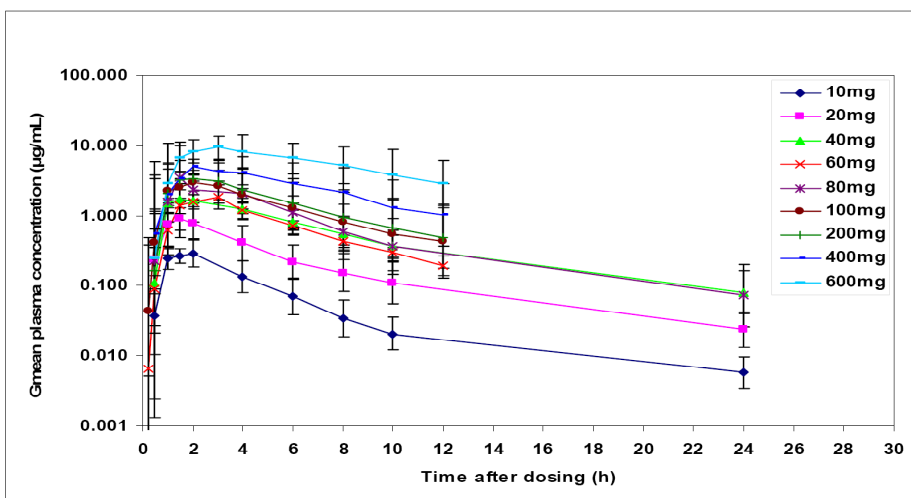
Supplementary figure 2: The structure of olaparib (4-[(3-[[4-cyclopropylcarbonyl]piperazin-1-yl]carbonyl]-4-fluorophenyl)methyl]phthalazin-1(2H)-one, also known as AZD2281 and KU-0059436.20



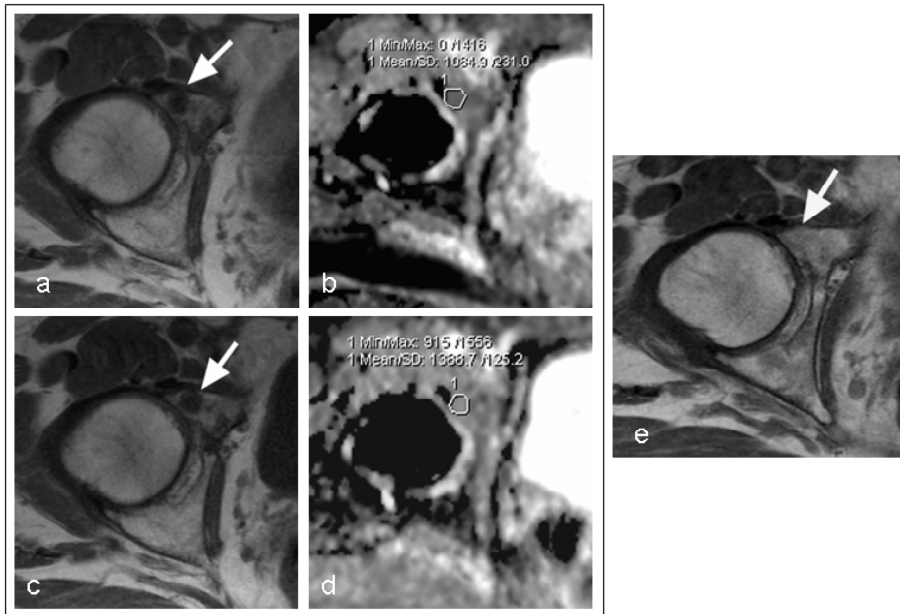
Supplementary figure 3: Hair follicle pharmacodynamic biomarker assay. Analysis of hair follicle cells for induction of γ H2AX foci as a downstream pharmacodynamic endpoint of the predicted mechanism of action of olaparib. The top diagram illustrates how in the setting of loss of PARP function an unrepaired DNA single-strand break (SSB) progresses to a double-strand break (DSB) upon encountering a replication fork; γ H2AX foci are formed in response to the DSB and can be detected by immunofluorescence labeling as red foci within the blue-stained nucleus in cells treated with a PARP inhibitor (PARPi, lower left).¹¹ The lower right diagram illustrates how each hair follicle is analyzed on 6 planes and up to 100 nuclei optically assessed by an observer blinded to patient olaparib dose. A cell is scored as positive if ≥ 10 small or >3 large foci per nucleus were seen. An immunofluorescence-labeled proliferation marker Ki67 (green) indicates the proliferating nature of the hair follicle surrogate tissue.



Supplementary figure 4: Pharmacokinetic studies. Geometric mean plasma concentration-time profiles following single oral dosing of olaparib to cancer patients. The drug administration schedule was adapted, based on acquired PK-PD data, from once daily (10 mg; 20 mg; 40 mg; 80 mg) to twice daily (60 mg to 600 mg) explaining the altered PK acquisition timepoints.



Supplementary figure 5: Diffusion-weighted magnetic resonance imaging (MRI) demonstrating disease regression in a patient with prostate cancer and BRCA2 mutation associated with a >50% decline in PSA. A 63-year-old man with BRCA2 mutation and castration resistant prostate cancer. T1-weighted MR images at the level of the right acetabulum in the pelvis obtained (a) prior to, and (c) three months after, initiating treatment showed no substantial change in a 13 mm low-signal intensity (dark) metastasis in the right acetabulum (arrows). Apparent diffusion coefficient (ADC) maps obtained by diffusion-weighted MRI (b) pre-treatment and (d) at three months after treatment showed ADC values increasing from $1.03 \times 10^{-3} \text{ mm}^2/\text{s}$ to $1.39 \times 10^{-3} \text{ mm}^2/\text{s}$ (>30% increase) at the site of metastatic disease (circled) consistent with disease regression. (e) T1-weighted image at one year after treatment showed resolution of disease (arrow). [Images courtesy of Dr Dow-Mu Koh, Royal Marsden Hospital, Sutton, UK].



CHAPTER 6.2

Olaparib (AZD2281) can be safely administered together with therapeutic doses of paclitaxel

David S. Boss, Andre Brunetto, Jana van der Sar, Jim Carmichael,
Stan Kaye , John Stone, Jos H. Beijnen, Johann de Bono,
Jan H.M. Schellens

Abstract

Background: Olaparib (AZD2281) is a potent, orally active inhibitor of PARP-1 and 2 that has demonstrated compelling activity in patients with BRCA mutated breast- and ovarian tumors. The objectives of this study were to investigate the safety and the pharmacokinetics of olaparib in combination with therapeutic doses of paclitaxel.

Methods: Patients received continuous olaparib orally at doses of 100 or 200 mg/day, and paclitaxel intravenously once weekly at a dose of 80 mg/m². Toxicities were monitored, and blood samples for pharmacokinetics of olaparib and paclitaxel were collected on day 4 (olaparib monotherapy) and day 8 (combination therapy) of the first treatment cycle.

Results: A total of 10 patients entered the study. No dose-limiting toxicities (DLTs) were observed, suggesting that both evaluated dose-levels were safe. The most frequently observed non-hematological toxicity was grade 1-2 fatigue, while grade 3-4 hematological toxicities were observed in one-third of the treated patients. Pharmacokinetic analysis revealed a significant reduction in exposure to olaparib of approximately 50 percent following co-administration of paclitaxel. A partial response was observed in a patient with BRCA deficient breast cancer.

Conclusion: Olaparib at doses of 100 and 200 mg bi-daily can be safely combined with 80 mg/m² paclitaxel given weekly. More research is needed to study the pharmacokinetic drug-drug interaction following administration of both compounds.

Introduction

DNA repair mechanisms are essential for maintaining genomic integrity and cell survival (1). Poly (ADP-ribose) polymerase 1 (PARP1) is a key molecule in the repair of DNA single strand breaks by a mechanism called Base Excision Repair (BER) (2). Inhibition of PARP activity leads to the persistence of single strand DNA breaks, which can progress to double strand DNA breaks when replication forks stall at the site of the single strand break. These double strand breaks are normally repaired by the error-free homologous recombination (HR) pathway, of which the tumor suppressor proteins BRCA1 and BRCA2 are essential components. Germline heterozygous mutations in BRCA1 or BRCA2 are associated with a high risk of developing a number of malignancies, including breast, ovarian, and prostate cancer. Loss of the wild-type BRCA allele in nascent tumor cells is the critical step in the carcinogenesis process, although the precise mechanisms of the oncogenic transformation remain to be elucidated (3).

The defects in HR that hallmark BRCA deficient tumors can be exploited as a target for cancer therapy, using PARP inhibitors (4). Inhibiting PARP leads to double-strand breaks that cannot be repaired by the HR deficient tumor cells, eventually leading to cell death (5). The normal cells, bearing a functional BRCA gene, are able to repair these breaks, since they have a functional HR pathway. This makes these cells relatively insensitive, providing a large therapeutic index for PARP inhibition in BRCA carriers.

Recently, impressive anti-tumor activity of single agent olaparib was observed in patients with BRCA mutated tumors at doses of 200 mg (6). This observation led to the initiation of several clinical studies combining olaparib with other anticancer agents. This report describes the feasibility of combining olaparib with therapeutic doses of paclitaxel, an anti-mitotic agent that has shown activity against various forms of cancer, including breast and ovarian cancer (7). The combination of these agents might hold promise in patients with BRCA mutated tumors, but also in other tumors with deficiencies in DNA repair pathways.

Patients and methods

Patient selection

Patients with advanced solid tumors refractory to standard therapies, or for whom no effective standard treatment existed, were eligible for this study. Other eligibility criteria were as follows: >18 years age; ECOG performance status ≤ 2 ; adequate bone marrow function, defined by haemoglobin ≥ 6.2 mM, absolute neutrophil count $\geq 1500 \times 10^6/L$, and platelets $\geq 100,000 \times 10^6/L$; adequate hepatic function, defined by total bilirubin $\leq 1.25 \times$ upper normal limit, AST (SGOT) $\leq 2.5 \times$ upper normal limit, and AST (SGOT) $\leq 2.5 \times$ upper normal limit; normal renal function, defined by serum creatinine $\leq 1.5 \times$ upper normal limit; and a minimum washout period of 4 weeks after any previous anti-cancer therapy.

Study design

The here described study was part of a two-centre phase I study investigating the administration of olaparib in combination with carboplatin alone, paclitaxel alone, and in combination with a paclitaxel/carboplatin (TC) doublet. This study was conducted at the Royal Marsden Hospital (UK) and the Netherlands Cancer Institute (Netherlands), but the patients included in the here described sub-study were all included at the Netherlands Cancer Institute. The primary objective of this sub-study was to determine the safety of combining a standard dose of weekly paclitaxel (80 mg/m²) with two different dose-levels of olaparib. The starting dose was olaparib 100 mg, and escalation to the second dose-level (200 mg) was based on the occurrence of Dose Limiting Toxicities (DLTs) in the first cohort. If one patient in a cohort of at least three patients would experience a DLT, that cohort was to be expanded to at least 6 patients, unless a second DLT would demonstrate that this dose-level was unsafe. The Maximum Tolerated Dose (MTD) was defined as the prior dose level below the drug-combination that caused DLT in at least 2 patients in a cohort of at least 3 patients who had completed one cycle of treatment.

Drug administration and dosing schedule

Olaparib was administered on an empty stomach orally twice daily continuously at doses of 100 mg BID (cohort 1) or 200 mg BID (cohort 2), in

combination with a fixed dose of 80 mg/m² weekly paclitaxel. Olaparib was administered twice daily alone for the first 7 days to allow samples to be taken for olaparib pharmacokinetics. Paclitaxel was administered on days 8, 15 and 22 of the first treatment cycle (35 days), and on days 1, 8 and 15 of all subsequent treatment cycles (28 days). Paclitaxel was administered as a 3 hour intravenous infusion, at least 1 hour after the patient had taken their olaparib capsules. All patients were to be dosed for up to 6 cycles, but could receive more than 6 cycles if it was considered to be in their best interest, which was left to the discretion of the investigator.

Toxicity criteria

All toxicities were monitored and graded using the NCI Common Terminology Criteria for Adverse Events (NCI CTCAE) version 3.0. Dose-limiting toxicity (DLT) was defined as the following study drug-related events experienced during Cycle 1: Thrombocytopenia with platelets $<25,000 \times 10^6/l \geq 7$ days; grade 4 neutropenia ≥ 7 days; grade 3 or 4 febrile neutropenia; any grade 3 or 4 non-hematological toxicity (excluding alopecia, and nausea, vomiting or diarrhea controlled by standard therapies); a delay of > 2 weeks for the next scheduled paclitaxel for reasons of drug-related toxicity.

Pharmacokinetic sampling

Blood samples for olaparib pharmacokinetics were collected on days 4 and 8, at the following time-points: Predose, 30 minutes after drug administration, and then at 1, 2, 3, 4, 6, and 8 hours post drug administration. Blood samples for paclitaxel pharmacokinetics were taken on days 8 and 9, at the following time points: Predose, 1 hour after start of infusion, at end of infusion, and at 6 and 24 hours after the completion of the infusion. Olaparib and paclitaxel concentrations were measured using validated liquid chromatography with mass spectrometry detection methods. The following pharmacokinetic parameters were derived, using PK Solutions: Peak plasma concentration (C_{max}), time to C_{max} (t_{max}), the total area under the plasma concentration-time curve (AUC), volume of distribution (V_{dd}), Clearance (Cl), and the elimination half-life (t_{1/2}).

Response measurements

Tumor assessments of anti-neoplastic activity were performed at baseline, and at the end of every two cycles. Response was assigned as complete response (CR), partial response (PR), stable disease (SD) or progressive disease (PD) at each scheduled imaging visit, according to the Response Evaluation Criteria in Solid Tumors (RECIST) guideline. Responses (PR or CR) were confirmed ≥ 4 weeks after the initial assessment.

Results

Patient characteristics

A total of 10 patients entered the study, of which 4 were included in cohort 1. One patient included in cohort 2 presented brain metastases only 1 day after study initiation, and was therefore unevaluable for toxicity, pharmacokinetics, and response assessments. The other 9 patients completed at least one course of treatment. The patient characteristics are summarized in table 1.

Safety

Nine patients were evaluable for adverse events. All treatment related adverse events that occurred during the first treatment cycle, as well as all observed laboratory abnormalities during the first treatment cycle, are shown in table 2. No DLTs were observed during the study. Most observed toxicities were mild (grade 1-2), excluding grade 3 hematological toxicities that were observed in 3 patients. The first patient reported grade 3 neutropenia, resulting in a delay of paclitaxel administration. His granulocyte values recovered to normal within a week, and he didn't stop the intake of olaparib. A second patient developed grade 3 leukocytopenia, lymphocytopenia, and neutropenia. She temporarily stopped treatment, until recovery of her blood values, which took 7 days. Finally, another patient had grade 4 neutropenia and grade 3 lymphocytopenia. This patient also stopped treatment until recovery, which was within 7 days. One patient experienced a grade 3 gamma-glutamyl transferrase elevation. However, these values recovered within 3 days to grade 2, and no intervention was taken. Another patient had high glucose values during course 1 (ctc grade 3). This patient entered the study with grade 2 hyperglycemia, and her glucose remained elevated during the study. She

Table 1: Patient characteristics

Characteristic	
Total number of patients (n)	10
Sex (male/female)	6/4
Age (median, range)	52 (30-63)
Tumor Characteristics (n)	
Breast	2
Ewing sarcoma	1
Kidney	1
Lung (Carcinoid)	1
Lung (NSCLC)	1
Melanoma	1
Mesothelioma	1
Oesophagus ca.	1
Ovarium ca.	1
Previous Chemotherapy (n)	
Yes/no	10/0
Previous Radiotherapy (n)	
Yes/no	4/6
Previous Surgery (n)	
Yes/no	10/0

continued without dose delays or interruptions. All non-hematological toxicities were modest, and did not exceed grade 1-2, with alopecia and fatigue as the most frequently observed side-effects.

Pharmacokinetics

Pharmacokinetic studies performed on day 4 of therapy revealed results similar to those reported in the olaparib phase I study that was published recently (6). The results are shown in table 3. Olaparib was absorbed rapidly, with a median maximal concentration 1 or 2 hours after dosing, depending on dose-level or day of administration. The terminal half-life of the drug was between 3.5 and 4 hours, and there was a less than dose-proportional increase in exposure, when doubling the dose from 100 to 200 mg. There was a significant decrease in exposure to olaparib following co-administration of paclitaxel (day 8). This decrease of up to almost 50 percent, was accompanied by an increase in distribution volume (V_{dd}/F) and clearance (Cl/F), which is possibly due to a reduced absorption of the drug. The elimination half-life of

olaparib after co-administration of paclitaxel did not change significantly (around 4 hours). The plasma concentration-time curves following administration of olaparib only (day 4) and olaparib plus paclitaxel (day 8) in a representative patient are shown in figure 1. The AUCs of all individual patients on day 4 and day 8 are shown in figure 2. Paclitaxel pharmacokinetics revealed a median area under the curve (AUC) of 4.4 $\mu\text{g}\cdot\text{h}/\text{ml}$, and a median elimination half-life of 16.6 hours.

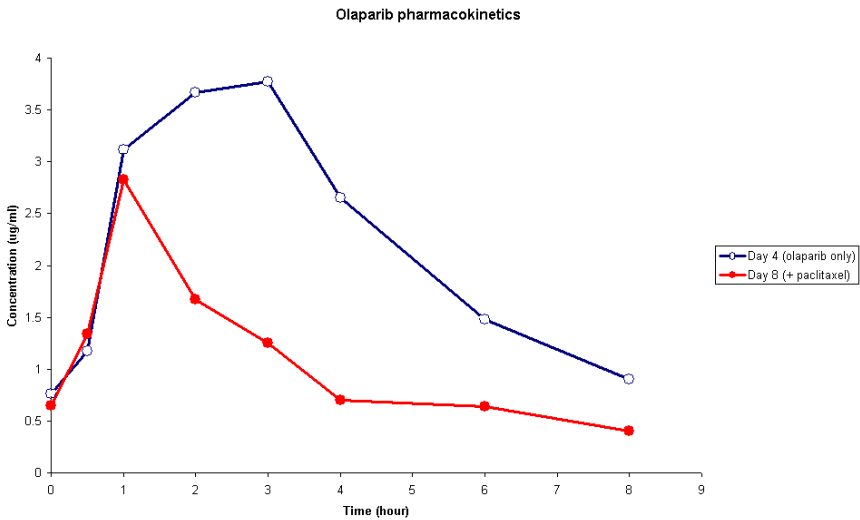
Table 2: Treatment-related adverse events, and laboratory abnormalities during the first treatment cycle.

Non-hematological adverse events					
	Grade 1 n (%)	Grade 2 n (%)	Grade 3 n (%)	Grade 4 n (%)	Total n (%)
Alopecia	4 (44%)	2 (22%)			6 (66%)
Fatigue	4 (44%)	2 (22%)			6 (66%)
Neuropathy	3 (33%)				3 (33%)
Stomatitis	3 (33%)				3 (33%)
Diarrhea	2 (22%)				2 (22%)
Epistaxis	2 (22%)				2 (22%)
Nausea	2 (22%)				2 (22%)
Vomiting	2 (22%)				2 (22%)
Arthralgia	1 (11%)				1 (11%)
Dizziness	1 (11%)				1 (11%)
Fever	1 (11%)				1 (11%)
Flu like symptoms	1 (11%)				1 (11%)
Myalgia	1 (11%)				1 (11%)
Laboratory abnormalities					
	Grade 1 n (%)	Grade 2 n (%)	Grade 3 n (%)	Grade 4 n (%)	Total n (%)
Hematology					
Leukocytopenia	2 (22%)	3 (33%)	1 (11%)		6 (66%)
Neutropenia (ANC)		2 (22%)	2 (22%)	1 (11%)	5 (55%)
Lymphocytopenia		2 (22%)	2 (22%)		4 (44%)
Clinical chemistry					
Hyperglycemia	4 (44%)	3 (33%)	1 (11%)		8 (88%)
Alanine aminotransferase	5 (55%)				5 (55%)
Gamma-glutamyl transferase	2 (22%)	2 (22%)	1 (11%)		5 (55%)
Alkaline phosphatase	4 (44%)				4 (44%)
Hypocalcemia	4 (44%)				4 (44%)
Creatinine	3 (33%)				3 (33%)
Aspartate aminotransferase	2 (22%)				2 (22%)
Hypercalcemia	2 (22%)				2 (22%)
Hyperkalemia	2 (22%)				2 (22%)
Hypernatremia	1 (11%)				1 (11%)
Hypoalbuminemia	1 (11%)				1 (11%)
Hypokalemia	1 (11%)				1 (11%)
Hyponatremia	1 (11%)				1 (11%)

Table 3: Olaparib pharmacokinetics

Parameter	100 mg olaparib		200 mg olaparib	
	day 4	day 8	day 4	day 8
Cmax (µg/ml)	4.0 (1.9-11.2)	3.0 (1.6-7.5)	4.2 (3.0-8.9)	2.8 (2.0-5.8)
Tmax (hours)	1.0 (1.0-2.0)	2.0 (1.0-4.0)	2.0 (2.0-3.0)	1.0 (1.0-2.0)
AUC ₀₋₈ (µg-hr/ml)	19.0 (6.9-70.2)	10.0 (5.2-47.0)	23.7 (14.9-51.2)	12.1 (9.1-26.9)
Ratio AUC ₀₋₈ day 8/day4	0.52		0.51	
AUC (µg-hr/ml)	24.3 (8.3-197.5)	12.9 (6.8-67.5)	31.9 (20.2-64.4)	23.3 (10.8-40.5)
Ratio AUC day 8/day4	0.53		0.73	
T _{1/2} (hr)	3.7 (1.9-11.5)	3.9 (3.3-4.0)	3.6 (2.9-8.5)	4.7 (3.0-9.6)
Cl/F (l/hr)	4.3 (0.5-12.1)	7.8 (1.5-14.8)	6.3 (3.1-9.8)	8.6 (4.9-18.6)
Vdd (l)	23.5 (8.4-33.4)	41.8 (8.4-81.2)	36.5 (12.9-51.4)	71.3 (35.3-115.4)

Figure 1: Olaparib plasma concentration-time curves with (day 8) and without (day 4) co-administration of paclitaxel. This figure shows representative curves of a patient treated with 200 mg olaparib, and 80 mg/m² paclitaxel.



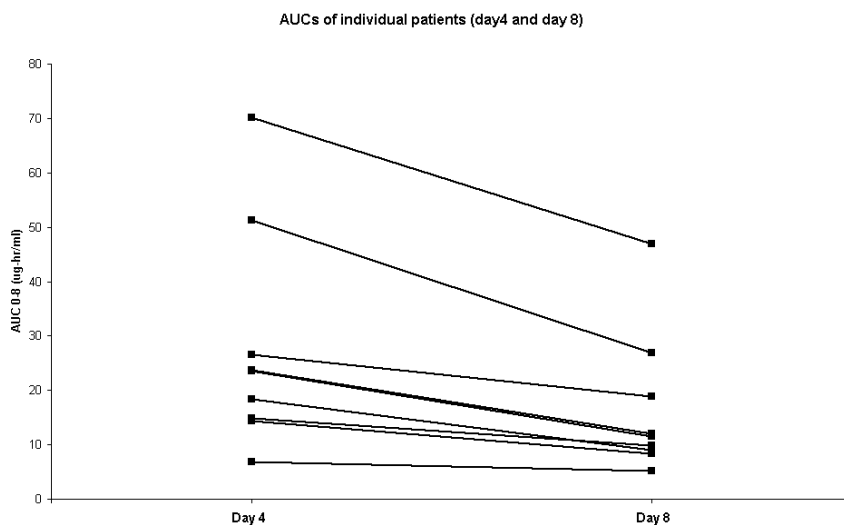


Figure 2: AUCs (0-8) on day 4 (single dose olaparib) and day 8 (after co-administration of paclitaxel).

Response

Nine patients had at least 1 response assessment following treatment in this study. The median treatment duration and best response per dose-level are given in table 4. At the 100 mg olaparib dose-level, one patient progressed after 2 cycles (8 weeks) of treatment. The three other patients treated at this dose-level remained stable for at least 24 weeks. Two of these patients were ongoing at the time of this report. This included a heavily pre-treated young male patient with Ewing sarcoma, who was on treatment for 50 weeks, and a breast cancer patient that was ongoing for 40 weeks. This patient, with a known BRCA2 mutation, had a dramatic CA15.3 tumor marker response, as can be observed in figure 3. However, according to RECIST, her best response was stable disease. She had been pre-treated for advanced disease with 5-FU, epirubicin and cyclophosphamide. At the 200 mg olaparib dose-level, 5 out of 6 patients could be evaluated for response. Two patients came off-study after the first evaluation, 8 weeks after initiation of treatment. The other patients remained on-study for 14, 20, and 24 weeks, respectively. Two of these patients were ongoing at the time of this report. A patient with breast cancer, with a known BRCA1 mutation, had a confirmed partial response after 4 cycles (16 weeks) of treatment, and continued at the time of this report, 20

Table 4: Treatment response

Dose-level	Median treatment duration (weeks)	Best response		
		PR	SD	PD
100 mg Olaparib (n=4)	32 (8-50)*		3	1
200 mg Olaparib (n=5)	14 (8-24)*	1	2	2
Total (n=9)	20 (8-50)*	1	5	3

* At the cut off date of this report, 4 patients (2 at each dose-level) were still ongoing. This includes patients with BRCA deficient breast cancer (n=2), Ewing sarcoma (n=1), and lung cancer (n=1).

weeks after initiation of olaparib treatment. She had been pre-treated for advanced disease with 5-FU, epirubicin and cyclophosphamide. The second ongoing patient was a patient with a neuroendocrine small cell lung tumor, who had stable disease after 2 cycles of treatment, and was ongoing 14 weeks after treatment initiation.

Olaparib tumor marker response

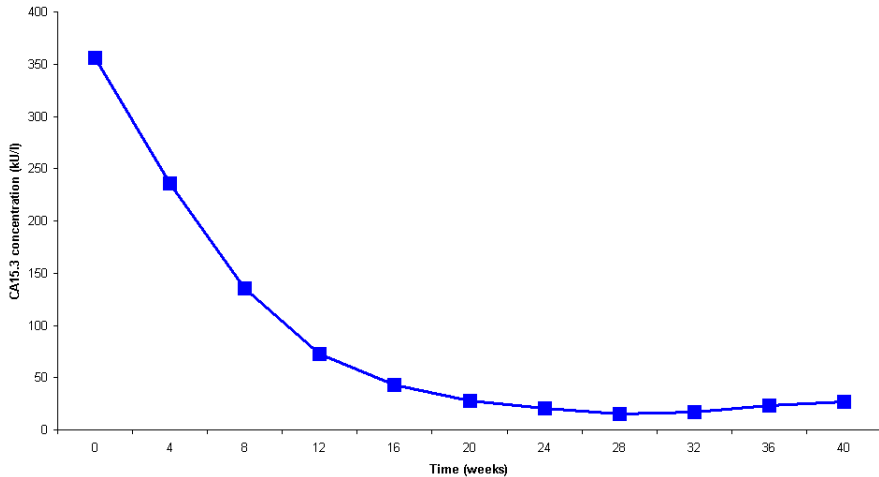


Figure 3: Tumor marker response of a breast cancer patient with a known BRCA2 mutation. She was treated with 100 mg olaparib bi-daily, and 80 mg/m² paclitaxel weekly. She had documented progressive disease prior to start and had been pretreated with 5-FU, epirubicin and cyclophosphamide for advanced disease.

Discussion

In this sub-study, part of a larger clinical trial combining olaparib with carboplatin, paclitaxel, or a carboplatin/paclitaxel doublet, we demonstrated that olaparib can be safely combined with therapeutic doses of paclitaxel. The applied doses of olaparib in this study (100 and 200 mg) were also biologically active doses, as demonstrated in the previous phase I trial with olaparib monotherapy (6). Weekly administration of paclitaxel was chosen as at this schedule paclitaxel is more active than at a 3-weekly schedule (8).

The observed non-hematological toxicities in this study were very mild, with fatigue and alopecia as most frequently observed side-effects. These toxicities were expected based on previous studies with both agents. The recently published olaparib monotherapy trial showed mild nausea and fatigue as predominant side-effects (6), and alopecia is a well known side-effect of paclitaxel administration (9). In this study, we observed some hematological toxicity. This can be attributed to the paclitaxel administration, since no hematological toxicities were observed in the monotherapy olaparib study, and bone marrow toxicity is a well-known side-effect of weekly paclitaxel.(9). All observed hematological toxicities were reversible, and did not lead to treatment withdrawal in any case.

Pharmacokinetic parameters derived after administration of olaparib only (day 4), and after administration of olaparib and paclitaxel (day 8) revealed a significant decrease in exposure to olaparib after co-administration of paclitaxel. It is unlikely that this is due to an effect of paclitaxel itself. The effects of paclitaxel could have influenced olaparib pharmacokinetics in two ways: First, by effecting the uptake in the intestine, due to an effect on P-glycoprotein. It is known that both paclitaxel and olaparib are P-gp substrates (10). Another effect of paclitaxel could have been the entrapment of olaparib in the central compartment by cremophor EL (a constituent of the paclitaxel formulation) micelles. However, both these effects would have led to an increased exposure to olaparib, while we found a decrease of about 50 percent. Based on the observation that both the volume of distribution (V_d/F) and the clearance (Cl/F) increased with comparable magnitudes following administration of paclitaxel, we hypothesized that this effect was due to a decreased bioavailability (F) of olaparib. Paclitaxel can not influence this, since it is given intravenously. The decreased bioavailability of olaparib may be the

consequence of a change in gastric pH, caused by the co-administration of ranitidine, an H₂ receptor antagonist that is given as pre-medication for paclitaxel. Further research to test this hypothesis is warranted.

The pharmacokinetics of paclitaxel were, with an elimination half-life of 16.6 hours and an exposure of 4.4 µg.h/ml, comparable with other studies investigating weekly paclitaxel administration (11).

Several patients included in this trial remained on-study for long periods of time, indicating beneficial activity of this combination. This is also illustrated by the responses we observed in patients harboring BRCA mutations. One heavily pre-treated patient with BRCA2 deficient breast cancer had stable disease as best response, accompanied by a dramatic CA15.3 tumor marker response. Another heavily pre-treated patient with BRCA1 deficient breast cancer had a confirmed PR. Both patients were ongoing at the time of this report. These results are in line with olaparib phase I data, and with phase II results that were recently presented for patients with BRCA mutated breast cancer (12,13). Interestingly, several patients without known BRCA deficiencies remained on study for long periods of time as well. A young heavily pre-treated male patient with Ewing sarcoma, for instance, was ongoing for 50 weeks at the time of this report.

In the recently published phase I study, an MTD of 400 mg olaparib BID was established as the maximal tolerable dose, but lower doses of 100 and 200 mg BID were found to be biologically active (6). These results justify the 100 and 200 mg olaparib doses we used in this study. However, it was recently shown that 400 mg olaparib is far more effective than lower doses of 100 mg, in patients with ovarian and breast cancer (12,13). The here described study only investigated the combination of 100 and 200 mg olaparib with paclitaxel, and therefore we can not conclude whether 400 mg of olaparib combined with clinically active doses of paclitaxel is safe. Moreover, due to possible synergy between olaparib and paclitaxel, lower olaparib doses might be sufficient to induce a powerful anti-tumor effect. It was shown in preclinical studies that continuous olaparib administration is optimal (10). Together with the optimal weekly paclitaxel schedule, the treatment schedule as used in this study can be considered optimal for this combination of drugs. Recent preclinical studies suggested that inhibition of PARP might induce paclitaxel resistance by induction of the PI3-kinase-Akt pathway (14). However, it needs to be stressed that this work, although of interest, was done in cell lines. The

extrapolation of preclinical results to the clinical situation is often difficult, due to differences in drug disposition and signal transduction pathways between the in vitro and in vivo situation. Altogether, we believe that these results should be interpreted cautiously.

In conclusion, we showed that olaparib at doses of 100 and 200 mg bi-daily can be safely combined with 80 mg/m² paclitaxel given weekly. The toxicities were very mild, excluding infrequently observed grade 3-4 hematological toxicities, that can be mainly attributed to paclitaxel administration. We found a significant decrease in olaparib exposure after co-administration of paclitaxel. We believe this effect may be due to an effect of ranitidine on the gastric pH, thereby influencing the bioavailability of olaparib. More research is needed to explore the mechanistic background of this PK interaction.

References

1. Hoeijmakers, J. H. Genome maintenance mechanisms for preventing cancer. *Nature*. 2001;411:366-374.
2. Dantzer, F., de La, Rubia G., Menissier-De Murcia, J.et al. Base excision repair is impaired in mammalian cells lacking Poly(ADP-ribose) polymerase-1. *Biochemistry*. 2000;39:7559-7569.
3. Evers, B. and Jonkers, J. Mouse models of BRCA1 and BRCA2 deficiency: past lessons, current understanding and future prospects. *Oncogene*. 2006;25:5885-5897.
4. Lord, C. J. and Ashworth, A. Targeted therapy for cancer using PARP inhibitors. *Curr.Opin.Pharmacol*. 2008;8:363-369.
5. Farmer, H., McCabe, N., Lord, C. J.et al. Targeting the DNA repair defect in BRCA mutant cells as a therapeutic strategy. *Nature*. 2005;434:917-921.
6. Fong, P. C., Boss, D. S., Yap, T. A.et al. Inhibition of Poly(ADP-Ribose) Polymerase in Tumors from BRCA Mutation Carriers. *N.Engl.J.Med*. 2009;361(2):123-34.
7. Rowinsky, E. K., Onetto, N., Canetta, R. M.et al. Taxol: the first of the taxanes, an important new class of antitumor agents. *Semin.Oncol*. 1992;19:646-662.
8. Seidman, A. D., Hudis, C. A., Albanell, J.et al. Dose-dense therapy with weekly 1-hour paclitaxel infusions in the treatment of metastatic breast cancer. *J.Clin.Oncol*. 1998;16:3353-3361.
9. Rowinsky, E. K., Eisenhauer, E. A., Chaudhry, V.et al. Clinical toxicities encountered with paclitaxel (Taxol). *Semin.Oncol*. 1993;20:1-15.
10. Rottenberg, S., Jaspers, J. E., Kersbergen, A.et al. High sensitivity of BRCA1-deficient mammary tumors to the PARP inhibitor AZD2281 alone and in combination with platinum drugs. *Proc.Natl.Acad.Sci.U.S.A*. 2008;105:17079-17084.
11. Fennelly, D., Aghajanian, C., Shapiro, F.et al. Phase I and pharmacologic study of paclitaxel administered weekly in patients with relapsed ovarian cancer. *J.Clin.Oncol*. 1997;15:187-192.
12. Tutt, A., Robson, M., Garber, J. E.et al. Phase II trial of the oral PARP inhibitor olaparib in BRCA-deficient advanced breast cancer. *J.Clin.Oncol*. 2009;27:Abstr. CRA501-
13. Audeh, M. W., Penson, R. T., Friedlander, M.et al. Phase II trial of the oral PARP inhibitor olaparib (AZD2281) in BRCA-deficient advanced ovarian cancer. *J.Clin.Oncol*. 2009;27:abstr. 5500-
14. Szanto, A., Hellebrand, E. E., Bognar, Z.et al. PARP-1 inhibition-induced activation of PI-3-kinase-Akt pathway promotes resistance to taxol. *Biochem.Pharmacol*. 2009;77:1348-1357

7

**The angiogenesis
inhibitor E7080**

CHAPTER 7.1

Phase I dose escalation study of E7080, an orally available multi-targeted angiogenesis inhibitor, in patients with advanced solid malignancies

David S. Boss, Hilary Glen, Jos H. Beijnen, Marianne Keessen,
Jan H. M. Schellens, Jeff T. R. Evans

Abstract

Purpose: E7080 is a potent inhibitor of the split-kinase family of the VEGF receptors Flt-1 and KDR. In addition, E7080 also potently inhibits FGFR1, PDGFR β , and c-kit tyrosine kinase activities. This study established the optimal dose, safety and pharmacokinetics of E7080 in patients with advanced solid malignancies.

Patients and methods: E7080 (0.2 to 32 mg) was administered orally on a once daily continuous dose schedule in cycles of 28 days. Sampling of blood and urine for pharmacokinetic studies was performed in all patients. Preliminary tumor response was assessed once every 2 cycles.

Results: 80 patients with documented Progressive Disease (PD) were included in the study. The most frequently observed adverse events were hypertension (36%) and gastrointestinal disorders including nausea, diarrhea, and stomatitis (35, 31 and 31%, respectively). Dose-limiting toxicities were grade 3 proteinuria (2 patients) at 32 mg, and the maximum tolerated dose was set at 25 mg. Eight patients (10%) had a partial response, and 40 (50%) patients had stable disease as best response, with some patients continuing on study after 131 weeks of treatment. Pharmacokinetic studies revealed dose-linearity, a half-life of around 7 hours, and a moderate volume of distribution. No accumulation was observed after 4 weeks of drug administration. Concomitant intake of food had no effect on exposure to E7080.

Conclusion: E7080 is safe and well tolerated at doses up to 25 mg/day. Promising signs of anti-cancer activity were observed in various tumor types, including melanoma and renal cell carcinoma.

Introduction

Angiogenesis, the formation of new blood vessels from a pre-existing vascular network, is essential for tumor growth and metastasis. Many molecules have been implicated as positive regulators of angiogenesis, including vascular endothelial growth factor (VEGF), fibroblast growth factor (FGF), and platelet-derived growth factor (PDGF). VEGF has been identified as a crucial regulator of physiologic and pathologic angiogenesis, acting primarily via activation of VEGF- receptor 2 (VEGFR-2; kinase insert domain receptor) (1). Increased VEGF expression has been associated with a poor prognosis in many cancers, exemplifying the significance of the VEGF pathway for the malignant process (2,3,4). The concept of targeting angiogenesis for tumor therapy was introduced already in the 1970s by Judah Folkman (5). However, it was not until recently that the first angiogenesis inhibitors reached the clinic. bevacizumab, a monoclonal antibody directed against VEGF-A, has demonstrated clinically relevant improvements in survival when added to conventional chemotherapy regimens in patients with colorectal and non-small cell lung cancer (6,7). Sorafenib and sunitinib, orally available multi-kinase inhibitors with activity against VEGF and PDGF receptors have shown promising antitumor activity in patients with renal cell carcinoma (8,9). E7080 is a novel, orally available multi-kinase inhibitor that prevents tumor angiogenesis, primarily via inhibition of the VEGF receptor KDR (VEGFR-2). E7080 also has activity against Flt-1 (VEGFR-1), fibroblast growth factor receptor 1 (FGF-R1), platelet-derived growth factor receptor beta (PDGFR- β), and c-kit (10). The effect of E7080 on c-kit signaling might also affect tumor cell proliferation, since this receptor, and its ligand stem cell factor (SCF) are expressed on tumor cells as well. Finally, E7080 might suppress the metastatic potential of tumor cells via inhibition of VEGF-R3 mediated lymphangiogenesis (11). This phase I study was initiated to determine the maximum tolerated dose (MTD), dose limiting toxicities (DLTs), pharmacokinetics, and antitumor activity of oral daily E7080 in patients with advanced solid malignancies.

Patients and methods

Patient selection

The study was conducted in adult (>18 years of age) patients with a histologically and/or cytologically confirmed solid tumor or lymphoma who

were resistant/refractory to approved therapies or for whom no appropriate therapies were available. Other criteria for inclusion were: A Karnofsky performance status $\geq 70\%$; adequate hematological function as defined by an absolute neutrophil count (ANC) of $\geq 1.5 \times 10^9$, platelet count of $\geq 100 \times 10^9$ and hemoglobin ≥ 5.6 mmol/l; adequate hepatic function as defined by serum bilirubin ≤ 25 $\mu\text{mol/l}$, ALT and AST ≤ 3 times the upper limit of normal; adequate renal function as defined by serum creatinine ≤ 1.5 times the upper limit of normal or a creatinine clearance ≥ 60 ml/min (Cockcroft–Gault formula). Previous treatment (including surgery and radiotherapy) had to be completed at least 4 weeks before study entry. Patients with centrally located or squamous cell carcinoma of the lung, brain tumors or brain metastases, uncontrolled infections, clinically significant cardiac impairment, bleeding or thrombotic disorders, or poorly controlled hypertension were excluded from the study. Other exclusion criteria included: the use of therapeutic doses of anticoagulants; a history of gastrointestinal malabsorption; proteinuria $>1+$, and pregnancy. The study protocol was approved by the Medical Ethics Committees of the participating hospitals and all patients gave written informed consent prior to inclusion in the study.

Study design

This phase I, open-label, multi-centre, dose escalation study assessed the safety, tolerability, anti-tumor activity and PK profile of E7080. Patients received E7080 orally once daily in 28 day cycles, until the occurrence of unacceptable toxicity not amenable to dose reduction or treatment interruption, or progressive disease. The starting dose of 0.2 mg/day was based on preclinical data. The selection of subsequent dose levels was performed according to an accelerated design: The next dose level was open for patient accrual after only the first patient in the previous cohort had completed cycle 1 with no drug related toxicity \geq Grade 1 (except alopecia, lymphopenia and anemia). Dose increases in subsequent cohorts were by 100% increments until any patient at a given dose level experienced \geq grade 2 toxicity. From that moment on, dose increases were 50% or less, depending on the seriousness of the toxicity, and all 3 patients at a given dose level were followed for a full cycle before the next dose level opened. If 1 out of 3 patients experienced a dose limiting toxicity (DLT) during the first cycle, 3 additional patients were to be treated at that dose level. The MTD was defined as the highest dose level at which no more than 1 out of 6 patients

experienced a DLT. An additional 12 patients were treated at the MTD dose level. Due to the occurrence of dose reductions at dose levels of 16 mg and higher, and observed activity at 12.5 mg, an additional 12 patients were enrolled at 12 mg. These cohort expansions allowed for further investigation into the tolerability and anti-tumor effect of E7080 both at MTD and a lower, possibly non-toxic dose, in a larger cohort of patients. All patients entering the MTD expansion cohort were asked to participate in the food-effect investigation. Patients entering this part of the study were randomly assigned to receive the cycle 1 day 15 dose of E7080 under fasting conditions (following an overnight fast of at least 10 hours), or following a high fat meal. In both cases, no food was allowed for 4 hours post dose. The patients assigned to receive the cycle 1 day 15 dose under fasting conditions then received the cycle 1 day 22 with a high fat meal, and vice versa. Blood samples for pharmacokinetic analyses were drawn as detailed in the pharmacokinetic studies section.

Toxicity criteria

Adverse events were monitored and graded according to the National Cancer Institute Common Toxicity Criteria (NCI- CTC) version 3.0 . A DLT was defined as any of the following drug related toxicities: Any grade 3 or higher hematological or non-hematological toxicity; Any repeated grade 2 hematological or non-hematological toxicity requiring dose reduction; Failure to administer $\geq 75\%$ of the planned dosage of E7080 during cycle 1 as a result of treatment-related toxicity.

Hypertension management

As E7080 is an angiogenesis inhibitor, and hypertension is a classical toxicity for this category of anticancer agents, hypertension was an expected side-effect. In this multi-centre study, antihypertensive drugs were prescribed to minimize these toxicities from the moment of their first occurrence (diastolic blood pressure ≥ 100 mg Hg). The prescribed drugs varied between the two participating hospitals, but generally included calcium-antagonists, Beta-blockers, ACE-inhibitors, and diuretics. Treatment with E7080 was interrupted until recovery, and patients continued on the same dose after blood pressure normalization. Dose-reductions were only given when blood pressure could not be adequately controlled with antihypertensive drugs.

Pharmacokinetic studies

Blood samples for pharmacokinetic analysis were collected on days 1 and 29 (day 1 cycle 2), immediately prior to the first dose, and then at 0.25, 0.5, 1, 1.5, 2, 2.5, 3, 5, 8, and 24 hours following the first dose of E7080. Trough samples were taken within 2 hours prior to E7080 administration on days 8, 15, and 22 of cycle 1, and on day 1 of each subsequent cycle. Patients entering the food-effect investigation provided blood samples at the same eleven time-points on days 1, 15, and 22 of cycle 1. PK blood samples were not collected from these patients on day 29, except for the pre-dose sample. A pre-dose sample as well as a 24 hour urine collection was performed on day 1 for all patients, and on day 29 for patients not participating in the food-effect investigation. For food-effect participants only a pre-dose sample was collected on day 29. The 24 hour urine collection was performed in three aliquots of 0-8 hours, 8-16 hours, and 16-24 hours after E7080 administration. E7080 concentrations in blood and urine were measured using a liquid chromatography-tandem mass spectrometry method. The pharmacokinetic parameters for plasma and urine were calculated using Winnonlin version 6.0 (Pharsight corporation, Mountain view, USA). In the food effect investigation, a 90% confidence interval for the log transformed C_{max} and AUC₀₋₂₄ (fed/fasted) were calculated using ANOVA. If a range within 80% to 125% was found, then the concomitant intake of food was considered not to modify the bioavailability of E7080.

Clinical activity measurements

All sites of malignant disease were determined at baseline by clinical examination and photography (for skin lesions), CT, or MRI scans, according to the Response Evaluation Criteria In Solid Tumors (RECIST) criteria (12). Thereafter, tumor assessments were performed by identical methods once every 2 treatment cycles. The clinical benefit ratio was calculated as the sum of all patients experiencing a complete response, partial response, or stable disease, divided by the total number of evaluable patients.

Results

Patient characteristics

A total of 80 patients with documented progressive disease were recruited between July 2005 and July 2008. The patient characteristics are summarized in table 1. All patients were evaluable for toxicity assessments. Eleven additional patients treated at the MTD dose-level were included in the food-effect study, and 6 additional patients were treated at the 12 mg dose-level. At the time of the database lock (October 2008), 14 patients (17.5%) were still on treatment.

Table 1: Patient characteristics

Characteristic	n	%
Total No. of patients	80	
Sex (male:female)	42-38	
Age (median, range)	54 (25-84)	
Performance status (Karnofsky)		
100	6	8
90	32	40
80	11	14
70	31	39
Tumor type		
Sarcoma	15	19
Melanoma	14	18
Colorectal	13	16
Renal	8	10
Oesophagus/Gastric	8	10
Lung	6	8
Pancreas	4	5
Ovarian ca.	3	4
Other	9	11

MTD and DLT

No DLTs were observed up to 6.4 mg. One patient treated at the 6.4 mg dose-level experienced a DLT (grade 3 febrile neutropenia), but this treatment did not influence the dose escalation plan, since it did not occur during the first treatment cycle. At the next dose-level (12.5 mg), initially, two out of six patients experienced a DLT. The first patient had grade 4 thrombocytopenia, and the second had a grade 3 proteinuria. The severity of the proteinuria in this patient was questioned, since her urine samples were collected wrongly, falsely elevating her urinary protein level. When the sample was collected correctly, she only had grade 2 proteinuria. Her E7080 had been interrupted

by this time, and was then slow to return to baseline. Moreover, she already had grade 1 proteinuria when she was screened for participation in the study. It was decided, as the majority of patients treated at the 12.5 mg dose-level were ongoing without side-effects, and as this episode of proteinuria was not clearly a DLT, to include another three patients at this dose-level. None of these extra patients experienced a DLT, and it was decided to increase the dose to 16 mg. At the 16 mg dose-level, one out of three patients experienced a DLT (grade 3 hypertension), and the cohort was expanded with three extra patients. None of these extra patients experienced a DLT, and the dose was again increased, to 20 mg. No DLTs were observed in the three patients treated at this dose-level, and also not in the three patients treated at the next dose-level of 25 mg. At 32 mg, two out of six patients experienced a DLT (both grade 3 proteinuria), and this dose-level was concluded to be intolerable. The MTD was set at the next-lower dose-level of 25 mg.

Adverse events

A total of 74 patients (92.5%) experienced drug-related adverse event, the most frequent were hypertension (36.5%), and gastrointestinal disorders including nausea, stomatitis and diarrhea (35, 31.3%, and 31.3%, respectively). The most frequently observed toxicities are summarized in table 2. Most toxicities were mild in origin (grade 1-2). The observed grade 3 and 4 toxicities (26.3 and 7.5% overall, respectively) consisted mainly of proteinuria, hypertension, and gastrointestinal complaints. There was a trend towards an increase in hypertension and proteinuria with increasing doses of E7080, as can be seen in table 3. Proteinuria was a DLT in three patients. The first patient, treated at 12.5 mg, experienced grade 3 proteinuria, which was considered a DLT. However, as stated in the above, the severity of this event was questioned. After stopping treatment, her proteinuria took more than two weeks to return grade 1, and hence she was taken off study. The second and third patient with proteinuria as DLT were both treated at 32 mg. Both patients experienced a grade 3 proteinuria, and treatment was interrupted. They continued with dose reductions and then both had further episodes of proteinuria, each time recovering within a week of stopping E7080. Ultimately, they ended up on maintenance doses of 8 and 10 mg/day respectively, but interestingly, on these lower maintenance doses they both went on to have PRs and remained on treatment for many months. Hypertension was a DLT in a patient treated at 16 mg. This patient ceased drug intake until normalization

Table 2: Treatment-related adverse events with an overall incidence $\geq 10\%$

Adverse Event	total (n=80)		0.2-6.4 mg (n=21)		12-20 mg (n=28)		25 mg (n=24)		32 mg (n=7)	
	n	%	n	%	n	%	n	%	n	%
Hypertension	29	36.3	2	9.5	10	35.7	13	54.2	4	57.1
Nausea	28	35.0	8	38.1	4	14.3	13	54.2	3	42.9
Diarrhea	25	31.3	4	19.0	5	17.9	12	50.0	4	57.1
Stomatitis	25	31.3	1	4.8	6	21.4	14	58.3	4	57.1
Lethargy	19	23.8	3	14.3	5	17.9	9	37.5	2	28.6
Vomiting	19	23.8	7	33.3	3	10.7	8	33.3	1	14.3
Hoarseness	18	22.5			4	14.3	11	45.8	3	42.9
Proteinuria	18	22.5	3	14.3	6	21.7	7	29.2	2	28.6
Dry Skin	14	17.5	1	4.8	3	10.7	10	41.7		
Fatigue	14	17.5	2	9.5	7	25.0	4	16.7	1	14.3
Anorexia	13	16.3	2	9.5	4	14.3	5	20.8	2	28.6
Constipation	12	15.0	2	9.5	1	3.6	8	33.3	1	14.3
Arthralgia	10	12.5	2	9.5	2	7.1	4	16.7	2	28.6
Headache	9	11.3			1	3.6	6	25.0	2	28.6
Abdominal Pain	8	10.0			1	3.6	7	29.2		

of his blood pressure, and continued with a dose reduction of 25 %. Also, anti-hypertensive medication was prescribed to control his blood-pressure during further treatment with E7080. The observed gastrointestinal toxicities were generally mild (57.5% grade 1-2, 7.6% grade 3-4), and consisted mainly of grade 1-2 nausea, diarrhea, stomatitis and vomiting. There was a dose-dependent increase in the occurrence of gastrointestinal toxicities. This accounted especially for stomatitis, although the severity was limited to grade 1-2. Hematological toxicities were very infrequently observed, with an overall incidence of 8.8% in the total population. However, two patients experienced grade 3-4 hematological toxicities that were considered DLTs. The first patient, treated at 6.4 mg, experienced a grade 3 febrile neutropenia. After cessation of E7080, his neutrophil count recovered to normal, but his platelet count dropped from CTC grade 2 to CTC grade 4, and he died shortly after this of overwhelming sepsis. The second patient, treated at 12.5 mg, experienced grade 4 thrombocytopenia. The thrombocytes levels in this patient returned to normal within a week after cessation of E7080 therapy. Both patients with hematological toxicities were heavily pretreated with multiple lines of chemotherapy, and their bone marrow reserve could have been seriously compromised at the time of study entry.

Table 3: Treatment-related hypertension, proteinuria, and stomatitis by CTC grade

Adverse Event	total (n=80)		0.2-6.4 mg (n=21)		12-20 mg (n=28)		25 mg (n=24)		32 mg (n=7)	
	n	%	n	%	n	%	n	%	n	%
Hypertension	29	36.3	2	9.5	10	35.7	13	54.2	4	57.1
Grade 1	6	7.5	1	4.8	2	7.1	1	4.2	2	28.6
Grade 2	15	18.8			6	21.4	9	37.5		
Grade 3	8	10.0	1	4.8	2	7.1	3	12.5	2	28.6
Proteinuria	18	22.5	3	14.3	6	21.4	7	29.2	2	28.6
Grade 1										
Grade 2	12	15.0	3	14.3	4	14.3	5	20.8		
Grade 3	6	7.5			2	7.1	2	8.3	2	28.6
Stomatitis	25	31.3	1	4.8	6	21.4	14	58.3	4	57.1
Grade 1	20	25.0	1	4.8	5	17.9	12	50.0	2	28.6
Grade 2	5	6.3			1	3.6	2	8.3	2	28.6

Pharmacokinetics

A total of 79 patients provided blood samples for pharmacokinetic analyses after a single dose of E7080 (table 4). After drug administration, E7080 was absorbed rapidly with maximum concentrations reached after 2 to 3 hours. Both the exposure to E7080 and the observed C_{max} concentrations increased linearly with increasing dose (figure 1), and the median half-life of E7080 varied between 5.4 and 8.3 hours at the higher dose-levels (6.4 mg or higher). The terminal elimination phase could not be estimated properly for several patients treated at the lower dose-levels (up to 3.2 mg), due to insufficient data points in the terminal phase. Consequently, no AUC_{inf}, half-life, clearance and volume of distribution could be reported for these patients. At the higher doses, the median clearance of E7080 ranged between 4.3 and 10.4 l/hr, while the drug had a moderate median volume of distribution ranging between 50.5 and 92.0 liter. Comparable results were obtained following multiple doses of E7080 (table 5, n=58). No accumulation was observed after multiple dosing of E7080 (the C_{max} values observed at steady state equaled those observed after a single dose). Analyses of urine samples collected up to 24 hours after the first dose revealed that less than 1% of E7080 was recovered unchanged in urine. The same was observed after multiple doses of E7080 (day 1, cycle 2). Eleven patients were included in the food-effect study. No effects of food on exposure or maximum achieved plasma concentrations were observed (AUC ratio fed:fasted of 1.01 with a 90% confidence interval of 0.84-1.22; C_{max} ratio fed:fasted of 0.98 with a 90% confidence interval of 1.72-1.34). However, there was a significant effect

Table 4: Pharmacokinetic parameters after a single dose of E7080.

Parameters after single doses of E7080	E7080 Dose											
	0.2 mg (n=4)	0.4 mg (n=4)	0.8 mg (n=4)	1.6 mg (n=3)	3.2 mg (n=3)	6.4 mg (n=3)	12 mg (n=10)	12.5 mg (n=9)	16 mg (n=6)	20 mg (n=3)	25 mg (n=22)	32 mg (n=7)
T _{max} (hr)	5.0 (2.1-5.0)	6.4 (2.5-7.8)	2.8 (2.5-5.0)	3.1 (1.0-7.8)	2.5 (2-24.1)	2 (1.0-3.1)	2.5 (1.0-12.3)	2.0 (1.0-2.5)	2.1 (2.1-3.0)	3.0 (1.6-3.0)	1.8 (1.0-3.0)	2.1 (1.0-7.1)
C _{max} (ng/ml)	0.7 (0.6-1.1)	1.6 (1.1-2.7)	3.8 (2.7-6.8)	24.7 (7.9-30.3)	49.8 (33.9-65.9)	131.8 (33.5-215.9)	239.2 (71.6-511.4)	178.3 (107.7-401.5)	397.7 (156.3-610.2)	402.1 (306.6-517.7)	598.0 (318.4-1285.4)	681.5 (235.2-914.3)
AUC ₀₋₂₄ (ng ^a ·hr/ml)	13.9 (9.6-19.8)	28.4 (21.5-50.5)	50.3 (43.2-61.7)	152.6 (140.7-367.5)	718.9 (432.6-844.1)	1280.8 (318.6-1918.6)	1586.2 (2890.3)	1132.7 (788.5-3263.5)	3096.4 (1084.6-6155.0)	3102.2 (2018.3-6019.0)	3923.8 (1495.4-9267.4)	5106.8 (1651.8-7471.6)
AUC _{inf} (ng ^a ·hr/ml)		155.9a		914.0a		1501.2 (369.7-2135.6)	1797.9 (1328.0-3072.4)b	1205.9 (838.1-3631.5)	3466.4 (1157.5-4608.2)	3398.3 (2159.8-7158.0)	4178.0 (1542.4-10299.8)c	4603.8 (1723.3-5992.2)d
T _{1/2} (hr)				4.5a	10.6a	8.3 (7.3-8.7)	6.1 (5.3-7.0)b	6.4 (5.3-8.9)	7.0 (5.9-8.7)	6.6 (6.0-8.3)	5.4 (4.5-8.3)c	5.5 (4.9-6.5)d
Cl/F (l/hr)				10.3a	3.5a	4.3 (3.0-17.3)	6.7 (3.9-9.0)b	10.4 (3.4-14.9)	4.9 (2.2-13.8)	5.9 (2.8-9.3)	6.0 (3.8-13.1)c	7.1 (18.6)d
V/F (l)				66.3a	53.6a	53.6 (31.4-206.7)	60.5 (31.5-77.6)	92.0 (33.6-133.6)	50.5 (27.4-117.4)	56.1 (33.6-79.4)	50.9 (33.8-121.4)c	58.7 (45.7-130.9)d

Several patients treated at the lower dose levels up to 3.2 mg had not enough data points in the terminal phase to estimate the half-life. For these patients, no AUC_{inf}, clearance, volume of distribution, and half-life was reported.

^a n=1, ^b n=9, ^c n=9, ^d n=21, ^e n=6

Table 5: Pharmacokinetic parameters after multiple doses of E7080.

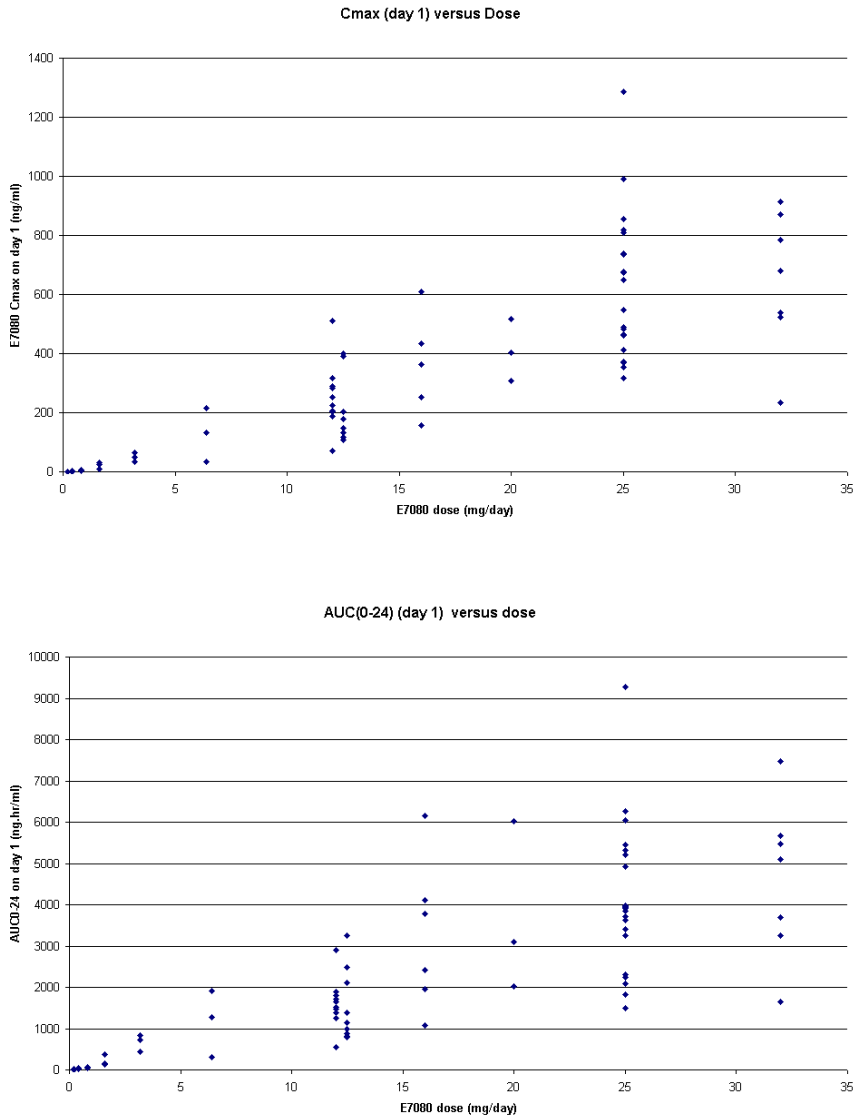
Parameters	E7080 Dose											
	0.2 mg (n=2)	0.4 mg (n=3)	0.8 mg (n=2)	1.6 mg (n=3)	3.2 mg (n=3)	6.4 mg (n=3)	12 mg (n=9)	12.5 mg (n=7)	16 mg (n=6)	20 mg (n=1)	25 mg (n=15)	32 mg (n=4)
doses of E7080	2.2	3.0	3.0	3.0	2.5	2.0	1.5	2.0	2.5	3.0	2.5	1.5
Tmax	(2.0-2.5)	(2.0-3.0)	(3.0-3.0)	(1.0-3.1)	(1.5-2.5)	(1.8-2.6)	(1.0-5.0)	(1.0-2.5)	(1.0-3.0)	3.0	(1.1-4.9)	(1.0-2.0)
Cmax	2.4	4.9	9.1	33.6	104.5	173.6	314.6	160.4	350.6	480.3	564.0	564.0
(ng/ml)	(2.0-2.8)	(4.3-7.3)	(7.0-11.3)	(27.3-48.6)	(59.0-112.9)	(73.8-344.2)	(70.7-519.9)	(119.3-372.5)	(193.4-599.2)	238.7	(279.5-1068.1)	(418.3-703.3)
AUC _{0-∞}	43.7	65.0	202.7	409.4	1041.3	1587.8	2228.6	1173.6	3133.5	4626.5	4709.8	4709.8
(ng*hr/ml)	(37.5-49.9)	(64.3-130.8)	a	(179.8-731.9)	(772.1-1128.6)	(664.1-3181.8)	(962.1-3094.6)	(987.6-3111.9)	(1364.3-5035.8)	2031.7	(1642.1-6615.3)	(2915.8-4882.8)
T _{1/2}	29.5	25.3	12.2	10.1	10.1	8.5	6.9	6.6	6.8	6.0	6.7	6.7
(hr)	(23.7-35.4)	(19.0-34.9)	20.8a	(4.8-15.6)	(8.6-11.2)	(7.8-8.8)	(5.1-9.0)	(5.4-8.4)	(5.8-8.3)	8.1	(4.6-8.1)	(6.5-7.3)
Cl/F	4.7	6.2	3.9	3.1	3.1	4.0	5.4	10.7	5.1	5.4	6.8	6.8
(l/hr)	(4.0-5.3)	(3.1-6.2)	4.0a	(2.2-8.9)	(2.8-4.1)	(2.0-9.6)	(3.6-12.5)	(4.0-12.0)	(2.8-11.7)	9.8	(3.8-15.2)	(5.2-11.0)
V/F	204.9	226.9	118.7	61.0	41.2	51.0	51.4	98.0	50.3	51.7	68.1	68.1
(l)	(137.1-272.7)	(83.6-310.2)	a	(38.3-88.0)	(38.3-67.1)	(22.5-117.7)	(29.6-124.4)	(40.3-146.1)	(33.7-97.4)	115.0	(28.7-102.0)	(50.3-103.3)

Pharmacokinetic parameters derived after 4 weeks of treatment with E7080.

a n=1

on the T_{max} , shifting from 2h post dose in the fasted group to 5h post dose in the fed group (median values; $p = 0.0025$).

Figure 1: Dose versus C_{max} concentrations of E7080 in plasma (upper), and dose versus exposure (AUC_{0-24}) to E7080 (lower).



Anti-tumor activity

A total of 63 patients was evaluable for at least 1 response assessment in the course of treatment. In total, 6 patients achieved a confirmed partial response, lasting from 4 to 20 cycles of treatment. The partial responses were observed in patients with renal cell carcinoma (3 patients), melanoma (2 patients), and soft tissue sarcoma (1 patient). In addition, two patients, one with nasopharynx carcinoma and one with ovarian carcinoma, also developed a >30% reduction in tumor volume. However, this could not be confirmed in a subsequent evaluation. The partial responses observed in the patients with renal cell carcinoma lasted 4, 4, and 18 cycles respectively, and the latter two were still in partial remission at the time of the database lock. Forty patients (50%) had stable disease as best response, and several patients remained on study for a long period of time. This includes a patient at 12.5 mg with epitheloid haemangioendothelioma who remained on study for 33 cycles, and was still ongoing at the time of the database lock. The observed responses in patients with melanoma and renal cell carcinoma are shown in figure 2. CT images of responding patients are shown in figure 3.

Table 6: Treatment duration and response according to RECIST

Dose level (mg/day)	No of patients	Duration in weeks (median, range)	Best Response			
			PR	SD	PD	NE
0.2-6.4	21	7 (0-87)	0 (0%)	7 (33%)	6 (29%)	8 (38%)
12-20	28	15 (0-131)	2 (7%)	15 (54%)	7 (25%)	4 (14%)
25	24	22 (1-57)	2 (8%)	16 (67%)	2 (8%)	4 (17%)
32	7	38 (0-67)	2 (29%)	4 (57%)	0 (0%)	1 (14%)
Total	80	14 (0-131)	6 (8%)	42 (53%)	15 (19%)	17 (21%)

Discussion

This report describes the results of a first-in-man study with E7080, a novel multi-kinase inhibitor. The MTD was set at 25 mg daily administration of E7080, and encouraging anti-tumor activity was observed in patients with renal cell carcinoma and melanoma.

Among the most profound adverse events in this study were hypertension and proteinuria, which are common side-effects for agents targeting angiogenesis

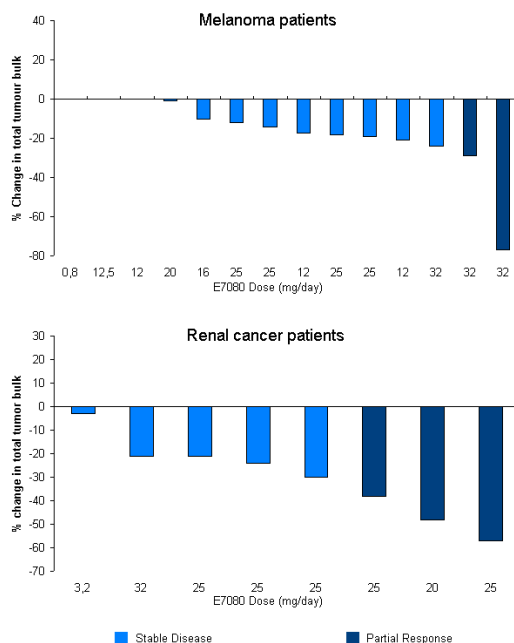


Figure 2: Waterfall plots representing changes in tumor size in patients with melanoma and renal cell carcinoma.

(13). The incidence of hypertension (36.3 % overall) was, although higher, in line with other studies where drugs targeting the VEGF-signaling pathway were evaluated (14). The incidence of proteinuria in this study was much higher compared with studies done with sorafenib and sunitinib, agents that target similar pathways (15,16). The incidence was 22.5 % overall, which is comparable with the incidence in clinical trials of bevacizumab (17). Extensive research has been done to explain the mechanistic background of hypertension and proteinuria after treatment with angiogenesis inhibitors, and the effects can be largely attributed to the blockade of VEGFR-2 signaling. It has been shown that VEGFR-2 signaling stimulates the production of mediators of vasodilatation, including nitric oxide (NO) and prostacyclin (PGI₂). A reduced level of these molecules results in an increase in vascular resistance, and thereby an increase in blood pressure (14,18). Proteinuria may be the consequence of treatment-induced hypertension, since it is known that there is a strong correlation between blood pressure and the development of proteinuria (19). But it is also known that VEGF has a direct cytoprotective

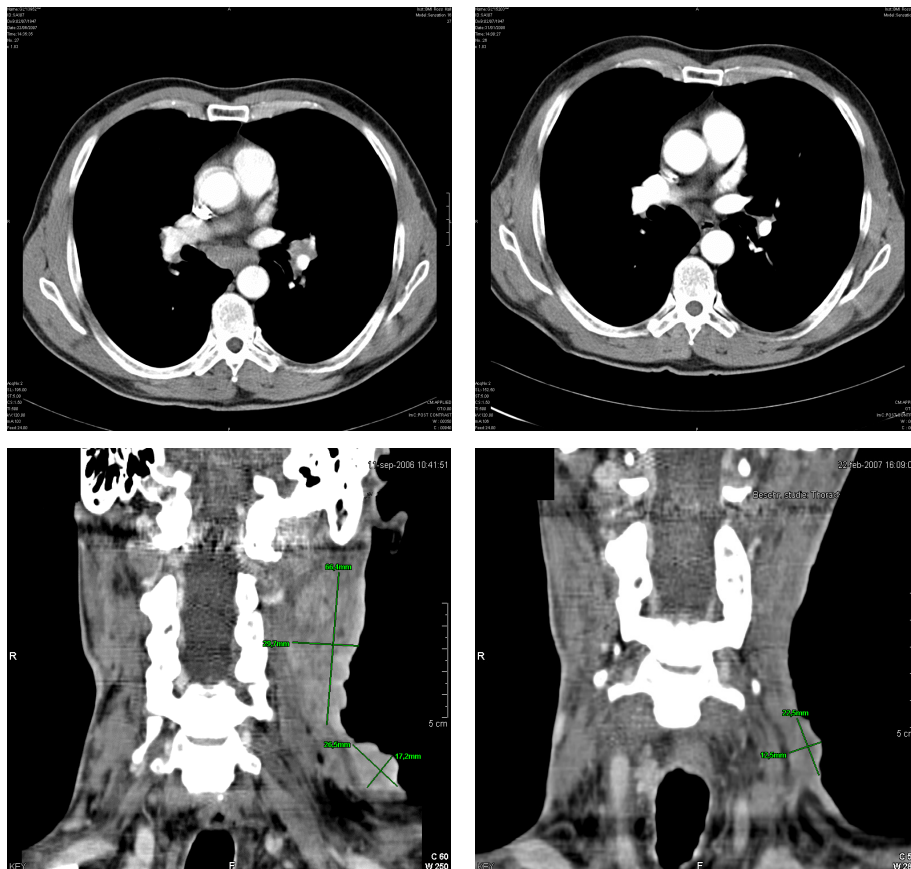


Figure 3: CT Scans of patients treated with E7080. Upper figures: CT evaluations of a patient with metastatic melanoma before (left) and after (right) 8 cycles (32 weeks) of treatment with E7080. This patient had an overall reduction in total tumor burden of 73%. Lower figures: CT evaluations of a patient with a nasopharynx carcinoma, before (left) and after (right) 6 cycles (24 weeks) of treatment with E7080. This patient had an overall reduction in total tumor burden of 41 %.

effect on endothelial cells, thereby maintaining the integrity of the glomerular filtration barrier. In this way, blocking VEGF signaling can also cause proteinuria independent of hypertension (14).

In this study, the treatment of patients who presented with hypertension and proteinuria was interrupted until recovery, and antihypertensive drugs were prescribed to minimize these toxicities from the moment of their first occurrence (diastolic blood pressure ≥ 100 mg Hg). The prescribed drugs included calcium-antagonists, Beta-blockers, ACE-inhibitors, and diuretics. Generally, the hypertension and proteinuria were well controlled by these

medications, and the patients could continue treatment at the same dose-level, although some patients required a dose-reduction before continuing treatment.

Gastrointestinal toxicities, including nausea, diarrhea, vomiting and stomatitis were also frequently observed in this study, although the severity was mostly limited to grade 1-2 toxicities. Stomatitis was frequently observed at the higher dose-levels, and in many cases lead to dose reductions and dose delays. Stomatitis is a toxicity that is commonly observed after treatment with angiogenesis inhibitors. Unfortunately, there is no adequate treatment for this problem. The patients in this study who reported stomatitis complained of pain in the mouth, especially when eating food. Moreover, taste alterations, and irritation and redness of the oral mucosa during and shortly after tooth brushing, were reported. The phenotype of this irritation closely resembles an allergic reaction, and to confirm this, a biopsy was taken from the tongue of a patient reporting these problems, shortly after she brushed her teeth. However, no abnormalities in the epithelial lining the tongue tissue, and no infiltration of eosinophil granulocytes in the underlining stroma, were found. The underlying mechanism of mucositis following treatment with angiogenesis inhibitors remains unclear (20).

Another side-effect that was observed in this trial, also more frequently at the higher doses, was hoarseness. This side-effect, albeit inconvenient for the patients, did not lead to dose reductions or dose delays. As with the stomatitis, hoarseness is commonly observed after treatment with angiogenesis inhibitors, but the etiology is unknown (20). The incidence of myelosuppression was very low (8 % overall), although two patients experienced hematological toxicities that were considered DLTs (grade 3 febrile neutropenia and grade 4 thrombocytopenia, respectively). It must be noted that these patients were very heavily pretreated, which possibly affected their bone marrow reserve prior to entry in this trial. The occurrence of thrombocytopenia is also observed after treatment with sunitinib (15), but not after treatment with sorafenib (16).

Pharmacokinetic analyses of E7080 revealed dose linearity, and an elimination half-life that was much shorter than those observed for the comparable agents sorafenib and sunitinib (15,21). Consequently, no drug accumulation was observed after 4 weeks of once-daily E7080 administration. These data

suggest that bi-daily dosing of E7080 might be a feasible strategy, and more research to investigate this is warranted.

Regarding the observed anti-tumor activity, 60 % of all patients derived clinical benefit (PR + SD) following treatment with E7080. This is a high percentage, especially for an unselected phase I population. The observed response-rates depended on the administered dose of E7080, with an increase in observed partial responses, and a decrease in progressive disease as best response, at the higher dose-levels. Special attention must be given to the observed responses in patients with melanoma (2 partial responses) and renal cell carcinoma (3 partial responses). As can be seen in the waterfall plots, none of the patients with these malignancies had an increase in tumor volume as best response during treatment with E7080, indicating the activity of the drug in these patients. The preliminary activity of E7080 in patients with renal cell cancer could be expected, since sorafenib and sunitinib, agents with comparable drug targets, are both registered for this indication (22,23). The preliminary activity of E7080 in patients with melanoma was less expected. As a single agent, sorafenib failed to demonstrate activity in patients with melanoma. This was disappointing, since a large proportion of melanomas carry a BRAF mutation, and sorafenib is known to inhibit both wild-type and mutated (V600E) BRAF (24). E7080 does not target BRAF, and therefore activity against melanoma was not expected, at least not at the level observed in this study.

The observed dose-dependent increase in hypertension, proteinuria and stomatitis following treatment with E7080 represent a significant problem when considering an advised phase II dose for E7080. There was a high number of dose-reductions and dose-delays at the MTD of 25 mg (91.7% and 83.3% during all cycles, respectively), suggesting that a lower dose is favorable for further development. However, there also appeared to be a relationship between the dose-levels and the likelihood of developing tumor response, and not all patients treated at 25 mg needed a dose reduction in the course of treatment. A recent study, presented at ASCO 2009, showed that patients with higher diastolic blood pressure levels (≥ 90 mm Hg) during treatment with axitinib responded better than patients with maximal blood pressure levels below 90 mm Hg (25). Evaluating E7080 in phase II studies at a lower dose will most probably lead to lower response rates. Moreover, the lower dose-levels in this study were not associated with reduced numbers of

dose-reductions or dose-delays (76.2% of the patients treated at doses between 0.2 and 6.4 mg had a dose-reduction, and an equal percentage a dose-delay). We therefore suggest a phase II starting dose of 25 mg/day. Patients who develop hypertension or proteinuria in the course of treatment should be adequately treated with antihypertensive drugs, just as we did in this study, and continue on the same dose if possible. In the case of stomatitis or other toxicities that can not be adequately treated, dose-reductions will be inevitable.

In conclusion, this study demonstrates that E7080 can be safely administered to patients with advanced solid tumors up to doses of 25 mg/day. The most prominent toxicities were dose-limiting proteinuria, hypertension, and gastrointestinal complaints. Compelling anti-tumor activity was observed in patients with melanoma and renal cell carcinoma. The results obtained in this study form an excellent basis for future phase II and probably phase III trials with this compound.

References

1. Ferrara, N., Gerber, H. P., and LeCouter, J. The biology of VEGF and its receptors. *Nat.Med.* 2003;9:669-676.
2. Gasparini, G. Prognostic value of vascular endothelial growth factor in breast cancer. *Oncologist.* 2000;5 Suppl 1:37-44.
3. Ishigami, S. I., Arij, S., Furutani, M.et al. Predictive value of vascular endothelial growth factor (VEGF) in metastasis and prognosis of human colorectal cancer. *Br.J.Cancer.* 1998;78:1379-1384.
4. Fontanini, G., Vignati, S., Boldrini, L.et al. Vascular endothelial growth factor is associated with neovascularization and influences progression of non-small cell lung carcinoma. *Clin.Cancer Res.* 1997;3:861-865.
5. Folkman, J. Anti-angiogenesis: new concept for therapy of solid tumors. *Ann.Surg.* 1972;175:409-416.
6. Hurwitz, H., Fehrenbacher, L., Novotny, W.et al. Bevacizumab plus irinotecan, fluorouracil, and leucovorin for metastatic colorectal cancer. *N.Engl.J.Med.* 2004;350:2335-2342.
7. Reck, M., von Pawel, J., Zatloukal, P.et al. Phase III trial of cisplatin plus gemcitabine cancer: AVAIL. *J.Clin.Oncol.* 2009;27:1227-1234.
8. Motzer, R. J., Hutson, T. E., Tomczak, P.et al. Sunitinib versus interferon alfa in metastatic renal-cell carcinoma. *N.Engl.J.Med.* 2007;356:115-124.
9. Escudier, B., Eisen, T., Stadler, W. M.et al. Sorafenib in advanced clear-cell renal-cell carcinoma. *N.Engl.J.Med.* 2007;356:125-134.
10. Matsui, J., Yamamoto, Y., Funahashi, Y.et al. E7080, a novel inhibitor that targets multiple kinases, has potent antitumor activities against stem cell factor producing human small cell lung cancer H146, based on angiogenesis inhibition. *Int.J.Cancer.* 2008;122:664-671.
11. Matsui, J., Funahashi, Y., Uenaka, T.et al. Multi-kinase inhibitor E7080 suppresses lymph node and lung metastases of human mammary breast tumor MDA-MB-231 via inhibition of vascular endothelial growth factor-receptor (VEGF-R) 2 and VEGF-R3 kinase. *Clin.Cancer Res.* 2008;14:5459-5465.
12. Therasse, P., Arbuck, S. G., Eisenhauer, E. A.et al. New guidelines to evaluate the response to treatment in solid tumors. European Organization for Research and

- Treatment of Cancer, National Cancer Institute of the United States, National Cancer Institute of Canada. *J.Natl.Cancer Inst.* 2000;92:205-216.
13. Launay-Vacher, V. and Deray, G. Hypertension and proteinuria: a class-effect of antiangiogenic therapies. *Anticancer Drugs.* 2009;20:81-82.
 14. Roodhart, J. M., Langenberg, M. H., Witteveen, E.et al. The molecular basis of class side effects due to treatment with inhibitors of the VEGF/VEGFR pathway. *Curr.Clin.Pharmacol.* 2008;3:132-143.
 15. Faivre, S., Delbaldo, C., Vera, K.et al. Safety, pharmacokinetic, and antitumor activity of SU11248, a novel oral multitarget tyrosine kinase inhibitor, in patients with cancer. *J.Clin.Oncol.* 2006;24:25-35.
 16. Strumberg, D., Awada, A., Hirte, H.et al. Pooled safety analysis of BAY 43-9006 (sorafenib) monotherapy in patients with advanced solid tumours: Is rash associated with treatment outcome? *Eur.J.Cancer.* 2006;42:548-556.
 17. Kamba, T. and McDonald, D. M. Mechanisms of adverse effects of anti-VEGF therapy for cancer. *Br.J.Cancer.* 2007;96:1788-1795.
 18. Verheul, H. M. and Pinedo, H. M. Possible molecular mechanisms involved in the toxicity of angiogenesis inhibition. *Nat.Rev.Cancer.* 2007;7:475-485.
 19. K/DOQI clinical practice guidelines on hypertension and antihypertensive agents in chronic kidney disease. *Am.J.Kidney Dis.* 2004;43:S1-290.
 20. Eskens, F. A. and Verweij, J. The clinical toxicity profile of vascular endothelial growth factor (VEGF) and vascular endothelial growth factor receptor (VEGFR) targeting angiogenesis inhibitors; a review. *Eur.J.Cancer.* 2006;42:3127-3139.
 21. Moore, M., Hirte, H. W., Siu, L.et al. Phase I study to determine the safety and pharmacokinetics of the novel Raf kinase and VEGFR inhibitor BAY 43-9006, administered for 28 days on/7 days off in patients with advanced, refractory solid tumors. *Ann.Oncol.* 2005;16:1688-1694.
 22. Escudier, B., Eisen, T., Stadler, W. M.et al. Sorafenib for Treatment of Renal Cell Carcinoma: Final Efficacy and Safety Results of the Phase III Treatment Approaches in Renal Cancer Global Evaluation Trial. *J.Clin.Oncol.* 2009;
 23. Motzer, R. J., Hutson, T. E., Tomczak, P.et al. Overall Survival and Updated Results for Sunitinib Compared With Interferon Alfa in Patients With Metastatic Renal Cell Carcinoma. *J.Clin.Oncol.* 2009;
 24. Eisen, T., Ahmad, T., Flaherty, K. T.et al. Sorafenib in advanced melanoma: a Phase II randomised discontinuation trial analysis. *Br.J.Cancer.* 2006;95:581-586.
 25. Rixe, O., Dutcher, K., Motzer, R.et al. Diastolic blood pressure (dBp) and pharmacokinetics (PK) as predictors of axitinib efficacy in metastatic renal cell cancer (mRCC). *J.Clin.Oncol.* 2009;27:Abstr. 5045-

CHAPTER 7.2

Serum β -HCG and CA-125 as tumor-markers in a patient with osteosarcoma: A case report

David S. Boss, Hilary Glen, Jos H. Beijnen, Daphne de Jong,
Jantien Wanders, Jeff T. R. Evans, Jan H.M. Schellens

Abstract

Introduction: Elevated β -HCG serum levels are usually an indication of pregnancy, or pregnancy related disorders, but can also be elevated in testis and germ cell tumors. HCG expression by osteosarcoma is a rare phenomenon, with a few documented cases. CA-125 is commonly used to monitor disease progress and treatment response in ovarian cancer. CA-125 expression in patients with osteosarcoma has not previously been documented.

Case report: Elevated β -HCG and CA-125 serum levels were observed in a female patient of 57 years of age with metastatic osteosarcoma during screening investigations prior to participation in a phase I clinical trial. Pregnancy was excluded. Immunohistochemical studies revealed the tumor to be the source of the elevated β -HCG serum levels. We found no CA-125 expression in tumor tissue. The patient was treated with E7080, a novel oral multi-targeted tyrosine kinase inhibitor. We measured serum β -HCG and CA-125 to monitor treatment response. She had a significant clinical and radiological response after 2 cycles of treatment, but developed progressive disease after the third cycle. The β -HCG serum levels seemed to better reflect her disease status than the other tumor marker CA-125.

Conclusion: When elevated, β -HCG serum levels in patients with osteosarcoma might be used to monitor treatment. Treatment of advanced osteosarcoma with tyrosine kinase inhibitors, including E7080, warrants further investigation.

Introduction

Human chorionic gonadotropin (HCG) and Cancer Antigen (CA)-125 are widely used as tumor markers in the management of malignant disease. HCG is a glycoprotein hormone that is synthesized by syncytiotrophoblasts in the placenta of pregnant women, starting 6 days after conception (1). It comprises a non-specific α subunit, which is shared with other pituitary hormones, and a specific β subunit. Elevated β -HCG serum levels are valuable in the diagnosis of pregnancy and pregnancy related disorders (2), but have also been observed in non-gestational disorders, including various forms of cancer (3). CA-125 is a high molecular weight membrane glycoprotein of unknown function. CA-125 serum levels are elevated in approximately 80% of patients with advanced stage epithelial ovarian cancer and are routinely used to monitor disease activity and treatment response in patients with ovarian cancer (4). Elevated CA-125 serum levels have also been observed in other malignancies, including mesothelioma (5), leukemia (6), non-Hodgkin's lymphoma (7) and breast cancer (8). Rarely, serum CA-125 can also be elevated in non-malignant disorders (9,10).

Osteosarcoma is the most common primary malignant tumor of bone with the most frequent presentation during the second and third decades of life. Osteosarcomas are highly aggressive tumors with high metastatic potential and are characterized by metastases primarily located in the lungs. The prognosis of osteosarcoma has improved significantly following the introduction of chemotherapy in the 1970s. The current standard of care for patients without metastasis includes radical surgery and adjuvant chemotherapy with cisplatin, doxorubicin and high-dose methotrexate, resulting in about 70% long-term disease-free survival (11). However, the prognosis for patients with metastatic osteosarcoma remains poor, with a 5-year survival rate of only 20% (12). There is no universally-accepted, standard of care, therapy regimen for patients with disease which is resistant to standard chemotherapy regimens (13).

Secretion of β -HCG by osteosarcomas is very uncommon, with only a few documented cases in the published literature (14). In contrast, we are not aware of any documented cases of secretion of CA-125 by osteosarcomas. In this report, we present the case of a patient with metastatic osteosarcoma who was found to have elevated serum levels of β -HCG and CA-125 during

screening investigations prior to participation in a phase I clinical trial,, and speculate on their potential use as markers of disease progression and treatment response in patients with osteosarcoma. .

Case report

A 57 year old woman initially presented in May 2006 with an osteosarcoma of the left femur with bilateral multiple pulmonary metastases. Following neo-adjuvant chemotherapy with doxorubicin and cisplatin (2 cycles) the primary tumour was resected in October 2006. She developed pulmonary metastases in December 2006, treated initially with palliative ifosfamide and etoposide (2 cycles) and subsequently with an experimental regimen comprising cyclophosphamide and imatinib (2 cycles). In July 2007, she underwent screening investigations prior to participation in a phase I clinical trial of the multi-targeted oral tyrosine kinase inhibitor, E7080. This study had been approved by the Research Ethics Committee of the Netherlands Cancer Institute, and the patient gave written informed consent. Elevated serum β -HCG and serum CA-125 levels of 1340 IU/l and 461 kU/l, respectively, were observed during these investigations (figure 1). Serum β -HCG analysis had been performed to exclude pregnancy prior to participation in a clinical trial of an experimental anti-cancer agent. Serum CA-125 had been measured as part of a panel of tumor markers when the patient first attended our unit. Additional diagnostic tests were performed to exclude pregnancy and to determine the source of the β -HCG and CA-125 secretion. Immunohistochemical studies revealed the tumor to be the source of the elevated β -HCG. However, immunohistochemical studies could not explain the high CA-125 serum levels (figure 2).

She commenced treatment with E7080, a novel tyrosine kinase inhibitor, which targets VEGFR-2, PDGFR- β , FGFR-1 and C-KIT. E7080 was administered orally in a continuous once-daily schedule at a dose of 32 mg, with each cycle of treatment consisting of 28 days of treatment. After the first cycle of treatment the serum β -HCG level had decreased from 1340 to 982.7 IU/l, and the serum CA-125 had decreased from 461 kU/l at baseline to 45 kU/l. Repeat disease assessment by CT scanning following 2 cycles of treatment demonstrated a decrease of about 20 percent in the sum of the longest diameters of the target lesions (figure 3), with an associated significant clinical improvement. However, at the start of the third cycle the serum β -HCG level

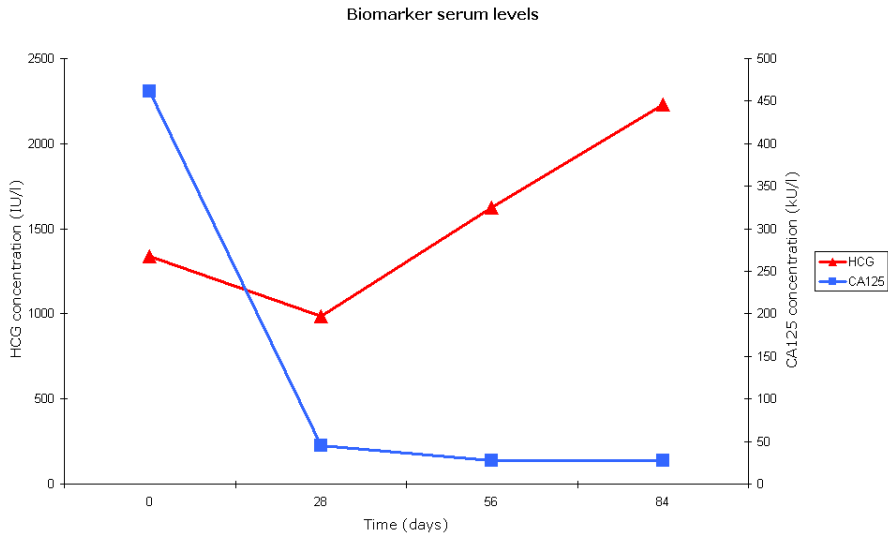


Figure 1: β -HCG and CA-125 serum concentrations during the course of experimental treatment with the multitargeted oral tyrosine kinase inhibitor E7080.

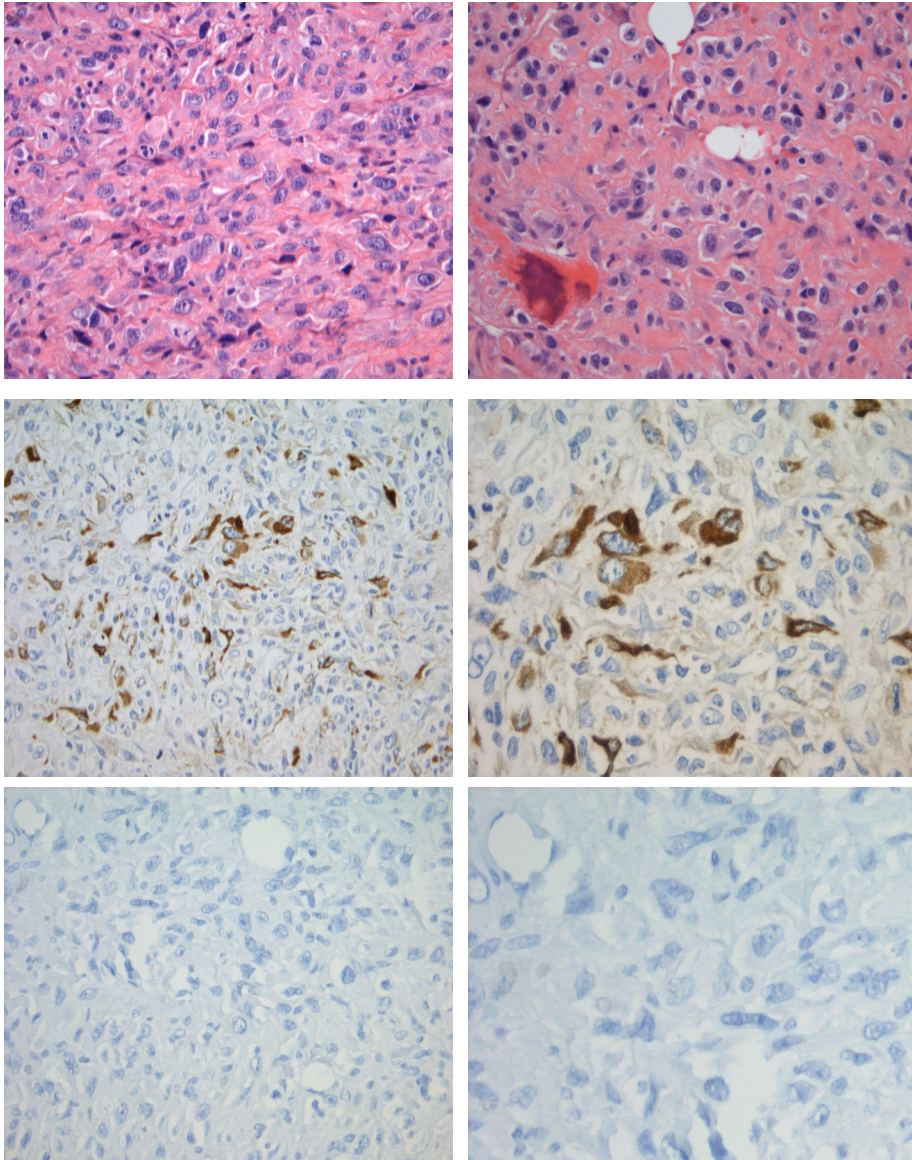
had increased to 1623 IU/l, while the CA-125 level continued to decrease to 28 kU/l. Study treatment was discontinued after 3 cycles due to clinical disease progression, which was confirmed by radiological (CT) disease assessment, with a further rise in the serum β -HCG to 2229 IU/l, although the CA-125 remained low (28 kU/l).

Discussion

To our knowledge, this is the first report of increased serum β -HCG and serum CA-125 levels in a patient with metastatic osteosarcoma. After initial commencement of treatment, both serum markers correlated with radiological regression of the tumor and with clinical benefit.. Subsequently, rising serum β -HCG levels also correlated with disease progression, although no such correlation was observed with serum CA-125 levels. Currently there are, no tumor markers of proven efficacy in the management of patients with osteosarcoma. Elevated serum β -HCG levels have been described in a number of patients with various malignancies, including osteosarcoma, and it has been shown in some of these cases that β -HCG serum levels can be used to monitor therapy (15). In the case we report here, we suggest that serum β -HCG, but

not CA-125, may be used to monitor disease progress and treatment response in patients with osteosarcoma who have elevated pre-treatment serum levels.

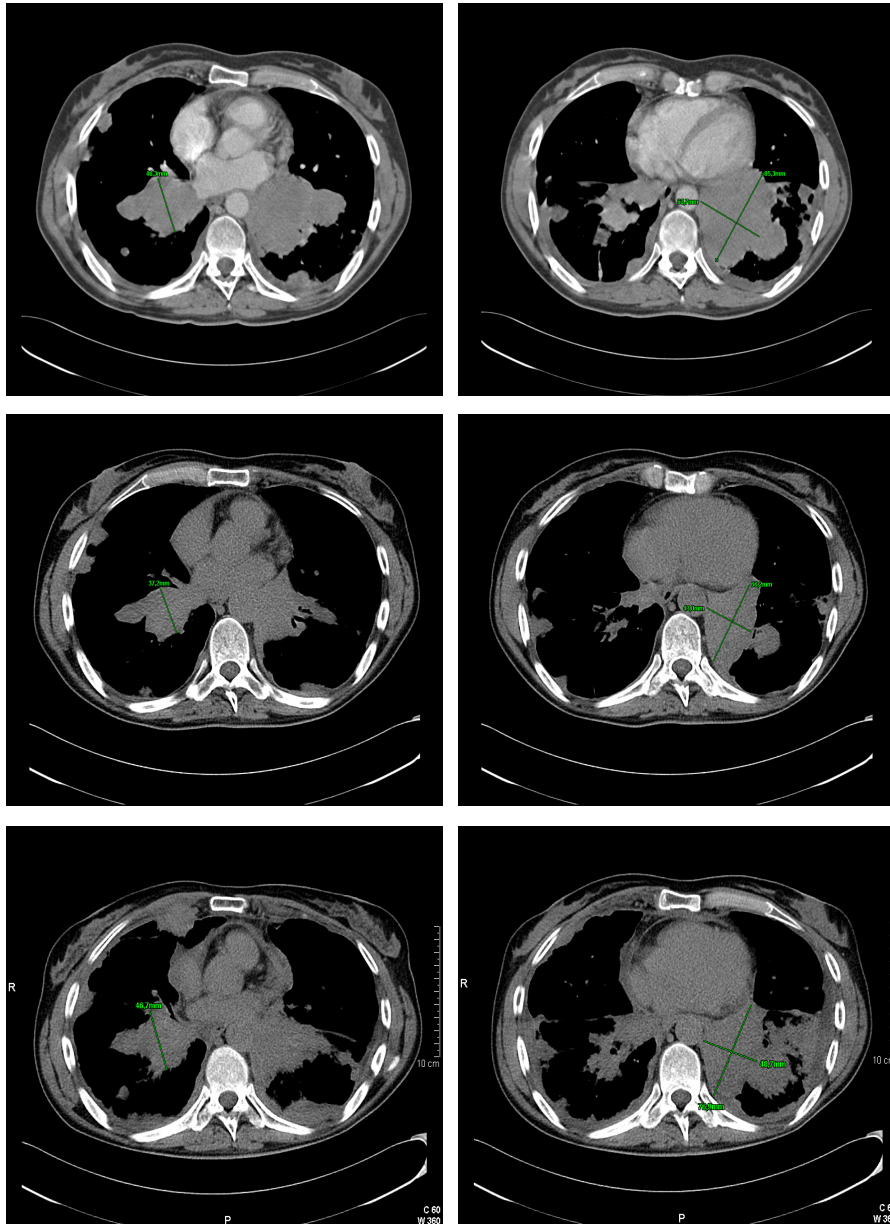
Figure 2: Immunohistochemical studies. The upper figures show osteosarcoma tumor sections stained with hematoxylin and eosin (H&E). The sections shown in the middle were stained for β -HCG. The brown spots clearly indicate β -HCG expression of the tumor tissue. The lower figures were stained for CA-125 expression. No CA-125 expression was observed in these sections. Left figures: Amplification 20X, right figures: Amplification 40X.



In our case, tumor expression of β -HCG, but not CA-125, was demonstrated by immunohistochemistry. However, these analyses were performed on the diagnostic tissue specimen which was collected in August 2006, almost one year before undergoing investigations prior to entering the phase I clinical trial of E7080. The serum CA-125 levels had increased significantly shortly before the patient entered the study (from 140 kU/l on the 11th of May 2007 to 461 kU/l at screening on the 5th of July 2007). Therefore, it is possible that tumor expression of CA-125, as determined by immunohistochemistry, may have been observed if further tumor biopsies had been taken at this time. Alternatively, sources other than the osteosarcoma might have caused the elevated CA-125 serum levels. Previously, it has been described that benign conditions including benign ascites, peritonitis and pelvis inflammatory disease can cause elevated CA-125 serum levels (16,17). Falsely elevated CA-125 serum levels have been reported in patients with CA-125 negative ovarian cancer (18) and, interestingly, in a patient with a CA-125 negative rhabdomyosarcoma (19). We found no non-malignant disorder in our patient that might have caused her CA-125 serum levels to be falsely elevated. Finally, discrepancies between CA-125 tumor staining and serum levels may be due to sensitivity problems of the immunohistochemical staining method in formalin-fixed and paraffin embedded tissue, as previously described (20).

Our patient was treated with E7080, an orally active small molecule tyrosine kinase inhibitor targeting VEGFR-2, PDGFR- β , FGFR-1 and C-KIT (21,22). This is of interest, since osteosarcomas are known to be hypervascular tumors (23). It has been shown that tumor VEGF-expression in patients with osteosarcoma correlates with a higher incidence of developing pulmonary metastases and worse overall and disease free outcome (24). Another study in patients with non-metastatic osteosarcoma also found an increased metastatic potential and a poorer prognosis in patients in whom the tumors overexpressed VEGF165, a splice variant of VEGF-A, compared with patients with VEGF165-negative tumors. However, there was no correlation between tumor VEGFR expression and survival in this study (25). The relationship between tumor VEGF expression and patient age was investigated by another group, since older patients (older than 40 years) with osteosarcoma have a poorer prognosis compared to younger patients. No relationship was found between the degree of VEGF expression and patient age (26).

Figure 3: CT scans of lung metastases before and after 2 cycles of treatment with E7080. Upper figures: baseline scans. Middle figures: Scans made after 2 cycles (56 days) of treatment. Lower figures: Scans made after 3 cycles (84 days). The scans show a good initial response to E7080, with reductions in tumor size of the indicated lesions. The patient progressed after 3 cycles of treatment. The longest diameter of the lesions indicated on the left changed from 46 mm at baseline to 37 mm after 2 cycles, and 47 mm after 3 cycles. The lesions indicated on the right changed from 85x64 mm at baseline to 66x43 mm after 2 cycles, and 77x49 mm after 3 cycles.



The importance of the VEGFR pathway for osteosarcoma growth raises the opportunity for therapeutic intervention with angiogenesis inhibitors. Several strategies might be employed in the near future, including antibodies targeting VEGF (bevacizumab), or small molecules targeting VEGFR (sunitinib, sorafenib or E7080). Our patient had a good initial response to treatment with E7080. Her physical condition improved, which coincided with radiological regression after two cycles of treatment. This was encouraging given her poor response to previous treatment regimens. Previously, she had progressed after two cycles of ifosfamide/etoposide and also after two cycles of cyclophosphamide/imatinib, the latter combination in an experimental protocol. The initial response to treatment of our patient was accompanied by a decline in β -HCG and CA-125 serum levels, possibly due to a direct effect of E7080 on the tumor cells. However, her β -HCG serum levels started to increase again after four weeks of therapy. This might be the result of tumor resistance to E7080 treatment. Interestingly, her CA-125 remained low, which might be explained by the heterogeneity of the tumor. We speculate that the tumor cells responsible for β -HCG production became resistant to E7080 treatment, while the CA-125 producing tumor cells remained sensitive. The mechanism by which the cells became resistant remains to be elucidated. The rapid surge in β -HCG levels is most likely due to an increased number of β -HCG producing tumor cells (tumor growth), but can also result from an increased β -HCG production per tumor cell. It has been shown that β -HCG is directly involved in the promotion of angiogenesis by increasing capillary formation and migration of endothelial cells. This effect might be the result of an HCG-induced increase in VEGF expression (27). We hypothesize that blocking the VEGF pathway by E7080 might induce the tumor cells to secrete more β -HCG, leading to increased VEGF production. However, we cannot confirm this hypothesis, as circulating VEGF levels were not measured during the course of therapy.

In conclusion, we present a rare case of a patient with a β -HCG-producing metastatic osteosarcoma in whom β -HCG serum levels seemed to better reflect the disease status than serum CA-125. Treatment of advanced osteosarcoma with angiogenesis inhibitors like E7080 warrants further investigation.

References

1. Keay, S. D., Vatish, M., Karteris, E. et al. The role of hCG in reproductive medicine. *BJOG*. 2004;111:1218-1228.
2. Fiala, C., Safar, P., Bygdeman, M. et al. Verifying the effectiveness of medical abortion; ultrasound versus hCG testing. *Eur.J.Obstet.Gynecol.Reprod.Biol.* 2003;109:190-195.
3. Demirtas, E., Krishnamurthy, S., and Tulandi, T. Elevated serum beta-human chorionic gonadotropin in nonpregnant conditions. *Obstet.Gynecol.Surv.* 2007;62:675-679.
4. Bast, R. C., Jr., Badgwell, D., Lu, Z. et al. New tumor markers: CA125 and beyond. *Int.J.Gynecol.Cancer.* 2005;15 Suppl 3:274-281.
5. Hedman, M., Arnberg, H., Wernlund, J. et al. Tissue polypeptide antigen (TPA), hyaluronan and CA 125 as serum markers in malignant mesothelioma. *Anticancer Res.* 2003;23:531-536.
6. de Larrea, C. F., Cibeira, M. T., Vallansot, R. et al. Increased serum tumor markers (CA125 and CA15.3) in primary plasma cell leukemia: a case report and review of the literature. *Clin.Lymphoma Myeloma.* 2008;8:312-314.
7. Dilek, I., Ayakta, H., Demir, C. et al. CA 125 levels in patients with non-Hodgkin lymphoma and other hematologic malignancies. *Clin.Lab Haematol.* 2005;27:51-55.
8. Leonard, G. D., Low, J. A., Berman, A. W. et al. CA 125 elevation in breast cancer: a case report and review of the literature. *Breast J.* 2004;10:146-149.
9. Goonewardene, T. I., Hall, M. R., and Rustin, G. J. Management of asymptomatic patients on follow-up for ovarian cancer with rising CA-125 concentrations. *Lancet Oncol.* 2007;8:813-821.
10. Sevinc, A., Adli, M., Kalender, M. E. et al. Benign causes of increased serum CA-125 concentration. *Lancet Oncol.* 2007;8:1054-1055.
11. Chou, A. J. and Gorlick, R. Chemotherapy resistance in osteosarcoma: current challenges and future directions. *Expert.Rev.Anticancer Ther.* 2006;6:1075-1085.
12. Lamoureux, F., Trichet, V., Chipoy, C. et al. Recent advances in the management of osteosarcoma and forthcoming therapeutic strategies. *Expert.Rev.Anticancer Ther.* 2007;7:169-181.
13. Sakamoto, A. and Iwamoto, Y. Current status and perspectives regarding the treatment of osteo-sarcoma: chemotherapy. *Rev.Recent Clin.Trials.* 2008;3:228-231.
14. Leidinger, B., Bielack, S., Koehler, G. et al. High level of beta-hCG simulating pregnancy in recurrent osteosarcoma: case report and review of literature. *J.Cancer Res.Clin.Oncol.* 2004;130:357-361.
15. Leidinger, B., Bielack, S., Koehler, G. et al. High level of beta-hCG simulating pregnancy in recurrent osteosarcoma: case report and review of literature. *J.Cancer Res.Clin.Oncol.* 2004;130:357-361.
16. Goonewardene, T. I., Hall, M. R., and Rustin, G. J. Management of asymptomatic patients on follow-up for ovarian cancer with rising CA-125 concentrations. *Lancet Oncol.* 2007;8:813-821.
17. Sevinc, A., Adli, M., Kalender, M. E. et al. Benign causes of increased serum CA-125 concentration. *Lancet Oncol.* 2007;8:1054-1055.
18. Tholander, B., Lindgren, A., Taube, A. et al. Immunohistochemical detection of CA-125 and carcinoembryonic antigen in ovarian tumors in relation to corresponding preoperative serum levels. *Int.J.Gynecol.Cancer.* 1992;2:263-270.
19. Holcomb, K., Francis, M., Ruiz, J. et al. Pleomorphic rhabdomyosarcoma of the uterus in a postmenopausal woman with elevated serum CA125. *Gynecol.Oncol.* 1999;74:499-501.
20. Tholander, B., Lindgren, A., Taube, A. et al. Immunohistochemical detection of CA-125 and carcinoembryonic antigen in ovarian tumors in relation to corresponding preoperative serum levels. *Int.J.Gynecol.Cancer.* 1992;2:263-270.
21. Matsui, J., Yamamoto, Y., Funahashi, Y. et al. E7080, a novel inhibitor that targets multiple kinases, has potent antitumor activities against stem cell factor producing human small cell lung cancer H146, based on angiogenesis inhibition. *Int.J.Cancer.* 2008;122:664-671.
22. Matsui, J., Funahashi, Y., Uenaka, T. et al. Multi-kinase inhibitor E7080 suppresses lymph node and lung metastases of human mammary breast tumor MDA-MB-231 via inhibition of vascular endothelial growth factor-receptor (VEGF-R) 2 and VEGF-R3 kinase. *Clin.Cancer Res.* 2008;14:5459-5465.

23. Ek, E. T., Ojaimi, J., Kitagawa, Y. et al. Does the degree of intratumoural microvessel density and VEGF expression have prognostic significance in osteosarcoma? *Oncol.Rep.* 2006;16:17-23.
24. Kaya, M., Wada, T., Akatsuka, T. et al. Vascular endothelial growth factor expression in untreated osteosarcoma is predictive of pulmonary metastasis and poor prognosis. *Clin.Cancer Res.* 2000;6:572-577.
25. Lee, Y. H., Tokunaga, T., Oshika, Y. et al. Cell-retained isoforms of vascular endothelial growth factor (VEGF) are correlated with poor prognosis in osteosarcoma. *Eur.J.Cancer.* 1999;35:1089-1093.
26. Ek, E. T., Ojaimi, J., Kitagawa, Y. et al. Outcome of patients with osteosarcoma over 40 years of age: is angiogenesis a marker of survival? *Int.Semin.Surg.Oncol.* 2006;3:7-
27. Reisinger, K., Baal, N., McKinnon, T. et al. The gonadotropins: tissue-specific angiogenic factors? *Mol.Cell Endocrinol.* 2007;269:65-80.

8

**The pan-HER
inhibitor PF00299804**

CHAPTER 8.1

Phase I dose escalation study of the pan-HER inhibitor, PF00299804, in patients with advanced malignant solid tumors

David S. Boss, Carolyn Britten, Pasi Jannë, Ross Camidge, Feng Guo, Jos H. Beijnen, Steven Wong, Stephen Letrent, Robert Millham, Ian Taylor, Jan H. M. Schellens, Gail Eckhardt.

Abstract

Purpose: PF00299804 is a potent, orally available, irreversible inhibitor of the HER1, HER2, and HER4 tyrosine kinase receptors. This first-in-human study investigated the safety and tolerability, pharmacokinetics (PK), and pharmacodynamics (PD) of PF00299804 in patients with advanced solid malignancies.

Patients and methods: PF00299804 was administered once daily continuously (part A), and intermittently (part B). Dose escalation proceeded until the occurrence of unmanageable toxicities. Toxicities were monitored, and blood samples were drawn for pharmacokinetic analyses. Skin biopsies were taken predose, and after 14 days of treatment, to establish a PK/PD relationship. Tumor response was measured once every 2 cycles.

Results: A total of 121 patients was included (111 in schedule A and 10 in schedule B). The MTD was set at 45 mg daily, the DLTs included stomatitis and skin toxicities. Most adverse events were mild (grade 1-2), and consisted of skin toxicities, fatigue, and gastrointestinal side-effects, including diarrhea, nausea, and vomiting. Pharmacokinetic analyses revealed dose-dependent increase of exposure to PF00299804, and a long terminal half-life of 46 to 72 hours. A dose-dependent increase in target inhibition was observed in skin biopsy samples. Four patients, all with non-small cell lung cancer, had a partial response following treatment with PF00299804.

Conclusions: PF00299804 can be safely administered up to a dose of 45 mg/day. Both continuous and intermittent treatment schedules were well tolerated, and encouraging signs of anti-tumor activity were observed in patients with NSCLC. The recommended dose for phase 2 studies is 45 mg once daily at a continuous schedule.

Introduction

The HER family of receptor tyrosine kinases comprises four members: epidermal growth factor receptor (EGFR, also called HER-1 or erbB1), HER-2 (also called erbB2/neu), HER-3 (erbB3) and HER-4 (erbB4). Upon ligand binding and subsequent homo- or heterodimerization, the HER receptors trigger various intracellular signaling pathways involved in cell proliferation and differentiation (1,2). Abnormal HER signaling contributes to malignant transformation via increased cell proliferation, evasion of apoptosis, induction of angiogenesis and metastatic spread. The overexpression of HER-family members is observed in a wide variety of malignancies, including lung, colon, breast and bladder cancer. HER-1 and HER-2 have been validated as therapeutic targets in several human tumors, including colorectal cancer, non-small cell lung cancer, head and neck cancer, and breast cancer (3,4,5). PF00299804 is a potent and highly selective irreversible small molecule inhibitor of HER-1, HER-2 and HER-4 (6,7). PF00299804 offers potential advances in targeting HER signaling pathways in 2 ways. First, it achieves irreversible inhibition via covalent modification of nucleophilic cysteine residues in the catalytic domains of the HER receptors. Irreversible inhibitors have been shown to induce a prolonged suppression of tyrosine kinase activity compared with reversible inhibitors, leading to improved antitumor activity (8). Moreover, irreversible binding induces ubiquitination and degradation of the targeted receptors, a property not shared by reversible HER inhibitors (9). Recently, it was shown that resistance through the secondary T790M mutation is the result of an increased affinity of the EGFR receptor for ATP, thereby minimizing the competitive advantage of the reversible inhibitors. Irreversible inhibitors like PF0299804 have the potential to overcome this form of resistance (10). Another advantage of PF00299804, in addition to its mode of binding, is its activity against more members of the HER family. There are strong rationales for the development of pan-HER inhibitors, agents that inhibit all HER family members. First, this offers the potential for use against a wider range of tumor types, since many tumors express multiple HER family members (11). Moreover, patients with cancers overexpressing more than one family member have a significantly poorer outcome than those with tumors that overexpress just one family member (12,13). PF00299804 is a potent inhibitor of HER-1, HER-2 and HER-4, with IC₅₀ values determined of 6.0, 45.7 and 74.0 nM, respectively. The selectivity of PF00299804 for the HER family is at least 500-fold relative to other kinases involved in signal

transduction, including JAK3, AKT, IGF-1R, and CDKs (IC50 values 3566, >40,000, >40,000 and >40,000, respectively) (6). Furthermore, PF00299804 shows promising pharmacokinetic properties across species and has a higher bioavailability, a longer half-life, and a larger volume of distribution relative to CI-1033, a first generation irreversible pan-HER inhibitor (7). In this first-in-human study we investigated the safety and tolerability, pharmacokinetics (PK), and pharmacodynamics (PD) of PF00299804 in patients with advanced solid malignancies.

Methods

Study design and treatment

This was a multi-center, open-label, dose-escalation, phase I study, that was conducted in accordance with International Conference on Harmonization Good Clinical Practice guidelines and applicable local regulatory requirements and laws. During the dose-escalation period, PF00299804 was administered on an empty stomach (no food for 2 hours before or after drug administration) as continuous daily oral doses in 21-day cycles (schedule A). Dose escalation was based on the occurrence of dose-limiting toxicities (DLTs) during cycle 1: Accelerated dose escalation proceeded in 100% increments until 1 patient experienced DLT and/or 2 patients experienced the same drug-related adverse event (AE) during the first treatment cycle. From this point, dose escalation continued according to a modified Fibonacci scheme (67%, 50%, and 40% followed by 33% thereafter). If a DLT was observed in one of the three initial patients treated at a dose level, up to three additional patients were enrolled into that cohort. Dose escalation continued until at least two of the three to six patients treated at that dose level experienced a DLT. The next-lower dose level was considered to be the maximum tolerable dose (MTD). A DLT was defined as any of the following events as classified according to the Common Terminology Criteria for Adverse Events (CTCAE) version 3.0 which was attributed to PF00299804 and occurred during the first 21 days of treatment (cycle 1): Grade 3 or 4 nausea, vomiting, or diarrhea despite the use of adequate/maximal medical intervention and/or prophylaxis; any other Grade 3 or greater non-hematological toxicity; delayed recovery from toxicity related to treatment with PF00299804 which delays scheduled re-treatment for >14 days; Grade 4 neutropenia (absolute neutrophil count (ANC) <500 cells/mm³) for five or more consecutive days or febrile neutropenia (ie, fever >38.5°C

with ANC <1000 cells/mm³); Grade 4 thrombocytopenia (<25,000 platelets/mm³) or bleeding requiring a platelet transfusion.

Intra-patient dose escalation was permitted if maximum toxicity during prior cycles of therapy was ≤ grade 2 and three patients receiving the next higher dose level had completed 3 weeks of therapy without experiencing DLT.

Following the dose escalation portion of the trial, PF00299804 was evaluated in MTD expansion cohorts as follows: At a dose of 33% higher than the MTD on an intermittent dosing schedule (schedule B) comprising oral once daily dosing for 2 weeks followed by 1 week off therapy repeated in 21-day cycles; On schedule A MTD to investigate the effects of food on PF00299804 PK; On schedule A MTD to investigate the effects of stomach pH on PF00299804 PK; On schedule A combined with a loading dose of MTD BID for 3 days followed by once daily dosing for the rest of cycle 1, then subsequent cycles at once daily dosing. Additional patients from potential target populations were enrolled into schedule A MTD expansion cohorts, including patients with primary/metastatic tumors with HER-1/EGFR, HER-2 and/or HER-3 gene amplification and/or, for cases of non-small cell lung cancer (NSCLC), HER-1/EGFR and HER-2 mutations, and patients with RAS wildtype NSCLC resistant or refractory to erlotinib or gefitinib.

Study population

Adults ≥18 years of age with a histologically or cytologically confirmed malignant solid tumor unresponsive to currently available therapies and for which there is no currently approved treatment likely to be tolerated or acceptable were included in this study. Other criteria for inclusion were an Eastern Cooperative Oncology Group performance status (ECOG PS) of 0 or 1, adequate organ and hematological function and informed consent. Exclusion criteria included surgical procedure <4 weeks before starting study treatment; prior chemotherapy, radiotherapy, biological or investigational agents <4 weeks before starting study treatment (6 weeks for mitomycin C, nitrosoureas and liposomal doxorubicin), although inhibitors of EGFR could be continued for up to 2 weeks after initiation of PF00299804 therapy provided that treatment-related toxicity had resolved; prior high-dose chemotherapy requiring hematopoietic stem cell transplantation within 12 months of study entry, uncontrolled or significant cardiovascular disease, clinically significant abnormalities of the cornea and a history of non-medically manageable grade 3 or grade 4 toxicity related to treatment with an inhibitor of HER1/EGFR.

Patients with a requirement for treatment with H2 antagonists and /or proton pump inhibitors or drugs highly dependent on CYP2D6 for metabolism were also excluded from this study

Assessments

The primary endpoints of this study were the MTD, defined as the highest dose associated with DLTs in less than 33% of patients receiving PF00299804 administered on a continuous daily dosing (CDD) schedule as well as the safety and tolerability of continuous and intermittent daily dosing as assessed by monitoring AEs and laboratory abnormalities (according to CTCAE version 3.0). Monitoring of vital signs, ECG and laboratory analyses were performed at specific time points throughout the study. Left ventricular ejection fraction (LVEF) was determined at baseline and at the end of treatment. An ophthalmic slit lamp eye examination was performed at baseline and when indicated clinically. Other endpoints included the clinical activity as well as pharmacokinetics and-dynamics of PF00299804. The preliminary anti-tumor activity was assessed using RECIST criteria. Tumor size assessments were included at baseline, and every 2 cycles after the initiation of CDD. The pharmacokinetics (PK) of a single dose of PF00299804 was assessed for each dose escalation cohort by administration of a single lead-in dose on an empty stomach at least 4 days prior to the initiation of CCD (dose levels up to 16 mg), or at least 10 days prior to the initiation of CCD (30, 45, and 60 mg dose levels) . Blood samples were collected pre-dose and at intervals up to 3 days (dose levels up to 16 mg) or up to 9 days (30, 45, and 60 mg) post-dose. Steady-state kinetics were assessed on day 14 of the first treatment cycle. Blood samples were collected prior to dosing and at intervals up to 24 hours post-dose. Additional pre-dose samples were collected during cycle 2. The effect of food and pH on PF00299804 PK was assessed prior to the initiation of CCD in patients enrolled into schedule A MTD expansion cohorts. Patients received PF00299804 orally on an empty stomach 20 days prior to the initiation of CCD and a second dose 10 days later following either a standard typical breakfast or immediately after administration of Maalox Maximum strength. Blood samples for PK analyses were collected immediately prior to dosing and at intervals up to 9 days. Patients then began schedule A CCD of PF00299804 on an empty stomach at the MTD (day1). The PK effects of a 45mg BID loading dose administered during the first 3 days of cycle 1 were assessed in patients enrolled into the schedule A MTD expansion cohort. Serial

blood samples were collected pre- and up to 24 hours post-dose on the initiation of QD dosing (day 4, cycle 1) and at steady state (day 1, cycle 2). Additional pre-dose samples were collected at intervals up to the beginning of cycle 3. Potential biomarkers of HER activity were analyzed in skin biopsies taken at baseline and at steady state (day 14, cycle 1). Descriptive statistics were used for the analysis of PK, safety and tumor response data.

Results

Patient characteristics and drug exposure

A total of 121 patients were enrolled into the study and treated with PF00299804 (111 in schedule A, 10 in schedule B). Patients' baseline characteristics are summarized in Table 1. Most patients had been heavily pretreated before entry in the study. The most common tumor types were NSCLC (43%), colorectal cancer (22%), and breast cancer (6%). Patients received a total of 425 treatment cycles of PF00299804 with a median of 2 cycles per patient (range, 1–30). Table 2 provides a dosing summary for these patients.

MTD and DLTs

The patients treated in this study received doses of PF00299804 ranging from 0.5 to 60 mg QD. Initially, no DLTs were observed up to 60 mg. At this dose-level, 4 patients experienced a DLT (grade 3 stomatitis (n=2), grade 3 palmar-plantar erythema, and grade 3 dehydration, respectively). Consequently, this dose-level was considered intolerable. At the next-lower dose-level of 30 mg, 1 out of 13 patients experienced a DLT (grade 3 oral mucositis), and the dose was escalated up to 45 mg. At this dose-level, only 1 out of 6 patients experienced a DLT (grade 3 rash), and The MTD was set at 45 mg. Only 1 additional DLT (grade 3 Acne) was observed in the MTD expansion cohorts, making the total number of DLTs at 45 mg 2 out of 53 treated patients. A summary of the observed DLTs per dose-level is given in table 2.

Safety and tolerability

The safety population comprised all patients who received at least one dose of PF00299804, and included 121 patients in total. All but one patients (120)

Table 1: Patient characteristics.

Patient characteristics	Schedule A (n=111)	Schedule B (n=10)
Mean age (SD), years	56.9 (11.3)	57.6 (13.4)
Male/female n (%)	52/59 (47/53)	1/9 (10/90)
Race, n, (%):		
White	99 (89%)	9 (90%)
Black	2 (2%)	0 (0%)
Asian	8 (7%)	1 (1%)
Other	2 (2%)	0 (0%)
Primary tumor		
NSCLC	48 (43%)	7 (70%)
Colorectal	24 (22%)	0 (0%)
Breast	7 (7%)	1 (10%) ⁽¹⁾
Ovarian	5 (5%)	0 (0%)
Biliary	4 (4%)	1 (10%)
Other	23 (21%)	1 (10%)
Prior treatment		
Chemotherapy, n (%)	95 (86%)	8 (80)
1 regimen	20 (18%)	1 (10%)
2 regimens	21 (19%)	1 (10%)
≥ 3 regimens	54 (49%)	6 (60%)
Surgery, n (%)	99 (89%)	10 (100%)
Radiotherapy, n (%)	59 (53%)	4 (40%)

experienced a total of 1395 AEs. Of these, 716 AEs, experienced by 110 patients, were considered to be related to the study drug (Schedule A: 101 patients, 629 AEs; Schedule B: 9 patients, 87 AEs). The most frequently occurring non-hematologic treatment-related AEs (all cycles) are summarized in Table 3. Most treatment-related adverse events were mild (grade 1-2), and no treatment related adverse events of severity higher than grade 3 were reported. On Schedule A, over all treatment cycles, the most frequently observed grade 1-3 AEs attributed to study drug included diarrhoea (66%), rash (45%), fatigue (34%) and nausea (32%), comparable with the most frequently observed toxicities on schedule B. Fourteen patients discontinued due to AEs (5 of these discontinuations were considered to be treatment-related), and. Thirty-one patients had dose interruptions as a result of treatment-related AEs (29 in schedule A and 2 in schedule B), and 8 patients continued with a reduced dose due to adverse events (7 in schedule A, 1 in schedule B). The observed non-hematologic laboratory abnormalities were

Table 2: Dose-limiting toxicities during treatment cycle 1 and median number of treatment cycles started

Dose (mg/day)	Evaluable patients (n)	DLTs (n)	Events (n/N)	Total no of cycles started per cohort:	Cycles started per patient: median (range)
0.5	3	None	0/3	8	2 (2-5)
1	3	None	0/3	5	2 (1-4)
2	3	None	0/3	6	2 (1-4)
4	5	None	0/3	40	4 (2-30)
8	3	None	0/3	10	4 (1-6)
16	4	None	0/4	14	2 (1-10)
30	13	Stomatitis	1/13	29	2 (1-9)
45	53	Rash, acne	2/53	212	2 (1-27)
45 (loading dose)	18	None		51	3 (1-6)
60	6	Stomatitis (n=2), palmar- plantar erythema , dehydration	4/6	10	1.5 (1-4)

mainly of grade 1 or grade 2 severity. Grade 3 non-hematologic laboratory abnormalities reported across the patient cohorts were reversible and comprised changes in gamma glutamyl transferase (n=19), alkaline phosphatase (n=8), hypophosphatemia (n=7), hyponatremia (n=6), hypermagnesemia (n=3), total bilirubin (n=3), hypoalbuminemia (n=3), aspartate aminotransferase (n=2), alanine amino transferase (n=2), hyperkalemia (n=1), hypokalemia (n=1), hypocalcemia (n=1), and hyperglycemia (n=1). Reported grade 4 non-hematologic laboratory abnormalities included hypercalcemia (n=3), hyponetremia (n=1), elevated gamma-glutamyl transferase (n=1) and elevated total bilirubin (n=1) were reported. Hematologic laboratory abnormalities were mainly of grade 1 or grade 2. A total of 10 patients experienced grade 3 hematological abnormalities, which included 9 patients with lymphocytopenia, and 1 patient with grade 3 hemoglobin toxicity. Grade 4 hematological abnormalities were observed in 5 patients treated in schedule A, and consisted of lymphocytopenia (n=3) and haemoglobin toxicity (n=2). One patient in schedule B experienced grade 4 thrombocytopenia. Urinalysis data was available for 79 patients. All incidences of protein in the urine were of grade 1

Table 3: Frequency of treatment-related AEs occurring in $\geq 15\%$ of the study population* (All treatment cycles).

Adverse Event	CTC Grade*			Total**
	Grade 1	Grade 2	Grade 3	
Schedule A				
Diarrhea	42 (38%)	20 (18%)	11 (10%)	73 (66%)
Rash	30 (27%)	16 (15%)	4 (4%)	50 (45%)
Fatigue	20 (18%)	15 (14%)	3 (3%)	38 (34%)
Nausea	28 (25%)	6 (5%)	1 (1%)	35 (32%)
Dry skin	29 (26%)	1 (1%)	0 (0%)	30 (27%)
Stomatitis	17 (15%)	9 (8%)	4 (4%)	30 (27%)
Anorexia	11 (10%)	9 (8%)	2 (2%)	22 (20%)
Dermatitis Acneiform	12 (11%)	3 (3%)	6 (5%)	21 (19%)
Vomiting	13 (12%)	3 (3%)	1 (9%)	17 (15%)
Schedule B				
Diarrhea	2 (20%)	5 (50)	2 (20%)	9 (90%)
Rash	4 (40%)	2 (20%)	0 (0%)	6 (60%)
Fatigue	0 (0%)	3 (30%)	1 (10%)	4 (40%)
Nausea	1 (10%)	2 (20%)	1 (10%)	4 (40%)
Vomiting	3 (30%)	1 (10%)	0 (0%)	4 (40%)
Anorexia	0 (0%)	3 (30%)	0 (0%)	3 (30%)
Dermatitis acneiform	0 (0%)	3 (30%)	0 (0%)	3 (30%)
Dry eye	1 (10%)	2 (20%)	0 (0%)	3 (30%)
Dry skin	1 (10%)	2 (20%)	0 (0%)	3 (30%)
Skin fissures	2 (20%)	1 (10%)	0 (0%)	3 (30%)
Stomatitis	1 (10%)	1 (10%)	1 (10%)	3 (30%)
Alopecia	2 (20%)	0 (0%)	0 (0%)	2 (20%)
Eye pain	2 (20%)	0 (0%)	0 (0%)	2 (20%)
Pruritus	2 (20%)	0 (0%)	0 (0%)	2 (20%)
Skin exfoliation	1 (10%)	0 (0%)	1 (10%)	2 (20%)

or 2 severity, with all but two grade 2 events occurring at a dose of 45 mg/day, and one grade 2 event occurring in schedule B, at a dose of 60 mg/day. Overall, protein in the urine was reported for 21 patients (27%). Treatment related eye disorders were infrequent, but included four grade 3 events, all at the 45 mg dose (conjunctivitis (n=2), conjunctival irritation and eyelid pruritus, respectively). No treatment-related cardiac disorders were reported.

Pharmacokinetics

All patients provided blood samples for pharmacokinetic analyses. The pharmacokinetic parameters after single and multiple dosing are provided in table 4. No pharmacokinetic parameters could be calculated for the 0.5 and 1.0 mg dose-levels after single dosing, since the concentrations at several time points were below the limit of quantitation for these dose-levels. After single dose administration, PF00299804 was orally absorbed with a median T_{max} of 2-4 hours in the dose levels up to 8 mg, and 6-7 hours in the dose levels of 16 mg and higher. In general, the mean C_{max} and AUC of PF00299804 increased with dose over the dose range evaluated. The half-life could not be adequately characterized due to a lack of sufficient sampling time in the 2 to 16 mg cohorts. With the extension of PK collection times, the half-life was 46-72 hours over the dose range of 30-60 mg, with a CV of 30-50%. Apparent clearance ranged from 19-29 L/hr and apparent volume of distribution ranged from 1920-2620 L across the 30mg to 60 mg dose level. After multiple doses, the mean AUC accumulation of PF00299804 (Rac) ranged from approximately 4- to 6-fold. The linearity ratio (R_{ss}) was close to 1 across the 30 mg to 60 mg dose range. No dose-dependent or time-dependent nonlinear PK were observed for PF00299804. In the food effect study (n=5), the median C_{max} was similar between patients with food (21 ng/ml) and without food (21.5 ng/ml). The median AUC_{inf} was also comparable (1850 ng*hr/ml versus 1940 ng*hr/ml). In the antacid effect study (n=8), also no effects were observed, with the same median C_{max} (22.1 ng/ml) in patients with and without antacid. Also, the median AUC_{inf} was similar in patients with (1820 ng*hr/ml) and without (1640 ng*hr/ml) antacid. Finally, 18 patients entered the loading dose cohort. The median C_{max} after the loading dose (cycle 1, day 4) was comparable with the C_{max} on day 1 of cycle 2 (101 ng/ml and 80 ng/ml, respectively). The exposure (AUC_{tau}) after the loading dose (1940 ng*hr/ml) was also comparable with that seen on day 1 of cycle 2 (1620 ng*hr/ml).

Pharmacodynamics

A total of 87 patients provided pre- and post-dose skin biopsy samples that were analysed to establish a PK-PD relationship. The PK-PD relationship was investigated by evaluating the correlation between PK exposure parameters at steady state (C_{max} , AUC_{tau} and C_{trough} on Cycle 1 Day 14, Cycle 2 Day 1 for

Table 4a: Mean pharmacokinetic parameters (%CV) after a single dose of PF00299804.

Parameters after single doses of PF00299804	Dose PF00299804								
	0.5 mg	1 mg	2 mg (n=1)	4 mg (n=1)	8 mg (n=3)	16 mg (n=4)	30 mg (n=13)	45 mg (n=50)	60 mg (n=15)
Tmax (hr)			2	4	4 (4-6)	7 (4-8)	6 (4-24)	6 (2-24)	6 (1-8)
Cmax (ng/ml)			2.1	2.7	3.1 (44.4)	11.8 (64.5)	17.3 (36.5)	26.2 (49.6)	38.1 (44.3)
AUC0-72 (ng*hr/ml)			9.5	21.6	70.2 (49.1)	348 (37.7)	572 (40.8)	1000 (36.4)	1560 (48.8)i
AUC0-216 (ng*hr/ml)							875 (52.7)b	1600 (34.0)d	2870 (45.0)g
AUCinf (ng*hr/ml)							1220 (54.2)a	1800 (33.8)e	3740 (44.8)h
T1/2 (hr)							45.7 (42.9)c	70.1 (30.5)	71.9 (50.0)f
Cl/F (l/hr)							28.9 (54.2)a	28.0 (34.4)e	18.5 (39.3)h
V/F (l)							2500 (9.1)a	2620 (33.4)e	1920 (51.6)h

a=2, b=3, c=11, d=44, e=37, f=14, g=9, h=6, i=16

loading dose cohort) and changes of PD biomarker endpoints (pMAPK, pSTAT3, Ki67 and p27) from baseline to steady state. An example of paired skin biopsy samples that show a reduction in Ki-67 and pMAPK following treatment with PF00299804 can be seen in figure 2. Biomarkers Ki67 and pMAPK appeared to have significant association with PK exposure ($P < 0.05$) (Table 5). Figure 3 shows the relationship between steady-state C_{trough} and % change from baseline of steady-state Ki67 and pMAPK. The percentage of change of Ki67 and pMAPK seemed to increase with their baseline values (Figure 4).

Antitumor activity

A total of 104 patients had at least one response evaluation following treatment with PF00299804. No complete responses were observed, but 4 patients (4%) with non-small cell lung cancer had a partial response. These

Table 4b: Mean pharmacokinetic parameters (%CV) after multiple doses of PF00299804.

Parameters after multiple doses of PF00299804	Dose PF00299804								
	0.5 mg (n=2)	1 mg (n=1)	2 mg (n=2)	4 mg (n=5)	8 mg (n=3)	16 mg (n=3)	30 mg (n=11)	45 mg (n=44)	60 mg (n=10)
Tmax (hr)	6 (6-6)	6	4 (4-4)	4 (4-6)	6 (4-8)	6 (4-6)	6 (4-24)	6 (0-24)	6 (0-24)
Cmax (ng/ml)	2.1 (1.2-3.1)	2.2	4.4 (4.2-4.6)	5.7 (7.0)	10.6 (50.5)	27.9 (25.8)	54.0 (38.4)	112 (42.6)	125 (39.7)
Cmin (ng/ml)	1.4 (0-2.7)	1.6	2.4 (2.0-2.9)	3.7 (23.4)	6.7 (52.4)	19.3 (24.5)	32.8 (49.6)	77.8 (46.9)	77.1 (64.5)
Cavg (ng/ml)	0.6 (0.6-0.7)	1.7	3.0 (2.5-3.6)	4.0 (35.3)	7.0 (78.6)	24.3 (27.7)	40.4 (40.1)	93.7 (46.6)	101 (45.0)
AUCtau (ng*hr/ml)	15.5 (13.9-17.1)	41.6	72.9 (60.2-85.7)	95.7 (35.3)	168 (78.6)	584 (27.7)	970 (40.1)	2250 (46.6)	2430 (45.0)
Rac			6.3	4.4	3.5 (53.4)	4.7 (34.1)	4.2 (24.3)	5.8 (46.9)	4.1 (47.8)
Rss							1.2 (5.7)	1.2 (35.2)	1.0 (26.2)

a=1, b=3, c=36, d=5

patients were treated in schedule A, at a dose of 16 mg (n=1) and 45 mg (n=2), and in schedule B, at a dose of 60 mg (n=1). Forty-two patients had stable disease as best response, and 50 patient had progressive disease at their first evaluation. Overall, 9 patients (9%) had a clinical benefit response, defined as complete response, partial response, or stable disease for at least 24 weeks.

Discussion

In this first-in-human study we show that PF00299804 administration is safe and well tolerated on both continuous and intermittent schedules. The MTD was set at 45mg daily, with only 2 DLTs (rash and acne) out of 53 evaluable patients treated at the MTD. This dose will be further evaluated in phase II studies. The most common treatment-related grade 3 adverse events were skin and gastrointestinal disorders for both continuous and intermittent dosing schedules. The higher incidence of the most common grade 3 AEs on

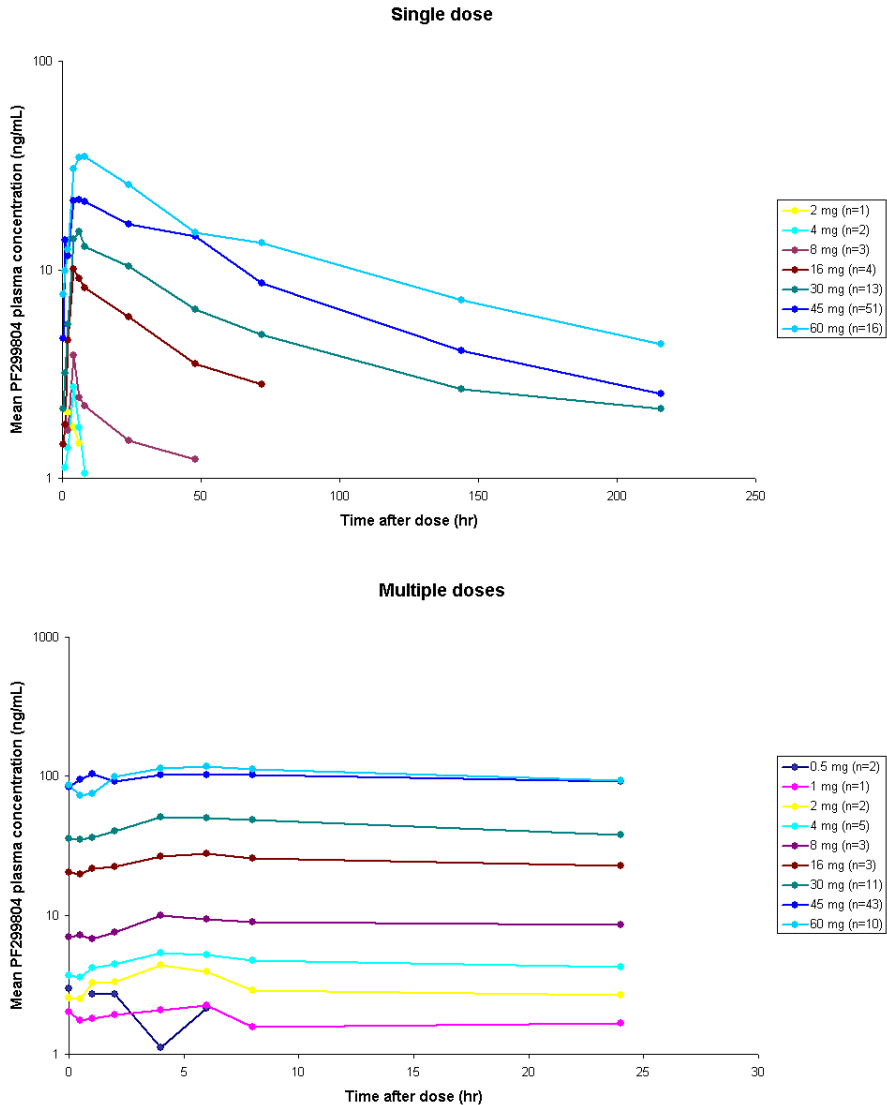


Figure 1: PK curves following single (upper) and multiple (lower) dosing of PF00299804. Median values are shown.

intermittent dosing was not significant and probably due to the relatively low patient numbers on this schedule.

Skin disorders are typical side-effects of agents targeting HER-driven pathways, and are observed following administration of both monoclonal antibodies and small molecule TKIs. Gastrointestinal complaints are more

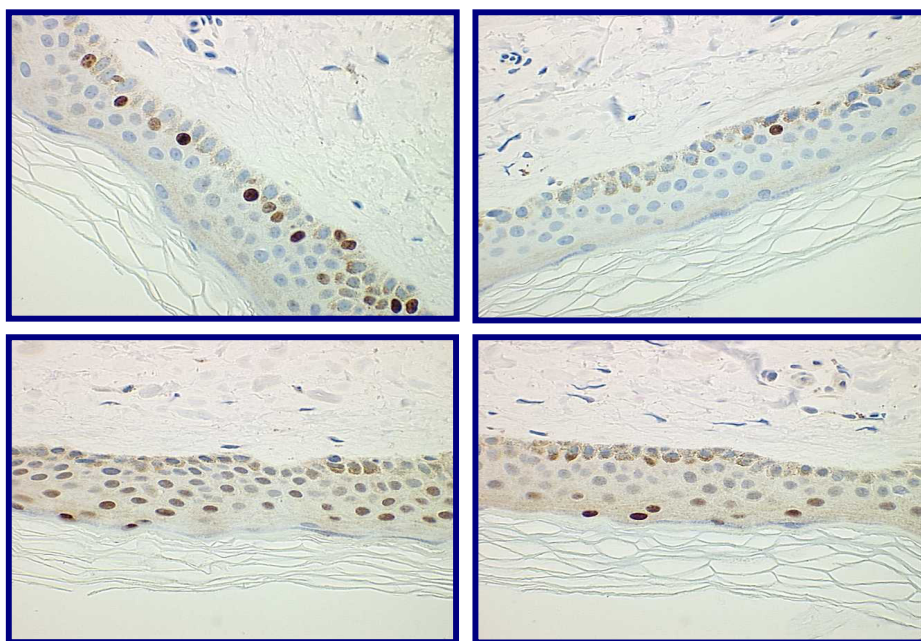


Figure 2: Decrease in Ki67 (top) and pMAPK (bottom) in skin biopsies. Left: Skin biopsies taken at baseline. Right: Skin biopsies taken at day 14 of the first treatment cycle. These samples were taken from a patient treated at the 45 mg dose-level.

frequently observed with orally administered agents, although trastuzumab is also known to induce gastrointestinal side-effects (14). The treatment related AEs and DLTs observed in this study are completely in line with the side-effects that were observed in other studies with inhibitors targeting multiple HER members. Lapatinib, for instance, shows a similar toxicity profile, with diarrhea, rash, nausea and fatigue as most profound side-effects (15). The safety of CI-1033 and HKI-272, both irreversible pan-HER inhibitors, was recently investigated in phase I studies. The DLTs for these agents were diarrhea and rash for CI-1033 (16), and rash for HKI-272 (17). Other toxicities observed in these studies included nausea, asthenia, vomiting and stomatitis, toxicities we also observed following administration of PF00299804.

Preclinical studies highlighted epithelial atrophy in the cornea as a potential safety concern. Although eye disorders were reported infrequently, treatment-related grade 3 events of conjunctivitis, conjunctival irritation and eyelid pruritus were documented. Likewise, preclinical studies suggested renal effects as a potential safety concern. Creatinine perturbations and urinary protein

Table 5: Pharmacokinetic/pharmacodynamic relations (PK/PD).

PD Biomarker	PK Parameters			
	Dose (n=87) P (rho)	Cmax (n=87) P (rho)	AUCtau (n=84) P (rho)	Ctrough (n=85) P (rho)
Ki67	0.223 (-0.132)	0.063 (-0.202)	0.038 (-0.229) *	0.019 (-0.258) *
pMAPK	0.0591 (-0.205)	0.001 (-0.371) *	0.001 (-0.376) *	0.001 (-0.377) *
pSTAT3	0.414 (-0.089)	0.387 (-0.094)	0.555 (-0.065)	0.791 (-0.029)
P27	0.569 (0.063)	0.986 (0.002)	0.972 (0.004)	0.895 (-0.015)

The Spearman correlation test was used. Values represent the correlation coefficient, with the p values between brackets. *: $p < 0.05$

were of low incidence and predominantly of grade 1 severity (maximum grade 2). Renal effects have been reported in other preclinical toxicology models of HER-1/EGFR inhibition, but these effects do not appear to translate into renal effects in human. PF00299804 appears to follow a similar pattern. In view of the documented association of trastuzumab with cardiotoxicity (18), cardiotoxicity generally, left ventricular ejection fraction (LVEF) and QTc intervals in particular were closely monitored in this study.

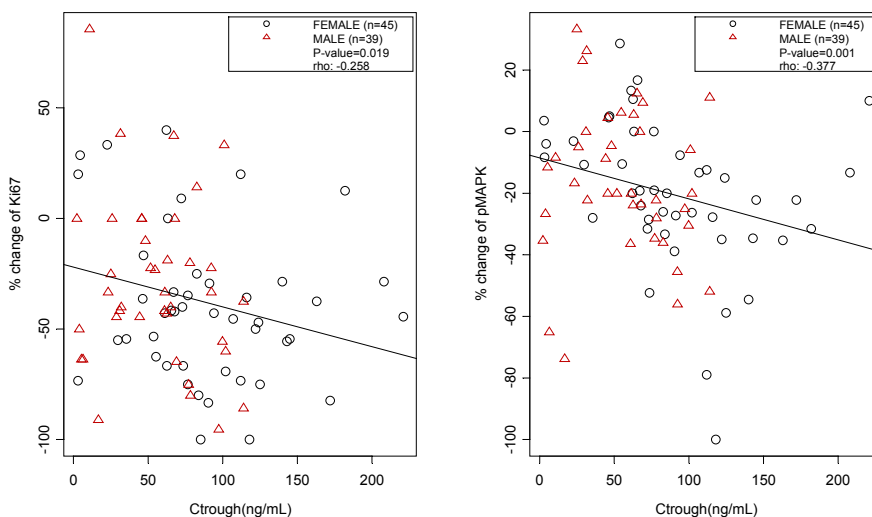


Figure 3 : The relationship between steady-state Ctrough and % change from baseline of steady-state Ki67 and pMAPK. Ctrough = trough concentration on Cycle 1 Day 14, or Cycle 2 Day 1 for loading dose cohort . % change = $100 \times (\text{SS}-\text{baseline})/\text{baseline}$

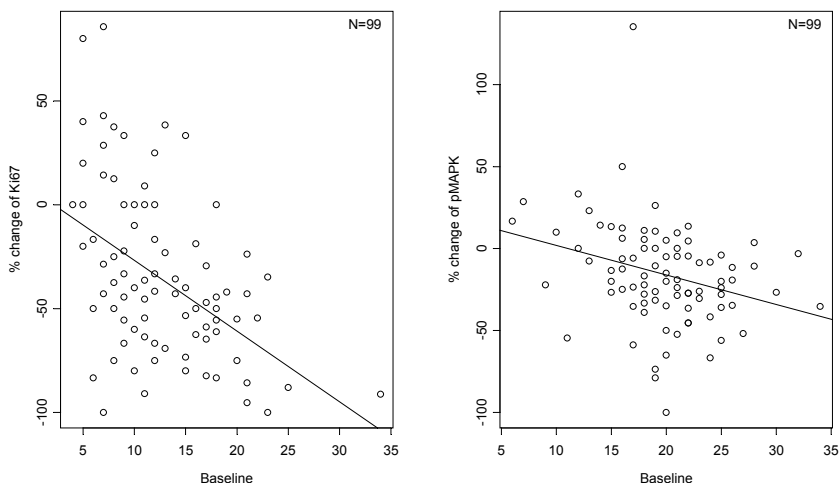


Figure 4: The relationship between baseline values and % change of biomarkers.

However, no incidences of treatment –related cardiotoxicity were reported, which is in line with the results of a meta-analysis that showed low levels of cardiotoxicity for lapatinib (19).

Pharmacokinetic analyses revealed a linear increase in exposure to PF00299804 with increasing doses. PF00299804 demonstrated a long half-life, and a very large volume of distribution, indicating extensive tissue penetration of the drug. The half-life of PF-00299804 is much longer than those observed for HKI-272, CI-1033, or EKB-569 (17,20,21). There was evidence of accumulation after multiple doses, but we did not observe increases in toxicity in patients that remained on-study for many cycles. No effect of food or antacid on PF00299804 pharmacokinetics was demonstrated, although no definitive conclusions can be drawn due to low numbers of patients in these expansion cohorts. Importantly, the systemic exposure at doses ≥ 30 mg/day exceeded the threshold targets for efficacy predicted from non-clinical studies. We also found a dose-dependent increase in target inhibition (decreases in MAPK phosphorylation, and Ki67, a marker for cell division) following treatment with PF00299804, results that are in line with those obtained with CI-1033 (20).

Preclinical studies with the irreversible dual EGFR/HER-2 inhibitor HKI-272 and the irreversible pan-HER inhibitors EKB-569 and CI-1033 have shown

inhibition of gefitinib resistant cell lines in vitro (22,23). However, recently it appeared that the efficacy of HKI-272 was disappointing in a phase 2 study in NSCLC patients pretreated with gefitinib/erlotinib (24). The CI-1033 phase 2 study in NSCLC patients also showed disappointing efficacy, although these patients were generally not gefitinib/erlotinib refractory or resistant (25). At present, no phase 2 data have been published for EKB-569. In the here reported study, four NSCLC patients had a partial response. Interestingly, all these patients had been pretreated with erlotinib or gefitinib, and two of these entered this study immediately after progressing on erlotinib or gefitinib. A total of 9 patients derived clinical benefit of treatment with PF00299804. One of these patients, a male patient with bronchoalveolar carcinoma, remained on study for over 2 years. His tumor load clearly reduced after initiation of treatment, but he never responded according to RECIST. Furthermore, his clinical condition improved after start of treatment with PF00299804.

In conclusion, PF00299804 can be safely administered up to a dose of 45 mg/day. Both continuous and intermittent treatment schedules were well tolerated, with gastrointestinal and skin toxicities as predominant side-effects. In this study, PF00299804 showed encouraging signs of antitumor activity in patients with NSCLC. The recommended dose for phase 2 studies is 45 mg once daily at a continuous schedule. PF00299804 is currently being assessed in phase 2 studies.

Acknowledgements

Editorial assistance was provided by ACUMED (Tytherington, UK) and funded by Pfizer Inc. This study was funded by Pfizer Inc.

References

1. Casalini, P., Iorio, M. V., Galmozzi, E. et al. Role of HER receptors family in development and differentiation. *J.Cell Physiol.* 2004;200:343-350.
2. Sergina, N. V. and Moasser, M. M. The HER family and cancer: emerging molecular mechanisms and therapeutic targets. *Trends Mol.Med.* 2007;13:527-534.
3. Ciardiello, F. and Tortora, G. EGFR antagonists in cancer treatment. *N.Engl.J.Med.* 2008;358:1160-1174.
4. Moasser, M. M. Targeting the function of the HER2 oncogene in human cancer therapeutics. *Oncogene.* 2007;26:6577-6592.
5. Press, M. F. and Lenz, H. J. EGFR, HER2 and VEGF pathways: validated targets for cancer treatment. *Drugs.* 2007;67:2045-2075.
6. Engelman, J. A., Zejnullahu, K., Gale, C. M. et al. PF00299804, an irreversible pan-ERBB inhibitor, is effective in lung cancer models with EGFR and ERBB2 mutations that are resistant to gefitinib. *Cancer Res.* 2007;67:11924-11932.

7. Gonzales, A. J., Hook, K. E., Althaus, I. W. et al. Antitumor activity and pharmacokinetic properties of PF-00299804, a second-generation irreversible pan-erbB receptor tyrosine kinase inhibitor. *Mol.Cancer Ther.* 2008;7:1880-1889.
8. Fry, D. W., Bridges, A. J., Denny, W. A. et al. Specific, irreversible inactivation of the epidermal growth factor receptor and erbB2, by a new class of tyrosine kinase inhibitor. *Proc.Natl.Acad.Sci.U.S.A.* 1998;95:12022-12027.
9. Citri, A., Alroy, I., Lavi, S. et al. Drug-induced ubiquitylation and degradation of ErbB receptor tyrosine kinases: implications for cancer therapy. *EMBO J.* 2002;21:2407-2417.
10. Yun, C. H., Mengwasser, K. E., Toms, A. V. et al. The T790M mutation in EGFR kinase causes drug resistance by increasing the affinity for ATP. *Proc.Natl.Acad.Sci.U.S.A.* 2008;105:2070-2075.
11. Nautiyal, J., Rishi, A. K., and Majumdar, A. P. Emerging therapies in gastrointestinal cancers. *World J.Gastroenterol.* 2006;12:7440-7450.
12. Abd El-Rehim, D. M., Pinder, S. E., Paish, C. E. et al. Expression and co-expression of the members of the epidermal growth factor receptor (EGFR) family in invasive breast carcinoma. *Br.J.Cancer.* 2004;91:1532-1542.
13. Bianchi, S., Palli, D., Falchetti, M. et al. ErbB-receptors expression and survival in breast carcinoma: a 15-year follow-up study. *J.Cell Physiol.* 2006;206:702-708.
14. Al Dasooqi, N., Bowen, J. M., Gibson, R. J. et al. Trastuzumab induces gastrointestinal side effects in HER2-overexpressing breast cancer patients. *Invest New Drugs.* 2008;
15. Moy, B. and Goss, P. E. Lapatinib-associated toxicity and practical management recommendations. *Oncologist.* 2007;12:756-765.
16. Calvo, E., Tolcher, A. W., Hammond, L. A. et al. Administration of CI-1033, an irreversible pan-erbB tyrosine kinase inhibitor, is feasible on a 7-day on, 7-day off schedule: a phase I pharmacokinetic and food effect study. *Clin.Cancer Res.* 2004;10:7112-7120.
17. Wong, K. K., Fracasso, P. M., Bukowski, R. M. et al. A phase I study with neratinib (HKI-272), an irreversible pan ErbB receptor tyrosine kinase inhibitor, in patients with solid tumors. *Clin.Cancer Res.* 2009;15:2552-2558.
18. Slamon, D. J., Leyland-Jones, B., Shak, S. et al. Use of chemotherapy plus a monoclonal antibody against HER2 for metastatic breast cancer that overexpresses HER2. *N.Engl.J.Med.* 2001;344:783-792.
19. Perez, E. A., Koehler, M., Byrne, J. et al. Cardiac safety of lapatinib: pooled analysis of 3689 patients enrolled in clinical trials. *Mayo Clin.Proc.* 2008;83:679-686.
20. Zinner, R. G., Nemunaitis, J., Eiseman, I. et al. Phase I clinical and pharmacodynamic evaluation of oral CI-1033 in patients with refractory cancer. *Clin.Cancer Res.* 2007;13:3006-3014.
21. Erlichman, C., Hidalgo, M., Boni, J. P. et al. Phase I study of EKB-569, an irreversible inhibitor of the epidermal growth factor receptor, in patients with advanced solid tumors. *J.Clin.Oncol.* 2006;24:2252-2260.
22. Carter, T. A., Wodicka, L. M., Shah, N. P. et al. Inhibition of drug-resistant mutants of ABL, KIT, and EGF receptor kinases. *Proc.Natl.Acad.Sci.U.S.A.* 2005;102:11011-11016.
23. Kwak, E. L., Sordella, R., Bell, D. W. et al. Irreversible inhibitors of the EGF receptor may circumvent acquired resistance to gefitinib. *Proc.Natl.Acad.Sci.U.S.A.* 2005;102:7665-7670.
24. Besse, B., Eaton, K. D., Soria, J. C. et al. Neratinib (HKI-272), an irreversible pan-ErbB receptor tyrosine kinase inhibitor: preliminary results of a phase 2 trial in patients with advanced non-small cell lung cancer. *Eur Journal Cancer.* 2008;6:Abstract 203-
25. Janne, P. A., von Pawel, J., Cohen, R. B. et al. Multicenter, randomized, phase II trial of CI-1033, an irreversible pan-ERBB inhibitor, for previously treated advanced non small-cell lung cancer. *J.Clin.Oncol.* 2007;25:3936-3944.

9

Sorafenib, gemcitabine and carboplatin

CHAPTER 9.1

Phase I pharmacokinetic study of sorafenib in combination with gemcitabine and carboplatin in patients with advanced solid tumors.

David S. Boss, Helgi H. Helgason, Robert Jansen, Annemarie Nol,
Nienke Lankheet, Hilde Rosing, Jos H. Beijnen,
Jan H. M. Schellens.

Interim analysis

Abstract

Introduction: Sorafenib, gemcitabine, and carboplatin are all active anticancer agents. In this phase I trial we studied the safety, pharmacokinetics, pharmacodynamics, and anti-tumor activity of this combination in patients with advanced solid malignancies.

Methods: Patients received sorafenib continuously, carboplatin on day 1, and gemcitabine on day 1 and 8 of each treatment cycle (21 days). The starting dose was set at 200 mg BID sorafenib, carboplatin AUC3, and 750 mg/m² gemcitabine. Toxicity was monitored, and blood samples were drawn during the first treatment cycle for pharmacokinetic analyses of sorafenib, carboplatin, gemcitabine, and intracellular gemcitabine-triphosphate measurements. Antitumor activity was assessed once every two cycles using RECIST criteria.

Results: At the time of this report, 10 patients were included. The starting dose-level appeared non-tolerable, with 3 out of 6 patients experiencing a DLT (grade 3 fatigue in all cases). Subsequently, three patients were treated with 200 mg sorafenib once daily, carboplatin AUC2, and gemcitabine 500 mg/m². No DLTs were observed. The most frequently observed treatment-related non-hematological toxicities included fatigue, alopecia, nausea and rash. Observed laboratory abnormalities included grade 3 liver function disturbances (GGT, ALS, and AST), grade 3 neutropenia, and grade 3-4 thrombocytopenia. Data obtained from pharmacokinetic and pharmacodynamic analyses were consistent with data from literature. One partial response was observed in a patient with melanoma treated at the starting dose-level, prolonged disease stabilizations were observed in 4 patients (27, 27, 27, and 24 weeks), of whom three patients were treated at the lower dose-level.

Conclusion: The starting dose of 200 mg BID sorafenib, carboplatin AUC3, and 750 mg/m² gemcitabine appeared non-tolerable. The study was ongoing at the time of this report to establish the maximum tolerable dose. Promising signs of anti-tumor activity were observed at both investigated dose-levels.

Introduction

Sorafenib (Bay 43-9006; Nexavar) is an orally available multi-kinase inhibitor that inhibits the activities of RAF kinase, vascular endothelial growth factor receptor, platelet-derived growth factor receptor, c-kit, Ret, and other receptor tyrosine kinases in vitro (1). In single-agent phase I studies, it was demonstrated that sorafenib had a favorable toxicity profile, as well as preliminary antitumor activity against various tumor types (2,3). The activity of sorafenib in patients with renal cell carcinoma (4) and hepatocellular carcinoma (5,6) led to FDA approval for these indications in 2005 and 2007, respectively. In vitro, synergy of sorafenib with several other anticancer drugs was demonstrated (7). In clinical trials, combining sorafenib with doxorubicin (8), dacarbazine (9), erlotinib (10), gefitinib (11) and gemcitabine (12) appeared to be well tolerated, while hints of antitumor activity were observed. Recently, it was shown that sorafenib was well tolerated up to doses of 400 mg BID when combined with carboplatin and paclitaxel (13). In the here described study we combined sorafenib with gemcitabine and carboplatin, two extensively used anticancer agents. Gemcitabine (2',2'-difluorodeoxycytidine, dFdC) is a nucleoside antimetabolite that has a wide spectrum of antitumor activity. Carboplatin is an analogue of cisplatin, but with a milder non-hematological toxicity profile and a broad spectrum of antitumor activity. The combination gemcitabine/carboplatin is FDA approved for the treatment of advanced ovarian cancer (14), but also showed activity in patients with non-small cell lung cancer (NSCLC) (15) and metastatic breast cancer (16). The wide activity of gemcitabine/carboplatin and sorafenib, together with the synergy of sorafenib with a variety of anticancer agents, led us to initiate a phase I study with these three compounds. In this study we aimed to assess the safety, pharmacokinetics and preliminary efficacy of gemcitabine, carboplatin and sorafenib in patients with advanced solid tumors.

Materials and methods

Study population

Patients with progressive advanced solid tumors who were considered for palliative gemcitabine plus carboplatin combination therapy were eligible. Other criteria for inclusion were: Age >18 years; WHO performance status ≤ 2 ; life expectancy > 3 months; evaluable or measurable disease according to

RECIST criteria; adequate hematological function as defined by an absolute neutrophil count (ANC) of $\geq 1.5 \times 10^9$, platelet count of $\geq 100 \times 10^9$ and Hemoglobin ≥ 6.2 mmol/l; adequate hepatic function as defined by serum bilirubin ≤ 1.25 times the upper limit of normal, ALT and AST ≤ 2.5 times the upper limit of normal (≤ 5 times the upper limit of normal in case of liver metastases); adequate renal function as defined by serum creatinine ≤ 1.25 times the upper limit of normal or creatinine clearance ≥ 50 ml/min (Cockcroft–Gault formula). Exclusion criteria included: Previous treatment with an investigational drug within 30 days before start of the study; radiotherapy within 2 weeks prior to study entry; major surgery within 4 weeks prior to study entry; use of any medications or substances known to effect the activity or pharmacokinetics of sorafenib; pregnancy or breast feeding (all patients had to use adequate contraceptive protection; uncontrolled or poorly controlled hypertension (systolic blood pressure ≥ 150 mm Hg, diastolic blood pressure ≥ 90 mmHg); systemic steroids within 2 weeks prior to study treatment; myocardial infarction or cerebrovascular accident (CVA) within 6 months prior to study treatment; congestive heart failure requiring medication; symptomatic brain metastases; uncontrolled infections; known human immunodeficiency virus (HIV) infection; known chronic or acute viral hepatitis. The study protocol was approved by the Medical Ethics Committee of the hospital and all patients had to give written informed consent.

Trial design and procedures

This phase I dose escalation study assessed the safety, tolerability, anti tumor activity and pharmacokinetics of gemcitabine, carboplatin and sorafenib. At screening, informed consent was obtained and a complete medical history, including concomitant medication and demographic data were recorded. The use of concomitant medication was recorded on days 1, 8 and 15 of the first 2 treatment cycles, and on days 1 and 8 of subsequent treatment cycles. Physical examinations and the assessments of vital signs, performance status, and routine clinical chemistry and hematology were performed at baseline on days 1, 8 and 15 of the first 2 treatment cycles, and on days 1 and 8 of subsequent treatment cycles. A 12-lead ECG was performed at baseline and at start of cycle 2 and every subsequent treatment cycle. A chest X-ray was performed at screening and after every 2nd treatment cycle.

Dosing schedule and dose escalation

Patients were treated in 21-day cycles. Carboplatin dosage was calculated using the target area under the free carboplatin plasma concentration versus time curve (AUC in min.mg/mL). We calculated the carboplatin dose using the Calvert formula (17), with GFR estimated using the formula of Cockcroft and Gault (18). Carboplatin was administered as a 30 minute intravenous infusion on the first day of each treatment cycle. Gemcitabine was administered as a 30 minute intravenous infusion, starting one hour after the completion of the carboplatin infusion on day 1, and on day 8 of each treatment cycle. Sorafenib was administered orally bi-daily on days 1-21 of each treatment cycle, and was taken prior to carboplatin on days 1, and prior to gemcitabine on days 8 of every treatment cycle. At least three patients were entered at each dose level. If a DLT occurred in a patient during cycle 1, 3 additional patients were enrolled at that dose level. The MTD was defined as the highest dose level not producing DLTs in more than 1/6 patients. The starting dose was set at carboplatin AUC 3, 750 mg/m² gemcitabine and 200mg BID sorafenib.

Toxicity criteria

The incidence and severity of AEs were evaluated and coded according to the National Cancer Institute Common Terminology Criteria of Adverse Events version 3.0 (19). DLT was defined as any of the following events during the first treatment cycle: Grade ≥ 3 non-hematological toxicity directly related to the study treatment (excluding untreated nausea, vomiting and diarrhea, and alopecia); grade ≥ 3 nausea, vomiting or diarrhea in the presence of maximal support; Inability to begin next course of treatment within 2 weeks of scheduled dosing due to toxicity; grade 4 thrombocytopenia ($<25 \times 10^9/l$); grade 4 neutropenia lasting over 7 consecutive days ($<25 \times 10^9/l$); grade 3 febrile neutropenia.

Pharmacokinetic analysis

All patients entering the study provided blood samples for pharmacokinetic analyses. Blood samples for the determination of sorafenib pharmacokinetics were taken on day 1 at baseline, and at 1, 2, 4, 6, 8 and 24 hours after oral administration. Additional samples were taken on days 8, and 22 (day 1 cycle 2) prior to drug administration. Plasma concentrations of sorafenib were

measured by a validated liquid chromatography/tandem mass spectrometry method. Blood samples for gemcitabine pharmacokinetics were taken on day 1 prior to the gemcitabine infusion, at the end of the gemcitabine infusion, and subsequently at 30 minutes, 2, 4, 6 and 22 hours after the end of the gemcitabine infusion. dFdC and dFdU pharmacokinetics were analysed as described previously (20) with the exception that we didn't add tetrahydrouridine to the sodium-heparine blood collection tubes. Intracellular concentrations of gemcitabine triphosphate (dFdCTP) were determined in white blood cells (PBMCs), according to a method that was described previously (21). For this analysis, blood samples were drawn on day 1 prior to the gemcitabine infusion, at the end of the gemcitabine infusion, 2 hours after the end of the gemcitabine infusion, and 22 hours after the end of the gemcitabine infusion. Blood samples for carboplatin pharmacokinetics were taken on day 1 prior to the carboplatin infusion, at the end of the carboplatin infusion, and 4 and 24 hours after the start of the carboplatin infusion. For the determination of free platinum, a validated Zeeman atomic absorption spectrometry method was used (22).

Clinical activity assessments

Clinical disease assessments and tumor marker assessments (if appropriate) were performed at baseline and every 4 weeks. Radiological disease assessments by CT or MRI were performed at baseline and after every 2nd treatment cycle. Tumor response was evaluated using RECIST criteria (23).

Results

Patients

At the time of this report, 10 patients had been included in the study. Baseline characteristics are summarized in table 1. All patients were in good condition, with a WHO performance score of 0 or 1. Patients with various tumor types were included in the study, including melanoma (n=2) and breast cancer (n=2). The patients received a total of 57 cycles, with a median of 7.5 cycles per patient.

Table 1: Patient characteristics

Characteristic	N	%
Total number of patients	10	
Sex (male:female)	5:5	
Age (median, range)	45 (33-68)	
Performance status		
0	3	30%
1	7	70%
Tumor type		
Breast Cancer	2	20%
Melanoma	2	20%
NSCLC	1	10%
Thymoma	1	10%
ACUP	1	10%
Desmoplastic small round cell	1	10%
Ovarium	1	10%
Mesothelioma	1	10%

MTD and DLT

Due to the emergence of 3 DLTs out of 6 evaluable patients at the starting dose-level, the protocol had to be amended with novel dose-levels, evaluating lower doses of the investigated drugs (table 2). The observed DLTs at dose-level 1 included grade 3 fatigue, grade 3 fatigue and grade 4 skin toxicity, and grade 3 fatigue and grade 4 thrombocytopenia, respectively. After amending the protocol, 3 patients entered the study at dose-level -4, and no DLTs were reported at this dose-level. Consequently, dose-level -4 was regarded safe, and escalation to dose-level -3 was planned at the time of this report.

Table 2: Dose-levels. Dose-level 1 was the starting dose in the original protocol. Due to unexpected toxicity at this dose-level (3 out of 6 patients developed a DLT), the protocol had to be amended, and new dose-levels (-4 to -1) were introduced.

Dose-level	Gemcitabine	Carboplatin	Sorafenib	DLT
1	750 mg/m ²	AUC3	200 BID	3/6
Protocol amendment				
-4	500 mg/m ²	AUC2	200	0/3
-3	500 mg/m ²	AUC2	200 BID	
-2	650 mg/m ²	AUC3	200 BID	
-1	650 mg/m ²	AUC3	200 BID	

Adverse events

The performance status of 1 patient treated at dose-level 1 dropped to WHO 3 early after start of treatment. She was taken off-study on her own request after 1 week of treatment, and was therefore considered unevaluable. All other patients (n=9) were evaluable for adverse events. Grade 3 laboratory abnormalities were frequently observed, and included hematological toxicities and liver function disturbances (table 3). Grade 3 lymphocytopenia was observed in 5 patients, thrombocytopenia in 3 patients, neutropenia in 2 patients, leucocytopenia in 1 patient, and hemoglobinemia in 1 patient. In case of grade 3 thrombocytopenia or neutropenia, treatment with gemcitabine and carboplatin was omitted until recovery, which was within a week in all cases. Grade 3 liver function disturbances included elevated plasma levels of Gamma-glutamyltransferase (GGT, n=3), alanine-aminotransferase (ALT, n=1), aspartate-aminotransferase (AST, n=1), and total bilirubin (n=1). In all these cases, gemcitabine, carboplatin, and sorafenib treatment was omitted until recovery, which was generally very slow. The first patient with grade 3 GGT serum levels had liver metastases prior to entry in the study, and she entered the study with grade 2 GGT serum levels. Her GGT serum levels reached grade 3 during course 1, and never returned to normal, as she went off-study due to disease progression after one cycle of treatment. The second patient with grade 3 GGT toxicity also had liver metastases and grade 2 GGT serum levels at baseline. He developed grade 3 GGT toxicity during cycle 2, and his treatment was ceased until recovery, which took 2 weeks. The third patient with liver toxicity was a female patient who developed grade 3 GGT, ALT, AST, and bilirubin toxicity during the third cycle of treatment. She complained of pain in the upper abdominal region, and presented with jaundice. Treatment was immediately stopped, and ultrasound imaging of the liver area was performed to investigate whether she had obstruction of her bile duct. This was not confirmed, and her liver functions slowly recovered to normal. She started cycle 4 of treatment with a delay of 2 weeks, and her sorafenib was stopped for 4 weeks in total. She continued on the same dose-level, and her liver enzyme serum levels did not exceed grade 1 during further treatment. One patient experienced a grade 4 thrombocytopenia. After stopping treatment, his serum thrombocyte levels returned to normal within a week, and he continued treatment with a dose reduction. Electrolyte disturbances were also regularly observed. These toxicities were generally modest and did not exceed grade 2, except grade 3 hypophosphatemia that was observed in 2

Table 3: Laboratory abnormalities per dose-level during all treatment cycles.

parameters	Dose-level 1 (n=6)				Dose-level -4 (n=3)				Total (n=9)
	Gr1	Gr2	Gr3	Gr4	Gr1	Gr2	Gr3	Gr4	
Hemoglobinemia	3	2	1		2	1			9 (100%)
Alanine aminotransferase	4	2			2		1		9 (100%)
Aspartate Aminotransferase	5				2		1		8 (88%)
Gamma-glutamyl transferase	4	2			1		1		8 (88%)
Hypophosphatemia		3	2		2	1			8 (88%)
Lymphopenia		2	3		1		2		8 (88%)
Thrombocytopenia	2		2	1		2	1		8 (88%)
Neutropenia	2	1	1		1	1	1		7 (77%)
Hypocalcemia	4	1			1	1			7 (77%)
Leucopenia		4				2	1		7 (77%)
Alkaline phosphatase	3	1			1				5 (55%)
Bilirubin total	3	1					1		5 (55%)
Hyperkalemia	2	1			1				4 (44%)
Hypoalbuminemia	1	1			1				3 (33%)
Hypercalcemia	1				2				3 (33%)
Hypokalemia	1				2				3 (33%)
Hyponatremia	2				1				3 (33%)
Hypernatremia	1				1				2 (22%)
Hypomagnesemia					1				1 (11%)
Creatinine					1				1 (11%)

patients, and recovered without intervention. Most non-hematological toxicities were modest and did not exceed grade 2 (table 4). Grade 3 fatigue was observed in 3 patients, accompanied by grade 4 rash in one of these patients. All patients recovered within one week after cessation of treatment. Two out of the three patients continued with dose reductions, while the third patient went off-study before restarting treatment.

Table 4: Treatment related non-hematological toxicities per dose-level during all treatment cycles.

parameters	Dose-level 1 (n=6)				Dose-level -4 (n=3)				Total (n=9)
	Gr1	Gr2	Gr3	Gr4	Gr1	Gr2	Gr3	Gr4	
Fatigue	2		3		2	1			8 (88%)
Alopecia	4				1	1			6 (66%)
Nausea	3				2				5 (55%)
Diarrhea	4								4 (44%)
Rash	2			1	1				4 (44%)
Stomatitis	4								4 (44%)
Neuropathy	1				2				3 (33%)
Vomiting	1				1	1			3 (33%)
Dizziness	1	1							2 (22%)
Dyspnoe	1	1							2 (22%)
Headache	1	1							2 (22%)
Hoarseness	2								2 (22%)
Obstipation	1				1				2 (22%)
Pain	2								2 (22%)
Anorexia					1				1 (11%)
Coughing	1								1 (11%)
Fever					1				1 (11%)
Infection					1				1 (11%)
Skin other	1								1 (11%)

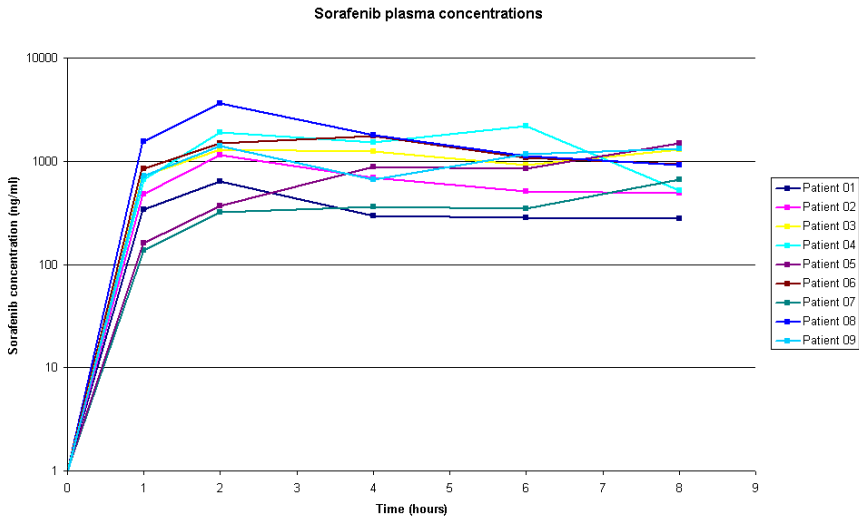
Pharmacokinetics

Plasma samples for sorafenib pharmacokinetics were collected from 9 patients. The individual curves are presented in figure 1, and the pharmacokinetic parameters are presented in table 5. This table includes patients treated at dose-levels 1 and -4, but all patients received the same dose of 200 mg sorafenib. Due to a large volume of distribution (median of 232 l), the measured plasma concentrations were low, with a median peak value of only 1.4 µg/ml. Due to these low plasma concentrations, there was an unpredictable concentration-time profile with multiple peaks. Consequently, it

Parameters	Median (Range)
Cmax (ng/ml)	1398 (634-3616)
Tmax (h)	4 (2-8)
AUC (0-8) (ng.h/ml)	7796 (2710-13731)
Vdd (l)	232 (87-657)

Table 5 (left): PK Sorafenib parameters derived from 9 patients, all after administration of a single dose of 200 mg sorafenib.

Figure 1 (below): Individual PK curves from 9 patients after receiving a single dose of 200 mg sorafenib.



was impossible to calculate the clearance and the elimination half-life in several patients. Plasma concentrations of gemcitabine (dFdC) and its metabolite dFdU were determined for 9 patients. Following administration of gemcitabine, dFdC was rapidly converted to its metabolite dFdU (figure 2). Consequently, dFdC concentrations in plasma dropped sharply, with an initial half-life of approximately 6 minutes (median values of 0.10 and 0.14 hours for the 500 and 750 mg-m² dose levels, respectively). The median elimination half-life of dFdC for both dose levels were 7.4 and 8.0 hours, respectively. The elimination half-life of dFdU at both dose levels was 22.9 and 12.5 hours, respectively. Plasma samples for carboplatin pharmacokinetics were collected from all patients (n=10). Carboplatin concentration measurements in ultrafiltrate revealed area under the curves that approximated the target area under the free carboplatin plasma curves that were calculated using the Calvert formula (table 7). Following administration, free carboplatin

Table 6: Gemcitabine (dFdC) and dFdU pharmacokinetic parameters.

Parameters dFdC	500 mg (n=2)	750 mg (n=7)
	Median (range)	
Cmax (ug/ml)	3.4 (1.0-5.8)	4.9 (2.9-15.1)
AUCinf (ug.hr/ml)	2.0 (0.7-3.2)	2.6 (1.8-8.2)
T1/2 init. (hours)	0.14 (0.10-0.18)	0.1 (0.09-0.15)
T1/2 elim.(hours)	7.4 (3.5-11.2)	8.0 (4.6-27.6) ^a
Parameters dFdU		
Cmax (ug/ml)	20.3 (13.7-26.8)	25.7 (18.1-34.3)
AUCinf (ug.hr/ml)	160.1 (155.2-165.0)	167.8 (136.5-207.2)
T1/2 elim. (hours)	22.9 (18.6-27.1)	12.5 (8.9-15.6)

^a n = 5

concentrations dropped rapidly, followed by a slower terminal elimination phase, with a half-life of approximately 4 hours (table 7, figure 3).

Pharmacodynamics

Nine patients provided white blood cells for intracellular dFdCTP concentration measurements. The results are shown in table 8 and figure 4. The peak dFdCTP concentrations, corrected for intracellular protein amounts, were observed at the end of gemcitabine infusion, or 2 hours post the end of infusion. The area under the dFdCTP in PBMCs versus time curve could be determined in 7 patients, and was 11.1 µg.hr/mg protein at the 500 mg gemcitabine dose (n= 1), and 7.7 µg.hr/mg protein at the 750 mg gemcitabine dose (n=6). The other 2 patients had no data at the 24h time-point. Consequently, also no terminal half-life could be determined in these patients. The median half-life for the different gemcitabine doses was 7.9 (500 mg gemcitabine, n= 1) and 11.1 (750 mg gemcitabine, n=6) hours, respectively. No correlation was found between the exposure to gemcitabine in plasma, and the intracellular dFdCTP levels (p=0.879, Spearman rank correlation test) (figure 4).

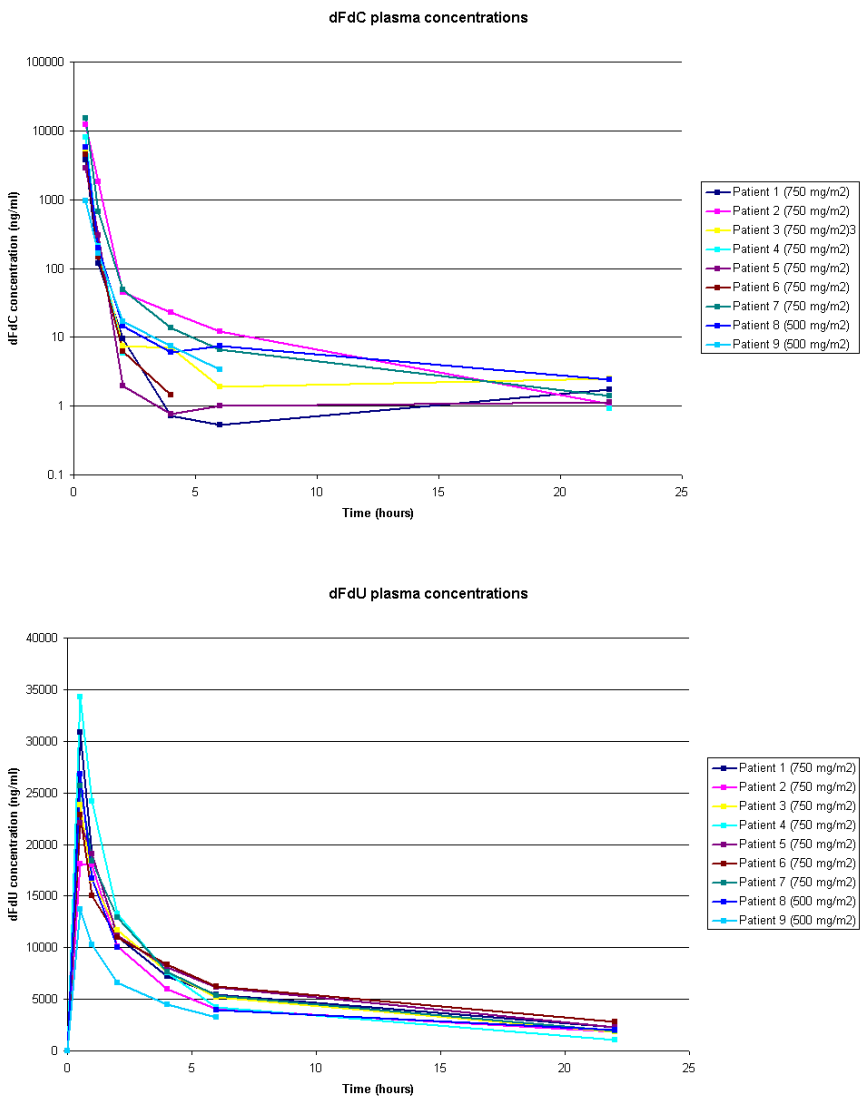


Figure 2: Individual dFdC (upper figure) and dFdU (lower figure) PK curves from 9 patients after receiving single doses of 750 mg/m² (n=7) or 500 mg/m² (n=2) gemcitabine.

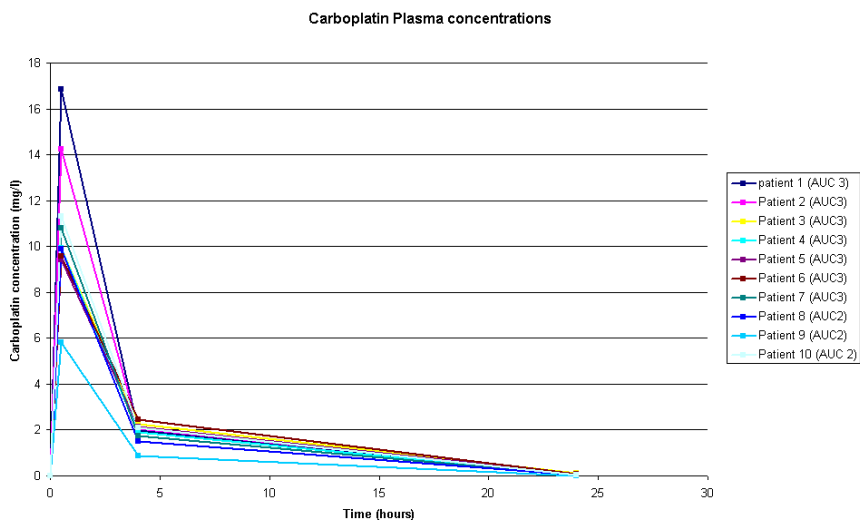
Antitumor activity

Eight patients had at least 1 response evaluation following treatment in this study. One patient with metastasized melanoma, treated at dose-level 1, had a confirmed partial response that lasted for 6 cycles. CT images of this patient,

Parameters	AUC 2 (n=3) Median (range)	AUC 3 (n=7) Median (range)
Cmax (mg/l)	9.9 (5.8-11.3)	10 (9.4-16.9)
AUCinf (mg.min/ml)	2.3 (1.4-2.9)	3.0 (2.6-3.5)
Clearance (ml/min)	114.8 (98.5-183.3)	119.7 (83.3-161.8)
T1/2 (hours)	3.7 (3.1-4.2)	4.0 (3.9-4.5)

Table 7 (left): PK Free carboplatin parameters derived from 10 patients treated at two different dose-levels.

Figure 3 (below): Individual concentration-time curves from 10 patient. Carboplatin concentrations were measured in ultrafiltrate.



who was pretreated with radiotherapy, chemotherapy (DTIC), and two lines of experimental therapy, are shown in figure 5. All other patients (n=7) had stable disease as best response. Some patients remained on-study for a long period of time, including a patient with a cortical thymoma, who remained on-study for 9 cycles (27 weeks). This patient went off-study upon his own request not due to progressive disease, but because it was anticipated that a maximum response of SD was achieved, and it was considered not in the benefit of the patient to continue treatment. Two patients with breast carcinoma, treated at dose-level -4, remained on treatment for 27 and 24 weeks, respectively. A patient with ovarium carcinoma, also treated at dose-level -4, remained on-study for 24 weeks. Median time of treatment at dose-level 1 was 12 weeks (range 2-27 weeks), the 3 patients treated at dose-level -4 remained on-study for 27, 27, and 24 weeks, respectively. Overall, the median time of treatment was 21 weeks, with a range of 2-27 weeks.

Table 8: Gemcitabine triphosphate (dFdCTP) concentrations in white blood cells

Parameters	500 mg (n=2)	750 mg (n=7)
	Median (range)	
Cmax (ng/mg protein)	533.5 (354.9-712.1)	410.7 (149.1-758.5)
AUCinf (ng.hr/mg protein)	11108 ^a	7711 ^b (5017-1251)
T1/2 (hours)	7.9 ^a	11.1 ^b (8.2-14.6)

^a n=1, ^b n=6

Discussion

This report described the experience of the first 10 patients that were treated with the combination of gemcitabine, carboplatin and sorafenib. The study was still ongoing at the time this report was written, and no MTD was reached. However, we did manage to identify a non-tolerable dose of 200 mg BID sorafenib, carboplatin AUC3 and 750 mg/m² gemcitabine.

At this dose-level, which was the starting dose-level, 3 out of 6 patients experienced a DLT, which was grade 3 fatigue in all cases. The incidence and severity of fatigue in this study was high, and unexpected. Fatigue was a DLT in the single agent sorafenib phase I study, but this was at a dose of 800 mg BID (24). Moreover, the incidence of fatigue following administration of gemcitabine/carboplatin is only infrequently observed (25). Other frequently observed non-hematological toxicities in this study included gastrointestinal side-effects including nausea, vomiting, and diarrhea. These toxicities are frequently observed following treatment with gemcitabine and carboplatin (except diarrhea) (26), and also after sorafenib administration (27). Sorafenib administration is probably also related to the occurrence of grade 4 rash, which was observed in one patient (28). It must be noted however, that higher doses were used in the referred studies.

The majority of the observed laboratory abnormalities can also be attributed to one or more of the administered agents. Bone marrow toxicity is a well known side-effect of carboplatin and gemcitabine (29), and was also observed in the phase I study with sorafenib and gemcitabine (30). Consequently, the high incidence of grade 3 thrombocytopenia and lymphopenia in this study was not surprising. This does not account for the frequently observed liver disturbances in this study. These are uncommon after administration of sorafenib alone

Chapter 9.1

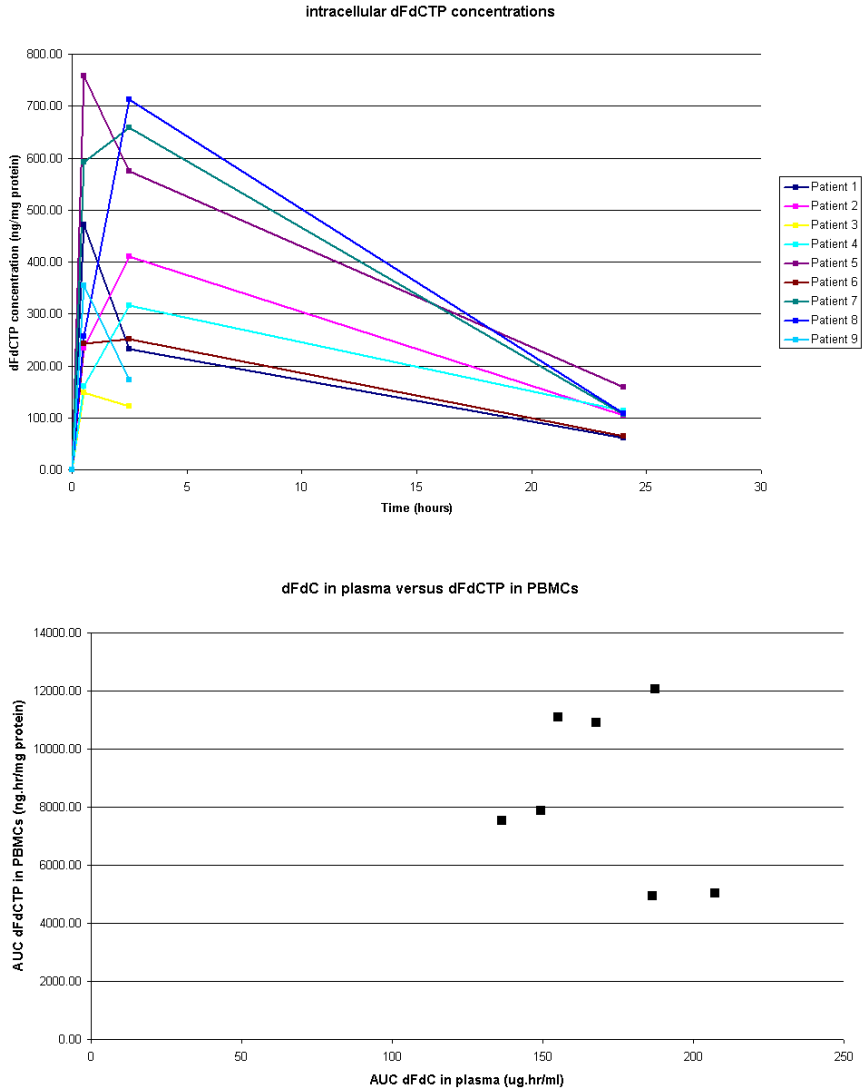


Figure 4: Intracellular dFdCTP concentrations (upper), and the relation between the exposure to gemcitabine and intracellular dFdCTP levels (lower). No correlation was found between the two parameters ($p=0.879$, spearman rank correlation test).

(31), and were also not observed following carboplatin and gemcitabine (32). However, grade 3 AST and ALT elevations were observed in the phase I study with sorafenib and gemcitabine (33). Grade 3 GGT toxicity was not reported in this study. The hypophosphatemia we observed in our study was probably related to sorafenib administration (34). In summary, most of the

hematological and non-hematological toxicities can be attributed to one or more of the administered agents. However, we did not expect a high incidence of these toxicities already at the starting dose-level.

When compared with other studies where sorafenib was combined with gemcitabine or platinum analogs, it appeared that in our study the tolerated doses are much lower. It has been demonstrated in phase I studies that full doses of sorafenib (400 mg BID) can be safely combined with high doses of oxaliplatin (35), gemcitabine (36), or even a carboplatin/paclitaxel doublet (37). In our study, only half the recommended sorafenib dose, together with relatively low doses of gemcitabine and carboplatin, appeared intolerable.

The low non-tolerable doses in our study, compared with the studies mentioned in the above, raise the hypothesis that this might be due to a chance effect. Generally, only small numbers of patients enter phase I studies, and the occurrence of multiple DLTs at the starting dose-level might simply be a consequence of bad luck. However, we believe this was not the case in our study, since all patients were in good condition (WHO score 0 or 1) at baseline. The DLT was fatigue grade 3 in all cases, which limits the hypothesis that these effects were due to a chance effect.

We believe that the unexpected high incidence of toxicities in this study can also not be attributed to pharmacokinetic interactions. The pharmacokinetics of sorafenib did not differ from that observed in literature (38), and we found no differences in exposure to carboplatin compared with the estimated target-exposure using the Calvert formula. Using sensitive detection methods (39), we were able to identify a terminal elimination half-life for dFdC of around 8 hours. This half-life is frequently not observed in clinical studies due to the low plasma concentrations at the terminal phase. The terminal half-life of dFdU at the 2 dose-levels was 12.5 and 22.9 hours, respectively. The analysis of dFdU concentrations in plasma is important, since dFdU is an active metabolite (40). We found no correlation between dFdC plasma concentrations and intracellular dFdCTP levels, which might be due to the low sample size (n=7).

We observed promising anti-tumor activity in this study. At the starting dose-level, a partial response was observed in a heavily pretreated patient with metastasized melanoma. This response might be due to the effects of sorafenib on BRAF, although it was demonstrated that single agent sorafenib

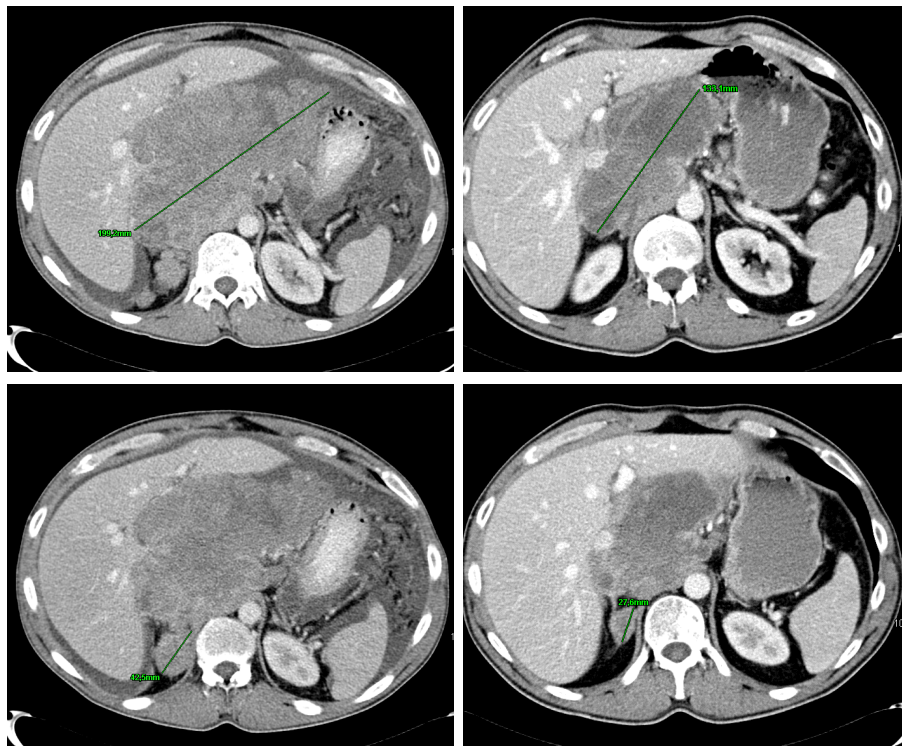


Figure 5: CT images of a melanoma patient treated at the starting dose-level of 750 mg/m² gemcitabine, AUC3 carboplatin and 200 mg BID sorafenib. This patient had a partial response following 2 cycles of treatment, that was confirmed after 4 and 6 cycles of treatment. Left images represent baseline scans, right images scans after 4 cycles (12 weeks) of treatment.

has little efficacy in advanced melanoma patients (41). Interestingly, we also observed promising activity at the lower dose-level, with three patients staying on treatment for 27, 27, and 24 weeks, respectively. These prolonged disease stabilizations suggest that the here studied drugs are active when combined, even at the lower dose-levels.

In conclusion, this report described the first experiences of 10 patients in a phase I trial with sorafenib, gemcitabine and carboplatin. The starting dose of 200 mg BID sorafenib, carboplatin AUC3, and 750 mg/m² gemcitabine was intolerable, with grade 3 fatigue as dose-limiting toxicity. The profile of the observed toxicities was not surprising given the toxicity profiles of the three administered drugs. The severity of the toxicities at the starting dose-level was surprising. The study is ongoing to establish the maximum tolerable dose for this combination of drugs.

Acknowledgement

We are grateful for the unrestricted grant from Bayer Healthcare, a division of Bayer Schering Pharma, and we thank Bienvenu Loumbé and Clifton Meije for supporting this trial.

References

1. Wilhelm, S. M., Carter, C., Tang, L. et al. BAY 43-9006 exhibits broad spectrum oral antitumor activity and targets the RAF/MEK/ERK pathway and receptor tyrosine kinases involved in tumor progression and angiogenesis. *Cancer Res.* 2004;64:7099-7109.
2. Clark, J. W., Eder, J. P., Ryan, D. et al. Safety and pharmacokinetics of the dual action Raf kinase and vascular endothelial growth factor receptor inhibitor, BAY 43-9006, in patients with advanced, refractory solid tumors. *Clin.Cancer Res.* 2005;11:5472-5480.
3. Strumberg, D., Richly, H., Hilger, R. A. et al. Phase I clinical and pharmacokinetic study of the Novel Raf kinase and vascular endothelial growth factor receptor inhibitor BAY 43-9006 in patients with advanced refractory solid tumors. *J.Clin.Oncol.* 2005;23:965-972.
4. Escudier, B., Eisen, T., Stadler, W. M. et al. Sorafenib in advanced clear-cell renal-cell carcinoma. *N.Engl.J.Med.* 2007;356:125-134.
5. Llovet, J. M., Ricci, S., Mazzaferro, V. et al. Sorafenib in advanced hepatocellular carcinoma. *N.Engl.J.Med.* 2008;359:378-390.
6. Cheng, A. L., Kang, Y. K., Chen, Z. et al. Efficacy and safety of sorafenib in patients in the Asia-Pacific region with advanced hepatocellular carcinoma: a phase III randomised, double-blind, placebo-controlled trial. *Lancet Oncol.* 2009;10:25-34.
7. Heim, M., Sharifi, M., Hilger, R. A. et al. Antitumor effect and potentiation or reduction in cytotoxic drug activity in human colon carcinoma cells by the Raf kinase inhibitor (RKI) BAY 43-9006. *Int.J.Clin.Pharmacol.Ther.* 2003;41:616-617.
8. Richly, H., Schultheis, B., Adamietz, I. A. et al. Combination of sorafenib and doxorubicin in patients with advanced hepatocellular carcinoma: results from a phase I extension trial. *Eur.J.Cancer.* 2009;45:579-587.
9. McDermott, D. F., Sosman, J. A., Gonzalez, R. et al. Double-blind randomized phase II study of the combination of sorafenib and dacarbazine in patients with advanced melanoma: a report from the 11715 Study Group. *J.Clin.Oncol.* 2008;26:2178-2185.
10. Duran, I., Hotte, S. J., Hirte, H. et al. Phase I targeted combination trial of sorafenib and erlotinib in patients with advanced solid tumors. *Clin.Cancer Res.* 2007;13:4849-4857.
11. Adjei, A. A., Molina, J. R., Mandrekar, S. J. et al. Phase I trial of sorafenib in combination with gefitinib in patients with refractory or recurrent non-small cell lung cancer. *Clin.Cancer Res.* 2007;13:2684-2691.
12. Siu, L. L., Awada, A., Takimoto, C. H. et al. Phase I trial of sorafenib and gemcitabine in advanced solid tumors with an expanded cohort in advanced pancreatic cancer. *Clin.Cancer Res.* 2006;12:144-151.
13. Flaherty, K. T., Schiller, J., Schuchter, L. M. et al. A phase I trial of the oral, multikinase inhibitor sorafenib in combination with carboplatin and paclitaxel. *Clin.Cancer Res.* 2008;14:4836-4842.
14. Pfisterer, J., Plante, M., Vergote, I. et al. Gemcitabine plus carboplatin compared with carboplatin in patients with platinum-sensitive recurrent ovarian cancer: an intergroup trial of the AGO-OVAR, the NCIC CTG, and the EORTC GCG. *J.Clin.Oncol.* 2006;24:4699-4707.
15. Wang, L. R., Huang, M. Z., Zhang, G. B. et al. Phase II study of gemcitabine and carboplatin in patients with advanced non-small-cell lung cancer. *Cancer Chemother.Pharmacol.* 2007;60:601-607.
16. Laessig, D., Stemmler, H. J., Vehling-Kaiser, U. et al. Gemcitabine and carboplatin in intensively pretreated patients with metastatic breast cancer. *Oncology.* 2007;73:407-414.

17. Calvert, A. H., Newell, D. R., Gumbrell, L. A. et al. Carboplatin dosage: prospective evaluation of a simple formula based on renal function. *J.Clin.Oncol.* 1989;7:1748-1756.
18. Cockcroft, D. W. and Gault, M. H. Prediction of creatinine clearance from serum creatinine. *Nephron.* 1976;16:31-41.
19. Cancer Therapy Evaluation Program NCI Common Terminology Criteria AE Version 3.0 (NCI-CTCAE v3.0). 2006;
20. Veltkamp, S. A., Jansen, R. S., Callies, S. et al. Oral administration of gemcitabine in patients with refractory tumors: a clinical and pharmacologic study. *Clin.Cancer Res.* 2008;14:3477-3486.
21. Veltkamp, S. A., Jansen, R. S., Callies, S. et al. Oral administration of gemcitabine in patients with refractory tumors: a clinical and pharmacologic study. *Clin.Cancer Res.* 2008;14:3477-3486.
22. van Warmerdam, L. J., van Tellingen, O., Maes, R. A. et al. Validated method for the determination of carboplatin in biological fluids by Zeeman atomic spectrometry. *Fresenius J.Anal.Chem.* 1995;351:1820-1824.
23. Therasse, P., Arbuck, S. G., Eisenhauer, E. A. et al. New guidelines to evaluate the response to treatment in solid tumors. European Organization for Research and Treatment of Cancer, National Cancer Institute of the United States, National Cancer Institute of Canada. *J.Natl.Cancer Inst.* 2000;92:205-216.
24. Strumberg, D., Richly, H., Hilger, R. A. et al. Phase I clinical and pharmacokinetic study of the Novel Raf kinase and vascular endothelial growth factor receptor inhibitor BAY 43-9006 in patients with advanced refractory solid tumors. *J.Clin.Oncol.* 2005;23:965-972.
25. Wang, L. R., Huang, M. Z., Zhang, G. B. et al. Phase II study of gemcitabine and carboplatin in patients with advanced non-small-cell lung cancer. *Cancer Chemother.Pharmacol.* 2007;60:601-607.
26. Wang, L. R., Huang, M. Z., Zhang, G. B. et al. Phase II study of gemcitabine and carboplatin in patients with advanced non-small-cell lung cancer. *Cancer Chemother.Pharmacol.* 2007;60:601-607.
27. Strumberg, D., Richly, H., Hilger, R. A. et al. Phase I clinical and pharmacokinetic study of the Novel Raf kinase and vascular endothelial growth factor receptor inhibitor BAY 43-9006 in patients with advanced refractory solid tumors. *J.Clin.Oncol.* 2005;23:965-972.
28. Lee, W. J., Lee, J. L., Chang, S. E. et al. Cutaneous adverse effects in patients treated with the multitargeted kinase inhibitors sorafenib and sunitinib. *Br.J.Dermatol.* 2009;
29. Wang, L. R., Huang, M. Z., Zhang, G. B. et al. Phase II study of gemcitabine and carboplatin in patients with advanced non-small-cell lung cancer. *Cancer Chemother.Pharmacol.* 2007;60:601-607.
30. Siu, L. L., Awada, A., Takimoto, C. H. et al. Phase I trial of sorafenib and gemcitabine in advanced solid tumors with an expanded cohort in advanced pancreatic cancer. *Clin.Cancer Res.* 2006;12:144-151.
31. Strumberg, D., Clark, J. W., Awada, A. et al. Safety, pharmacokinetics, and preliminary antitumor activity of sorafenib: a review of four phase I trials in patients with advanced refractory solid tumors. *Oncologist.* 2007;12:426-437.
32. Tomizawa, Y., Ishihara, S., Iijima, H. et al. A phase I dose escalation study of biweekly gemcitabine and carboplatin in completely resected stage IB-IIIa nonsmall cell lung cancer. *Am.J.Clin.Oncol.* 2007;30:498-502.
33. Siu, L. L., Awada, A., Takimoto, C. H. et al. Phase I trial of sorafenib and gemcitabine in advanced solid tumors with an expanded cohort in advanced pancreatic cancer. *Clin.Cancer Res.* 2006;12:144-151.
34. Kane, R. C., Farrell, A. T., Saber, H. et al. Sorafenib for the treatment of advanced renal cell carcinoma. *Clin.Cancer Res.* 2006;12:7271-7278.
35. Kupsch, P., Henning, B. F., Passarge, K. et al. Results of a phase I trial of sorafenib (BAY 43-9006) in combination with oxaliplatin in patients with refractory solid tumors, including colorectal cancer. *Clin.Colorectal Cancer.* 2005;5:188-196.
36. Siu, L. L., Awada, A., Takimoto, C. H. et al. Phase I trial of sorafenib and gemcitabine in advanced solid tumors with an expanded cohort in advanced pancreatic cancer. *Clin.Cancer Res.* 2006;12:144-151.
37. Flaherty, K. T., Schiller, J., Schuchter, L. M. et al. A phase I trial of the oral, multikinase inhibitor sorafenib in combination with carboplatin and paclitaxel. *Clin.Cancer Res.* 2008;14:4836-4842.

38. Strumberg, D., Clark, J. W., Awada, A. et al. Safety, pharmacokinetics, and preliminary antitumor activity of sorafenib: a review of four phase I trials in patients with advanced refractory solid tumors. *Oncologist*. 2007;12:426-437.
39. Vainchtein, L. D., Rosing, H., Thijssen, B. et al. Validated assay for the simultaneous determination of the anti-cancer agent gemcitabine and its metabolite 2',2'-difluorodeoxyuridine in human plasma by high-performance liquid chromatography with tandem mass spectrometry. *Rapid Commun. Mass Spectrom*. 2007;21:2312-2322.
40. Veltkamp, S. A., Pluim, D., van Eijndhoven, M. A. et al. New insights into the pharmacology and cytotoxicity of gemcitabine and 2',2'-difluorodeoxyuridine. *Mol. Cancer Ther*. 2008;7:2415-2425.
41. Eisen, T., Ahmad, T., Flaherty, K. T. et al. Sorafenib in advanced melanoma: a Phase II randomised discontinuation trial analysis. *Br.J.Cancer*. 2006;95:581-586.

10

Conclusion and Perspectives

Chapter 10: Conclusion and perspectives

With the shift from classical cytotoxic drugs to targeted anticancer agents, the clinical development program of drug candidates is changing as well. The focus is now, more than in the era of the classical anticancer drugs, on pharmacodynamic analyses. This even accounts for the early clinical trials, as described in this thesis.

The adage: "The higher the dose, the more effective", has been the golden standard in the era of the classical cytotoxic agents, justifying the use of the MTD as the recommended phase II dose. Targeted agents act specifically on a single or a set of target molecules, thereby minimizing the side-effects. Therefore, these drugs might be effective at doses far lower than the MTD. Also, the RECIST approach, by looking at size differences only, might not be the best way to judge whether a drug is active or not. This especially accounts for targeted drugs, as has been shown for imatinib. In chapter 2, the use of combined PET/CT imaging in the development of novel anticancer drugs was reviewed. Combined PET/CT can aid in the development of novel anticancer drugs by various means, including earlier response measurements, and assessment of various pharmacodynamic parameters. Despite the clear advantages of PET/CT over single CT, all here described phase I studies used standard RECIST criteria for response evaluations. PET scans were made in the studies with AZD1152 (chapter 3.2) and PF00299804 (chapter 8.1, data not included), but no metabolic responses were observed. Several factors might have attributed to these disappointing results. First, the investigated compounds could have lacked the potency needed to induce a metabolic response. Alternatively, the patients included may not have had appropriate tumor types for FDG-PET evaluation. FDG-PET measurements are not suitable for slowly growing tumors, for instance. It must be stated that AZD1152 and PF00299804 are not the ideal candidate drugs for FDG-PET evaluations, since they are not expected to induce a metabolic response. In stead, E7080 would have made a great candidate. This drug inhibits c-kit, a tyrosine kinase that is involved in regulation of the glucose transporter GLUT-1, and is therefore expected to inhibit the uptake of FDG in tumor cells. Imatinib, perhaps the best example of a drug whose activity can be excellently evaluated by FDG-PET, also inhibits c-kit. Unfortunately, no FDG-PET scans were made in the here described phase I study with E7080 (chapter 7.1).

Several of the here reported phase I studies did use alternative endpoints to assess the efficacy of the investigational drugs, with varying degrees of success. The use of pharmacodynamic assays was more successful in the studies where tumor biopsies were obtained prior to and after administration of the investigational drug(s). Although considered invasive, looking at effects in tumor tissue is still the best way to assess pharmacodynamic effects *in vivo*. Alternatively, surrogate tissues like skin biopsies or peripheral blood mononuclear cells (PBMCs) can be used. However, the obtained results in these tissues might not always correlate with effects on the tumor itself. We observed this in our phase I study with carboplatin and topotecan (chapter 5), where we investigated the schedule-dependent toxicity of this combination. We found no correlation between the formation of platinum adducts in PBMCs and in tumor tissue. These effects can be explained by differences between the tumor target and the surrogate target. In our example, differences in DNA repair mechanisms between tumor cells and PBMCs might attribute to differences in outcome of the assay.

The phase I study with AZD5438 (chapter 4), an orally available inhibitor of cyclin-dependent kinase-2, failed to demonstrate pharmacodynamic effects at all, unfortunately due to poor quality of the collected PBMC and hair follicle samples. Earlier pharmacodynamic studies with AZD5438 in healthy volunteers were successful, highlighting the difficulties of translating pharmacodynamic measurements from healthy volunteer studies to trials involving patients with advanced cancer.

Fortunately, we managed to obtain valuable pharmacodynamic results in other trials, for instance in the phase I trial with the pan-HER inhibitor PF-00299804 (chapter 8). We demonstrated significant reduction in MAPK phosphorylation (a biomarker for HER-signaling) and Ki-67 expression (a marker for cell division) in skin biopsy samples following treatment with the investigational agent. Moreover, we found a relationship between the administered dose and the degree of target inhibition.

In the study with olaparib (AZD2281, chapter 6.1), we found that doses far below the MTD induced significant target inhibition in tumor tissue, suggesting that the administration of lower doses of the drug might be sufficient to induce a therapeutic effect. This finding was confirmed in the expansion phase of the study, where patients with BRCA mutated tumors were included. These

patients received doses of 200 mg BID, while the MTD was set at 400 mg BID. Significant antitumor effects were observed in these patients.

This finding brings us to another important point: The issue of selecting patients for trials with targeted agents. In the aforementioned trial with the PARP inhibitor olaparib we observed little efficacy in patients with various solid malignancies (BRCA wild-type tumors), even at the MTD of 400 mg BID. However, as expected from preclinical studies in mouse models, patients with BRCA-mutated cancers responded much better. These effects can be explained by the nature of the BRCA-deficient tumor cells. They are unable to repair the damage caused by olaparib, since they lack the functional homologous recombination repair pathway that is needed for repair of double-strand DNA breaks. This will eventually lead to cell death. Cells with a functional homologous recombination pathway can repair their damaged DNA, and survive. The phase I study with olaparib is a good example of how preclinical findings can be translated into an effective anticancer therapy for a selective patient population.

In future studies with targeted anticancer agents, patient selection based on tumor characteristics will, and should become more and more routine practice. As for today, we have to distinguish drugs that very specifically target one tumor type, like the PARP inhibitor AZD2281, from drugs with potential antitumor activity against a wider range of tumor types, like the angiogenesis inhibitor E7080. It is more challenging to select a specific patient population for trials with agents belonging to the latter category. In order to be able to select patients for future clinical studies with targeted agents, more knowledge about the mechanism of action of the investigational agents is needed. Also, in the near future, molecular testing of tumor tissue must become cheaper, faster, and easier in order to make patient selection for phase I clinical trials routine practice.

Several of the investigational agents that were described in this thesis have advanced to phase II clinical trials, while the development of others stalled after termination of the phase I trial. olaparib, E7080 and PF00299804 have shown to be active drugs in the here described phase I trials. olaparib is currently undergoing phase II clinical testing, and encouraging results of two phase II trials in patients with BRCA deficient breast and ovarian cancer were presented at ASCO this year. Without doubt, there is a bright future for this

drug in patients with BRCA deficient cancers, or even in other cancers with defined DNA repair deficiencies, especially homologous recombination deficiency. However, as there are several competitive PARP inhibitors in development, the future of olaparib does not only depend on its activity, but also on the study-design of the future phase II and phase III studies evaluating the drug. Olaparib was the first PARP inhibitor to be tested in patients with BRCA deficient cancers, giving the compound a lead compared with other compounds of the same class. Currently, many combination studies with olaparib are ongoing. Preclinical work revealed the combination of PARP inhibitors with platinum compounds to be synergistic. This combination might be the most potent, but also leads to enhanced toxicities, predominantly myelosuppression. It is essential to identify a schedule that allows a dose-intensity leading to efficacy and manageable toxicities. Based on the mechanism of action of PARP inhibitors, one could suggest a lead-in period of olaparib of 4 or 5 days, followed by a standard dose of carboplatin or a carboplatin/paclitaxel doublet, once every 4 weeks. The combination of olaparib with carboplatin or carboplatin/paclitaxel is currently undergoing clinical evaluation, also in the Netherlands Cancer Institute.

For E7080, phase II studies should be planned in patients with melanoma and renal cell carcinoma, since the drug showed impressive activity against these tumor types in the phase I study described in this thesis. In these phase II studies, E7080 should be dosed at its MTD of 25 mg, despite the toxicities that were observed in patients receiving this dose. Lower dose-levels of E7080 will inevitably lead to lower response rates, and the most profound toxicities (hypertension and proteinuria) can be treated with commonly applies antihypertensive drugs. A challenge in the development of E7080 will be to deal with the stomatitis that we observed when the drug was given at higher, efficacious doses. At present, there is no remedy for this side-effect, of which the etiology is unclear.

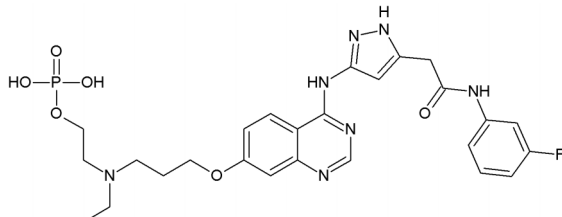
Finally, PF00299804 showed activity in patients with NSCLC that were previously pre-treated with the reversible EGFR inhibitors gefitinib or erlotinib. Phase II studies in patients with advanced NSCLC are ongoing at the recommended phase II dose of 45 mg. Recent results of phase II studies with competitive irreversible HER inhibitors were rather disappointing, hopefully PF00299804 will do better.

In conclusion, in this thesis several phase I studies are described with novel, targeted anticancer agents. Some of these studies successfully implemented pharmacodynamic analyses, although never as a primary endpoint. Future studies with targeted agents should focus more on these pharmacodynamic endpoints, and patients for these studies should be included based on their tumor characteristics. As for the compounds discussed in this thesis: Some of the here described agents are currently being evaluated in phase II clinical trials. The future of these agents does not only depend on their activity, but also on the design of the studies evaluating their activity.

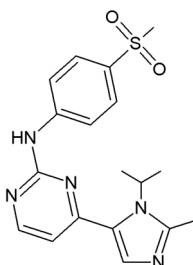
Chemical structures

Chemical structures of investigated molecules in this thesis

Chapter 3.2: AZD1152

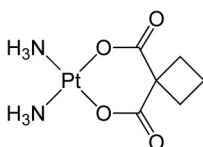


Chapter 4: AZD5438

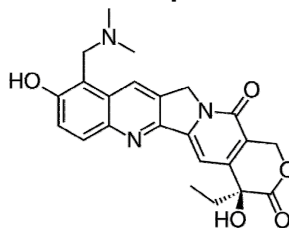


Chapter 5

Carboplatin

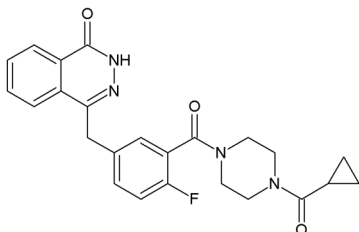


Topotecan

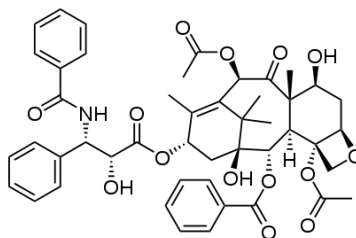


Chapter 6

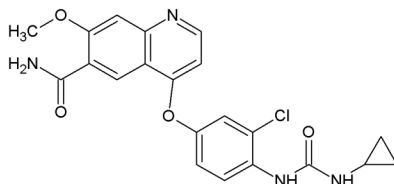
AZD2281



Paclitaxel



Chapter 7: E7080

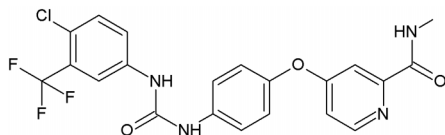


Chapter 8: PF00299804

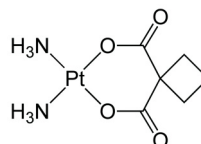
The chemical structure of PF00299804 was not available at the time this thesis was completed.

Chapter 9

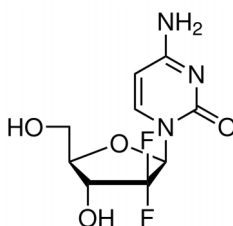
Sorafenib



Carboplatin



Gemcitabine



Summary

Summary

Despite the advances in the treatment of cancer, the disease is still responsible for approximately 40.000 deaths per year in the Netherlands only. The high incidence and death rates for this disease strongly advocate the search for better treatment options. Unfortunately, the clinical development program for any given investigational anti-cancer agent is time-consuming and expensive.

Following successful preclinical evaluation, the first clinical studies with novel anti-cancer agents are performed to assess the safety of the investigational drugs, and to determine the maximum tolerable dose (MTD) in patients with advanced disease, for whom no standard treatment options are available. Also important in these studies are the pharmacokinetic analyses. Serial blood samples were collected following drug administration to investigate how the agent behaves in the human body. The incorporation of pharmacodynamic endpoints is becoming increasingly important in these studies. This thesis describes several phase I studies with novel anti-cancer agents, or combinations of anti-cancer agents.

Chapter 2.1 describes the use of the combined PET/CT scanner in drug development. PET/CT combines the functional images of the PET scan with the anatomical information provided by the CT scan. PET/CT can be used in drug development in several ways. First, by assessing the early response to treatment with investigational agents. Using FDG-PET, it is possible to determine the metabolic activity of the tumor, which often gives a better indication of disease activity compared with conventional anatomical imaging methods. FDG-PET has become a valuable tool for response assessments, because metabolic responses are often observed earlier in the course of therapy than changes in tumor size. Using other PET tracers, PET/CT can also be used for drug biodistribution studies and pharmacodynamic studies, making this imaging modality a versatile and valuable tool in drug development. The use of FDG-PET for assessment of response to treatment with sorafenib, a multi-kinase inhibitor, is discussed in **chapter 2.2**. FDG-PET might be valuable for this purpose.

The topic of **Chapter 3** is aurora kinase inhibitors, a novel class of anticancer agents. The aurora kinase family consists of three family members, designated

aurora A, B, and C. Aurora kinase A and B play important roles in mitosis and cell division, and upregulation of these proteins is observed in several tumor types. Several inhibitors of aurora kinase A, aurora kinase B, or both, are currently in clinical development, which is reviewed in **chapter 3.1**. A phase I study with one of these compounds, AZD1152, is described in **chapter 3.2**. AZD1152 is a selective inhibitor of aurora kinase B, and was investigated in two different dosing schedules. We found that AZD1152 could be safely administered as a 2-hour infusion once weekly, and once every 14 days. Neutropenia was the most frequent, and dose-limiting toxicity for both schedules. The maximum tolerable doses for both schedules were 200 and 450 mg, respectively. Pharmacokinetic studies revealed dose-linearity, and a rapid conversion from the pre-drug AZD1152 to the active moiety AZD1152-hQPA. Due to disappointing anti-tumor activity in this single-agent study in patients with solid tumors, future studies should explore AZD1152 in patients with hemato-oncological malignancies, or as part of a combination regimen in solid tumors.

Chapter 4 describes three phase I studies with AZD5438, an orally available inhibitor of cyclin-dependent kinase 2 (CDK2) and CDK1 complexes. CDKs are core components of the cell cycle machinery, and drive the transition between cell cycle phases. The three here described phase I studies investigated AZD5438 administration four times daily once every seven days, for 14 consecutive days followed by seven days of rest, or continuously. The drug was well tolerated in a weekly dosing schedule, but not in the continuous dosing schedules. Pharmacokinetic studies demonstrated high inter-patient variability and accumulation after multiple doses, and pharmacodynamic assessments did not reveal consistent trends. Following the tolerability and exposure data from these studies, the clinical development program for AZD5438 was discontinued.

Topotecan, a topoisomerase-I inhibitor, and carboplatin, a cisplatin analogue, are both active anticancer drugs. The combination of these drugs is synergistic and schedule-dependent. To investigate this schedule dependency in the clinic, a phase I clinical trial was designed, which is described in **chapter 5**. The phase I study consisted of two parts. In part 1, patients received carboplatin on day 1 and topotecan on days 1, 2, and 3 (C→T schedule). In part 2, topotecan was administered on days 1, 2, and 3, followed by carboplatin on day 3 (T→C schedule). Pharmacodynamic assessments were performed in

tumor tissue as well as in white blood cells to investigate schedule dependent effects of this drug combination. It appeared that the T→C schedule was better tolerated, with less hematological and non-hematological toxicities. These effects could not be attributed to a pharmacokinetic interaction, because we found no difference in clearance and exposure to carboplatin and topotecan between the two schedules. Also, no schedule dependent effects were seen in platinum-DNA levels and topoisomerase activity in white blood cells and tumor tissue. Other than the investigated pharmacodynamic factors must explain the schedule dependent differences in toxicities.

Chapter 6 describes two phase I studies with the Poly(ADP-ribose) polymerase (PARP) inhibitor olaparib (AZD2281). PARP-1 is an enzyme that plays a key role in the repair of DNA single strand breaks via the base excision repair (BER) pathway. Inhibition of PARP leads to the accumulation of single strand DNA breaks, which can result in DNA double-strand breaks when replication forks stall at the site of the single strand break. Normally, double strand breaks are effectively repaired by a mechanism called homologous recombination. However, BRCA deficient tumor cells have no functional homologous repair mechanism, which makes these cells extremely sensitive to PARP inhibition. In **chapter 6.1**, the first phase I trial with olaparib is presented. Not only was olaparib well tolerated up to doses of 400 mg bi-daily, the drug appeared very effective in patients with BRCA deficient malignancies at lower doses of 200 mg. Over half of the patients with BRCA deficient ovarian, breast and prostate cancer derived clinical benefit from treatment with olaparib. Pharmacodynamic studies confirmed PARP inhibition in surrogate and tumor tissue. These results lead to the initiation of several studies combining olaparib with a variety of anti-cancer agents. One of these studies is described in **chapter 6.2**. In this study, olaparib was combined with the anti-mitotic agent paclitaxel. Patients received olaparib continuously at doses of 100 or 200 mg bi-daily, and paclitaxel once weekly at a dose of 80 mg/m². No dose-limiting toxicities were observed, suggesting that both dose-levels were safe. Interestingly, pharmacokinetic analyses revealed a significant reduction in exposure to olaparib of approximately 50 percent following co-administration of paclitaxel. More research is needed to study the mechanistic background of this interaction.

Another anti-tumor strategy is angiogenesis inhibition, which is described in **chapter 7**. Angiogenesis, the formation of new blood vessels from a pre-

existing vascular network, is essential for tumor growth and metastasis. E7080 is an orally available multi-kinase inhibitor that prevents tumor angiogenesis, primarily via inhibition of the vascular endothelial growth factor (VEGF) receptor KDR. E7080 also has activity against platelet-derived growth factor receptor (PDGFR), fibroblast growth factor receptor 1 (FGFR-1), and c-kit. In **chapter 7.1**, the first phase I study with E7080 in patients with advanced solid tumors is described. The drug was administered once daily up to doses of 32 mg. The maximum tolerable dose was 25 mg, and the dose-limiting toxicity was proteinuria. The most frequently observed toxicities were hypertension, gastrointestinal disorders, and stomatitis. Pharmacokinetic studies revealed dose-linearity and a half-life of around 7 hours. Promising signs of anti-cancer activity were observed in various tumor types, including melanoma and renal cell carcinoma. The case of a patient with osteosarcoma that was included in this study is presented in **chapter 7.2**. Elevated β -HCG and CA-125 serum levels were observed when this patient was screened for participation in the trial. Elevated β -HCG serum levels are usually an indication of pregnancy, and are rarely observed in patients with osteosarcoma. Elevated CA-125 serum levels in patients with osteosarcoma had not previously been documented. Immunohistochemical studies revealed the tumor to be the source of the elevated β -HCG serum levels, but we found no CA-125 expression in tumor tissue. Pregnancy was excluded, and the patient was treated with E7080. We measured both β -HCG and CA-125 serum levels to monitor treatment response. The β -HCG serum levels seemed to better reflect her disease status than the other tumor marker CA-125.

Yet another class of targeted anti-cancer agents constitute the HER-inhibitors. One of such agents, PF00299804, is described in **chapter 8**. the HER family of receptor tyrosine kinases comprises four members, designated HER1, HER2, HER3, and HER4. Upon ligand binding, and subsequent homo- or heterodimerization, the HER receptors trigger various intracellular signal transduction pathways involved in cell proliferation and differentiation. The overexpression of HER family members is observed in a wide variety of malignancies, and HER1 and HER2 have been validated as therapeutic targets in several human tumors. PF00299804 is an orally available, irreversible inhibitor of HER1, HER2, and HER4. In the here described phase I study, PF00299804 was administered once daily continuously (part A) and intermittently (part B) to patients with advanced solid tumors. The maximum tolerable dose was set at 45 mg daily, the dose-limiting toxicities included

Summary

stomatitis and skin toxicities. The pharmacokinetics revealed dose linearity and a long half-life of 46 to 72 hours. A dose-dependent increase in target inhibition was observed in skin biopsy samples. Encouraging signs of anti-tumor activity were observed in patients with non-small cell lung cancer.

The last phase I study in this thesis is described in **chapter 9**. This study explored the safety, pharmacokinetics, and pharmacodynamics of sorafenib in combination with gemcitabine and carboplatin. Sorafenib is an orally available multi-kinase inhibitor with anti-angiogenic properties that is registered for the treatment of renal cell carcinoma and hepatocellular carcinoma. The combination of gemcitabine, a nucleoside antimetabolite, and carboplatin is approved for the treatment of advanced ovarian cancer, but also showed activity in patients with non-small cell lung cancer and breast cancer. In this study, patients received sorafenib continuously, carboplatin on day 1, and gemcitabine on days 1 and 8 of each treatment cycle (21 days). The starting dose (200 mg bi-daily sorafenib, carboplatin AUC3, gemcitabine 750 mg/m²) appeared non-tolerable with three out of six patients experiencing a dose-limiting toxicity (grade 3 fatigue in all cases). Subsequently, the protocol was amended, and novel dose-levels were investigated. Data obtained from pharmacokinetic and pharmacodynamic analyses were consistent with data from literature. The study was ongoing at the time of the report to establish the maximum tolerable dose of this combination.

In conclusion, several phase I studies with novel anti-cancer agents are reported in this thesis. Several of the here described compounds are now under evaluation in phase II studies. Future studies with targeted agents should focus more on pharmacodynamic endpoints, and patients for future phase I studies should be included based on their tumor characteristics. PET/CT might be a helpful tool for both these purposes.

Samenvatting

Samenvatting

Ondanks de vooruitgangen die de afgelopen jaren gemaakt zijn in de behandeling van kanker, is de ziekte nog altijd verantwoordelijk voor ongeveer 40.000 doden per jaar, in Nederland alleen. De hoge incidentie- en sterftcijfers pleiten voor meer onderzoek naar betere behandelmethoden van deze ziekte. Helaas is de ontwikkeling van nieuwe anti-kanker medicijnen een tijdrovend en geldverslindend proces.

Volgend op succesvolle preklinische onderzoeken worden de eerste klinische studies met nieuwe anti-kanker medicijnen, zogenaamde fase I studies, uitgevoerd in patiënten voor wie geen standaardbehandeling meer mogelijk is. Deze studies worden vooral uitgevoerd om de veiligheid en de maximaal verdraagbare dosering (MTD) te onderzoeken. Een andere belangrijke component van deze studies is de farmacokinetiek. Door middel van een reeks bloedafnames na toediening van het onderzochte medicijn wordt gekeken hoe het middel zich in het menselijk lichaam gedraagt. Maar ook farmacodynamische eindpunten, als maat voor de effectiviteit van de onderzochte middelen, worden steeds belangrijker in deze vroege klinische studies. In dit proefschrift worden verscheidene fase I studies beschreven met nieuwe anti-kanker medicijnen, of combinaties van anti-kanker medicijnen.

Hoofdstuk 2.1 beschrijft de toepassing van de PET/CT scanner bij de ontwikkeling van nieuwe medicijnen tegen kanker. De PET/CT scanner combineert de functionele beelden van de PET scanner met de anatomische beelden van de CT scanner. Gecombineerde PET/CT kan op diverse manieren bijdragen aan de ontwikkeling van nieuwe anti-kanker middelen. Ten eerste door de vroege respons op behandeling met nieuwe middelen te meten. Met behulp van FDG-PET is het mogelijk om de metabole activiteit van de tumor te meten. Dit geeft vaak een betere indicatie van ziekte activiteit dan de standaard anatomische imaging methodieken. FDG-PET is waardevol gebleken bij het meten van respons op behandeling met diverse anti-kanker middelen, aangezien metabole veranderingen vaak eerder optreden dan veranderingen in tumorgrootte. Door gebruik te maken van andere PET-tracers kan PET/CT ook gebruikt worden voor geneesmiddel biodistributie studies, en farmacodynamische studies. Bij elkaar genomen maakt dit de PET/CT scanner tot een veelzijdig en waardevol apparaat bij de ontwikkeling van nieuwe anti-kanker medicijnen. Het gebruik van FDG-PET voor het meten van respons op

behandeling met sorafenib, een multi-kinase remmer, wordt besproken in **hoofdstuk 2.2**. FDG-PET lijkt erg geschikt te zijn voor dit doeleinde.

Hoofdstuk 3 handelt over de aurora kinase remmers, een nieuwe klasse anti-kanker middelen. De aurora kinase familie bestaat uit drie leden: Aurora kinase A, B, en C. Van aurora kinase A en B is bekend dat ze een belangrijke rol spelen bij mitose en celdeling, en dat overexpressie van deze eiwitten voorkomt bij verschillende soorten tumoren. Diverse remmers van aurora A, aurora B, of beide aurora kinases, zijn momenteel in klinische ontwikkeling. Een overzicht van deze middelen wordt gegeven in **hoofdstuk 3.1**. Een fase I studie met een van deze nieuwe middelen, AZD1152, staat beschreven in **hoofdstuk 3.2**. AZD1152, een selectieve remmer van aurora kinase B, werd in twee verschillende toedieningschema's onderzocht. De toediening van AZD1152 per 2-uurs infuus eenmaal per week en eens per 14 dagen bleek beiden veilig. De meest voorkomende bijwerking was neutropenie, en dit was ook de dosis-limiterende toxiciteit voor beide schema's. De maximaal verdraagbare dosering was 200 mg voor het wekelijkse schema, en 450 mg wanneer het middel eens per 2 weken toegediend werd. De farmacokinetiek van AZD1152 bleek lineair, en het middel werd snel na toediening omgezet in de actieve vorm AZD1152-hQPA. Vanwege de bescheiden anti-tumor activiteit van AZD1152 als monotherapie in patiënten met solide tumoren, zouden toekomstige studies met dit middel zich moeten richten op patiënten met hematologische tumoren, of op combinaties met andere anti-kanker middelen of radiotherapie.

Hoofdstuk 4 beschrijft drie fase I studies met het middel AZD5438, een oraal beschikbare remmer van cyclin-dependente kinase 2 (CDK2) en CDK1 complexen. CDKs zijn betrokken bij de overgang tussen de verschillende fasen van de celcyclus. De hier beschreven studies onderzochten AZD5438 in drie verschillende toedieningschema's: viermaal daags eens per 7 dagen, viermaal daags voor 14 opeenvolgende dagen gevolgd door een rustweek, en viermaal daags in een continue schema. Het middel werd goed verdragen in het wekelijkse schema, maar niet in de continue schema's. De farmacokinetiek was onvoorspelbaar, had een hoge inter-patiënt variabiliteit, en er vond ophoping plaats na continue toediening van het middel. Farmacodynamische onderzoeken lieten geen consistente trends zien. Tezamen hebben deze resultaten geleid tot het stopzetten van de ontwikkeling van AZD5438 als nieuw anti-kanker middel.

Topotecan, een topoisomerase-I remmer, en carboplatine, een cisplatine analoog, zijn beiden actieve anti-kanker middelen. De combinatie van deze middelen is synergistisch, en deze synergie is schema-afhankelijk. Om deze schema-afhankelijkheid te onderzoeken in de kliniek, werd er een klinische studie ontworpen, die beschreven staat in **hoofdstuk 5**. Deze fase-I studie bestond uit twee delen. In het eerste deel kregen patiënten carboplatine toegediend op dag 1, gevolgd door toediening van topotecan op dagen 1, 2, en 3 (C→T schema). In het tweede deel werd topotecan toegediend op dagen 1, 2, en 3, gevolgd door carboplatine toediening op dag 3 (T→C schema). Farmacodynamische onderzoeken werden uitgevoerd op tumor weefsel en in witte bloedcellen, om de schema-afhankelijke effecten van deze combinatie te bekijken. Het T→C schema werd beter verdragen dan het C→T schema, met minder hematologische en minder niet-hematologische bijwerkingen. Deze effecten waren niet het gevolg van een farmacokinetische interactie, aangezien er geen verschillen in klaring van en blootstelling aan carboplatine en topotecan werden gevonden tussen de verschillende schema's. Ook werden er geen schema-afhankelijke effecten gezien in platinum-adduct vorming en topoisomerase activiteit in witte bloedcellen en tumor weefsel. Andere farmacodynamische factoren dan diegene die in dit onderzoek beschreven worden moeten de schema-afhankelijke verschillen in toxiciteit verklaren.

Hoofdstuk 6 beschrijft twee fase-I studies met de Poly(ADP-ribose) polymerase (PARP) remmer olaparib (AZD2281). PARP-1 is een enzym dat een belangrijke rol speelt bij het repareren van enkelstrengs DNA breuken via een mechanisme dat ook wel base excision repair (BER) genoemd wordt. Remming van PARP leidt tot de ophoping van enkelstrengs DNA breuken, en dat kan weer leiden tot de vorming van dubbelstrengs DNA breuken, wanneer de cel zich wil delen. Het replicatiecomplex, bestaande uit diverse enzymen die DNA-strengen scheiden, vermenigvuldigen, en weer aan elkaar plakken, loopt dan namelijk vast op de enkelstrengs breuken in het DNA. De hierdoor gevormde dubbelstrengs DNA breuken kunnen normaliter gerepareerd worden door een mechanisme dat homologe recombinatie heet. Echter, BRCA deficiënte tumoren missen dit mechanisme, en zijn daarom extreem gevoelig voor PARP remmers. In **hoofdstuk 6.1** wordt de eerste fase-I studie met olaparib (AZD2281), een PARP remmer, beschreven. Niet alleen werd het middel goed verdragen tot doseringen van 400 mg tweemaal daags, ook bleek het middel erg effectief in patiënten met BRCA deficiënte tumoren, zelfs bij lagere doseringen van 200 mg tweemaal daags. Meer dan de helft van de behandelde

patiënten met BRCA deficiënte eierstok-, borst-, of prostaattumoren hadden baat bij de behandeling met olaparib, doordat hun tumoren kleiner werden, of tenminste vier maanden niet toenamen in grootte. Farmacodynamische studies toonden remming van PARP aan in witte bloedcellen en tumorweefsel van behandelde patiënten. Deze resultaten hebben geleid tot de initiatie van diverse studies waarbij olaparib gecombineerd werd met verscheidene anti-kanker middelen. Een van deze studies staat beschreven in **hoofdstuk 6.2**. In deze fase-I studie werd olaparib gecombineerd met de mitoseremmer paclitaxel. Patiënten namen olaparib tweemaal daags in op doseringen van 100 of 200 mg, en kregen eenmaal per week 80 mg/m² paclitaxel toegediend. Geen dosis-limiterende toxiciteiten werden waargenomen, wat aangaf dat deze combinatie van middelen goed verdragen werd. Een interessante bevinding in deze studie was dat de blootstelling aan olaparib gehalveerd werd na gelijktijdige toediening van paclitaxel. Meer onderzoek is nodig om het mechanisme achter deze farmacokinetische interactie uit te zoeken.

Een andere strategie om tumorcellen te doden, is door remming van angiogenese, wat beschreven wordt in **hoofdstuk 7**. Angiogenese, de aanmaak van nieuwe bloedvaten vanuit een bestaand vasculair netwerk, is essentieel voor tumoren om te kunnen groeien en uit te kunnen zaaien (metastaseren). E7080 is een oraal beschikbare multi-kinase remmer die de angiogenese remt, vooral door de signalering van de vascular endothelial growth factor (VEGF) receptor KDR te blokkeren. E7080 remt ook receptoren van andere groeifactoren, zoals platelet-derived growth factor receptor (PDGFR), fibroblast growth factor receptor 1 (FGFR-1) en c-kit. In **hoofdstuk 7.1** wordt de eerste fase-I studie met E7080 in patiënten met vergevorderde solide tumoren beschreven. Het middel werd eenmaal daags ingenomen tot doseringen van 32 mg. De maximaal verdraagbare dosering was 25 mg, en de dosis-limiterende toxiciteit was proteïnurie. De meest voorkomende bijwerkingen waren hypertensie, maagdarmklachten en stomatitis. De farmacokinetiek van E7080 was lineair, en het middel had een halfwaardetijd van ongeveer 7 uur. Veelbelovende tekenen van anti-tumor activiteit werd waargenomen in patiënten met uitgezaaide melanomen en nierceltumoren. Een case-report van een patiënt met een osteosarcoom die in deze studie werd behandeld wordt gepresenteerd in **hoofdstuk 7.2**. Verhoogde β -HCG en CA-125 serum concentraties werden gemeten toen deze patiënt gescreend werd voor deelname aan de studie. Verhoogde β -HCG serum concentraties zijn normaliter een aanwijzing voor zwangerschap, en worden maar zelden gezien

in patiënten met osteosarcoom. Verhoogde CA-125 serum concentraties zijn nog nooit gerapporteerd voor patiënten met osteosarcoom. Immunohistochemische studies toonden aan dat de tumor de bron was van de verhoogde β -HCG serum concentraties, maar we vonden geen CA-125 expressie in het tumorweefsel. De patiënt bleek niet zwanger, en werd vervolgens in studieverband behandeld met E7080. We vervolgden haar β -HCG en CA-125 serum concentraties tijdens haar behandeling. De β -HCG serum concentraties correleerden beter met de status van de ziekte dan de andere tumor marker CA-125.

Weer een andere klasse anti-kanker middelen zijn de HER-remmers. Een van deze middelen, PF00299804, wordt beschreven in **hoofdstuk 8**. De HER familie van receptor tyrosine kinases bestaat uit vier leden: HER1, HER2, HER3, en HER4. Na het binden van een ligand aan het extracellulaire domein van de HER receptoren (uitgezonderd HER2 dat geen ligand heeft), vindt er homo- of hetero-dimerisatie plaats, gevolgd door activatie van diverse intracellulaire signaal transductie routes die betrokken zijn bij celdeling en celdifferentiatie. De overexpressie van HER familieleden komt voor bij uiteenlopende vormen van kanker, en diverse nieuwe anti-kanker medicijnen grijpen aan op de HER1 en HER2 receptoren. PF00299804 is een oraal beschikbare, irreversibele remmer van de HER1, HER2, en HER4 receptoren. In de fase-I studie die hier beschreven wordt, werd PF00299804 eenmaal daags ingenomen in een continu schema (deel A) of discontinu (deel B) door patiënten met vergevorderde vormen van kanker. De maximaal verdraagbare dosering was 45 mg eenmaal daags, en de dosis-limiterende toxiciteiten waren stomatitis en huidproblemen. De farmacokinetiek van PF00299804 was lineair, en het middel had een lange halfwaardetijd van tussen de 46 en 72 uren. Een dosis-afhankelijke afname van celdeling en toename in remming van intracellulaire signaaltransductie routes werd geobserveerd in huidbiopt samples. Veelbelovende tekenen van anti-tumor activiteit werd geobserveerd in patiënten met niet-kleincellig long carcinoom.

De laatste fase-I studie van dit proefschrift wordt beschreven in **hoofdstuk 9**. Deze studie onderzocht de veiligheid, farmacokinetiek, en farmacodynamiek van sorafenib in combinatie met gemcitabine en carboplatine. Sorafenib is een oraal beschikbare multi-kinase remmer met angiogenese remmende eigenschappen, die geregistreerd is voor de behandeling van niercel tumoren en hepatocellulair carcinoom. De combinatie van gemcitabine, een nucleoside

antimetabool, en carboplatine is geregistreerd voor de behandeling van vergevorderde eierstok tumoren, maar is ook actief in patiënten met niet-kleincellig long carcinoom en borstkanker. In deze studie kregen patiënten carboplatine toegediend op dag 1, en gemcitabine op dag 1 en 8, van iedere behandelkuur (21 dagen). De sorafenib tabletten werden iedere dag ingenomen. Het eerste dosis niveau (sorafenib 200 mg tweemaal daags, carboplatine AUC3, en gemcitabine 750 mg/m²) bleek niet tolerabel, aangezien drie van de zes patiënten een dosis-limiterende toxiciteit ervoer (graad 3 vermoeidheid in alle gevallen). Vervolgens werd het protocol voor deze studie geamendeerd met nieuwe dosis niveaus, met lagere doseringen van alle onderzochte middelen. De maximaal toleerbare dosering was nog niet vastgesteld, en de studie liep nog op het moment dat dit proefschrift voltooid werd. De farmacokinetiek van alle drie de middelen, en de gemcitabine trifosfaat data kwamen beiden overeen met data uit de literatuur.

Samengevat beschrijft dit proefschrift verscheidene fase-I studies met nieuwe, doelgerichte anti-kanker middelen. Een aantal van deze middelen worden inmiddels in fase II studies getest op effectiviteit. Toekomstige fase I studies met doelgerichte middelen moeten zich vaker richten op farmacodynamische eindpunten, om sneller effectiviteit, of het gebrek hieraan, aan te kunnen tonen. Bovendien moeten patiënten in toekomstige fase-I studies vaker gerekruteerd worden op basis van de moleculaire eigenschappen van hun tumor. Imaging technieken zoals de PET/CT scanner kunnen waardevol zijn voor beide hierboven genoemde doeleinden.

Dankwoord

Dankwoord

De afgelopen jaren heb ik met veel plezier aan dit promotieonderzoek gewerkt, en er zijn een heleboel mensen die hier op enigerlei wijze aan bijgedragen hebben. Ik hoop dat ik niemand vergeten ben, en mocht dit wel het geval zijn dan bied ik hier bij voorbaat al mijn excuses voor aan.

Op de eerste plaats wil ik alle patiënten bedanken die mee hebben gewerkt aan de klinische onderzoeken. Misschien is de meest waardevolle kennis die ik de afgelopen jaren heb opgedaan wel afkomstig van de patiënten waar ik een groot deel van de tijd mee door gebracht heb. Jullie optimisme, vertrouwen en levenslust hebben me doen realiseren hoe waardevol het leven is.

Mijn promotoren, prof. dr. Jan Schellens en prof. dr. Jos Beijnen, wil ik bedanken voor de uitstekende begeleiding van mijn onderzoek. Beste Jan, ik heb enorm veel geleerd de afgelopen vier jaren, en daar ben jij grotendeels verantwoordelijk voor. De manier waarop jij de kliniek combineert met wetenschappelijk onderzoek is bewonderenswaardig. Bedankt voor je leerzame commentaar op mijn manuscripten en presentaties, en ook bedankt dat je me de mogelijkheid gegeven hebt om tot tweemaal toe een congres in het buitenland te bezoeken. Beste Jos, ook al was ons contact minder intensief, ik heb toch erg veel gehad aan jouw kritische blik op mijn manuscripten. Zonder jouw nuttige toevoegingen waren de manuscripten een stuk minder goed geworden. Ook zeer bedankt voor het mogelijk maken van de analytische ondersteuning voor enkele studies die in dit proefschrift beschreven staan.

De leescommissie, bestaande uit prof. dr. G. A. M. S. van Dongen, prof. dr. D. J. Richel, prof. dr. E. E. Voest, prof. dr. A. de Boer, en prof. dr. A. C. G. Egberts, ben ik zeer erkentelijk voor het lezen en beoordelen van mijn proefschrift.

Zeker de eerste drie jaren van mijn promotietraject heb ik voornamelijk doorgebracht in de kinetiekrimte op afdeling 4C van het Nederlands Kanker Instituut. Het was een klein hokje zonder uitzicht op buiten, maar het gezelschap vergoedde veel. En daarmee bedoel ik mijn collega-OIOs waar ik later op terugkom, en de (kinetiek)verpleegkundigen. Beste Ans, Annette, Thea, Karina, Noëlle, Mariska, Annemiek, Marjolein, en alle andere

verpleegkundigen, bedankt voor alle hulp en gezelligheid. Ik vond jullie gezelschap uiterst prettig, en zal jullie missen. Hopelijk houden we contact!

Ook met de nurse-practitioners Jana, Marja, Margaret, Marianne, Annemarie en Emmy was het prettig samenwerken. Bedankt voor de uitstekende voorlichting en begeleiding van de patiënten, en voor het ter beschikking stellen van de drop-pot. Ik kom eerdaags een zak snoep brengen om het goed te maken. Magda, bedankt voor je hulp bij het opzoeken van statussen, planningsgegevens en allerlei andere zaken.

Beste Marja, de teleconferenties waren vaak lang en soms op onhandige tijdstippen. Toch was het altijd even gezellig. Ik vind het knap hoe je alle studies op de rit weet te houden. Dit uiteraard mede door de geweldige ondersteuning van Brenda. Beste Brenda, ik vind dat je geweldig werk verzet, en ben erg blij dat jullie eindelijk de kamer gekregen hebben waar jullie recht op hebben. Bedankt voor de gezelligheid, en de prima samenwerking.

Zonder alle hulp van Jolanda was de totstandkoming van dit proefschrift nooit zo gladjes verlopen. Beste Jolanda, jouw vrolijkheid werkte aanstekelijk, en ik heb met veel plezier met je samengewerkt. Bedankt voor alle hulp bij het gereedmaken van alle formulieren en mappen die nodig zijn om te kunnen promoveren.

En dan het trialbureau. Hier heb ik flink wat uurtjes doorgebracht, onder andere met het invullen van de altijd gezellige CRFs. Gelukkig was er altijd wat te eten op het trialbureau, zodat ik nooit met honger naar huis ging. Beste Lidwina, Christiane, Marianne, Marjolijn, Marjolein, Ludy, Annelies, Josien, Frauwkje, Irene en de rest: Bedankt voor deze goede zorgen, en ook bedankt voor alle hulp wanneer ik weer eens aankwam met een vraag over een van de vele klinische studies. Mariëlle bedankt voor de gezellige lunches.

I would like to thank John Stone and Philip van der Veen for their assistance with the olaparib manuscripts. Dear John and Philip, many thanks for your help. It was a pleasure working with you. Dear Bob (Milham), many thanks for your assistance with the PF00299804 manuscript. I couldn't have done this without your help, and I enjoyed working with you.

Dankwoord

Angela, bedankt voor het inplannen van de vele patiënten voor de klinische studies. Het moet heel wat werk geweest zijn om alle patiënten op de juiste dagen te laten starten. Rene en Jannie, bedankt voor de ondersteuning op de afdeling. Brigitte en Cecile, bedankt voor alle hulp met de QA en GCP zaken. Zonder jullie controle was alles ongetwijfeld in de soep gelopen.

De nurse-practitioners van de dagbehandeling wil ik bedanken voor hun hulp bij het opzetten van de Herceptin studie. Ook al heeft deze studie mijn proefschrift niet gehaald, ik vond de samenwerking erg prettig. Annelies, bedankt voor je interesse in mijn onderzoek, en heel erg veel succes met de afronding van je eigen promotieonderzoek. De verpleegkundigen van de dagbehandeling wil ik bedanken voor alle bloedafnames die ze voor mij gedaan hebben.

Over bloedafnames gesproken: Grote dank is verschuldigd aan de dames van de prikpoli. Honderden buisjes bloed werden afgenomen voor mijn onderzoek, en het ging (bijna) altijd goed. Beste Els, Herma, Chris, Carmen, Edith, Mandy, Sabine, Tineke, Loubna, Carla en iedereen die ik vergeten ben, hartelijk dank hiervoor! Jullie zullen wel eens gek geworden zijn wanneer ik weer eens niet te bereiken was om een buisje af te halen. Ik beloof dat dit vanaf nu niet meer voor zal komen.

De OIOs van afdeling B7, voorheen H6, wil ik bedanken voor de gezellige samenwerking. Beste Lot, je was de enige medisch bioloog onder mijn collega OIOs, en dat scheidt gelijk een band. Bedankt voor je gezelligheid, en ook voor het recept van de Javaanse gehaktballetjes. Beste Maarten, bedankt voor de vele grappen en grollen in de kinetiekruimte en ver daarbuiten, en succes met de afronding van je promotie volgend jaar. Suzanne, ook jij bedankt voor de prettige samenwerking, en ook jouw promotie gaat helemaal goed komen! Beste Sander en Roos, kinetiekers in ruste, bedankt dat jullie me wegwijs gemaakt hebben in de wereld van de kinetiek. Ik vond het altijd fijn samenwerken met jullie. Leuk dat jullie elkaar nu ook buiten het werk gevonden hebben. Dick, bedankt voor al je hulp bij diverse studies. Je was er altijd als ik je hulp nodig had, en het was prettig samenwerken.

In het Slotervaart ziekenhuis was ik minder vaak te vinden, maar als ik er moest wezen, voelde ik me er altijd welkom. Beste Hilde, bedankt voor de gastvrijheid op het lab, en voor je geweldige hulp bij het meten van de

monsters van enkele hier beschreven studies. Beste Alwin, je was altijd enthousiast als ik met een kinetiek probleem aan kwam zetten, en wist ook altijd de oplossing voor het probleem te vinden. Bedankt voor alle hulp, en ook voor de gezelligheid bij het uitstapje in Orlando. Roel, bedankt voor je hulp met computerproblemen in de keet, en voor de altijd spetterende "state of the week". De analisten van de Slotervaart apotheek wil ik bedanken voor de analytische ondersteuning

Dan de OIOs uit de keet. Allereerst wil ik mijn (ex-) kamergenoten bedanken voor de prettige samenwerking. Anthe, Tessa, Corine en Markus, ik heb veel van jullie geleerd, en er was altijd plaats voor gezelligheid. Ron, bedankt voor je hulp met PK problemen, en voor het pimpen van "het lelijke figuur" uit dit proefschrift. We blijven de kwakzalverij bestrijden! Rik, ondanks je voorkeur voor die club uit Amsterdam konden we het goed vinden. Ik mail je wel als Ajax weer eens verloren heeft. Mariska, je was een gezellige buurvrouw. Succes met de laatste loodjes, ook al wegen die het zwaarst. Stijn, de ASCO trip naar Orlando was niet alleen erg leerzaam, maar dankzij jouw aanwezigheid ook erg gezellig. Volgende keer de Summit Plummet! Ly, de NKI soap zit er eindelijk op. Misschien in de toekomst op de televisie? Bedankt voor alle, daar komt het woord weer, gezelligheid. Fijn dat je mijn paranimf wilt zijn!

Ook alle "andere" OIOs wil ik bedanken voor de fijne tijd, een aantal in het bijzonder. Beste Wandena, bedankt voor de fijne samenwerking bij het overdragen van enkele van jouw studies. Nienke, bedankt voor het meten van alle sorafenib monsters, en succes met de nibjes!! Robert, bedankt voor het meten van alle trifosfaatjes, en voor je hulp bij het layouten. Joost, jij hebt me ook enorm geholpen bij het layouten, zowel technisch als psychisch (Fransie Duits). Bedankt hiervoor! Anne-Charlotte, ook jij bedankt voor de fijne samenwerking, en succes met het vervolg van je eigen promotietraject! Carola en Marie-Christine, bedankt voor de prettige samenwerking bij de (in dit boekje ontbrekende) Herceptin studie. Rob, Thomas, Johannes en Robert: Het was geweldig om deel uit te maken van het beruchte Slotervaart voetbalelftal.

Voordat ik in Amsterdam begon met mijn OIO carrière heb ik anderhalf jaar stage gelopen in het Antonius Ziekenhuis te Nieuwegein, onder begeleiding van dr. Wim Gerritsen. Beste Wim, ook al heb je niet direct bijgedragen aan het onderzoek dat in dit proefschrift beschreven wordt, toch ben ik je dank

Dankwoord

verschuldigd. Je hebt me met je humor en kennis enorm geënthousiasmeerd voor het klinische onderzoek waardoor ik vastbesloten was om een klinisch promotieonderzoek te doen. Je werkt inmiddels niet meer in Nieuwegein waardoor het een stuk lastiger is geworden om je op te zoeken voor een bakkie koffie. Gelukkig is er internet zodat we elkaar kunnen blijven mailen. We houden contact!

Beste Nick, ook al hebben we elkaar de afgelopen vier jaar eigenlijk niet vaak genoeg gezien, ik vond het altijd fijn om mijn promotie-sores met iemand te kunnen delen die in het zelfde schuitje zat. Binnenkort is het voor jou ook zo ver! Hopelijk zien we elkaar de komende tijd vaker, wie weet pakken we het tennissen weer op. Fijn dat je mijn paranimf wilt zijn!

Beste Johan, bedankt voor de vele gezellige avondjes voetbal kijken, potjes FIFA–en op de X–Box (volgens mij sta ik trouwens nog steeds een potje voor, maar dat ter zijde), buzen en guitar hero op de PS3, biertjes drinken bij Els, et cetera. Altijd prettig om te kunnen ontspannen na de lange dagen in Amsterdam, en met jou in de buurt was ontspanning nooit ver weg. Bedankt daarvoor! De gezellige avondjes zullen zeker voortgezet worden, en wie weet voetballen we over een jaartje wel weer samen, op het veld of in de zaal.

Verder wil ik graag mijn familie bedanken voor hun steun en interesse de afgelopen jaren. Lieve oma, ik vind het een eer dat u bij de promotieplechtigheid aanwezig zult zijn. Lieve pa en ma, bedankt voor alle steun de afgelopen jaren. Jullie interesse in mijn werk is enorm gewaardeerd, en onovertroffen. Pa, jouw vele muzikale suggesties hebben het fileleed de afgelopen jaren behoorlijk verzacht. Goede muziek in de auto maakte de tochten niet minder lang maar wel een stuk draaglijker. Ma, bedankt voor het schilderen van de voor- en achterkant van het proefschrift. Het is hartstikke mooi geworden! Lieve Suus en Ray, ook jullie bedankt voor jullie interesse in mijn werkzaamheden. We zien elkaar veel te weinig, hopelijk gaat daar snel verandering in komen. We spreken gauw weer wat af.

En als laatste: Lieve Eva, bedankt voor je ondersteuning de afgelopen jaren. Het was altijd fijn thuiskomen na de lange dagen in het NKI, en de vele uren in de file. Ik ben heel gelukkig met je!

David

Curriculum Vitae

List of publications

Curriculum Vitae

David Sebastiaan Boss werd geboren op 8 september 1979 te Utrecht. In 1998 behaalde hij het VWO diploma aan het Anna van Rijn college te Nieuwegein. In datzelfde jaar begon hij aan de studie biomedische wetenschappen aan de Universiteit van Utrecht. Tijdens zijn studie heeft hij een hoofdvakstage gelopen op de afdeling virologie onder begeleiding van dr. C.A.M. de Haan. Het onderwerp van deze stage was "foreign gene expression in Coronaviruses". Hierna liep hij een bijvakstage op het klinisch chemisch laboratorium van het st. Antonius ziekenhuis te Nieuwegein, onder begeleiding van dr. W.B. Gerritsen. Het onderwerp van deze stage was "MECC study: on-pump versus off-pump CABG". De masterfase van zijn studie werd afgerond met het schrijven van een afstudeerscriptie, getiteld "Biomarkers and cardiac surgery". Ook bij het schrijven van deze scriptie werd hij begeleid door dr. W.B. Gerritsen. In april 2005 rondde hij zijn studie af, waarna hij in mei van datzelfde jaar begon als onderzoeker in opleiding op de afdeling medische oncologie in het Antoni van Leeuwenhoek ziekenhuis en de apotheek van het Slotervaart ziekenhuis te Amsterdam. In deze periode werd het in dit proefschrift beschreven onderzoek uitgevoerd onder begeleiding van prof. dr. J.H.M. Schellens en prof. dr. J.H. Beijnen.

Curriculum Vitae

David Sebastiaan Boss was born on September 8, 1979 in Utrecht. In 1998 he received his VWO exam at the Anna van Rijn college in Nieuwegein. In the same year he started to study biomedical sciences at Utrecht University. His main research project was performed at the virology department of Utrecht University. This project, supervised by dr. C.A.M. de Haan, was entitled "foreign gene expression in Coronaviruses". Subsequently he did a second research project at the clinical laboratory of the st. Antonius hospital in Nieuwegein. This project, entitled "MECC study: on-pump versus off-pump CABG", was supervised by dr. W.B. Gerritsen. The writing of his master thesis, entitled "Biomarkers and cardiac surgery" was also supervised by dr. W.B. Gerritsen. He received his Master's degree in April 2005. In May 2005 he started his PhD project at the division of medical oncology of the Antoni van Leeuwenhoek hospital and the department of pharmacy of the Slotervaart hospital in Amsterdam. In this period the research as described in this thesis was carried out under the supervision of prof. dr. J.H.M. Schellens and prof. dr. J.H. Beijnen.



List of publications

Articles related to this thesis:

Safety, tolerability, pharmacokinetics and pharmacodynamics of the oral cyclin-dependent kinase inhibitor AZD5438 when administered at continuous and intermittent dosing schedules in patients with advanced solid tumours.
Boss DS, Schwartz GK, Middleton MR, Amakye DD, Swaisland H, Midgley RS, Ranson M, Danson S, Calvert H, Plummer R, Morris C, Carvajal RD, Chirieac LR, Schellens JH, Shapiro GI.
Ann Oncol. In press

Clinical experience with Aurora kinase inhibitors: A review.
Boss DS, Beijnen JH, Schellens JH.
Oncologist. 2009;14(8):780-93

Inhibition of Poly(ADP-Ribose) Polymerase in Tumors from BRCA Mutation Carriers.
Fong PC, **Boss DS**, Yap TA, Tatt A, Wu P, Mergui-Roelvink M, Mortimer P, Swaisland H, Lau A, O'Connor MJ, Ashworth A, Carmichael J, Kaye SB, Schellens JH, de Bono JS.
N Engl J Med. 2009;361(2):123-34

Phase I Pharmacokinetic and Pharmacodynamic study of Carboplatin and Topotecan administered intravenously every 28 days to Patients with malignant solid Tumors.
Boss DS, Siegel-Lakhai WS, van Egmond-Schoemaker NE, Pluim D, Rosing H, Ten Bokkel-Huinink WW, Beijnen JH, Schellens JH.
Clin Cancer Res. 2009;15(13):4475-83

Development and validation of an enzyme-linked immunosorbent assay for the quantification of trastuzumab in human serum and plasma. Damen CW, de Groot ER, Heij M, **Boss DS**, Schellens JH, Rosing H, Beijnen JH, Aarden LA.
Anal Biochem. 2009;391 (2): 114-120

Application of PET/CT in the Development of Novel Anticancer Drugs.
Boss DS, Olmos RV, Sinaasappel M, Beijnen JH, Schellens JH.
Oncologist. 2008;13(1):25-38

In Reply
Boss DS, Olmos RV, Sinaasappel M, Beijnen JH, Schellens JH.
Oncologist 2008;13(6):736-737

Articles not related to this thesis:

Malondialdehyde in plasma, a biomarker of global oxidative stress during mini CABG as compared to on- and off-pump CABG; a pilot study.
Gerritsen WB, van Boven WJ, **Boss DS**, Haas FJ, van Dongen EP, Aarts JP.
Interact Cardiovasc Thorac Surg. 2006;5(1):27-31

Coronaviruses as vectors: stability of foreign gene expression.
de Haan CA, Haijema BJ, **Boss D**, Heuts FW, Rottier PJ.
J Virol. 2005;79(20):12742-51

Abstracts

Phase I, pharmacokinetic, and pharmacodynamic study of carboplatin and topotecan administered in two different schedules.

Boss DS, Siegel-Lakhai WS, Schoemaker-van Egmond NE, Pluim D, Rosing H, Ten Bokkel-Huinink WW, Beijnen JH, Schellens JH.
ASCO annual meeting 2009, Orlando, US

First-in-human (FIH) study of PF-00299804 in advanced cancer patients: correlation between pharmacokinetics (PK) and pharmacodynamics (PD).
Schellens JH, Guo F, Janne PA, Eckhardt SG, Camidge DR, Taylor I, Lucca J, **Boss DS**, Wong SG, Britten CD
European Organisation for Research and Treatment of Cancer (EORTC)
21 – 24 october 2008, Geneva, Switzerland

Preliminary activity and safety results from a phase I clinical trial of PF-00299804, an irreversible pan-HER inhibitor, in patients (pts) with NSCLC.
Janne PA, Schellens JH, Engelman JA, Eckhardt SG, Millham R, Denis LJ, Britten CD, Wong SG, **Boss DS**, Camidge DR.
ASCO annual meeting 2008, Chicago, US

First-in-Human (FIH) study of PF-0299804 in advanced cancer patients: correlation between pharmacokinetics (PK) and pharmacodynamics (PD).
Schellens JH, Guo F, Janne PA, Eckhardt SG, Camidge DR, Taylor I, Lucca J, **Boss DS**, Wong SG, Britten CD.
ASCO annual meeting 2008, Chicago, US

A phase I study of E7080 in patient (pts) with advanced malignancies.
Glen H, **Boss DS**, Morrison R, Roelvink M, Wanders J, Mazur A, Gupta A, Das A, Evans TR, Schellens J.
ASCO annual meeting 2008, Chicago, US

AZD2281 (Ku-0059436), a PARP (Poly ADP-ribose Polymerase) inhibitor with single agent anticancer activity in patients with BRCA deficient ovarian cancer: results from a phase I study.
Fong PC, **Boss DS**, Carden CP, Roelvink M, De Greve J, Gourley CM, Carmichael J, De Bono JS, Schellens JH, Kaye SB.
ASCO annual meeting 2008, Chicago, US

First in human phase I pharmacokinetic (PK) and pharmacodynamic (PD) study of KU-0059436 (Ku), a small molecule inhibitor of Poly ADP-Ribose Polymerase (PARP).
Boss DS, Fong PC, Yap TA, Roelvink M, Tutt A, Carmichael J, O' Connor M, Kaye SB, Schellens JHM, de Bono JS.
EACPT 2007, Amsterdam, the Netherlands

List of publications

A Phase I dose finding study of E7080 in patients with advanced malignancies.
Boss DS, Glen H, Evans TRJ, Roelvink M, Saro JM, Bezodis P, Copalu W, Das A, Croswell G, Schellens JHM.
EACPT 2007, Amsterdam, the Netherlands

First in human phase I pharmacokinetic (PK) and pharmacodynamic (PD) study of KU-0059436 (Ku), a small molecule inhibitor of Poly ADP-Ribose Polymerase (PARP).
Yap TA, **Boss D**, Fong PC, Roelvink M, Tutt A, Carmichael J, O' Connor M, Kaye SB, Schellens JHM, de Bono JS.
ASCO annual meeting 2007, Chicago, US

A Phase I dose finding study of E7080 in patients with advanced malignancies.
Glen H, **Boss DS**, Evans TRJ, Roelvink M, Saro JM, Bezodis P, Copalu W, Das A, Croswell G, Schellens JHM.
ASCO annual meeting 2007, Chicago, US

Phase I and Pharmacological study of the novel aurora kinase inhibitor AZD1152.
Schellens JHM, **Boss D**, Witteveen PO, Zandvliet A, Beijnen JH, Voogel-Fuchs M, Morris C, Wilson D, Voest DD.
ASCO annual meeting 2006, Atlanta, US